The Impact of Adipose-Associated Stromal Cells on the Metastatic Potential of Ovarian Cancer

Amanda Ann Shea

Dissertation submitted to the faculty of Virginia Polytechnic Institute and State University in partial fulfillment of the requirements for the degree of

Doctor of Philosophy
In
Human Nutrition, Foods and Exercise

Eva M. Schmelz, Chair
Paul C. Roberts
Matthew W. Hulver
Madlyn I. Frisard

December 9, 2013
Blacksburg, Virginia

Keywords: ovarian cancer, obesity, adipose tissue, stromal vascular fraction, progenitor cells

The Impact of Adipose-Associated Stromal Cells on the Metastatic Potential of Ovarian Cancer

Amanda Ann Shea

ABSTRACT

Obesity is a major global health concern due to its steadily increasing rates and significant contribution to numerous diseases, including cancer. Ovarian cancer specifically, is associated with a 30% increased risk with obesity, although the mechanisms for this are unknown.[1] Waist-to-hip ratio has been especially associated with ovarian cancer,[2,3] suggesting that visceral fat may be the greatest contributor. Here, we investigated individual visceral fat depots as independent contributors to cancer progression, specifically focusing on adipose tissue-derived stem and progenitor cells, which have previously been shown to be recruited by cancer cells and participate in cancer progression. We confirmed that ovarian cancer tumor burden was indeed significantly increased in mice on a high fat as compared to low fat diet. To further investigate mechanisms, we examined changes in progenitor populations that occurred in intra-abdominal parametrial (pmWAT), retroperitoneal (rpWAT), and omental (omWAT) white adipose tissue (WAT) depots with cancer presence. The greatest tumor burden was evident in omWAT, which also displayed an increase in $CD45^-$ cells but a decrease in adipose progenitor cells (APC) and endothelial progenitor cells, suggesting that there was an increase in stromal cells, but that the stem cells were pushed towards differentiation. PmWAT and rpWAT showed remarkably stable progenitor populations. However, a tumor from pmWAT had a significant presence of $CD45^-$ cells, actually matching that of its surrounding tissue and differing from the omWAT tumors, indicating that

microenvironment has a major influence on tumor stromal cells. We also found that with high fat diet, many cancer-associated changes were exacerbated, such as an increased inflammatory response in all tissues and further decreases in APCs in omWAT. *In vitro* studies further confirmed that ovarian cancer cells and SVF cells were able to directly interact. Additionally, SVF cells were able to increase the proliferation, mobility, and invasiveness of cancer cells. Conversely, co-culturing also enhanced the proliferation and mobility of SVF cells, providing further evidence that SVF cells may be recruited by cancer cells and that their relationship may be bilateral. Thus, this study provides a good foundation for examining the cellular contributions of adipose tissue to cancer. By further characterizing the mechanism for the association between obesity and cancer development, we could find novel targets to decrease the progress of cancer development in at-risk obese individuals.

1. Olsen C, Green, A, Whiteman, D, Sadeghi, S, Kolahdooz, F, Webb, P. Obesity and the risk of epithelial ovarian cancer: a systemic review and meta-analysis. *Eur J Cancer.* 2007;43:690-709.

2. Mink PJ, Folsom AR, Sellers TA, Kushi LH. Physical activity, waist-to-hip ratio, and other risk factors for ovarian cancer: a follow-up study of older women. *Epidemiology.* Jan 1996;7(1):38-45.

3. Delort L, Kwiatkowski F, Chalabi N, Satih S, Bignon YJ, Bernard-Gallon DJ. Central adiposity as a major risk factor of ovarian cancer. *Anticancer Res.* Dec 2009;29(12):5229-5234.

Attributions

Several colleagues aided in the writing and research behind the chapters presented as part of this dissertation. A brief description of their contributions is included here.

Chapter 3. PRELIMINARY DATA: INTRA-ABDOMINAL FAT DEPOTS REPRESENT DISTINCT IMMUNOMODULATORY MICROENVIRONMENTS

Chapter 3 was published in PlosOne.

Cohen, C.A. was a PhD student in the Roberts lab in the Biomedical Sciences and Pathobiology (DBSP) department at VT. As co-author of this paper, she aided in the design and performance of the experiments, collection and analysis of data, generation of figures, interpretation of data and the writing of this paper.

Heffron, C.L. was a member of the Roberts lab in the Biomedical Sciences and Pathobiology (DBSP) department at VT. As a co-author of this paper, she aided in experimental planning, animal work and sample collection and processing.

Schmelz, E.M. is the Principal Investigator of the Schmelz lab in the HNFE department at VT. As a co-author of this paper, she aided in the design of these experiments, the interpretation of data and the writing of this paper, and provided editorial comments; she was co-principal investigator for one of the grants supporting this research.

Roberts, P.C. is the Principal Investigator of the Roberts lab in the DBSP department at VT. As a co-author of this paper, he aided in the design of these experiments, the interpretation of data and the writing of this paper, and provided editorial comments; he was co-principal investigator for one of the grants supporting this research.

Chapter 4. **HIGH FAT FEEDING INTIATES CHANGES IN INTRA-ABDOMINAL FAT DEPOT PROGENITOR POPULATIONS**

Cohen, C.A. aided in animal handling, sample collection and processing.

Heffron, C.L. aided in animal handling, sample collection and processing.

Schmelz, E.M. aided in the design of these experiments, the interpretation of data and the editing of this chapter.

Roberts, P.C. aided in the design of these experiments, the interpretation of data and the editing of this chapter.

Chapter 5. **CHANGES IN ADIPOSE PROGENITOR POPULATIONS ARE ASSOCIATED WITH ENHANCED OVARIAN CANCER PROGRESSION IN MICE ON A HIGH FAT DIET**

Cohen, C.A. aided in animal handling, sample collection and processing.

Heffron, C.L. aided in animal handling, sample collection and processing.

Schmelz, E.M. aided in the design of these experiments, the interpretation of data and the editing of this chapter.

Roberts, P.C. aided in the design of these experiments, the interpretation of data and the editing of this chapter.

Chapter 6. **WHITE ADIPOSE TISSUE STROMAL VASCULAR CELLS ENHANCE OVARIAN CANCER AGGRESSIVENESS IN VITRO**

Schmelz, E.M. aided in the design of these experiments, microscopy work, the interpretation of data and the editing of this chapter.

Roberts, P.C. aided in the design of these experiments, microscopy work, the interpretation of data and the editing of this chapter.

Table of Contents

TABLE OF FIGURES

TABLE OF TABLES

TABLE OF ABBREVIATIONS

αSMA: alpha smooth muscle actin
APC: Adipose progenitor cell
BM: Bone marrow
BMI: Body mass index
BSA: Bovine serum albumin
CEC: Circulating endothelial cell
COL1: Collagen 1
DC: Dendritic cell
DMEM: Dulbecco's Modified Eagle Medium
EC: Endothelial cell
EOC: Epithelial ovarian cancer
EPC: Endothelial progenitor cell
FACS: Fluorescent activated cell sorting
FFL: Firefly luciferase
FN1: Fibronectin 1
GFP: Green fluorescent protein
HPC: Hematopoietic progenitor cell
HSC: Hematopoietic stem cell
IP: Intraperitoneal
MOSE: Mouse ovarian surface epithelial cell
MOSE-E: early passage MOSE cell
MOSE-L FFL: late passage MOSE cell transfected with firefly luciferase
MS1: MILES SVEN, mouse endothelial cell
MSC: Mesenchymal stem cell
omWAT: Omental WAT
PBS: Phosphate buffered saline
pmWAT: Parametrial WAT
PSF: Peritoneal serous fluid
PCI: Peritoneal Cancer Index
PCR: Polymerase chain reaction
rpWAT: Retroperitoneal WAT
qRT-PCR: Quantitative real time polymerase chain reaction
STIC: Serous tubal intraepithelial carcinoma
SVF: Stromal vascular fraction
S-WAT: subcutaneous WAT
TAF: Tumor associated fibroblast
TNC: Tenascin C
VEGF: Vascular endothelial growth factor
V-WAT: Visceral WAT
WAT: White adipose tissue

Chapter 1: INTRODUCTION

Ovarian cancer is the fifth leading cause of cancer deaths among women in the United States, resulting in an estimated 22,280 new cases and 15,500 deaths in 2012.[1] Due to a lack of efficient methods of early detection and accurate molecular markers, ovarian cancer is generally found at later stages when the survival rates are severely diminished. Indeed, greater than 70% of patients are diagnosed with advanced stage disease when the 5-year survival rate is less than 20%.[2]

A potential obstacle in reducing the incidence of ovarian cancer is the current obesity epidemic. In 2008, 68% of Americans were overweight or obese and if the trend continues, this number is projected to be at 86.3% by 2030.[3,4] Obesity has been linked to numerous health conditions including cancer. In 2003, it was estimated that overweight and obesity were responsible for 14% of all cancer deaths in men and 20% of those in women in the United States.[5] Specifically focusing on ovarian cancer, a meta-analysis of 28 studies found that there is an estimated 30% increased risk of ovarian cancer with overweight and obesity.[6] Currently, the mechanism for how obesity contributes to ovarian cancer is unknown. A potential factor is adipose tissue reorganization, which may lead to an increase in the number and mobilization of stromal cells from the expanded adipose tissue in obese individuals. The stromal vascular fraction (SVF) of adipose tissue may serve as a reservoir for stem and progenitor cells, which can be recruited to promote tumor formation, enhancing ovarian cancer growth and metastatic potential. This study aims to determine if obesity enhances ovarian cancer progression in a mouse model and if the presence of tumor cells induces a shift in SVF cell populations within various intra-abdominal adipose depots. Further, we will determine if there is a

direct association between adipose tissue SVF cells and mouse ovarian cancer cells *in vitro*, and if SVF cells can enhance cancer cell proliferation, mobility and invasive potential. This study will determine if there is indeed a link between obesity and ovarian cancer progression and will further characterize novel targets for ovarian cancer therapy.

1. Society AC. *Cancer Facts & Figures 2012*. Atlanta: American Cancer Society;2012.

2. Balch C, Fang, F, Matei, D, Huang, T, Nephew, K. Minireview: Epigenetic Changes in Ovarian Cancer. *Endocrinology*. 2009;150(9):4003-4011.

3. Flegal K, Carroll, M, Ogden, C, Curtin, L. Prevalence and trends in obesity among US adults, 1999-2008. *JAMA*. 2010;303(3):235-241.

4. Wang Y, Beydoun, M, Liang, L, Caballero, B, Kumanyika, S. Will all Americans become overweight or obese? Estimating the progression and cost of the US obesity epidemic. *Obesity*. 2008;16(10):2323-2330.

5. Calle EE, Rodriguez C, Walker-Thurmond K, Thun MJ. Overweight, obesity, and mortality from cancer in a prospectively studied cohort of U.S. adults. *N Engl J Med*. Apr 24 2003;348(17):1625-1638.

6. Olsen C, Green, A, Whiteman, D, Sadeghi, S, Kolahdooz, F, Webb, P. Obesity and the risk of epithelial ovarian cancer: a systemic review and meta-analysis. *Eur J Cancer*. 2007;43:690-709.

Chapter 2: REVIEW OF LITERATURE

Epithelial Ovarian Cancer

While epithelial ovarian cancer (EOC) accounts for a majority of ovarian malignancies, very little is known about its pathophysiology, creating considerable difficulties in determining strategies for prevention and treatment. There is significant heterogeneity among EOCs, including variable clinical manifestations and underlying molecular characterizations, multiple histologically defined subtypes such as serous, endometrioid, clear cell, and mucinous, as well as a differentiation between type I and type II malignancies (Type I ovarian cancers are of lower malignant potential, but exhibit alterations in various biological events as they progress from benign to malignant, including microsatellite instability and mutations in K-Ras, B-Raf, β-catenin, and PTEN[1,2,3]. Type II carcinomas are highly aggressive and frequently display mutations in p53, resulting in rapid progression, often in the absence of a benign precursor lesion[1,2]). Additionally, a recent hypothesis suggests that what is currently considered ovarian cancer may actually be metastases to the ovaries from the fallopian tubes. It should be noted that the ovaries are of mesodermal epithelium origin, while the cervix, endometrium, and fallopian tubes are derived from the mullerian ducts[4]. Histologically, the layer of mesothelium over the ovaries bears no resemblance to serous, endometrioid, mucinous, clear cell, or transitional carcinomas[4]. The previously prevailing theory hypothesized that the mesothelium overlaying the ovaries invaginates into the underlying stroma to form inclusion cysts. These cysts, under the influence of local factors, could undergo malignant transformation resulting in carcinomas. Inclusion cysts lined by ciliated (mullerian type) epithelium are observed in the ovarian cortex, but there are no

documented examples of the transition to carcinomas.[5] Indeed, no precursor lesions resembling ovarian carcinomas have been found on the ovaries, but early invasive tubal carcinomas have been found in women with the genetic predisposition to ovarian cancer.[6] These lesions are referred to as serous tubal intraepithelial carcinomas (STICs) and are found in the fallopian tubes of 70% of sporadic (non-hereditary) ovarian and peritoneal serous carcinomas.[7] Thus STICs, which are almost always detected in the fimbria, may be the source of ovarian serous carcinomas. Further, nearly all STICs overexpress p53 and STICs associated with concomitant ovarian carcinoma often share morphological features and identical p53 mutations.[7] In addition, ovarian carcinomas commonly express PAX8, a mullerian marker, but not calretinin, which is a mesothelial marker.[8] Hence, it is possible that ovarian carcinomas are actually secondary metastases. This is very important for determining effective preventive and treatment strategies. If what is currently considered primary ovarian cancer is actually a metastasis, then it is critical to find earlier targets to effectively prevent late-stage cancer. The data on the potential contributions of adipose-associated cells presented in this review apply regardless of the origin of ovarian cancer since the role of these cells as cancer support apply more to cancer progression than cancer initiation and thus it is likely that adipose-associated cells can increase malignant potential at any stage of cancer development. However, this unclear definition of ovarian cancer is important when evaluating current literature as the heterogeneity of EOC may impact the actual contribution of established correlating factors as well as responsiveness to treatments. This may also account for some of the variability between studies.

EOC is difficult to compare to other cancers because of its unique progression. EOC dissemination is very rarely hematogenous and is instead spread by exfoliation into the peritoneal cavity.[9] As shown in figure 1, exfoliated ovarian cancer cells are sloughed from the ovaries and can aggregate to form homogenous or heterogenous multicellular spheroids that can disseminate throughout the abdomen by bulk flow of peritoneal serious fluid. In many cases, peritoneal dissemination is accompanied by the formation of ascites, which is fluid accumulation resulting from increased vascular permeability, lymphatic obstruction, and fluid influx due to increased concentration of proteins and other factors secreted by tumor cells.[10,11,12,13] Tumor spheroids or single cells in the ascites eventually engraft onto the mesentery lining or surface of other organs in the peritoneal cavity and initiate metastatic outgrowths.

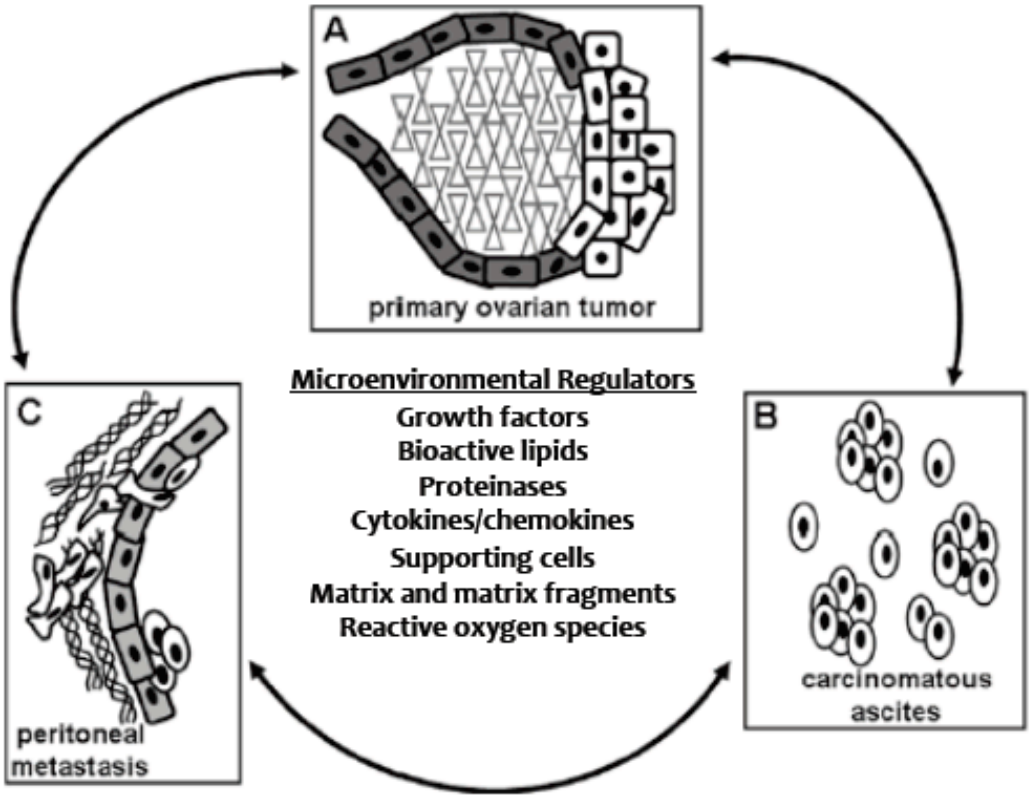

Figure 2.1. Progression of epithelial ovarian cancer. Ovarian epithelial cells become malignant, forming primary tumors on the ovaries (A). Cancer cells are sloughed off into the ascites fluid where they can aggregate (B) and eventually engraft onto the surface of other organs or the lining of the peritoneal cavity (C). This process is impacted by numerous microenvironmental regulators **Reproduced and edited from Cancer Treatment Research, January 2009, Vol 149, Pages 319-334 with permission from Springer Publishing.

EOC initiation and metastasis are influenced by numerous variables. Risk for ovarian cancer development increases with age, infertility, menopause, use of hormone replacement therapy, family history of ovarian or breast cancer, use of talc in the abdominal or perineal region, presence of polycystic ovary syndrome or endometriosis, and high body mass index.[15-19] Alternatively, high gravidity, hysterectomy, incomplete pregnancies, earlier age at first birth, unilateral oophorectomy and oral contraceptive use are associated with a reduced risk for ovarian cancer.[15-17,20] These associations have led to many theories for the developmental origin of EOC.

The most widely considered theories are incessant ovulation, gonadotropin stimulation, hormonal stimulation, and inflammation. The *incessant ovulation hypothesis* proposes that rupture of the ovulating follicle damages the ovarian surface epithelium and this continuous cycle of injury and repair leads to greater susceptibility to errors during replication. The *inflammation hypothesis* similarly proposes that the ovulatory process is injurious and induces inflammation, causing frequent damage and turnover of the ovarian surface epithelium during each ovulatory cycle, leading to an increased risk of mutation errors and cancer risk. Conversely, the *gonadotropin* and *hormonal stimulation hypotheses* focus on hormones. While the *gonadatropin hypothesis* theorizes that excessive follicle stimulating hormone and luteinizing hormone exposure increases stimulation of the ovarian surface epithelium, leading to malignant transformation, the *hormonal stimulation hypothesis* proposes that excess androgen stimulation of the

ovarian surface epithelium (OSE) leads to increased cancer risk while progesterone stimulation has a protective effect.[21]

As none of these theories have been accepted as the predominant cause of EOC, it is likely that factors from each, in addition to factors that have not yet been elucidated, all contribute to its pathogenesis. Interestingly, an obese state influences many of the biological processes, such as inflammation and hormone bioavailability, that are thought to contribute to ovarian cancer development, making a case for obesity being a potential factor in EOC pathogenesis.

Current theories on the contribution of obesity to ovarian cancer

While many studies point to an association between obesity and ovarian cancer development and progression, the dynamics of this relationship are unclear due to limited and conflicting data. Evaluation of a potential correlation has been hampered by inconsistent approaches in defining both obesity and ovarian cancer, as well as variations in methodology. While some studies use self-reported "usual body mass index (BMI) before diagnosis" or "usual weight as an adult" and do not find a correlation between obesity and EOC,[22-24] this could be due to ambiguity of time frame, variations in location of fat storage (visceral versus subcutaneous), fluctuations in weight, underestimation of weight or other sources or error. It is also important to note that currently published studies often differ with respect to the definition of obesity (not all use BMI), time of weight measurement (time of diagnosis versus prior to diagnosis), subject age, menopausal status, and measurement of risk. A meta-analysis of 28 studies, which took these factors into consideration, using only population based case-controlled or cohort studies with a clear definition of obesity based on BMI, found an estimated 30%

increased risk of epithelial ovarian cancer in obese women. There was also a 22% increased risk with adolescent obesity, although this was not adjusted for adult BMI.[25] Other studies have reported that even with no evidence of an association between recent BMI or adult weight and ovarian cancer risk, higher BMI in young adulthood was still associated with an increased risk of premenopausal ovarian cancer.[26] In addition, studies that evaluated BMI five years prior to diagnosis, increased BMI has been found to be an independent prognostic factor in ovarian cancer.[27,28] A correlation has also been found with a BMI of greater than 25 and both decreased disease-free survival and overall survival time,[29] although again, other studies have found no correlation found between BMI and survival, adding to the inconsistency of reported data.[30,31]

Despite conflicting evidence, most studies suggest a correlation between ovarian cancer and obesity. With an increasingly obese population, this could be a significant problem. Taking into account the theories for the different developmental origins of ovarian cancer and the impact of obesity on these factors, new paradigms are evolving on how obesity could be a major contributing factor. Figure 2 depicts some of the numerous pathways that can be implicated in the association between obesity and cancer development, including inflammation, increased energy supply, aberrant insulin signaling, and changes in adipokine production.

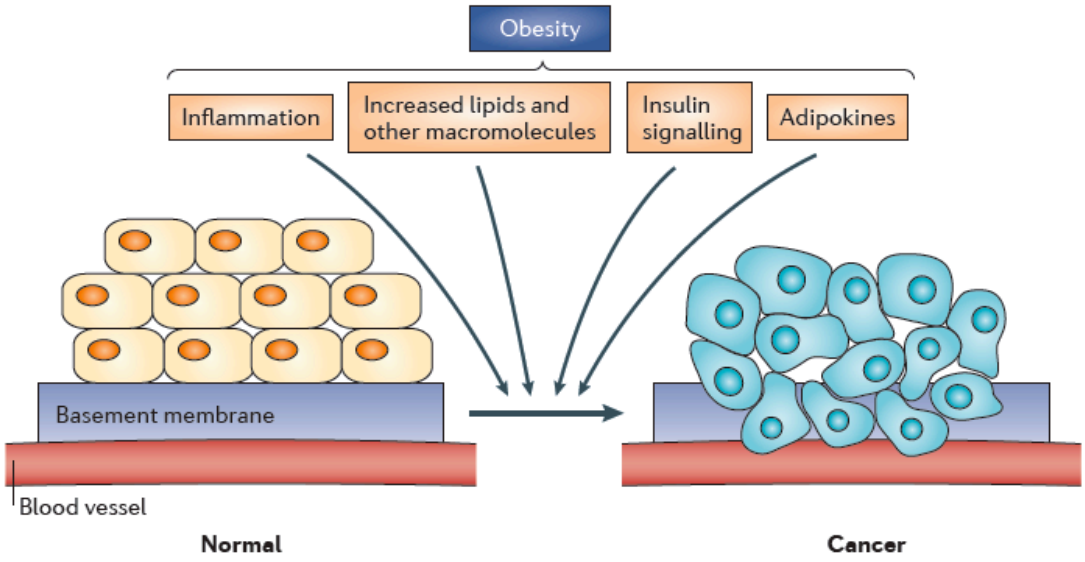

Figure 2.2. Pathways that may link obesity and cancer. **Reproduced from Nature Reviews Cancer, December 2011, Vol 11, No. 12, Pages 886-895 with permission from Nature Publishing Group.

Obesity is characterized by chronic low-grade inflammation, which can have profound effects on cancer progression. During states of excess energy, there is rapid expansion of adipose tissue. As the tissue expands, the blood vessels present are no longer able to supply oxygen to all cells, resulting in areas of local hypoxia.[33,34] This can lead to adipocyte death and consequently an influx of $CD8^+$ T cells followed by infiltration of macrophages which form crown-like structures around necrotic adipocytes.[35] The influx and activation of immune cells leads to an increase in production of inflammatory mediators such as ICAM1, MMP2, MCP3, VEGF, HIF1α, NFkB, IL1, IL6, MIF, IL-18, TNFα, TGFβ, MIP1α, SAA, PAI, and RANTES which are produced locally by adipocytes, immune cells or in many cases, both.[33,34,36-38] When prolonged, this inflammatory state can lead to low-grade systemic inflammation. This can then impact other biological processes, for example, by increasing insulin resistance and oxidative

damage, creating a protumorigenic environment.[39-43] Chronic inflammation has been associated with an increased risk for numerous cancers including colon,[44] gastric,[45] lung,[46] and potentially ovarian[47] cancer, while decreased risk has been reported with increased intake of NSAIDs.[48,49] With the recurring inflammation due to ovulation that may already instigate ovarian cancer, the low-grade inflammation associated with obesity may further promote ovarian cancer development.

Obesity is also associated with changes in both production and sensitivity to leptin. The synthesis of leptin in adipocytes is influenced by numerous humoral or paracrine factors, most notably insulin,[50] cortisol,[51] tumor necrosis factor-alpha (TNF-α),[52] and glucocorticoids[53]. Importantly, leptin production by adipocytes is increased with food intake and obesity in order to regulate appetite and satiety.[54,55] Obesity is also associated with leptin insensitivity, which results in further increased serum levels.[56] Leptin can contribute to cancer development by various mechanisms. In addition to appetite regulation, leptin targets vascular endothelium and induces neoangiogenesis and vascular remodeling as well as enhancement of endothelial cell proliferation.[57,58] Leptin has also been shown to act as a mitogen, transforming factor, or migration factor for many different cell types, including smooth muscle cells,[59] colon cells,[60] and mammary epithelial cells.[61] With increased circulating leptin levels, this could augment the ability of tumors to grow, form blood vessels, and metastasize.

Adiposity also influences the synthesis and bioavailability of numerous hormones. Obesity is associated with increased serum estrogens, which have been linked to malignancies such as breast and endometrial cancer, potentially due to overstimulation of proliferation and mutagenesis.[62-66] Androgenicity, as determined by free testosterone, is

increased with greater waist-to-hip ratio[67] and has been linked to ovarian cancer. Indeed, 90% of ovarian cancers express androgen receptors[68] and androgen production increases in carcinomas, while decreasing with chemotherapy.[69] Augmented androgen production is also one of the main characterizations for polycystic ovary syndrome[70] which has a suggested association with increased risk for ovarian cancer.[19] In addition, free insulin-like growth factor (IGF) is often increased with obesity and a strong direct relationship has been found between circulating IGF-1 levels and risk of developing ovarian cancer before age 55.[71]

Thus there are numerous factors that may contribute to a correlation between obesity and ovarian cancer risk and it is probable that each of these factors further influence each other. However, a potential cellular component should not be overlooked. The tumor milieu is composed of not only cancer cells, but also various supporting cells such as progenitors, leukocytes, fibroblasts, and endothelial cells. Cells that can be induced to become tumor-associated can have a significant impact on disease outcome and should thus be further investigated as targets of cancer development and treatment research. With an increasingly obese population and adipose tissue harboring various cell types susceptible to mobilization and utilization, it is critical that adipose tissue-derived cells are investigated for cancer promoting potential.

White Adipose Tissue

White adipose tissue (WAT) was once thought to be a passive reservoir for the storage of excess energy and is now becoming increasingly recognized for its other roles in immune and endocrine function, thermoregulation, and tissue repair. The origin and development of adipocytes and adipose tissue is not completely understood, but is the

focus of intense research as its complexity and role in other biological processes are becoming more apparent.

Adipose tissue development begins during gestation in higher mammals[72] and shortly after birth in rodents.[73] Dense regions of multipotent mesenchymal stem cells (MSCs) associated with vascular structures form at sites where adipose tissue will develop. Within these regions, MSCs undergo conversion into adipoblasts that eventually become lineage-committed preadipocytes. Following stimulation, preadipocytes undergo differentiation into mature, lipid-filled, insulin-sensitive adipocytes.[73] Throughout life, adipose tissue can expand and shrink in response to fluctuations in energy balance. Expansion occurs via hypertrophy of existing fat cells due to accumulation of triglycerides and/or hyperplasia, which involves the differentiation of preadipocytes to mature adipocytes.[74,75]

There are two main subtypes of WAT: visceral and subcutaneous. While subcutaneous fat is found underneath the skin, visceral fat surrounds the organs in the abdominal cavity and has a greater association with increased risk for many chronic diseases. Figure 3c shows the localization of various fat pads. It should be noted that there is some indiscriminate use of the term 'visceral' fat. While some authors include all intra-abdominal fat depots in this description, others use 'visceral' only to apply to fat depots that are drained by the hepatic portal vein, namely omental and mesenteric fat pads, and excluding others such as the perigonadal, retroperitoneal, and perirenal fat pads that are all intra-abdominal but are drained by the vena cava.[76]

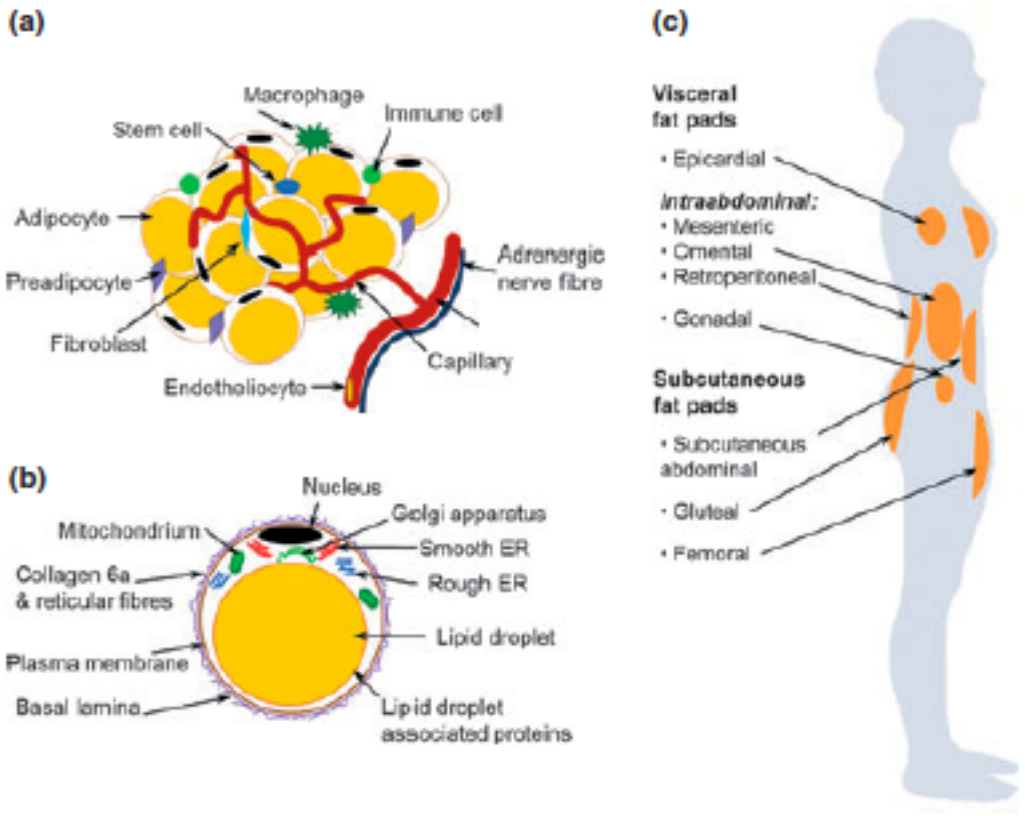

Figure 2.3. WAT structure and distribution in the human body. (A) Cell types present in WAT. (B) Structure of an adipocyte. (C) Localization of major fat pads in the human body. **Reproduced from Acta Physiologica, January 2012, Issue 2, Pages 194-208 with permission from John Wiley & Sons, Inc.

The *portal theory* suggests that exaggerated hepatic delivery of free fatty acids and proinflammatory cytokines originating from increased visceral adipose tissue mass drained by the hepatic portal vein in obese individuals, is responsible for insulin resistance and metabolic deterioration.[77] In support of this, Rytka et al[78] transplanted epididymal fat pads between mouse littermates, into either the parietal peritoneum, which is drained by the vena cava, or into the mesentery which is drained by the hepatic portal vein and found that only the mice receiving transplanted fat into portal vein-drained regions developed insulin resistance. That being said, those with greater abdominal fat, as measured by an increased waist-to-hip ratio or waist circumference, also known as

having the android 'apple-shaped' body are more at risk for disease than those with a gynoid or 'pear-shaped' body (which carry more weight in their lower body).[79,80] Indeed, in some studies where BMI, as an indicator of overall body fat, was not associated with ovarian cancer, increased waist-to-hip ratio was positively correlated with an increased risk.[81,82] Thus, while BMI is commonly used to determine obesity, often waist-to-hip ratio is a better prognostic indicator since it is more specific for where the excess adipose tissue is localized.

In addition to drainage, the various fat depots also differ with respect to tissue dynamics (tendency to respond to excess calories with a hypertrophic versus a hyperplastic response), adipokine release, hormonal responses, vascularization, innervation, and abundance of non-adipocyte cells, which all impact the specific function of each individual fat depot. Importantly, adipose tissue is composed of not only adipocytes (as shown in figure 3a), but also encompasses many different cell types residing within the stroma, collectively referred to as the stromal vasculature fraction (SVF). Cells of the SVF include but are not limited to endothelial cells, leukocytes, fibroblasts, pericytes, hematopoietic stem cells (HSCs), and mesenchymal stem cells (MSCs).[83,84] The cellular composition of the SVF can vary significantly between adipose tissue depots as well as between individuals due to factors such as age, obesity, and disease status. For example, in obese individuals, macrophages can represent up to 40% of the cells in WAT, while they comprise under 10% in lean individuals.[85] Fat depots can also differ in cellular composition in the homeostatic state. For example, omental fat contains opaque patches composed of a diverse set of leukocytes, which are referred to as 'milky spots'.[86] These milky spots are not found in other fat depots and so omental fat

exclusively, is considered a secondary, peripheral lymphoid organ.[86,87] Hence the cellular composition of the SVF is extremely important to WAT function and can influence many other factors such as vascularization, tissue remodeling and cytokine secretion.

Adipocytes have a unique cytokine expression profile including adipokines (cytokines produced almost exclusively by adipocytes) such as leptin, adiponectin, resistin, and visfatin, as well as other cytokines including TNFα, VEGF, PAI-1, IL-6, IL-1 and MCP-1.[88,89] However, adipocytes from different fat depots also have distinct secretory profiles. For example, visceral adipose tissue produces more inflammatory cytokines such as IL-6, VEGF, PAI-1, angiotensin, and MCP-1 and less adipokines such as leptin and adiponectin than subcutaneous adipocytes.[88-93] The difference in cytokine expression between fat depots may be a contributing factor as to why increased adiposity in specific regions may be more associated with disease status than others.

Fat depots also differ in storage capacity and mechanisms of expansion. Subcutaneous adipocytes have a greater ability to expand with obesity,[90] while visceral adipocytes are less responsive to the anti-lipolytic affects of insulin and display higher rates of lipolysis and release of fatty acid into circulation.[94,95,96] Visceral fat also has elevated LDL and triglyceride storage and increased insulin-stimulated glucose uptake as compared to subcutaneous fat.[96,97] Hence, visceral fat is suggested to be more dynamic and metabolically responsive to changes in energy balance. However, it should be noted that most studies compare one specific "visceral" fat pad to one subcutaneous fat pad, which may not adequately reflect the profile of all fat depots within each subtype. As noted above, differences are evident between varying locations of visceral or subcutaneous fat, including with respect to lipid storage. For example, Tchoukalova et

al.[98] found that overfeeding of normal-weight adults, led to a gain of only about 1.6 kg of lower-body subcutaneous fat resulting in an increase of approximately 2.6 billion new adipocytes within eight weeks. Interestingly, in the same individuals, no significant increase in adipocyte number in abdominal subcutaneous fat was noted, but rather a significant increase in adipocyte size. In addition, there is also individual variation in sites of lipid storage, as evidenced by the diversity of human body types. The fact that some people gain more weight than others with similar dietary habits and the phenomenon of individual tendencies to store excess energy in different fat depots provides evidence that adipose tissue development and reorganization is an extremely complex process.

Even preadipocytes are unique among different fat depots. Preadipocytes in abdominal subcutaneous fat are distinct from those in mesenteric or omental fat, with respect to proliferative potential, replicative subtype abundance, capacity for adipogenesis, susceptibility to apoptosis, and gene expression profiles. Cloned subcutaneous preadipocytes differentiate more rapidly than cloned omental preadipocytes and a higher percentage of subcutaneous cells are capable of differentiation.[99] Pluripotency of adipocyte precursors is also highest in subcutaneous fat, followed by mesenteric fat and lastly, omental fat.[100] This suggests that while mesenteric and omental fat are both visceral fat depots, mesenteric preadipocytes may be more similar to subcutaneous than omental preadipocytes.[101] With numerous fat pads and only a few characteristics examined, a more extensive comparison of cells, including preadipocytes, in each depot is needed.

To add another layer of complexity, even mature adipocytes have been shown to de-differentiate and participate in cancer progression. These de-differentiated adipocytes display multilineage potential towards adipocyte, chondrocyte, and osteoblast lineages, which is similar to typical mesenchymal stem cell potential.[102] Little is known about the mechanism for this, although TNFα and IL-11 have been shown to inhibit differentiation and induce de-differentiation.[103,104] Mature adipocytes can also increase invasive potential of human and murine cancer cells both *in vitro* and *in vivo*.[105] Adipocytes likewise have an altered phenotype when cultured with cancer cells.[105] These cancer-associated adipocytes are pushed towards de-differentiation characterized by a loss of lipids, decreased adipocyte markers including PPARγ and C/EBPα, and an overexpression of proteases such as MMP-11 and pro-inflammatory cytokines IL-1 and IL-6.[103,105] Indeed, adipocytes interacting with cancer cells at the invasive front become smaller and increase expression of MMP-11, both effects of which are not seen in more distal adipocytes.[106] Decreased mature adipocytes, increased altered adipocytes, and an increased population of peritumoral fibroblasts, (which are unique from other tumoral myofibroblasts in their expression of MMP-11 and lack of αSMA), have been found in tumors such as human breast carcinomas, suggesting a relationship between adipocyte and tumor-associated fibroblast populations.[105] Interestingly, peritumoral fibroblasts are suggested to be derived from de-differentiated adipocytes.[107] It has not yet been determined if adipocytes from all fat depots are equally susceptible to this process, but the ability of cancer cells to modulate the behavior of adipocytes to promote cancer development further increases the cancer-promoting potential of adipose tissue and the possible contribution of obesity.

Given the morphologic and functional differences between the various fat pads, it has been suggested that while each depot is composed of similar cells, they may represent distinct endocrine organs. Each depot and the cells within it could contribute to biological processes in different ways and some depots may be more associated with pathologic events than others. Since numerous factors including adipokine and cytokine production, increasing metabolic disorders such as diabetes and insulin resistance, changes in hormone production, or turnover and mobilization of progenitors may be involved in cancer progression, it is important to think of these processes as a complex interactive system where each facet may affect others. Their modulation in turn may differentially affect other parts of the system or the instigating cells, adding reciprocal or multi-directional events in a time-dependent manner. Thus while the focus of this review is on non-adipocyte cells localized to adipose tissue, it is critical to keep in mind the functions of adipose tissue as a whole, including the interplay between fat depots and how this can affect homeostasis of the entire body.

White Adipose Tissue Stromal Vascular Cells and Ovarian Cancer

Collectively, the functions of WAT SVF cells range from clearance of dead cells and generation of new adipocytes to production of cytokines and formation of new blood vessels. Importantly, these cells can impact not only the local adipose tissue environment, but can also have systemic effects, including a role in tumor formation. Zhang et al.[109] found that $CD13^{-}CD45^{-}CD29^{+}$ SVF cells isolated from the WAT of GFP mice (which constitutively express green fluorescent protein (GFP) in all cells), homed to tumors when injected either intravenously or subcutaneously. Even more representative of actual recruitment from tissue, when SVF cells were consistently administered in low

doses over six weeks in mice with Kaposi sarcoma or prostate cancer xenografts, SVF cells significantly increased tumor burden as compared to mice injected with control cells.[109] Further, SVF cells could be recruited directly from fat pads. Following gonadal fat pad transfer from GFP mice into nude mice, cancer cells were grafted 2cm away from the fat pad. Numerous GFP^+ cells were found in the tumors and tumor growth rate was significantly increased in mice with fat pad transplants. Immunofluorescence analysis revealed that the GFP^+ cells within the tumors were localized mainly in the stromal or perivascular regions and occasionally within the vasculature, with about 5-10% of cells expressing CD31, suggesting some endothelial cell differentiation.[109] Importantly, this was the first study to demonstrate that WAT SVF cells can not only home to tumors, but are also able to provide a growth advantage. It also provided evidence that this process is indeed biologically relevant as cells can be recruited directly from WAT. However, numerous other questions remain unresolved such as: Which population of SVF cells is contributing to cancer growth or are many different cell types responsible? Are cells more frequently mobilized from BM or WAT? What determines where cells are recruited from? How would recruitment be affected in immunocompetent mice? How would obesity influence these dynamics? Is there a direct association between fat pad size, number of recruited cells, and tumor burden? Would the inflammatory environment associated with obesity inhibit or enhance cell mobilization and tumorigenesis? Would individuals with more visceral versus subcutaneous fat have more SVF contribution to cancer progression? Can we manipulate any of these processes to affect cancer outcome? These questions highlight that this area of research is still in its infancy.

One of the first steps towards an understanding of SVF cells and their interactions with cancer cells is to characterize the composition of the WAT SVF and determine the differentiation potential of each cell type. WAT SVF comprises many stem and progenitor cell populations with multipotent potential (as shown in figure 4), which are similar to those of the BM, but with unique characteristics. Martin-Padura et al.[110] reported that human WAT is indeed a rich reservoir of $CD34^+$ progenitor cells. Compared to BM-derived $CD34^+$ cells mobilized in blood, these purified human WAT-derived $CD34^+$ cells expressed similar levels of stemness-related genes (SOX2, Nanog, LIF, WNT3A), but significantly increased levels of angiogenesis-related genes (VEGFR1 and 2, VE-Cadherin, VCAM1, etc.) and increased FAP-α, a suppressor of anti-tumor immunity. In vivo, the co-injection of human WAT-$CD34^+$ cells with MDA-MB-436 breast cancer cells enhanced xenograft vascularization and significantly increased tumor growth and the number of metastases in NOD/SCID mice. As these progenitors were capable of generating mature endothelial cells and endothelial tube-like structures, it is probable that endothelial differentiation contributed to tumor vascularization.[110] However, the exact nature of these cells is unknown as CD34 is a common hematopoietic primitive cell marker found on multiple cell types including the poorly defined WAT resident stem cells, endothelial progenitors, a subset of MSCs, and hematopoietic stem cells (HSCs).[111-113]

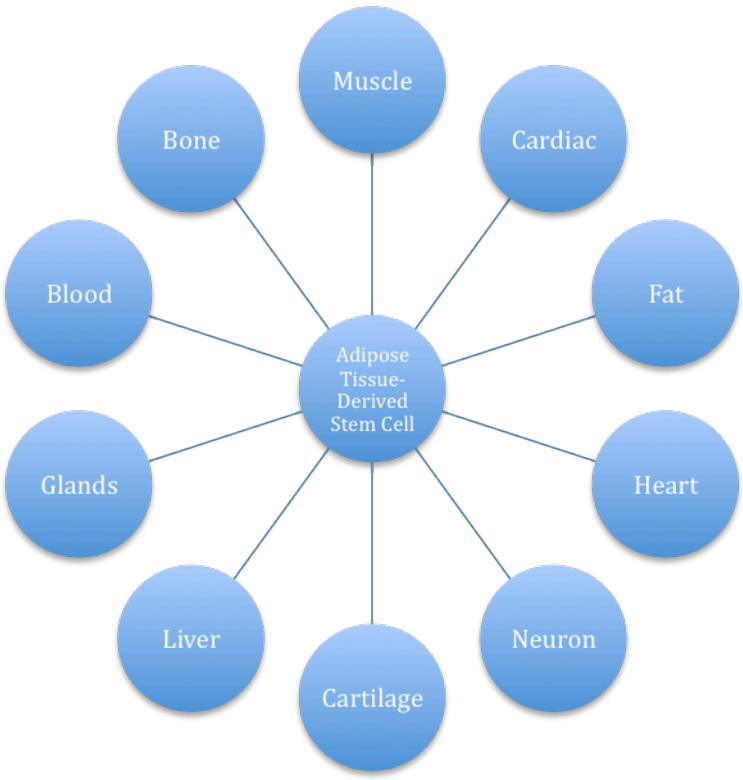

Figure 2.4. Differentiation potential of WAT-derived stem cells.

Hematopoietic Stem Cells

HSCs reside primarily in the BM and give rise to cells of myeloid (monocytes, neutrophils, basophils, erythrocytes, platelets, etc) and lymphoid (B cells, T cells, NK cells) lineages.[114] Recent studies suggest that HSCs may also be precursors for a subset of BM-derived adipocytes. HSCs originate from the bone marrow and indeed, the population of hematopoietic progenitor cells (HPC) is about 14-fold less in WAT SVF compared to BM. However, these WAT-HSCs are still capable of forming hematopoietic colonies including erythroid, granulocyte, macrophage, and megakaryote colonies and are able to home to the BM of irradiated recipients and provide long-term reconstitution of hematopoiesis.[115] Majka et al.[116] additionally found that not only were HSCs present in WAT, but demonstrated for the first time that they were able to differentiate into adipocytes. Using mice in which LacZ expression was restricted to hematopoietic cells

of myeloid lineage, they detected a significant number of adipocytes expressing LacZ, confirming that cells of a myeloid origin can and do differentiate into adipocytes *in vivo*. Interestingly, they also found that BM-derived adipocytes showed a preferential accumulation in visceral depots including gonadal and perirenal as opposed to subcutaneous and intrascapular fat pads. There was also a larger frequency of BM-derived adipocytes in females versus males and an increase in frequency with age.[116]

BM-derived adipocytes and adipocytes derived from WAT residents differ in their secreted cytokine profile. For example, BM-derived adipocytes have a decreased secretion of leptin and increased production of IL-6 and the chemokines CXCL12, CXCL9, and CXC3CL1.[116] It is interesting to note that BM-derived adipocytes preferentially accumulate in visceral fat, which is recognized for lower leptin production,[90] higher numbers of macrophages,[117] and greater inflammatory cytokine production[88,117] than subcutaneous fat. Thus, this accumulation of BM-derived adipocytes may contribute to the differential expression of hormones and cytokines from visceral versus subcutaneous WAT. Together, these studies suggest a link between BM-derived adipocyte accumulation with an enhanced state of inflammation and further recruitment of immune and progenitor cells.

HSCs from WAT can also differentiate and participate in carcinogenesis as tumor-associated leukocytes including macrophages[118] or dendritic cells,[119] which can be polarized by cancer cells to suppress cytotoxic immune responses against cancer cells while increasing production of pro-inflammatory cytokines. While these cells are not discussed in this review, they are also important contributors to cancer development.

Mesenchymal Stem Cells

MSCs may also participate in cancer progression and have been much more widely studied than HSCs in regards to both adipose tissue and cancer. MSCs can give rise to adipocyte, chondrocyte, endothelial, epithelial, hematopoietic support, hepatocyte, neuronal, myogenic, and osteoblast lineages[120-126] and have been isolated from many different tissues including BM, peripheral blood, cord blood, cord Wharton's jelly, adipose tissue, amniotic fluid, compact bone, periosteum, synovial membrane, synovial fluid, articular cartilage and fetal tissue.[127] MSCs have also been implicated in cancer progression and thus are an obvious cellular target when trying to link WAT SVF cells and ovarian cancer. MSCs have efficient homing capabilities potentially via migration towards chemotactic stimuli. Expression of chemokine receptors CCR1, CCR2, CCR3, CCR4, CCR7, CCR9, CXCR4, and CXCR5 are upregulated on the surface of MSCs in response to inflammatory signals,[128] which are produced by injured tissue, adipose tissue in obese individuals, and tumors. This may explain how MSCs are able to migrate to areas of injury as well as tumor tissue.[129] Indeed, tumors are often considered a 'wound that never heals' since cancer cells express many of the same hypoxia and inflammatory factors that are evident in wounds and they have a similar influx of leukocytes and stromal cells.[129]

Due to their effective homing abilities, the use of MSCs and other progenitors as anti-tumoral, targeted drug delivery vehicles are actively being investigated.[130,131] Komarova et al.[132] found that intraperitoneal (ip)-injected MSCs preferentially homed to SKOV3 human ovarian xenografts in immunodeficient mice and that this property could be exploited by loading the MSCs with genetically modified oncolytic viruses. Tumor burden was significantly decreased in mice injected with loaded MSCs, as compared to

uninfected MSCs and even as compared to mice ip-injected with the virion not attached to a carrier, demonstrating that the homing mechanism is specific to tumors. Furthermore, the oncolytic adenovirus-loaded MSC treatment also increased survival, proving to be an effective technique.[132] However, while this confirms that MSCs can efficiently target ovarian cancer xenografts, these studies provide very little information on the origin of MSCs. Interestingly, in a model of hindlimb ischemia, non-BM-derived cells accounted for approximately 60% of circulating progenitors and 74% of the cells that incorporated into the ischemic hindlimb, which suggests that tissue sources besides BM may be important for the recruitment of progenitor cells during injury and cancer.[133] Still, the extent to which cells are recruited from WAT is unknown along with the mechanism for mobilization of MSCs, the frequency of this process, and the impact of different pathological states such as obesity. Unfortunately, most of the information we have on the activity of WAT-derived stem and progenitor cells in cancer are from co-injection studies, which overlooks the recruitment process.

As mentioned previously, it has been suggested that BM-derived cells can be recruited to WAT where they can differentiate into adipocytes. Crossno et al.[134] transplanted GFP-labeled BM into wild-type recipient mice and detected GFP^+ adipocytes, again demonstrating that there are BM-derived preadipocytes. Further, they found that the number of BM-derived adipocytes in both omental and dorsal fat was increased in mice given a high fat diet. These BM-derived cells expressed factors associated with terminal adipocyte differentiation including C/EBPa, PPARy, adiponectin, leptin, perilipin, and fatty acid binding protein. There was also a significantly increased number of $GFP^+CD45^-Sca1^+$ cells, indicative of MSCs, in the

peripheral blood and a significantly decreased number in the omental fat of mice on a high fat diet.[134] The decrease of these cells in WAT could be explained by an efflux of MSCs from the tissue or by the loss of Sca1 as the cells differentiate into mature adipocytes. The latter would indicate that MSCs can be mobilized not only due to injury or cancer, but also as needed for expansion of adipose tissue or conversely, as a result of increased WAT and inflammation. Again, there is almost no information on how these cells are actually recruited and what facilitates this process. For example, does an increase in energy balance result in an initial increase in adipocyte hypertophy or hyperplasia? Does the recruitment of immune cells precede the recruitment of HSCs, MSCs or other progenitors? At what point are progenitors recruited from outside the WAT?

Understanding how MSCs may function within the tumor microenvironment and how they may effect cancer progression is critical to determining effective treatment strategies. Most studies show that MSC incorporation into tumors increases tumor burden and metastatic potential.[109,135,136] While there are different functions MSCs may perform, the most commonly reported roles are as differentiated tumor-associated fibroblasts (TAF), endothelial cells, or pericytes, which can have a profound impact on cancer development, as shown in figure 5. Spaeth et al.[137] induced a TAF phenotype by culturing MSCs in SKOV3-conditioned medium and found that when MSCs were administered with SKOV3 cells, those tumors were significantly larger with a more enhanced stromal contribution than controls. There was also increased expression of stromal proteins associated with an aggressive or invasive phenotype, including Tenascin C, Thrombospondin 1, and MMP-11, which are secreted by fibroblast-like cells. Also,

the expression of pericyte/myofibroblast markers including α-smooth muscle actin (αSMA) and desmin were elevated, which was not seen when cancer cells were injected without MSCs.[137] Bexell et al.[138] observed that grafted MSCs migrate to glioma endothelium and expressed αSMA, neuron-glia 2, and platelet derived growth factor receptor β (PDGFRβ), but did not express endothelial markers or impact tumor microvessel density. In contrast, Suzuki et al.[136] found that co-injection of MSCs with B16-LacZ melanoma cells resulted in a significant increase in tumor volume as compared to melanoma cells injected alone and resulted in more blood vessels and a larger vessel area. The MSCs were associated with tumor vessels and some were $CD31^+$ but did not express αSMA, suggesting endothelial differentiation.[136] This variation in reported differentiation of MSCs in tumors suggests that distinct tumor microenvironments influence MSC differentiation either directly by paracrine factors or indirectly by influence from other cells present in the tumor milieu. An additional source of variability among studies could be reflected in the different immunophenotyping of MSCs. There is not a clear combination of surface markers to define MSCs and most markers used are also present on various other cell types. Subgroups of these populations may be more predisposed to differentiate towards a particular cell type, so using a poorly defined cell

population could produce widely varied results.

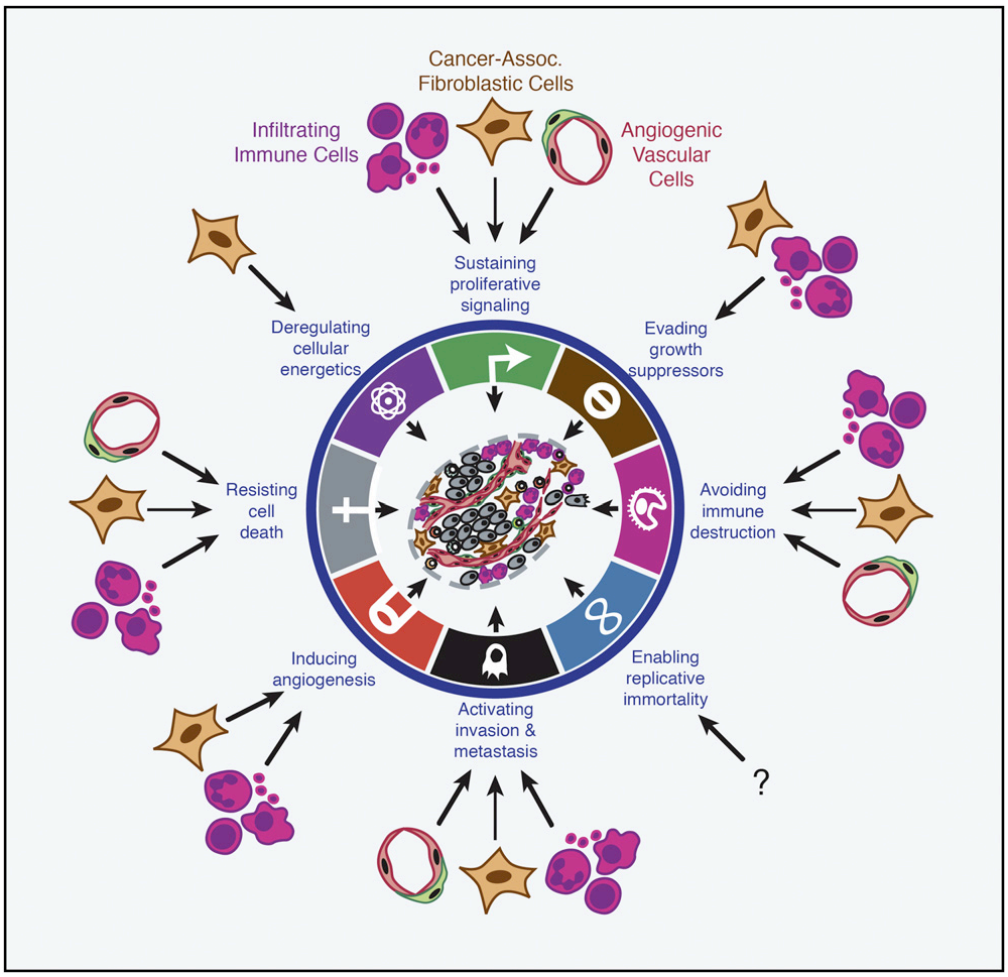

Figure 2.5. Multifactoral contributions of activated/recruited stromal cells to the hallmarks of cancer. Cancer-associated fibroblasts/myofibroblasts and angiogenic vascular cells such as endothelial cells and percytes can be critical players in cancer progression. **Reproduced from Cancer Cell, March 2012, Vol 21, No. 3, Pages 309-322 with permission from Elsevier Publishing.

MSCs can enhance tumor development by other mechanisms including by promotion of vascularization. Human MSCs and adipose progenitors produce VEGF, which is further subject to upregulation in response to proinflammatory mediators such as TNFα.[140] VEGF directly affects vasculogenesis by stimulating target cells with VEGF receptors. Endothelial cells grown in conditioned medium from WAT-derived MSCs increased cell growth and decreased apoptosis, both effects of which were enhanced by

hypoxic WAT-derived MSC conditioned medium. As previously discussed, hypoxia is also characteristic of an obese environment.[141] When cultured $CD31^-$ (an endothelial cell marker) human WAT SVF cells were injected into the hindlimbs of mice after 15 days of hindlimb ischemia, there was a significantly improved angiographic score and blood flow accompanied by numerous human $CD31^+$ cells lining regenerated blood vessel walls.[125] This indicated that human SVF progenitors can differentiate into $CD31^+$ endothelial cells and contribute to vascular regeneration. Angiogenesis and increased vascularization of tumors is essential to tumor development as it provides a nutrient and oxygen supply as well as a means of metabolite disposal, without which, the cancer cells would eventually die. Hence, recruitment of MSCs or other endothelial progenitor cells to aid in new blood vessel formation is essential for tumor growth and metastasis.

WAT-derived stem cells can also contribute to angiogenesis by serving as vasculature-supporting cells. Omental stem cells were found to home to endometrial tumors and significantly increase tumor growth, even as compared to stem cells isolated from subcutaneous fat, which did not increase tumor growth.[142] While these cells did not express $CD31^+$ after tumor incorporation, the WAT stem cells were associated with the $CD31^+$ endothelium. These omental-derived stem cells also increased endometrial cancer cell proliferation, tumor vascularization and significantly decreased necrosis at the tumor centers (9-22% necrosis in tumors from mice that were injected with omental stem cells versus 48% in PBS injected controls).[142] Thus WAT-derived stromal cells, especially from visceral fat, can be recruited to tumors and increase vascularization by serving as endothelial or endothelial support cells, enhancing the viability of cancer cells.

MSCs can also aid in the establishment of an immunosuppressive microenvironment that may be important for immune evasion. WAT-derived MSCs have immunomodulatory properties demonstrated by suppression of mixed lymphocyte reactions, inhibition of lymphocyte proliferation in response to mitogens, and an inability to induce a response from allogenic lymphocytes.[143] Indeed, both human and mouse WAT-derived MSCs have been shown to control graft-versus-host disease, which occurs when the immune system of the host rejects transplanted tissue from a donor.[144,145] When recruited to tumors, this immunomodulation ability could allow the tumor cells to escape immune surveillance and evade clearance. This is supported by the observation that when B16 melanoma cells or MSCs alone were implanted into C3H mice, no tumors formed. However, when the melanoma cells were implanted into C3H mice together with MSCs, tumors rapidly developed with a tumor incidence of 57% at day 30.[146] As B16 cells rapidly form tumors in syngeneic C57BL/6 mice but elicit an immune response in C3H mice and do not form tumors, this suggests that growth was allowed in C3H mice with co-injected MSCs due to downregulation of an immune response. Thus MSCs that are recruited to ovarian tumors may provide a survival and growth advantage via immunosuppression.

In addition to incorporation into tumors, changes in MSC and other cell populations in the peritoneal serous fluid may be critical to ovarian cancer development. Ovarian cancer is largely restricted to the peritoneal cavity where advanced stages are commonly associated with ascites accumulation. The cell and molecular composition of the ascites plays an important role in cancer progression as the cells present are the most likely to be incorporated into tumors. Various small molecules including inflammatory

mediators, bioactive lipids, proteolytic enzymes, shed plasma membrane particles, growth factors and extracellular matrix components, as well as many different cell types such as leukocytes, stem and progenitor cells, and other stromal cells can be found at varying levels in the cancerous ascites.[14] Indeed, McLean et al.[147] demonstrated that cells with MSC markers ($CD44^{+}CD73^{+}CD90^{+}$) made up approximately 6% of the cell population in human ovarian cancer ascites. These cells could potentially associate with ovarian cancer cells and incorporate into multicellular spheroids, enhancing invasion and metastatic potential of the cancer cells. As MSCs can be identified in greater than 90% of human ovarian carcinomas,[147] this suggests that an MSC-ovarian tumor interaction is important to cancer development. Thus, an increase in available MSCs, such as during obesity, could directly contribute to disease progression.

The source of MSCs also appears to be important for cancer promotion. In a study on ovarian cancer, while BM-derived MSCs did not significantly increase tumor growth when co-injected with SKOV3 cells, WAT-derived MSCs led to a significant expansion of the cancer cells,[147] suggesting that WAT-MSCs are functionally distinct from BM-MSCs and may be predisposed to cancer promotion. With the close proximity of multiple fat depots to the ovaries, WAT-MSCs may be more likely to be recruited.

Endothelial and Endothelial Progenitor Cells

Endothelial cells are also actively involved in cancer progression. Circulating endothelial cells (CEC) and endothelial progenitor cells (EPC) are increased in the peripheral blood of patients with various malignancies including breast, prostate, gastric, colonic, renal, cervical and ovarian cancer.[148-151] In breast cancer and lymphoma patients, both resting and activated CECs were increased five-fold in cancer patients versus controls and were significantly correlated with plasma VCAM-1 and VEGF levels.

In lymphoma patients in complete remission and breast cancer patients following a quadrantectomy, the number of CECs present dropped to control levels, suggesting that high CEC levels may be an indicator of poor prognosis.[151] While CECs are associated with cancer progression, the origin of these increased CEC and EPC populations are controversial. Whether endothelial cells are recruited from tissues by tumors or if they originate from the tumor vasculature and are detached from the endothelium due to vascular dysfunction is unknown. While an increase in CECs has been associated with perturbation of the endothelium,[152] ECs and/or EPCs also incorporate into tumor endothelium, increase vascularization in tumors, and ultimately enhance tumor growth.[153] Thus further studies are needed to determine what factors facilitate increased CECs.

Regardless, endothelial cells are critical to cancer growth and indeed tumor-associated endothelial cells can originate from WAT. A study by Kidd et al.[154] found that five weeks after injection of ID8 ovarian tumor cells, 91+/- 6% of the $CD31^+$ endothelial cells present in the tumors were of non-BM origin. To determine if WAT was a potential source of these non-BM-derived cells, they next transplanted GFP^+ WAT and later injected E0771 breast cancer cells adjacent to the fat pad. After two weeks, numerous GFP^+ cells were found in the proximal tumor tissue, with 18% of those cells positive for CD31, suggesting that tumors in close proximity to WAT could use the tissue as a significant source of recruitable endothelial cells (or progenitors that can differentiate towards an endothelial lineage).[154]

The effect of obesity on these pro-angiogenic cells is not well defined. The ability of BM progenitors, including EPCs, to respond to mobilization stimuli seems to decline with age,[155] but may increase with obesity. Bellows et al.[156] found that there was

a five-fold increase in $CD34^+$ circulating progenitor cells, including hematopoietic and endothelial precursors, with a BMI of greater than 30, as compared to those with a BMI of less than 30. Conversely, other studies report that there are decreased numbers of circulating EPCs with obesity and that EPC migration and colony formation is inhibited with obesity and elevated leptin levels.[157,158] This may be transient and the increase in CECs and EPCs at earlier stages in obesity may reflect recruitment to the adipose tissue, where they are maintained, resulting in subsequent decrease in circulating levels. In support of the latter, one study reported that the overweight group, although statistically insignificant, had increased numbers of CECs, while the obese group displayed decreased numbers.[158] This may be an indicator of progressive effects on cell population changes with obesity and should be investigated as a time-course experiment with diet-induced obesity.

Increased adiposity is also associated with EPC dysfunction characterized by diminished capacity to release angiogenic cytokines, increased apoptotic susceptibility, and reduced cell migration.[159] It is unclear how potential cellular dysfunction due to obesity would affect the association and interaction of CECs or EPCs with cancer cells.

Fibrocytes and Myofibroblasts

Other cell types influenced by adiposity include fibrocytes and myofibroblasts, which are involved in wound healing, tissue remodeling, and cancer progression. While fibroblasts are tissue-resident cells, fibrocytes are BM-derived cells that can be recruited from the peripheral blood in response to injury, whereupon they can differentiate into fibroblast or myofibroblast-like cells to participate in wound repair[160]. Fibrocytes are unique $CD45^+$ (a pan-leukocyte marker) cells, which also express primitive cell marker CD34.[161] They are similar to monocytes in their expression of CD11b and antigen

presenting capabilities and are similar to fibroblasts in their expression of collagen I.[161] Interestingly, $CXCR4^{+}Col1^{+}CD45RO^{+}CD14^{-}CD68^{-}$ fibrocytes isolated from circulation are also capable of adipogenic differentiation *in vitro* and are able to form adipose tissue with associated neovascularization *in vivo*.[162] As fibrocytes express an array of chemokine receptors including CCR7, CXCR4, CCR5 and CCR3, the recruitment of fibrocytes is thought to be chemokine-mediated.[163] CCL2, CCL3, CCL5, CCL7, and CCL8, all of which can bind to chemokine receptors on fibrocytes, are upregulated in both subcutaneous and visceral fat in obese patients.[164] Thus with obesity, there may be increased traffic of fibrocytes to WAT to serve as pre-adipocytes.

While present in normal tissue in an immature state, fibrocytes display phenotypic differences in wounds and malignancies. In benign breast lesions and chronic pancreatitis, there is an influx of fibrocytes along with the appearance of myofibroblasts, which are not present in healthy tissue. Further, in invasive breast and pancreatic cancer, there is a complete loss of fibrocytes and an accumulation of αSMA+ myofibroblasts, suggesting that fibrocytes may be myofibroblast precursors.[165,166]

Myofibroblasts secrete a plethora of modulatory proteins that can influence cancer cells, including matrix metalloproteinases that remodel extracellular matrix in support of invasion and metastasis, growth factors to promote cancer cell proliferation, cytokines and chemokines for cell recruitment, as well as extracellular matrix proteins for adhesion and motility support.[167] $CD45^{+}CD34^{+}CD14^{-}$ fibrocytes can be induced to express myofibroblast αSMA and a substantial portion of the myofibroblasts isolated from wounds co-express fibrocyte markers CD45 and CD13, which are not expressed by fibroblasts, suggesting that myofibroblasts are likely derived from a common fibrocyte

precursor.[168] A study that transplanted BM from male to female mice, found Y chromosomes in a majority of myofibroblasts in wounded tissue, confirming fibrocyte and BM origin.[168] In addition, human cancer lines (including breast, pancreatic, colon, and hematologic) are capable of recruiting BM-derived vascular endothelial cells and myofibroblasts. Xenografts from cell lines that recruited a larger number of these cell types also had a greater proportion of stromal contribution,[169] which is important as tumors need stroma to grow beyond 1-2mm.[170] Stroma, consisting of vasculature, extracellular matrix, and supporting cells, provides mechanical support, a source of growth factors and cytokines, as well as the vascular supply for nutrients, gas exchange, and waste disposal. Indeed, in some common carcinomas, stroma can account for over 90% of the total tumor mass.[171]

WAT appears to be a significant source of tumor-associated fibroblasts/myofibroblasts. Breast tumors that were transplanted near fat pads, were infiltrated with WAT-derived stromal cells after just two weeks. Of the WAT-derived cells, 56% were positive for αSMA, indicating a myofibroblast.[154] In addition, 2% and 7% of the WAT-derived cells were positive for fibroblast activation protein and fibroblast specific protein respectively, which are markers of 'pathology-associated' fibroblasts or activated fibroblasts.[154] Another study that injected adipose-derived stem cells into the tail veins of mice, found that the stem cells were able to home to 4T1 breast cancer tumors and that association with the tumors increased myofibroblast differentiation.[172] The percentage of αSMA^+ WAT-derived cells increased by 15% when the WAT-derived cells were co-injected with 4T1 spheroid-forming cells, suggesting that tumor association pushes these cells towards myofibroblast differentiation.[172] In addition, incorporation of

these WAT-derived cells enhanced vascularity and capillary density as well as growth of breast tumors.[172]

Thus WAT is a rich reservoir of stem and progenitor cells that can be recruited to participate in cancer progression. Since early tumors may not have the means for increasing systemically circulating chemokine levels sufficient to recruit cells from BM, visceral WAT may serve as a more responsive reservoir to low levels of localized chemokines. In addition to being more proximal to the ovaries, the number of viable stem cells that can be retrieved from adipose tissue is much greater than from bone marrow. Between 0.5 x 10^6 and 20 x 10^6 stem cells can be retrieved from 100g of fat, while only approximately 0.006-0.06 x 10^6 stem cells can be isolated from 100ml of BM.[121,173,174] WAT also contains about 263-fold more CD45-CD34+ EPCs per ml in humans and about 179-fold more in mice than BM.[110] The number of EPCs and HPCs in the WAT SVF are also positively correlated with BMI and age in humans and a high fat diet further increases the number of EPCs and HPCs in the WAT of mice.[110,175] With increased numbers of progenitor cells in WAT with obesity, there is greater availability of cells for recruitment, which may positively impact tumor growth.

The close proximity of the ovaries to various fat depots may also be useful as a metastatic niche. Metastatic ovarian cancer is often found localized to the omentum and indeed the omentum is almost always removed during surgical debulking as a preventative measure against ovarian cancer relapse.[176] Currently, it is unknown whether ovarian cancer cells home to the omentum because it represents a highly conducive tumor microenvironment or are filtered by the omentum due to bulk flow of the peritoneal fluid. It is noteworthy that ovarian cancer metastasis to the omentum often results in solid

tumor formation virtually devoid of adipocytes.[177] Additionally, after ip-injection of ovarian cancer cells, a majority of the cells are found localized to the omentum within 20 minutes, suggesting an exceptionally advantageous environment for growth.[178] *In vitro*, omental adipocytes induce migration and significantly increase invasiveness of SKOV3 cells as compared to co-culture with subcutaneous adipocytes.[178] Adipocytes can also promote the growth of cancer cells by various mechanisms, including by serving as a lipid source of energy. Nieman et al.[178] found that omental adipocytes loaded with fluorescently-labeled fatty acids actually transferred lipids to ovarian cancer cells when co-cultured together, which was further characterized by lipolysis in adipocytes and beta-oxidation in cancer cells. There was also an upregulation of fatty acid binding protein 4 (FABP4) in omental metastases as compared to primary ovarian tumors, which was largely restricted to cells at the adipocyte-tumor cell interface.[178] Interestingly, FABP4 deficiency impaired metastatic tumor growth, indicating that fatty acid uptake was extremely important to metastasis and that adipocytes, serving as an energy depot, allow ovarian cancer cells to grow and metastasize.[178] It stands to reason that hypertrophy of fat depots, including the omental fat pad, as a result of obesity, could readily support more aggressive expansion of ovarian cancer within the peritoneal cavity. Further, adipocytes from obese individuals have changes in secretory profiles that promote cancer growth. Conditioned medium from visceral adipocytes from obese individuals was able to significantly increase proliferation of esophageal and colorectal cancer cells, while visceral adipocytes from lean individuals and adipocytes from subcutaneous fat did not increase growth rate.[179]

These observations of the pleiotropic effects of expanded adipose tissue on cancer progression support the '*seed and soil*' or *pre-metastatic niche hypothesis,* which suggests that a conducive microenvironment must be formed in order for tumor cells to be able to engraft and proliferate at secondary sites.[180] For example, a study by Kaplan et al.[181] found that BM-derived precursor cells expressing VEGFR1 home to tumor-specific pre-metastatic sites and form clusters before the arrival of tumor cells. By blocking VEGFR1 with antibodies or ablating cells expressing the receptor, the formation of pre-metastatic clusters was abrogated and tumor metastasis was prevented, indicating that the primary tumor actively modifies distant locations prior to metastasis. This is highly relevant to ovarian cancer, since the peritoneal cavity comprises its metastatic environment and cancer cells are in close proximity to suitable tissues that are highly dynamic and modifiable. Of note, the production of chemokines and other immunomodulatory molecules by ovarian cancer cells could help recruit cells to the peritoneal cavity and/or polarize cells present towards a cancer promoting phenotype, further transforming the peritoneal microenvironment towards one favoring attachment and expansion of cancer. Thus, WAT represents an exceptional metastatic site in some instances and a source of factors that can be exploited to modify a metastatic niche in others. As many of the advantageous factors discussed are enhanced with obesity, it is reasonable to speculate that an obese state activates this highly conducive microenvironment, facilitating ovarian cancer metastasis.

Conclusion and Aims

Once considered merely a depository for excess lipids, adipose tissue is now recognized as an endocrine organ with central roles in numerous biological processes. With an increasing global obesity epidemic, the implications of these functions are

becoming ever more apparent. As adipose tissue serves as a reservoir for various stem and progenitor populations, it may be an important source of cells to be recruited as tumor support. Progenitor cells are mobilized in response to cancer development and a large percentage of these cells are derived from non-BM sources. It has also been demonstrated that cells can be recruited directly from WAT and incorporated into the tumor stroma, enhancing both cancer progression and metastasis. Since ovarian cancer disseminates within the unique microenvironment of the peritoneal cavity, the close proximity to various visceral fat pads may be advantageous, providing optimal binding sites with pre-existing energy depots. Additionally, some studies have demonstrated that obesity increases the abundance of stem and progenitor cells both in adipose tissue and circulation. There have also been reports that many BM-derived cells are capable of adipocyte differentiation and can incorporate into the adipose tissue as needed for tissue expansion and thus also have increased availability as a result of obesity. This may be exploited by ovarian cancer, which is often closely associated with fat pads, especially the omentum. Cancer cells can utilize fat depots as a supply for nutrients, recruitable stromal cells, and as a source of inflammatory mediators and growth factors that provide tumors with a growth advantage and increase metastatic potential. It stands to reason that an obese state would provide more energy, an increase in availability of progenitor and stromal cells, and an increased inflammatory microenvironment, all of which may be more opportune than a lean environment.

The pleiotropic influence of adipose tissue on numerous cellular processes necessitates a complete inquiry into how obesity could impact ovarian cancer development and metastasis. Not only is ovarian cancer inadequately characterized itself,

but so are the mechanisms involved in adipose tissue reorganization and the actual consequence of obesity on ovarian cancer progression. The stromal cells of the adipose tissue are poorly defined and most studies investigating the properties of these cells and their affect on cancer, fail to use methods that would demonstrate the actual probability of their contribution and the mechanism of recruitment. Additionally, conflicting surface marker characterizations for the same cell types make comparisons between studies difficult at best. For example, MSCs, HSCs, and other progenitors share numerous surface markers and yet many studies look at populations of cells by defined by only one or two markers, which could encompass numerous different cell types. With the cell types in current studies determined based on loosely defined criteria, it is possible that much of the information published now will have to be revised when the cell types are further analyzed by more comprehensive means. Further, there are considerable discrepancies in the terminology used to define distinct cell types. For instance, pericytes are also called mural cells and are additionally sometimes considered myofibroblasts and even suggested to be MSCs. This further muddies the waters when trying to pinpoint the effects of specific cell types on certain processes. To add further complications, new cell types or subtypes are constantly being identified or new traits are being applied to previously characterized cell types. This is problematic when trying to determine which cell type or what activation or differentiation state of a specific cell type impacts cancer progression. Without being able to accurately differentiate one cell from another, it is very difficult to characterize cell-cell interactions and determine which cells should be targeted.

Besides basic immunophenotyping, there is still much work to be done to accurately elucidate a potential correlation between obesity and cancer. The actual changes that occur in progenitor populations within each fat depot needs to be determined as well as a definitive assessment of changes in the circulating progenitor populations present in peripheral blood as a consequence of obesity. Further the origin of these cell types and the delineation of the site-specific factors that impact cell recruitment needs clarification. The cellular content of ascites, which is poorly defined, needs further characterization with respect to content of progenitor populations during non-obese and obese states. More importantly, the kinetics of progenitor populations within the peritoneal cavity as a consequence of exfoliated cancer cell accumulation needs to be determined. There may be a defined window of opportunity to restrict their recruitment by cancer cells and limit metastases. Subsequent to identification of the key players in the regulation of peritoneal dissemination of ovarian cancer, it will be crucial to determine how these cells contribute to metastasis, whether it is by serving as stromal contributers, producers of growth factors and anti-apoptotic signals, sources of energy, means of immune evasion, or all of the above. Obesity may contribute to cancer progression in a more indirect fashion by its global, systemic effects such as insulin resistance and low-grade chronic inflammation, which may globally mobilize and activate progenitor cells. While there is strong anecdotal evidence that stem and progenitors derived from WAT may be involved in ovarian cancer progression, only once we have characterized the sequence of progressive events and identified what factors impact these processes can we determine how to therapeutically or even prophylactically target these events to impede cancer progression. With more research focus on the effect of WAT-derived stem and

progenitor populations on ovarian cancer, new treatment options targeting risk factors may allow us to develop novel strategies to prevent aggressive ovarian cancer.

Specific Aims

This study aims to determine how high fat diet and weight gain can enhance ovarian cancer progression in a mouse model. We will additionally characterize the progenitor populations present in various intra-abdominal adipose depots as well as determine how these populations change with high fat feeding and the presence of tumor cells. This will shed light on a potential correlation between expanded adipose tissue and cancer risk. Further, we will conduct an initial characterization of the association between adipose tissue-derived SVF cells and mouse ovarian cancer cells *in vitro*, and determine if SVF cells can enhance cancer cell proliferation, mobility and invasive potential. This will provide more information on how cancer is actually affected by SVF cells. Thus, this study will determine if there is indeed a link between obesity and ovarian cancer progression and will further identify novel cellular targets for ovarian cancer therapy. The specific aims are as follows:

Aim 1- Characterize the SVF cell populations and whole-tissue gene expression profiles of intra-abdominal adipose depots of mice on a low fat versus high fat diet.

Rationale*:* Each adipose tissue depot is unique and may play a different role in pathological conditions. When evaluating the impact of adipose tissue on specific processes, many studies choose a single depot, or one subcutaneous and one visceral depot to represent adipose tissue as a whole. However, this may be misleading as each depot may have its own distinct contribution. In murine studies, the most commonly

utilized intra-abdominal fat depot is perigonadal fat (epididymal in males and parametrial in females), although it has no human counterpart. This aim will provide a comprehensive analysis of basal immune and progenitor populations in parametrial WAT, as well as omental WAT (a "true" visceral fat depot) and retroperitoneal WAT (an intra-abdominal depot that is not drained by the portal vein, but does have a human counterpart) in mice on low fat versus high fat diets.

Hypothesis: Each fat depot represents a unique intra-abdominal microenvironment distinguished by differing stromal vascular cell populations and contrasting whole-tissue gene expression profiles. Additionally, we hypothesize that distinct changes in progenitor populations will occur in with high fat feedings in all tissues.

Aim 2- Determine the impact of high fat feeding on ovarian cancer tumor burden and characterize changes in SVF cell populations that occur with ovarian cancer in mice on a low fat versus high fat diet.

Rationale*:* Obesity has been linked to numerous cancers and many studies suggest that it may increase the risk of development and death due to ovarian cancer. Obesity is associated with expansion of adipose tissue and potential increases in stem and progenitor populations present within the fat. This increase in progenitor cells may contribute to cancer progression by serving as a source of recruitable cells that can be incorporated into tumors, enhancing the survival and aggressiveness of cancer cells.

Hypothesis: Mice on a high fat diet will have a higher tumor burden score than those on a low fat diet. Additionally, there will be changes in progenitor populations in the fat depots as well as the blood and peritoneal serous fluid of mice injected with cancer cells. Similarly, qRT-PCR will demonstrate enhanced expression of chemoattractants in the fat

depots of mice on a high fat diet and with injection of MOSE-L FFLs as compared to either (high fat diet or cancer injection) individually.

Aim 3- Characterize the relationship between SVF progenitor cells and MOSE-L FFL cells in vitro.

Rationale*:* Tumor-associated cells, including stromal cells, are critical for tumor formation and growth. It is probable that stromal cells from proximal tissues, such as adipose tissue, are recruited by cancer cells and can enhance cancer progression. Aim 3 will investigate the *in vitro* interactions of SVF and MOSE-L FFL cells to determine if their association initiates changes in proliferation, mobilization, or invasive capacity of the other cell type.

Hypothesis: SVF cells will be able to directly interact with MOSE-L FFL cells causing behavioral changes in both cell types. We hypothesize that the presence of SVF cells will increase MOSE-L FFL proliferation, mobility, and invasive capacity. Additionally, the presence of MOSE-L FFLs may increase proliferation and mobility of SVF cells.

References

1. Singer G, Stohr R, Cope L, et al. Patterns of p53 mutations separate ovarian serous borderline tumors and low- and high-grade carcinomas and provide support for a new model of ovarian carcinogenesis: a mutational analysis with immunohistochemical correlation. *Am J Surg Pathol.* Feb 2005;29(2):218-224.

2. Caduff RF, Svoboda-Newman SM, Ferguson AW, Johnston CM, Frank TS. Comparison of mutations of Ki-RAS and p53 immunoreactivity in borderline and malignant epithelial ovarian tumors. *Am J Surg Pathol.* Mar 1999;23(3):323-328.

3. Singer G, Oldt R, 3rd, Cohen Y, et al. Mutations in BRAF and KRAS characterize the development of low-grade ovarian serous carcinoma. *J Natl Cancer Inst.* Mar 19 2003;95(6):484-486.

4. Kurman RJ, Shih Ie M. The origin and pathogenesis of epithelial ovarian cancer: a proposed unifying theory. *Am J Surg Pathol.* Mar 2010;34(3):433-443.

5. Cheng W, Liu J, Yoshida H, Rosen D, Naora H. Lineage infidelity of epithelial ovarian cancers is controlled by HOX genes that specify regional identity in the reproductive tract. *Nat Med.* May 2005;11(5):531-537.

6. Callahan MJ, Crum CP, Medeiros F, et al. Primary fallopian tube malignancies in BRCA-positive women undergoing surgery for ovarian cancer risk reduction. *J Clin Oncol.* Sep 1 2007;25(25):3985-3990.
7. Kindelberger DW, Lee Y, Miron A, et al. Intraepithelial carcinoma of the fimbria and pelvic serous carcinoma: Evidence for a causal relationship. *Am J Surg Pathol.* Feb 2007;31(2):161-169.
8. Li J, Abushahin N, Pang S, et al. Tubal origin of 'ovarian' low-grade serous carcinoma. *Mod Pathol.* Nov 2011;24(11):1488-1499.
9. Lengyel E. Ovarian cancer development and metastasis. *Am J Pathol.* Sep 2010;177(3):1053-1064.
10. Mesiano S, Ferrara N, Jaffe RB. Role of vascular endothelial growth factor in ovarian cancer: inhibition of ascites formation by immunoneutralization. *Am J Pathol.* Oct 1998;153(4):1249-1256.
11. Shield K, Ackland ML, Ahmed N, Rice GE. Multicellular spheroids in ovarian cancer metastases: Biology and pathology. *Gynecol Oncol.* Apr 2009;113(1):143-148.
12. Kuk C, Kulasingam V, Gunawardana CG, Smith CR, Batruch I, Diamandis EP. Mining the ovarian cancer ascites proteome for potential ovarian cancer biomarkers. *Mol Cell Proteomics.* Apr 2009;8(4):661-669.
13. Feldman GB. Lymphatic obstruction in carcinomatous ascites. *Cancer Res.* Feb 1975;35(2):325-332.
14. Barbolina MV, Moss NM, Westfall SD, et al. Microenvironmental regulation of ovarian cancer metastasis. *Cancer Treat Res.* 2009;149:319-334.
15. Booth M, Beral V, Smith P. Risk factors for ovarian cancer: a case-control study. *Br J Cancer.* Oct 1989;60(4):592-598.
16. Riman T, Dickman PW, Nilsson S, et al. Risk factors for invasive epithelial ovarian cancer: results from a Swedish case-control study. *Am J Epidemiol.* Aug 15 2002;156(4):363-373.
17. Lubin F, Chetrit A, Freedman LS, et al. Body mass index at age 18 years and during adult life and ovarian cancer risk. *Am J Epidemiol.* Jan 15 2003;157(2):113-120.
18. Whittemore AS. Personal characteristics relating to risk of invasive epithelial ovarian cancer in older women in the United States. *Cancer.* Jan 15 1993;71(2 Suppl):558-565.
19. Schildkraut JM, Schwingl PJ, Bastos E, Evanoff A, Hughes C. Epithelial ovarian cancer risk among women with polycystic ovary syndrome. *Obstet Gynecol.* Oct 1996;88(4 Pt 1):554-559.
20. Purdie D, Green A, Bain C, et al. Reproductive and other factors and risk of epithelial ovarian cancer: an Australian case-control study. Survey of Women's Health Study Group. *Int J Cancer.* Sep 15 1995;62(6):678-684.
21. Fleming JS, Beaugie CR, Haviv I, Chenevix-Trench G, Tan OL. Incessant ovulation, inflammation and epithelial ovarian carcinogenesis: revisiting old hypotheses. *Mol Cell Endocrinol.* Mar 9 2006;247(1-2):4-21.
22. Nagle CM, Purdie DM, Webb PM, Green A, Harvey PW, Bain CJ. Dietary influences on survival after ovarian cancer. *Int J Cancer.* Aug 20 2003;106(2):264-269.

23. Moysich KB, Baker JA, Menezes RJ, et al. Usual adult body mass index is not predictive of ovarian cancer survival. *Cancer Epidemiol Biomarkers Prev.* Mar 2007;16(3):626-628.
24. Schildkraut JM, Halabi S, Bastos E, Marchbanks PA, McDonald JA, Berchuck A. Prognostic factors in early-onset epithelial ovarian cancer: a population-based study. *Obstet Gynecol.* Jan 2000;95(1):119-127.
25. Olsen C, Green, A, Whiteman, D, Sadeghi, S, Kolahdooz, F, Webb, P. Obesity and the risk of epithelial ovarian cancer: a systemic review and meta-analysis. *Eur J Cancer.* 2007;43:690-709.
26. Fairfield KM, Willett WC, Rosner BA, Manson JE, Speizer FE, Hankinson SE. Obesity, weight gain, and ovarian cancer. *Obstet Gynecol.* Aug 2002;100(2):288-296.
27. Zhang M, Xie X, Lee AH, Binns CW, Holman CD. Body mass index in relation to ovarian cancer survival. *Cancer Epidemiol Biomarkers Prev.* May 2005;14(5):1307-1310.
28. Kjaerbye-Thygesen A, Frederiksen K, Hogdall EV, et al. Smoking and overweight: negative prognostic factors in stage III epithelial ovarian cancer. *Cancer Epidemiol Biomarkers Prev.* Apr 2006;15(4):798-803.
29. Pavelka JC, Brown RS, Karlan BY, et al. Effect of obesity on survival in epithelial ovarian cancer. *Cancer.* Oct 1 2006;107(7):1520-1524.
30. Matthews KS, Straughn JM, Jr., Kemper MK, Hoskins KE, Wang W, Rocconi RP. The effect of obesity on survival in patients with ovarian cancer. *Gynecol Oncol.* Feb 2009;112(2):389-393.
31. Backes FJ, Nagel CI, Bussewitz E, Donner J, Hade E, Salani R. The Impact of Body Weight on Ovarian Cancer Outcomes. *Int J Gynecol Cancer.* Oct 8 2011.
32. Khandekar MJ, Cohen P, Spiegelman BM. Molecular mechanisms of cancer development in obesity. *Nat Rev Cancer.* Dec 2011;11(12):886-895.
33. Rausch ME, Weisberg S, Vardhana P, Tortoriello DV. Obesity in C57BL/6J mice is characterized by adipose tissue hypoxia and cytotoxic T-cell infiltration. *Int J Obes (Lond).* Mar 2008;32(3):451-463.
34. Ye J, Gao Z, Yin J, He Q. Hypoxia is a potential risk factor for chronic inflammation and adiponectin reduction in adipose tissue of ob/ob and dietary obese mice. *Am J Physiol Endocrinol Metab.* Oct 2007;293(4):E1118-1128.
35. Cinti S, Mitchell G, Barbatelli G, et al. Adipocyte death defines macrophage localization and function in adipose tissue of obese mice and humans. *J Lipid Res.* Nov 2005;46(11):2347-2355.
36. Nishimura S, Manabe I, Nagasaki M, et al. CD8+ effector T cells contribute to macrophage recruitment and adipose tissue inflammation in obesity. *Nat Med.* Aug 2009;15(8):914-920.
37. Kanda H, Tateya S, Tamori Y, et al. MCP-1 contributes to macrophage infiltration into adipose tissue, insulin resistance, and hepatic steatosis in obesity. *J Clin Invest.* Jun 2006;116(6):1494-1505.
38. Trayhurn P, Wood IS. Signalling role of adipose tissue: adipokines and inflammation in obesity. *Biochem Soc Trans.* Nov 2005;33(Pt 5):1078-1081.
39. Hsing AW, Gao YT, Chua S, Jr., Deng J, Stanczyk FZ. Insulin resistance and prostate cancer risk. *J Natl Cancer Inst.* Jan 1 2003;95(1):67-71.

40. Nunez NP, Oh WJ, Rozenberg J, et al. Accelerated tumor formation in a fatless mouse with type 2 diabetes and inflammation. *Cancer Res.* May 15 2006;66(10):5469-5476.
41. Federico A, Morgillo F, Tuccillo C, Ciardiello F, Loguercio C. Chronic inflammation and oxidative stress in human carcinogenesis. *Int J Cancer.* Dec 1 2007;121(11):2381-2386.
42. Bruning PF, Bonfrer JM, van Noord PA, Hart AA, de Jong-Bakker M, Nooijen WJ. Insulin resistance and breast-cancer risk. *Int J Cancer.* Oct 21 1992;52(4):511-516.
43. Trevisan M, Liu J, Muti P, Misciagna G, Menotti A, Fucci F. Markers of insulin resistance and colorectal cancer mortality. *Cancer Epidemiol Biomarkers Prev.* Sep 2001;10(9):937-941.
44. Rutter M, Saunders B, Wilkinson K, et al. Severity of inflammation is a risk factor for colorectal neoplasia in ulcerative colitis. *Gastroenterology.* Feb 2004;126(2):451-459.
45. Ernst P. Review article: the role of inflammation in the pathogenesis of gastric cancer. *Aliment Pharmacol Ther.* Mar 1999;13 Suppl 1:13-18.
46. Azad N, Rojanasakul Y, Vallyathan V. Inflammation and lung cancer: roles of reactive oxygen/nitrogen species. *J Toxicol Environ Health B Crit Rev.* Jan 2008;11(1):1-15.
47. Ness RB, Cottreau C. Possible role of ovarian epithelial inflammation in ovarian cancer. *J Natl Cancer Inst.* Sep 1 1999;91(17):1459-1467.
48. Schreinemachers DM, Everson RB. Aspirin use and lung, colon, and breast cancer incidence in a prospective study. *Epidemiology.* Mar 1994;5(2):138-146.
49. Farrow DC, Vaughan TL, Hansten PD, et al. Use of aspirin and other nonsteroidal anti-inflammatory drugs and risk of esophageal and gastric cancer. *Cancer Epidemiol Biomarkers Prev.* Feb 1998;7(2):97-102.
50. Malmstrom R, Taskinen MR, Karonen SL, Yki-Jarvinen H. Insulin increases plasma leptin concentrations in normal subjects and patients with NIDDM. *Diabetologia.* Aug 1996;39(8):993-996.
51. Newcomer JW, Selke G, Melson AK, Gross J, Vogler GP, Dagogo-Jack S. Dose-dependent cortisol-induced increases in plasma leptin concentration in healthy humans. *Arch Gen Psychiatry.* Nov 1998;55(11):995-1000.
52. Medina EA, Stanhope KL, Mizuno TM, et al. Effects of tumor necrosis factor alpha on leptin secretion and gene expression: relationship to changes of glucose metabolism in isolated rat adipocytes. *Int J Obes Relat Metab Disord.* Aug 1999;23(8):896-903.
53. Papaspyrou-Rao S, Schneider SH, Petersen RN, Fried SK. Dexamethasone increases leptin expression in humans in vivo. *J Clin Endocrinol Metab.* May 1997;82(5):1635-1637.
54. Maffei M, Halaas J, Ravussin E, et al. Leptin levels in human and rodent: measurement of plasma leptin and ob RNA in obese and weight-reduced subjects. *Nat Med.* Nov 1995;1(11):1155-1161.
55. Klok MD, Jakobsdottir S, Drent ML. The role of leptin and ghrelin in the regulation of food intake and body weight in humans: a review. *Obes Rev.* Jan 2007;8(1):21-34.

56. Bonadonna RC, Groop L, Kraemer N, Ferrannini E, Del Prato S, DeFronzo RA. Obesity and insulin resistance in humans: a dose-response study. *Metabolism.* May 1990;39(5):452-459.
57. Park HY, Kwon HM, Lim HJ, et al. Potential role of leptin in angiogenesis: leptin induces endothelial cell proliferation and expression of matrix metalloproteinases in vivo and in vitro. *Exp Mol Med.* Jun 30 2001;33(2):95-102.
58. Sierra-Honigmann MR, Nath AK, Murakami C, et al. Biological action of leptin as an angiogenic factor. *Science.* Sep 11 1998;281(5383):1683-1686.
59. Huang F, Xiong X, Wang H, You S, Zeng H. Leptin-induced vascular smooth muscle cell proliferation via regulating cell cycle, activating ERK1/2 and NF-kappaB. *Acta Biochim Biophys Sin (Shanghai).* May 15 2010;42(5):325-331.
60. Hardwick JC, Van Den Brink GR, Offerhaus GJ, Van Deventer SJ, Peppelenbosch MP. Leptin is a growth factor for colonic epithelial cells. *Gastroenterology.* Jul 2001;121(1):79-90.
61. Dieudonne MN, Machinal-Quelin F, Serazin-Leroy V, Leneveu MC, Pecquery R, Giudicelli Y. Leptin mediates a proliferative response in human MCF7 breast cancer cells. *Biochem Biophys Res Commun.* Apr 26 2002;293(1):622-628.
62. Austin H, Austin JM, Jr., Partridge EE, Hatch KD, Shingleton HM. Endometrial cancer, obesity, and body fat distribution. *Cancer Res.* Jan 15 1991;51(2):568-572.
63. MacDonald PC, Siiteri PK. The relationship between the extraglandular production of estrone and the occurrence of endometrial neoplasia. *Gynecol Oncol.* Aug 1974;2(2-3):259-263.
64. Key TJ, Appleby PN, Reeves GK, et al. Body mass index, serum sex hormones, and breast cancer risk in postmenopausal women. *J Natl Cancer Inst.* Aug 20 2003;95(16):1218-1226.
65. Marquez DC, Pietras RJ. Membrane-associated binding sites for estrogen contribute to growth regulation of human breast cancer cells. *Oncogene.* Sep 6 2001;20(39):5420-5430.
66. Liehr JG. Is estradiol a genotoxic mutagenic carcinogen? *Endocr Rev.* Feb 2000;21(1):40-54.
67. Evans DJ, Hoffmann RG, Kalkhoff RK, Kissebah AH. Relationship of androgenic activity to body fat topography, fat cell morphology, and metabolic aberrations in premenopausal women. *J Clin Endocrinol Metab.* Aug 1983;57(2):304-310.
68. Kuhnel R, de Graaff J, Rao BR, Stolk JG. Androgen receptor predominance in human ovarian carcinoma. *J Steroid Biochem.* Mar 1987;26(3):393-397.
69. Mahlck CG, Backstrom T, Kjellgren O. Androstenedione production by malignant epithelial ovarian tumors. *Gynecol Oncol.* Oct 1986;25(2):217-222.
70. Apridonidze T, Essah PA, Iuorno MJ, Nestler JE. Prevalence and characteristics of the metabolic syndrome in women with polycystic ovary syndrome. *J Clin Endocrinol Metab.* Apr 2005;90(4):1929-1935.
71. Lukanova A, Lundin E, Zeleniuch-Jacquotte A, et al. Body mass index, circulating levels of sex-steroid hormones, IGF-I and IGF-binding protein-3: a cross-sectional study in healthy women. *Eur J Endocrinol.* Feb 2004;150(2):161-171.

72. Poissonnet CM, Burdi AR, Garn SM. The chronology of adipose tissue appearance and distribution in the human fetus. *Early Hum Dev.* Sep 1984;10(1-2):1-11.
73. Ailhaud G, Grimaldi P, Negrel R. Cellular and molecular aspects of adipose tissue development. *Annu Rev Nutr.* 1992;12:207-233.
74. Gruen R, Hietanen E, Greenwood MR. Increased adipose tissue lipoprotein lipase activity during the development of the genetically obese rat (fa/fa). *Metabolism.* Dec 1978;27(12 Suppl 2):1955-1966.
75. Ochi M, Yoshioka H, Sawada T, Kusunoki T, Hattori T. New adipocyte formation in mice during refeeding after long-term deprivation. *Am J Physiol.* Mar 1991;260(3 Pt 2):R468-474.
76. Wronska A, Kmiec Z. Structural and biochemical characteristics of various white adipose tissue depots. *Acta Physiol (Oxf).* Jan 7 2012.
77. Bjorntorp P. "Portal" adipose tissue as a generator of risk factors for cardiovascular disease and diabetes. *Arteriosclerosis.* Jul-Aug 1990;10(4):493-496.
78. Rytka JM, Wueest S, Schoenle EJ, Konrad D. The portal theory supported by venous drainage-selective fat transplantation. *Diabetes.* Jan 2011;60(1):56-63.
79. Rimm AA, Hartz AJ, Fischer ME. A weight shape index for assessing risk of disease in 44,820 women. *J Clin Epidemiol.* 1988;41(5):459-465.
80. Janssen I, Katzmarzyk PT, Ross R. Body mass index, waist circumference, and health risk: evidence in support of current National Institutes of Health guidelines. *Arch Intern Med.* Oct 14 2002;162(18):2074-2079.
81. Delort L, Kwiatkowski F, Chalabi N, Satih S, Bignon YJ, Bernard-Gallon DJ. Central adiposity as a major risk factor of ovarian cancer. *Anticancer Res.* Dec 2009;29(12):5229-5234.
82. Mink PJ, Folsom AR, Sellers TA, Kushi LH. Physical activity, waist-to-hip ratio, and other risk factors for ovarian cancer: a follow-up study of older women. *Epidemiology.* Jan 1996;7(1):38-45.
83. Zuk PA, Zhu M, Ashjian P, et al. Human adipose tissue is a source of multipotent stem cells. *Mol Biol Cell.* Dec 2002;13(12):4279-4295.
84. Mitchell JB, McIntosh K, Zvonic S, et al. Immunophenotype of human adipose-derived cells: temporal changes in stromal-associated and stem cell-associated markers. *Stem Cells.* Feb 2006;24(2):376-385.
85. Weisberg SP, McCann D, Desai M, Rosenbaum M, Leibel RL, Ferrante AW, Jr. Obesity is associated with macrophage accumulation in adipose tissue. *J Clin Invest.* Dec 2003;112(12):1796-1808.
86. Krist LF, Eestermans IL, Steenbergen JJ, et al. Cellular composition of milky spots in the human greater omentum: an immunochemical and ultrastructural study. *Anat Rec.* Feb 1995;241(2):163-174.
87. Dux K, Rouse RV, Kyewski B. Composition of the lymphoid cell populations from omental milky spots during the immune response in C57BL/Ka mice. *Eur J Immunol.* Aug 1986;16(8):1029-1032.
88. Fain JN, Madan AK, Hiler ML, Cheema P, Bahouth SW. Comparison of the release of adipokines by adipose tissue, adipose tissue matrix, and adipocytes

from visceral and subcutaneous abdominal adipose tissues of obese humans. *Endocrinology.* May 2004;145(5):2273-2282.

89. Satoor SN, Puranik AS, Kumar S, et al. Location, location, location: Beneficial effects of autologous fat transplantation. *Sci Rep.* 2011;1:81.

90. Van Harmelen V, Reynisdottir S, Eriksson P, et al. Leptin secretion from subcutaneous and visceral adipose tissue in women. *Diabetes.* Jun 1998;47(6):913-917.

91. Einstein FH, Atzmon G, Yang XM, et al. Differential responses of visceral and subcutaneous fat depots to nutrients. *Diabetes.* Mar 2005;54(3):672-678.

92. Christiansen T, Richelsen B, Bruun JM. Monocyte chemoattractant protein-1 is produced in isolated adipocytes, associated with adiposity and reduced after weight loss in morbid obese subjects. *Int J Obes (Lond).* Jan 2005;29(1):146-150.

93. Drolet R, Belanger C, Fortier M, et al. Fat depot-specific impact of visceral obesity on adipocyte adiponectin release in women. *Obesity (Silver Spring).* Mar 2009;17(3):424-430.

94. Ostman J, Arner P, Engfeldt P, Kager L. Regional differences in the control of lipolysis in human adipose tissue. *Metabolism.* Dec 1979;28(12):1198-1205.

95. Engfeldt P, Arner P. Lipolysis in human adipocytes, effects of cell size, age and of regional differences. *Horm Metab Res Suppl.* 1988;19:26-29.

96. Bolinder J, Kager L, Ostman J, Arner P. Differences at the receptor and postreceptor levels between human omental and subcutaneous adipose tissue in the action of insulin on lipolysis. *Diabetes.* Feb 1983;32(2):117-123.

97. Lundgren M, Buren J, Ruge T, Myrnas T, Eriksson JW. Glucocorticoids down-regulate glucose uptake capacity and insulin-signaling proteins in omental but not subcutaneous human adipocytes. *J Clin Endocrinol Metab.* Jun 2004;89(6):2989-2997.

98. Tchoukalova YD, Votruba SB, Tchkonia T, Giorgadze N, Kirkland JL, Jensen MD. Regional differences in cellular mechanisms of adipose tissue gain with overfeeding. *Proc Natl Acad Sci U S A.* Oct 19 2010;107(42):18226-18231.

99. Tchkonia T, Giorgadze N, Pirtskhalava T, et al. Fat depot origin affects adipogenesis in primary cultured and cloned human preadipocytes. *Am J Physiol Regul Integr Comp Physiol.* May 2002;282(5):R1286-1296.

100. Tung KH, Goodman MT, Wu AH, et al. Reproductive factors and epithelial ovarian cancer risk by histologic type: a multiethnic case-control study. *Am J Epidemiol.* Oct 1 2003;158(7):629-638.

101. Tchkonia T, Lenburg M, Thomou T, et al. Identification of depot-specific human fat cell progenitors through distinct expression profiles and developmental gene patterns. *Am J Physiol Endocrinol Metab.* Jan 2007;292(1):E298-307.

102. Matsumoto T, Kano K, Kondo D, et al. Mature adipocyte-derived dedifferentiated fat cells exhibit multilineage potential. *J Cell Physiol.* Apr 2008;215(1):210-222.

103. Meng L, Zhou J, Sasano H, Suzuki T, Zeitoun KM, Bulun SE. Tumor necrosis factor alpha and interleukin 11 secreted by malignant breast epithelial cells inhibit adipocyte differentiation by selectively down-regulating CCAAT/enhancer binding protein alpha and peroxisome proliferator-activated receptor gamma: mechanism of desmoplastic reaction. *Cancer Res.* Mar 1 2001;61(5):2250-2255.

104. Engelman JA, Berg AH, Lewis RY, Lisanti MP, Scherer PE. Tumor necrosis factor alpha-mediated insulin resistance, but not dedifferentiation, is abrogated by MEK1/2 inhibitors in 3T3-L1 adipocytes. *Mol Endocrinol.* Oct 2000;14(10):1557-1569.

105. Dirat B, Bochet L, Dabek M, et al. Cancer-associated adipocytes exhibit an activated phenotype and contribute to breast cancer invasion. *Cancer Res.* Apr 1 2011;71(7):2455-2465.

106. Andarawewa KL, Motrescu ER, Chenard MP, et al. Stromelysin-3 is a potent negative regulator of adipogenesis participating to cancer cell-adipocyte interaction/crosstalk at the tumor invasive front. *Cancer Res.* Dec 1 2005;65(23):10862-10871.

107. Tan J, Buache E, Chenard MP, Dali-Youcef N, Rio MC. Adipocyte is a non-trivial, dynamic partner of breast cancer cells. *Int J Dev Biol.* 2011;55(7-9):851-859.

108. Tang QQ, Lane MD. Adipogenesis: From Stem Cell to Adipocyte. *Annu Rev Biochem.* Mar 29 2012.

109. Zhang Y, Daquinag, A, Traktuev, D, Amaya-Manzanares, F, Simmons, P, March, K, Pasqualini, R, Arap, W, Kolonin, M. White adipose tissue cells are recruited by experimental tumors and promote cancer progression in mouse models. *Cancer Res.* 2009;69(12):5259-5266.

110. Martin-Padura I, Gregato G, Marighetti P, et al. The white adipose tissue used in lipotransfer procedures is a rich reservoir of CD34+ progenitors able to promote cancer progression. *Cancer Res.* Nov 3 2011.

111. Matsuoka S, Ebihara Y, Xu M, et al. CD34 expression on long-term repopulating hematopoietic stem cells changes during developmental stages. *Blood.* Jan 15 2001;97(2):419-425.

112. Urbich C, Dimmeler S. Endothelial progenitor cells functional characterization. *Trends Cardiovasc Med.* Nov 2004;14(8):318-322.

113. Traktuev DO, Merfeld-Clauss S, Li J, et al. A population of multipotent CD34-positive adipose stromal cells share pericyte and mesenchymal surface markers, reside in a periendothelial location, and stabilize endothelial networks. *Circ Res.* Jan 4 2008;102(1):77-85.

114. Gunsilius E, Gastl G, Petzer AL. Hematopoietic stem cells. *Biomed Pharmacother.* May 2001;55(4):186-194.

115. Han J, Koh YJ, Moon HR, et al. Adipose tissue is an extramedullary reservoir for functional hematopoietic stem and progenitor cells. *Blood.* Feb 4 2010;115(5):957-964.

116. Majka SM, Fox KE, Psilas JC, et al. De novo generation of white adipocytes from the myeloid lineage via mesenchymal intermediates is age, adipose depot, and gender specific. *Proc Natl Acad Sci U S A.* Aug 17 2010;107(33):14781-14786.

117. Harman-Boehm I, Bluher M, Redel H, et al. Macrophage infiltration into omental versus subcutaneous fat across different populations: effect of regional adiposity and the comorbidities of obesity. *J Clin Endocrinol Metab.* Jun 2007;92(6):2240-2247.

118. Solinas G, Germano G, Mantovani A, Allavena P. Tumor-associated macrophages (TAM) as major players of the cancer-related inflammation. *J Leukoc Biol.* Nov 2009;86(5):1065-1073.
119. Fricke I, Gabrilovich DI. Dendritic cells and tumor microenvironment: a dangerous liaison. *Immunol Invest.* 2006;35(3-4):459-483.
120. Koh YJ, Koh BI, Kim H, et al. Stromal vascular fraction from adipose tissue forms profound vascular network through the dynamic reassembly of blood endothelial cells. *Arterioscler Thromb Vasc Biol.* May 2011;31(5):1141-1150.
121. Strem BM, Hicok KC, Zhu M, et al. Multipotential differentiation of adipose tissue-derived stem cells. *Keio J Med.* Sep 2005;54(3):132-141.
122. Gimble JM, Guilak F. Differentiation potential of adipose derived adult stem (ADAS) cells. *Curr Top Dev Biol.* 2003;58:137-160.
123. Gimble J, Guilak F. Adipose-derived adult stem cells: isolation, characterization, and differentiation potential. *Cytotherapy.* 2003;5(5):362-369.
124. Brzoska M, Geiger H, Gauer S, Baer P. Epithelial differentiation of human adipose tissue-derived adult stem cells. *Biochem Biophys Res Commun.* Apr 29 2005;330(1):142-150.
125. Planat-Benard V, Silvestre JS, Cousin B, et al. Plasticity of human adipose lineage cells toward endothelial cells: physiological and therapeutic perspectives. *Circulation.* Feb 10 2004;109(5):656-663.
126. Seo MJ, Suh SY, Bae YC, Jung JS. Differentiation of human adipose stromal cells into hepatic lineage in vitro and in vivo. *Biochem Biophys Res Commun.* Mar 4 2005;328(1):258-264.
127. Augello A, Kurth TB, De Bari C. Mesenchymal stem cells: a perspective from in vitro cultures to in vivo migration and niches. *Eur Cell Mater.* 2010;20:121-133.
128. Ponte AL, Marais E, Gallay N, et al. The in vitro migration capacity of human bone marrow mesenchymal stem cells: comparison of chemokine and growth factor chemotactic activities. *Stem Cells.* Jul 2007;25(7):1737-1745.
129. Kidd S, Spaeth E, Dembinski JL, et al. Direct evidence of mesenchymal stem cell tropism for tumor and wounding microenvironments using in vivo bioluminescent imaging. *Stem Cells.* Oct 2009;27(10):2614-2623.
130. Nakamura K, Ito Y, Kawano Y, et al. Antitumor effect of genetically engineered mesenchymal stem cells in a rat glioma model. *Gene Ther.* Jul 2004;11(14):1155-1164.
131. Ferrari N, Glod J, Lee J, Kobiler D, Fine HA. Bone marrow-derived, endothelial progenitor-like cells as angiogenesis-selective gene-targeting vectors. *Gene Ther.* Apr 2003;10(8):647-656.
132. Komarova S, Kawakami Y, Stoff-Khalili MA, Curiel DT, Pereboeva L. Mesenchymal progenitor cells as cellular vehicles for delivery of oncolytic adenoviruses. *Mol Cancer Ther.* Mar 2006;5(3):755-766.
133. Aicher A, Rentsch M, Sasaki K, et al. Nonbone marrow-derived circulating progenitor cells contribute to postnatal neovascularization following tissue ischemia. *Circ Res.* Mar 2 2007;100(4):581-589.
134. Crossno JT, Jr., Majka SM, Grazia T, Gill RG, Klemm DJ. Rosiglitazone promotes development of a novel adipocyte population from bone marrow-derived circulating progenitor cells. *J Clin Invest.* Dec 2006;116(12):3220-3228.

135. Karnoub AE, Dash AB, Vo AP, et al. Mesenchymal stem cells within tumour stroma promote breast cancer metastasis. *Nature.* Oct 4 2007;449(7162):557-563.
136. Suzuki K, Sun R, Origuchi M, et al. Mesenchymal stromal cells promote tumor growth through the enhancement of neovascularization. *Mol Med.* 2011;17(7-8):579-587.
137. Spaeth EL, Dembinski JL, Sasser AK, et al. Mesenchymal stem cell transition to tumor-associated fibroblasts contributes to fibrovascular network expansion and tumor progression. *PLoS One.* 2009;4(4):e4992.
138. Bexell D, Gunnarsson S, Tormin A, et al. Bone marrow multipotent mesenchymal stroma cells act as pericyte-like migratory vehicles in experimental gliomas. *Mol Ther.* Jan 2009;17(1):183-190.
139. Hanahan D, Coussens LM. Accessories to the crime: functions of cells recruited to the tumor microenvironment. *Cancer Cell.* Mar 20 2012;21(3):309-322.
140. Wang M, Crisostomo PR, Herring C, Meldrum KK, Meldrum DR. Human progenitor cells from bone marrow or adipose tissue produce VEGF, HGF, and IGF-I in response to TNF by a p38 MAPK-dependent mechanism. *Am J Physiol Regul Integr Comp Physiol.* Oct 2006;291(4):R880-884.
141. Rehman J, Traktuev D, Li J, et al. Secretion of angiogenic and antiapoptotic factors by human adipose stromal cells. *Circulation.* Mar 16 2004;109(10):1292-1298.
142. Klopp AH, Zhang Y, Solley T, et al. Omental adipose tissue-derived stromal cells promote vascularization and growth of endometrial tumors. *Clin Cancer Res.* Feb 1 2012;18(3):771-782.
143. Puissant B, Barreau C, Bourin P, et al. Immunomodulatory effect of human adipose tissue-derived adult stem cells: comparison with bone marrow mesenchymal stem cells. *Br J Haematol.* Apr 2005;129(1):118-129.
144. Yanez R, Lamana ML, Garcia-Castro J, Colmenero I, Ramirez M, Bueren JA. Adipose tissue-derived mesenchymal stem cells have in vivo immunosuppressive properties applicable for the control of the graft-versus-host disease. *Stem Cells.* Nov 2006;24(11):2582-2591.
145. Fang B, Song Y, Liao L, Zhang Y, Zhao RC. Favorable response to human adipose tissue-derived mesenchymal stem cells in steroid-refractory acute graft-versus-host disease. *Transplant Proc.* Dec 2007;39(10):3358-3362.
146. Djouad F, Plence P, Bony C, et al. Immunosuppressive effect of mesenchymal stem cells favors tumor growth in allogeneic animals. *Blood.* Nov 15 2003;102(10):3837-3844.
147. McLean K, Gong Y, Choi Y, et al. Human ovarian carcinoma-associated mesenchymal stem cells regulate cancer stem cells and tumorigenesis via altered BMP production. *J Clin Invest.* Jul 1 2011.
148. Blann AD, Woywodt A, Bertolini F, et al. Circulating endothelial cells. Biomarker of vascular disease. *Thromb Haemost.* Feb 2005;93(2):228-235.
149. Beerepoot LV, Mehra N, Vermaat JS, Zonnenberg BA, Gebbink MF, Voest EE. Increased levels of viable circulating endothelial cells are an indicator of progressive disease in cancer patients. *Ann Oncol.* Jan 2004;15(1):139-145.

150. Kim HK, Song KS, Kim HO, et al. Circulating numbers of endothelial progenitor cells in patients with gastric and breast cancer. *Cancer Lett.* Jul 30 2003;198(1):83-88.
151. Mancuso P, Burlini A, Pruneri G, Goldhirsch A, Martinelli G, Bertolini F. Resting and activated endothelial cells are increased in the peripheral blood of cancer patients. *Blood.* Jun 1 2001;97(11):3658-3661.
152. Goon PK, Boos CJ, Lip GY. Circulating endothelial cells: markers of vascular dysfunction. *Clin Lab.* 2005;51(9-10):531-538.
153. Asahara T, Masuda H, Takahashi T, et al. Bone marrow origin of endothelial progenitor cells responsible for postnatal vasculogenesis in physiological and pathological neovascularization. *Circ Res.* Aug 6 1999;85(3):221-228.
154. Kidd S, Spaeth E, Watson K, et al. Origins of the tumor microenvironment: quantitative assessment of adipose-derived and bone marrow-derived stroma. *PLoS One.* 2012;7(2):e30563.
155. Thijssen DH, Vos JB, Verseyden C, et al. Haematopoietic stem cells and endothelial progenitor cells in healthy men: effect of aging and training. *Aging Cell.* Dec 2006;5(6):495-503.
156. Bellows CF, Zhang Y, Simmons PJ, Khalsa AS, Kolonin MG. Influence of BMI on Level of Circulating Progenitor Cells. *Obesity (Silver Spring).* Feb 3 2011.
157. Wolk R, Deb A, Caplice NM, Somers VK. Leptin receptor and functional effects of leptin in human endothelial progenitor cells. *Atherosclerosis.* Nov 2005;183(1):131-139.
158. MacEneaney OJ, Kushner EJ, Van Guilder GP, Greiner JJ, Stauffer BL, DeSouza CA. Endothelial progenitor cell number and colony-forming capacity in overweight and obese adults. *Int J Obes (Lond).* Feb 2009;33(2):219-225.
159. MacEneaney OJ, Kushner EJ, Westby CM, et al. Endothelial progenitor cell function, apoptosis, and telomere length in overweight/obese humans. *Obesity (Silver Spring).* Sep 2010;18(9):1677-1682.
160. Metz CN. Fibrocytes: a unique cell population implicated in wound healing. *Cell Mol Life Sci.* Jul 2003;60(7):1342-1350.
161. Bucala R, Spiegel LA, Chesney J, Hogan M, Cerami A. Circulating fibrocytes define a new leukocyte subpopulation that mediates tissue repair. *Mol Med.* Nov 1994;1(1):71-81.
162. Hong KM, Burdick MD, Phillips RJ, Heber D, Strieter RM. Characterization of human fibrocytes as circulating adipocyte progenitors and the formation of human adipose tissue in SCID mice. *FASEB J.* Dec 2005;19(14):2029-2031.
163. Abe R, Donnelly SC, Peng T, Bucala R, Metz CN. Peripheral blood fibrocytes: differentiation pathway and migration to wound sites. *J Immunol.* Jun 15 2001;166(12):7556-7562.
164. Huber J, Kiefer FW, Zeyda M, et al. CC chemokine and CC chemokine receptor profiles in visceral and subcutaneous adipose tissue are altered in human obesity. *J Clin Endocrinol Metab.* Aug 2008;93(8):3215-3221.
165. Barth PJ, Ebrahimsade S, Ramaswamy A, Moll R. CD34+ fibrocytes in invasive ductal carcinoma, ductal carcinoma in situ, and benign breast lesions. *Virchows Arch.* Mar 2002;440(3):298-303.

166. Barth PJ, Ebrahimsade S, Hellinger A, Moll R, Ramaswamy A. CD34+ fibrocytes in neoplastic and inflammatory pancreatic lesions. *Virchows Arch.* Feb 2002;440(2):128-133.
167. De Wever O, Demetter P, Mareel M, Bracke M. Stromal myofibroblasts are drivers of invasive cancer growth. *Int J Cancer.* Nov 15 2008;123(10):2229-2238.
168. Mori L, Bellini A, Stacey MA, Schmidt M, Mattoli S. Fibrocytes contribute to the myofibroblast population in wounded skin and originate from the bone marrow. *Exp Cell Res.* Mar 10 2005;304(1):81-90.
169. Sangai T, Ishii G, Kodama K, et al. Effect of differences in cancer cells and tumor growth sites on recruiting bone marrow-derived endothelial cells and myofibroblasts in cancer-induced stroma. *Int J Cancer.* Jul 20 2005;115(6):885-892.
170. Folkman J. Tumor angiogenesis: therapeutic implications. *N Engl J Med.* Nov 18 1971;285(21):1182-1186.
171. Dvorak HF. Tumors: wounds that do not heal. Similarities between tumor stroma generation and wound healing. *N Engl J Med.* Dec 25 1986;315(26):1650-1659.
172. Muehlberg FL, Song YH, Krohn A, et al. Tissue-resident stem cells promote breast cancer growth and metastasis. *Carcinogenesis.* Apr 2009;30(4):589-597.
173. Pittenger MF, Mackay AM, Beck SC, et al. Multilineage potential of adult human mesenchymal stem cells. *Science.* Apr 2 1999;284(5411):143-147.
174. Varma MJ, Breuls RG, Schouten TE, et al. Phenotypical and functional characterization of freshly isolated adipose tissue-derived stem cells. *Stem Cells Dev.* Feb 2007;16(1):91-104.
175. Ellis JR, McDonald RB, Stern JS. A diet high in fat stimulates adipocyte proliferation in older (22 month) rats. *Exp Gerontol.* 1990;25(2):141-148.
176. Steinberg JJ, Demopoulos RI, Bigelow B. The evaluation of the omentum in ovarian cancer. *Gynecol Oncol.* Jul 1986;24(3):327-330.
177. Clark R, Krishnan V, Schoof M, et al. Milky spots promote ovarian cancer metastatic colonization of peritoneal adipose in experimental models. *Am J Pathol.* Aug 2013;183(2):576-591.
178. Nieman KM, Kenny HA, Penicka CV, et al. Adipocytes promote ovarian cancer metastasis and provide energy for rapid tumor growth. *Nat Med.* 2011;17(11):1498-1503.
179. Lysaght J, van der Stok EP, Allott EH, et al. Pro-inflammatory and tumour proliferative properties of excess visceral adipose tissue. *Cancer Lett.* Dec 15 2011;312(1):62-72.
180. Psaila B, Lyden D. The metastatic niche: adapting the foreign soil. *Nat Rev Cancer.* Apr 2009;9(4):285-293.
181. Kaplan RN, Riba RD, Zacharoulis S, et al. VEGFR1-positive haematopoietic bone marrow progenitors initiate the pre-metastatic niche. *Nature.* Dec 8 2005;438(7069):820-827.

Chapter 3: PRELIMINARY DATA: INTRA-ABDOMINAL FAT DEPOTS REPRESENT DISTINCT IMMUNOMODULATORY MICROENVIRONMENTS

Cohen CA, Shea AA, Heffron CL, Schmelz EM, Roberts PC. Intra-abdominal fat depots represent distinct immunomodulatory microenvironments: a murine model. PLoS One. 2013;8(6):e66477. *Co-first authors

Abstract

White adipose tissue (WAT) is a multi-faceted endocrine organ involved in energy storage, metabolism, immune function and disease pathogenesis. In contrast to subcutaneous fat, visceral fat (V-WAT) has been associated with numerous diseases and metabolic disorders, indicating specific functions related to anatomical location. Although visceral depots are often used interchangeably in V-WAT-associated disease studies, there has been a recent subdivision of V-WAT into ‘‘true visceral’’ and non-visceral intra-abdominal compartments. These were associated with distinct physiological roles, illustrating a need for depot-specific information. Here, we use FACS analysis to comparatively characterize the leukocyte and progenitor populations in the stromal vascular fraction (SVF) of peritoneal serous fluid (PSF), parametrial (pmWAT), retroperitoneal (rpWAT), and omental (omWAT) adipose tissue from seven-month old C57BL/6 female mice. We found significant differences in SVF composition between all four microenvironments. PSF SVF was comprised almost entirely of CD45+ leukocytes (.99%), while omWAT contained less, but still almost two-fold more leukocytes than pmWAT and rpWAT (75%, 38% and 38% respectively; $p<0.01$). PmWAT was composed primarily of macrophages, whereas rpWAT more closely resembled omWAT, denoted by high levels of B1 B-cell and monocyte populations. Further, omWAT harbored significantly higher proportions of T-cells than the other tissues, consistent with

its role as a secondary lymphoid organ. These SVF changes were also reflected in the gene expression profiles of the respective tissues. Thus, intra-abdominal fat pads represent independent immunomodulatory microenvironments and should be evaluated as distinct entities with unique contributions to physiological and pathological processes.

Introduction

White adipose tissue (WAT) is the largest endocrine organ in the body, comprising up to 45% of total body composition in obese individuals (BMI≥30), having dramatic effects both locally and systemically. Once thought to be a passive reservoir for excess energy storage, WAT is increasingly recognized for its role in metabolism, immune and endocrine function, thermoregulation, and tissue repair.[1] Its function in both physiological and pathological processes may be impacted by either tissue resident adipocytes or the stromal vascular fraction (SVF), which includes leukocytes, mesenchymal stem cells, adipocyte progenitors, fibroblasts, and endothelial cells.[2] Recent studies indicate functional differences in adipose tissue depots related to anatomical location, specifically between subcutaneous fat (S-WAT) and visceral fat (V-WAT). While expansion of S-WAT is associated with improved insulin sensitivity and decreased risk of type 2 diabetes, V-WAT expansion is linked to an increased risk of cardiovascular disease, glucose dysregulation, hypertension, and certain cancers.[3] Functional and secretory differences between V-WAT and S-WAT include increased lipolysis and expression of inflammatory molecules, and decreased angiogenesis, production of adiponectin and leptin, and responsiveness to insulin.[4] Although V-WAT only comprises ~10% of total body fat, it is strongly correlated with increased morbidity and mortality.[4,5]

Recently, V-WAT has been further classified based on drainage, distinguishing "true" V-WAT depots, e.g. omental and mesenteric fat drained by the portal vein, from intra-abdominal ("non-visceral") depots, drained by the inferior vena cava, including perigonadal (parametrial in females, epididymal in males), retroperitoneal, and perirenal fat.[6,7] To date, studies comparing S-WAT and V-WAT are inconsistent in their use of V-WAT, with different fat pads often used interchangeably, although distinct depots are reportedly unique in tissue dynamics (hypertrophic versus hyperplastic response to excess calories), adipokine release, hormonal responses, vascularization, innervation, and abundance of non-adipocyte components.[6,7] Due to this diversity, it is possible that individual fat pads play differential roles in the pathogenesis of specific diseases. Thus, it is critical that the inherent differences between intra-abdominal fat depots are properly characterized instead of designating one to represent the contribution of V-WAT as a whole.

Although there is no human counterpart, perigonadal fat is often utilized in murine studies of V-WAT-associated diseases, primarily due to its ease of access and relative abundance.[7] As it is a recent delineation, many adipose characterization studies have not distinguished between true visceral and non-visceral intra-abdominal fat or do not specify the type of V-WAT, making depot-specific conclusions difficult. However, one study demonstrated that differences in fat pad composition and functionality endure after transplantation to different anatomical sites, indicating additional factors, such as SVF content, may contribute to functional heterogeneity.[8] While many studies focus on WAT transcriptome, proteome or secretome, limited information exists on the cellular composition of individual depots. Given the metabolic and immunological relevance of

V-WAT, there is clearly a need for elucidation of *depot-specific* SVF composition and gene expression profiles in order to provide a more comprehensive understanding of these distinct microenvironments within the peritoneal cavity. Here, we utilized fluorescence-activated cell sorting (FACS) to comparatively characterize the SVF of parametrial WAT (pmWAT), retroperitoneal WAT (rpWAT), omental WAT (omWAT), and the peritoneal serous fluid (PSF), to determine whether they represent unique microenvironments. We also performed qRT-PCR to assess differences in the gene expression profiles. Our results suggest that pmWAT, rpWAT, omWAT, and PSF represent distinct microenvironments with unique cellular composition in the homeostatic state, supporting our hypothesis that distinct fat depots possess inherent properties that may differentially impact disease states.

Methods

Animals

Female C57/BL6 mice (Harlan Laboratories) were housed five per cage in a controlled environment (12 hour light/dark cycle at 21°C) with free access to water and food (18% protein rodent chow, Teklad Diets). Mice were sacrificed at 24 weeks of age (27g average body weight) by CO_2 asphyxiation. All animal procedures were approved by the Virginia Tech Institutional Animal Care and Usage Committee.

Adipose tissue and peritoneal serous fluid harvest

PmWAT, rpWAT and omWAT were harvested from each mouse, weighed, rinsed with calcium- and magnesium-deficient phosphate buffered saline ($PBS^{-/-}$), and processed for FACS or placed into RNAlater (Qiagen) and stored at -80°C. Resident peritoneal cavity cells were collected via peritoneal lavage with 5ml of $PBS^{-/-}$. The effluent was

centrifuged, subjected to erythrocyte lysis (155mM NH_4Cl, 10mM $KHCO_3$, 0.1mM EDTA),[2] and further processed as described below.

Tissue Digestion

SVF from individual fat depots (n=10) were isolated from digested tissue[9,10] with minor modifications to improve yields. OmWAT was digested in GKN-buffer containing 1.8mg/ml Type IV collagenase, 10% FBS, and 0.1mg/ml DNase. The pmWAT and rpWAT digest buffer included a 1:1 ratio of Krebs-Ringer bicarbonate buffer and collagenase solution (1mg type I collagenase, 10mg BSA, and 2mM $CaCl_2$ in 1ml PBS). Following digest at 37°C for 45 min, cells were passed through a 40µm cell strainer, and erythrocytes were lysed.

FACS Analysis

Cell suspensions were washed in flow buffer (2% BSA in $PBS^{-/-}$), blocked with Fc block (BD Biosciences) for 10 minutes at 4°C, rinsed and subsequently incubated with fluorochrome-labeled antibody combinations (available upon request) for 20 min at 4°C. Fluorochrome-labeled antibodies specific for mouse CD45, CD11b, CD11c, F4/80, Ly6C, MHCII, CD34, CD31, CD4, CD44, CD62L, CD25, CD69, B220, CD19, NK1.1, CD73, Flk-1 and Ly6G were obtained from eBioscience (San Diego, CA). CD105 and Ly6a/e antibodies were obtained from BioLegend (San Diego, CA) and Ly6G, CD3, CD8, CD80, CD117 and MR antibodies were obtained from BD Biosciences (San Jose, CA). Prior to analysis, cells were washed twice and resuspended in $PBS^{-/-}$ with propidium iodide for dead cell exclusion. FACS was performed on a FACSAria (BD Biosciences) and data was analyzed using Flowjo (TreeStar) software.

RNA extraction

WAT was homogenized in Qiazol (Qiagen), and RNA was purified using an RNeasy Lipid Tissue Kit (Qiagen), according to manufacturer's instructions. RNA concentration was determined using a NanoDrop1000 spectrophotometer.

Quantitative real-time PCR

RNA (n=6 per tissue) was subjected to the iScript cDNA synthesis system (Biorad) according to manufacturer's protocol. qRT-PCR was performed with 12.5ng cDNA per sample using gene-specific SYBR Green primers (primer sequences are available upon request) designed with Beacon Design software. SensiMix SYBR and Fluorescein mastermix (Quantace) was used in a 15μL reaction volume. qRT-PCR was performed for 42 cycles at 95°C for 15 sec, 58-60°C for 15 sec, and 72°C for 15 sec, preceded by a 10 min incubation at 95°C on the ABI 7900HT (Applied Biosystems). Melt curves were performed to ensure fidelity of the PCR product. The housekeeping gene was L19 and the ddCt method[11] was used to determine fold differences.

Statistical Analysis

Data was expressed as mean ± standard error of mean (SEM). FACS and qRT-PCR data were analyzed using a one-way ANOVA coupled with a Tukey Post-hoc test in Graphpad Prism. Differences were considered statistically significant at $p<0.05$.

Results

To date, studies investigating the contribution of V-WAT to various diseases have often used intra-abdominal fat pads interchangeably. Considering the reported differences between S-WAT and V-WAT, we believe it is important to determine whether intra-abdominal fat pads are indeed similar with respect to their SVF cellular composition, or represent unique signaling microenvironments that may differentially impact intra-

peritoneal processes. Here, we use pmWAT due to its widespread application in murine studies, omWAT due to its classification as a "true" visceral fat and importance in immunological surveillance, and rpWAT due to its characterization as a non-visceral intra-abdominal fat depot with a human counterpart.

Seven-month old female C57/BL6 mice were chosen to match the endpoint of many WAT studies that place young mice on specialized treatment regimens for several weeks or months.[12-15] This age also allows sufficient fat accumulation for comprehensive FACS analysis of the SVF. Additionally, female mice were utilized because of gender-related differences in adipose accumulation and the importance of omWAT in gynecological diseases, such as ovarian cancer.[14,16]

Fat depot size and cellularity

As expected, pmWAT was the largest fat depot while omWAT represented the smallest (Figure 3.1 A). Despite its significantly smaller size, omWAT yielded total numbers of SVF cells similar to pmWAT, whereas rpWAT had a significantly smaller SVF population ($p<0.0001$) (Figure 3.1 B). Thus, 20 times more SVF cells *per milligram of tissue* were isolated from omWAT, as compared to pmWAT ($p=0.009$) or rpWAT ($p=0.01$) (Figure 3.1 C).

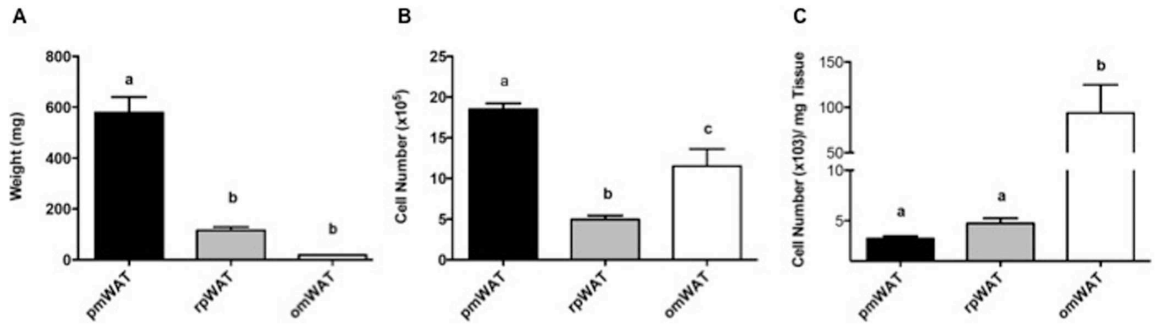

Figure 3.1. Adipose tissue depot weight and SVF cell counts. (A) Whole tissue weight. (B) Total number of SVF cells isolated from the digestion of each tissue. (C) Number of SVF cells isolated from the digestion of each milligram (mg) of adipose tissue. pmWAT; parametrial WAT,

rpWAT; retroperitoneal WAT, omWAT; omental WAT. [a,b,c] Unlike letters indicate significance, p,0.05.

Fat depot SVF characterization

Individual fat depots were characterized via FACS analysis to identify depot-specific differences; PSF was included as an established immunologically active microenvironment present within the peritoneal cavity.[17,18] Leukocyte subsets were identified based on well-defined surface markers (Figure 3.2). First, viable cells (propidium iodide exclusion) were separated into $CD45^+$ leukocytes and $CD45^-$ stromal constituents. The $CD45^+$ population was subsequently separated into R1 (lymphocyte) and R2 (monocyte/granulocyte) gates based on forward/side scatter (Figure 3.2 A). T-lymphocyte subsets within the $CD3^+$ fraction (R1) were further separated into $CD4^+$ T-helper (T_h) cells, $CD8^+$ T-cytotoxic (T_c) cells, $NK1.1^+$ natural killer T-cells (NKT), or $CD4^-CD8^-$ double-negative (DN) cells (Figure 2b). $CD19^+$ B-cells, distributed within both the R1 and R2 gates, were gated into B1 ($B220^{lo/+}CD11b^+$) and B2 ($B220^{lo/+}CD11b^-$) subsets (Figure 3.2 C). Monocyte/granulocyte populations (R2) were classified based on CD11b, CD11c and F4/80 staining, followed by analysis of additional surface markers (Ly6C, Ly6G, mannose receptor [MR], CD80, CD69 and CD93) (Figure 3.2 D).

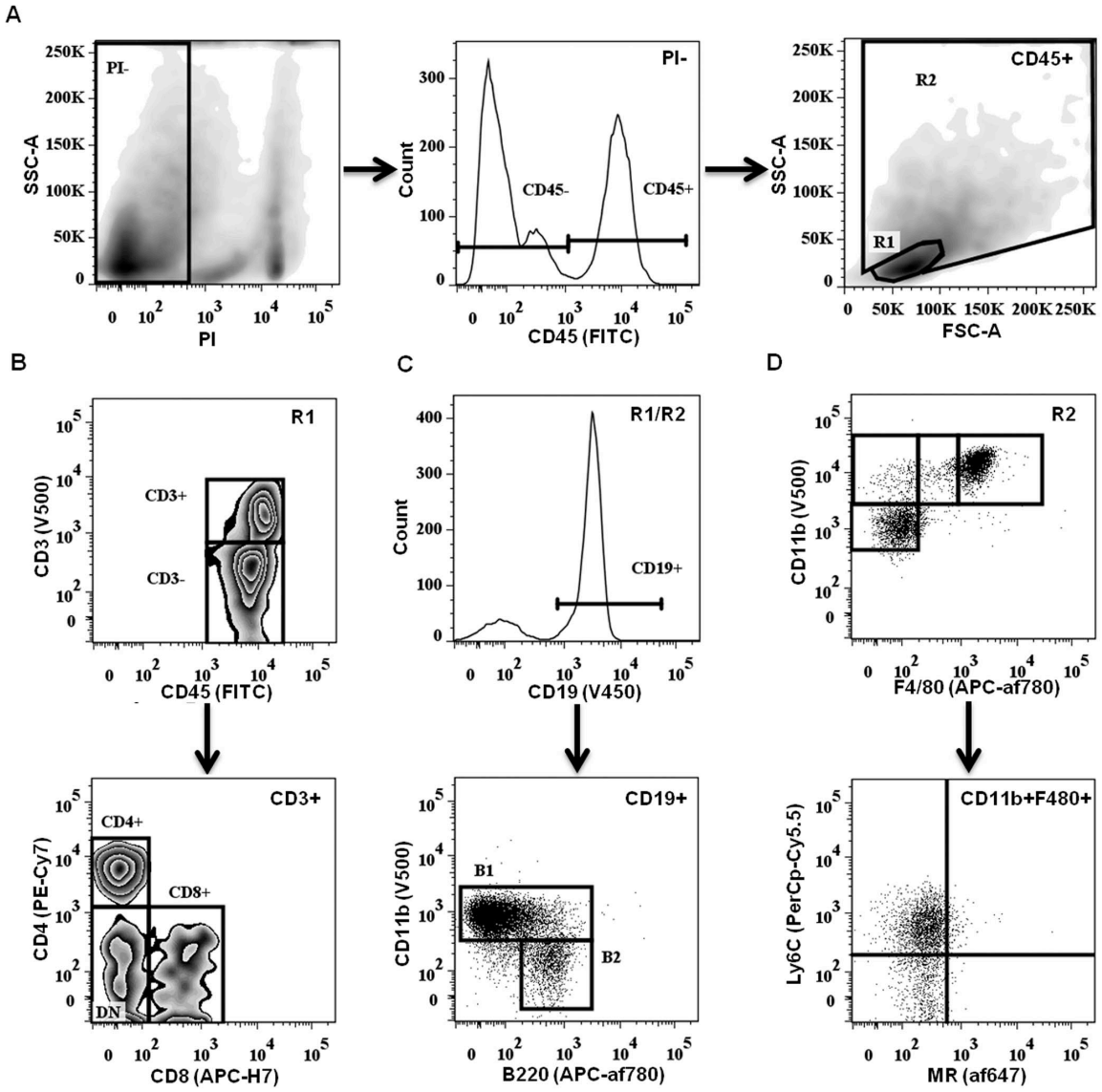

Figure 3.2. Flow cytometric analysis gating strategy. (A) Digested tissue samples were subjected to PI live/dead cell exclusion and $CD45^+$ leukocytes were divided into R1 (lymphocytes) and R2 (mono-, granulocytes) gates based on forward/side scatter followed by doublet exclusion. (B) $CD3^+$ T cells from R1 were further subclassified either as CD4+ T_H, $CD8^+$ T_C or DN (double negative). (C) CD19+ B cells from R1 and R2 were further subclassified into $CD11b^+$ B1 or CD11b2 B2. (D) Monocytic populations from R2 were classified based on CD11b, F4/80 and CD11c (not shown) staining, and further subdivided based on activation markers.

Table 3.1. Leukocyte characterization of immune microenvironments

Cell Type (origin)	Markers	pmWAT	rpWAT	omWAT	PSF
$CD45^+$ (of viable)		38.1 (3.6)	38.1 (2.5)	75.4 (1.2)	99.1 (0.3)
Lymphocytes (R1)		29.0 (3.1)	29.1 (3.0)	53.0 (8.3)	62.0 (1.1)
Mono/Granulocytes (R2)		62.2 (3.0)	61.1 (3.5)	39.3 (8.3)	34.7 (3.1)
B1-B	$CD19^+CD11b^+B220^{lo/+}$	11.5 (1.7)	40.0 (2.1)	25.0 (1.1)	38.1 (1.2)
B2-B	$CD19^+CD11b^-B220^{lo/+}CD5^-$	0.9 (0.2)	2.2 (0.4)	7.1 (0.9)	4.9 (0.8)
T_H	$CD3^+CD4^+$	4.6 (0.8)	3.7 (0.6)	12.8 (1.8)	3.1 (0.2)
T_C	$CD3^+CD8^+$	1.2 (0.1)	1.2 (0.2)	3.9 (0.5)	0.7 (0.1)
NKT	$CD3^+NK1.1^+$	0.9 (0.1)	0.7 (0.1)	0.6 (0.1)	0.3 (0.1)
T_{REG}	$CD3^+CD4^+CD25^+$	0.8 (0.3)	1.5 (0.4)	2.5 (0.2)	1.6 (0.2)
$CD3^+CD4^-CD8^-NK1.1^-$		2.4 (0.2)	2.3 (0.4)	4.5 (0.4)	0.4 (0.1)
Myeloid precursors	$CD3^-B220^-NK1.1^-CD11b^{hi}$	5.1 (0.6)	5.2 (0.4)	4.8 (0.3)	2.0 (0.1)
mNK	$NK1.1^+CD11b^+CD3^-$	3.4 (0.3)	3.0 (0.3)	1.4 (0.2)	1.3 (0.1)
preNK	$NK1.1^+CD11b^-CD3^-$	0.9 (0.1)	0.5 (0.1)	0.6 (0.1)	0.1 (0.04)
DCs(I)	$CD11c^+CD11b^{lo/+}$	6.7 (0.4)	8.3 (0.5)	7.6 (0.7)	4.6 (0.4)
DCs (II)	$CD11b^{+/lo}CD11c^+F4/80^-$	3.7 (1.5)	11.3 (6.4)	11.5 (4.0)	3.8 (1.5)
LPMs	$CD11b^+F4/80^+$	3.6 (0.6)	3.1 (0.5)	1.1 (0.2)	21.0 (1.4)
SPMs	$CD11b^+F4/80^{lo}$	41.6 (2.1)	22.9 (1.2)	11.1 (1.2)	2.9 (1.1)
Monocytes (I)	$CD11b^+F4/80^-$	1.4 (0.6)	2.2 (3.8)	4.0 (1.7)	0.2 (0.1)
Monocytes (II)	$CD11b^{hi}F4/80^-$	1.4 (1.1)	4.4 (1.4)	6.1 (2.4)	5.0 (2.2)
PMNs	$CD11b^+Ly6G^+Ly6C^+$	0.4 (0.1)	0.8 (0.1)	0.04 (0.03)	0
PreBoMs	$CD19^+CD11b^{hi}B220^{lo}F480^+CD93^+CD69^+$	0	0	0	0.7 (0.1)

Data are presented as % of total $CD45^+$ (+/− standard error of the mean). pmWAT, parametrial fat; rpWAT, retroperitoneal fat; omWAT, omental fat; and PSF, peritoneal serous fluid. T_H, Helper T cells; T_C, cytotoxic T cells; NKT, natural killer T cells; T_{REG}, regulatory T cells; DCs, dendritic cells; LPMs, large peritoneal macrophages; SPMs, small peritoneal macrophages; PMNs, neutrophils; and PreBoMs, pre-B or –macrophage cells.

Markers defining specific populations and distribution of leukocyte subsets within the respective fat pads are detailed in Figure 3.3. The compositional profiles of individual fat depots were clearly different, supporting the hypothesis that each fat depot is a unique microenvironment harboring distinct immune cell populations. All three fat depots contained a large $CD45^-$ population within the SVF, whereas the PSF was limited to $CD45^+$ leukocytes (99.1%). Consistent with its role as a secondary lymphoid organ, omWAT contained a twofold higher $CD45^+$ population than pmWAT and rpWAT ($p<0.001$).

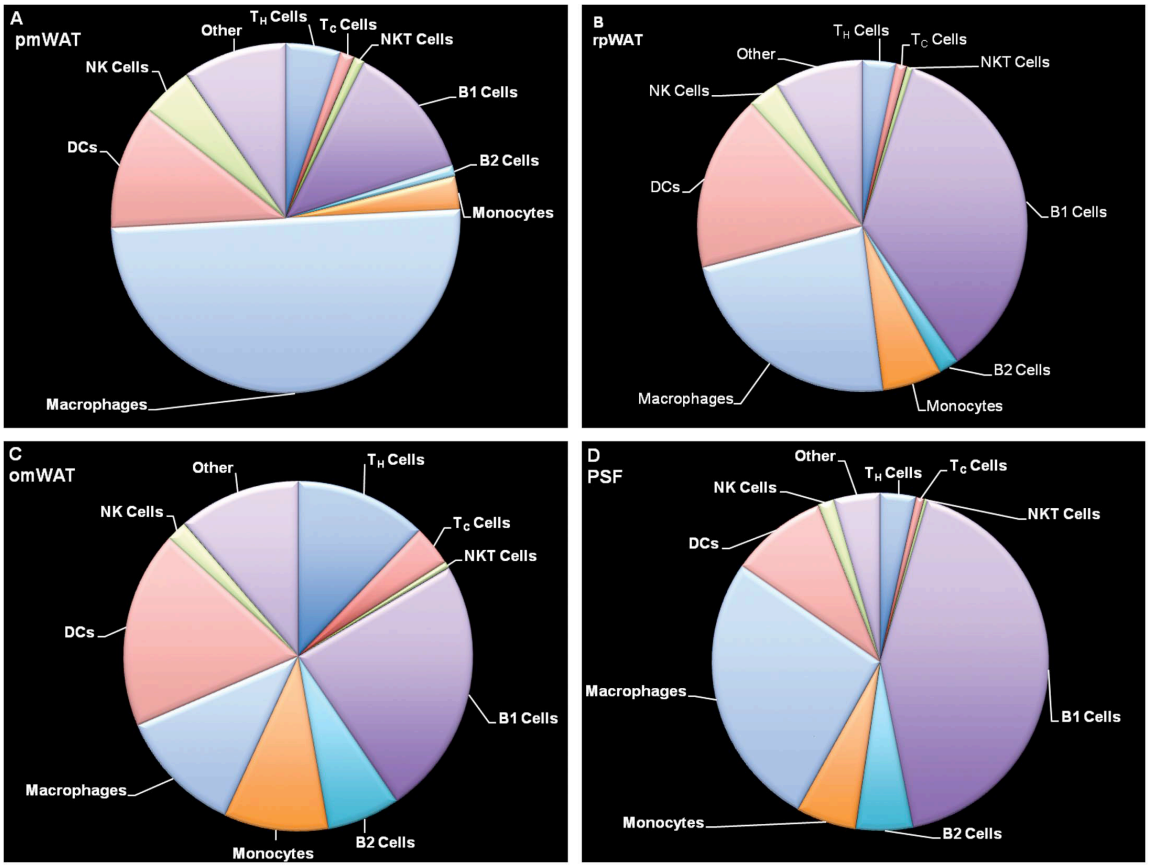

Figure 3.3. Flow cytometric analysis of leukocyte populations in the SVF of (A) pmWAT, (B) rpWAT, (C) omWAT and (D) PSF. Natural killer (NK) cells include mNKs and preNKs, dendritic cells (DC) include DC (I) from R1 and DC (II) from R2, macrophages include large (LPMs) and small (SPM) peritoneal macrophages, monocytes include monocytes (I) ($CD11b^{+}F4/80^{+}$) and monocytes (II) ($CD11b^{lo}F4/80^{-}$) populations, and ‘‘other’’ includes regulatory T cells (Treg), $CD3^{+}CD4^{+}CD8^{+}NK1.1^{+}$ subset, and myeloid precursors from R1, as well as neutrophils (PMNs), and pre-B or –macrophage cells (PreBoMs) from R2.

Overall Distribution

Of total compartmental leukocytes, pmWAT contained the highest proportion of macrophages (Mθs) (45.2%), with smaller populations of B-cells (12.9%), T-cells (8.2%) and monocyte subsets (2.8%) (Figure 3). The immune composition of rpWAT displayed distinct similarities (larger B1- and dendritic cell (DC) and monocyte populations) to omWAT whereas T- and natural killer (NK) cell frequencies (7.3%; 3.5%) more closely matched those of pmWAT, its non-visceral counterpart. OmWAT had proportionally

more T-cells (21.5%), DCs (19.1%) and B-cells (35.5%) than pmWAT or rpWAT (Figure 3). Confirming previous reports[17], PSF contained a large proportion of B1-cells (38.1%), Mθs (21.0%) and DCs (8.7%), consistent with ongoing immunosurveillance in the peritoneal cavity (Figure 3.3).

Lymphocyte Characterization

T-cells were most heavily represented in omWAT, consistent with its role in antigen presentation and development of cell-mediated responses.[19] This corresponds to high expression of *Ccl21*, a chemoattractant important in the homing of T-cells to lymphoid organs. PmWAT and rpWAT had threefold fewer T-cells ($p<0.0001$) than omWAT, although the T_h:T_c ratio in all four microenvironments was 4:1. There were no significant depot-specific differences within the memory ($CD44+/CD62L^{+/-}$) or naïve ($CD44^{-}/CD62L^{+}$) T_h or T_c subsets (data not shown). The proportion of NKT-cells was significantly lower in PSF than all fat depots ($p<0.001$). Interestingly, the majority (>60%) of NK-cells within all four compartments were $CD94^{hi}$, which has recently been associated with increased proliferation, production of IFNy, and target cell lysis.[20] Further, the $CD27^{hi}$ subset of mature NK (mNK) cells in omWAT was twofold higher ($p<0.001$, data not shown) than the other microenvironments. CD27 expression has been linked to increased responsiveness to chemokines and interactions with DCs, again consistent with the role of omWAT as a major peritoneal immunosurveillance organ.[21]

Monocyte/Granulocyte Characterization

Within the R2 gate, four populations based on relative CD11b and F4/80 expression were discernible. Previous reports have described two functionally distinct macrophage subsets within the PSF: the "large peritoneal macrophages" (LPMs), named

for their increased forward/side scatter (predominant in the homeostatic state), and "small peritoneal macrophages" (SPMs) which increase following LPS stimulation.[22] The largest R2 population present within the PSF was the $CD11b^{+}F4/80^{+}$-LPMs, (61.7%), followed by $CD11b^{+}F4/80^{lo}$-SPMs, and $CD11b^{+}F4/80^{-}$- (I) and $CD11b^{lo}F4/80^{lo}$-monocyte (II) populations present at 8.3%, 3.5%, and 23.5%; respectively (Figure 3.4 A, B).

In contrast, the predominant R2 population in pmWAT was SPMs (77.7%), with minor populations of LPMs (7.0%) and monocytes (I and II) (7.6%; 5.4%). Similarly, in rpWAT the SPM population was predominant (42.4%), with LPMs representing only 5.7% of total cells within the R2 gate. However, the monocytic (I and II) subsets represented a significant proportion (31.7%, and 17.1%; respectively) of the R2 gate. The omWAT R2 composition was also defined by a predominant SPM subset (30.9%), with the LPMs and monocytes (I and II) comprising 3.1%, 27.9%, and 34.6%; respectively.

A CD80/MR expression profile was used to evaluate depot-specific differences in macrophage activation status. SPMs residing within PSF and omWAT expressed CD80, whereas pmWAT and rpWAT SPMs were $CD80^{-}$. MR expression was only noted in SPMs isolated from PSF, omWAT and rpWAT (Figure 3.4 C). This further suggests that depot-specific factors inherently contribute to activation or differentiation of their inherent SVF leukocytes.

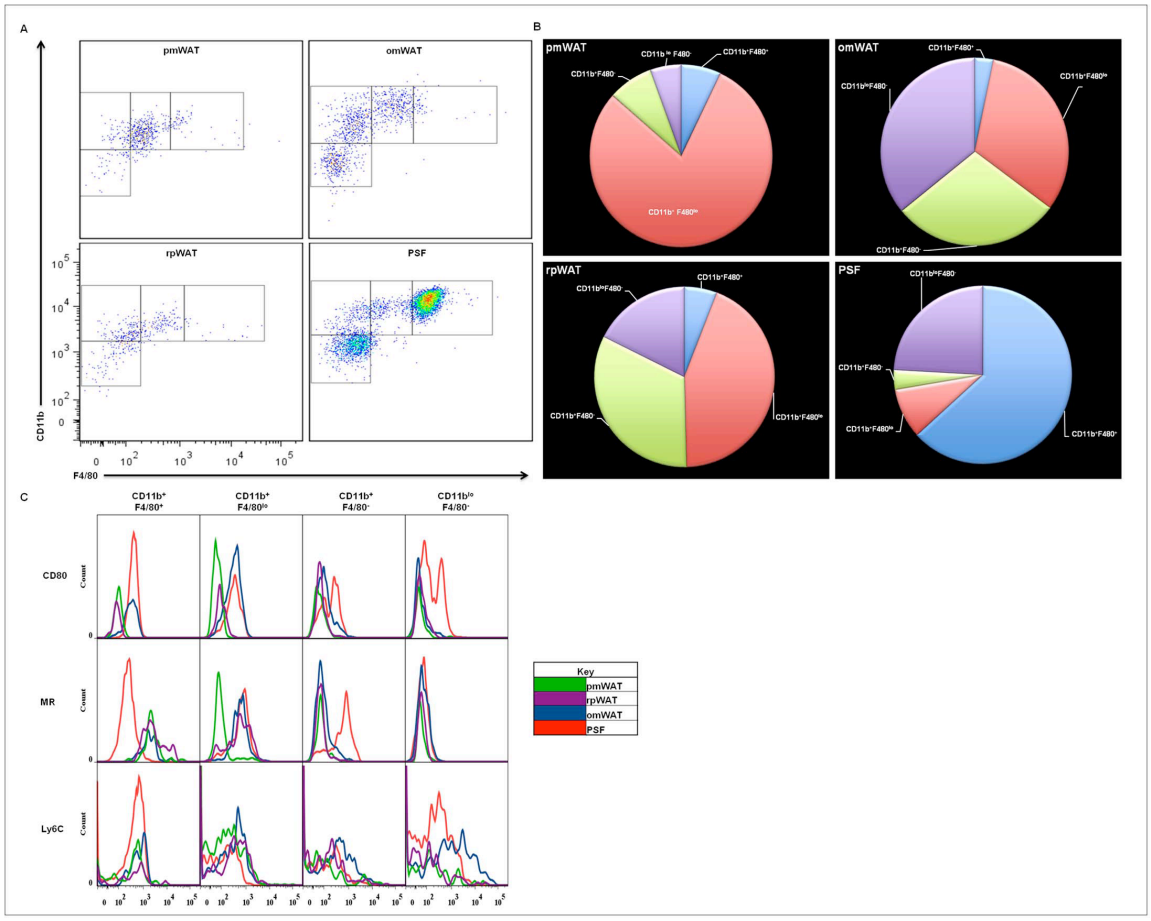

Figure 3.4. Myeloid populations found in pmWAT, rpWAT, omWAT and PSF. (A) Resident myeloid populations differ in a microenvironment specific manner. (B) Differential CD11b and F4/80 expression displayed as a percentage of total R2 gate. (C) Activation status of respective myeloid populations differ in a microenvironment-specific manner.

PreBoMs

During analysis, a small, distinct $CD45^{+}$ cell population (0.7%) was identified within the PSF that was not present in the fat depots. We refer to this subset as "PreBoMs" (pre-B or -macrophages) due to their expression of unique and potentially novel surface markers (Figure 3.5). These cells were $CD19^{+}B220^{lo/+}$, expressed high levels of CD11b and were found within the R2 gate, implying a more granular phenotype. Additionally, they expressed CD93, a premature B-cell marker, and CD69, an early activation marker. Similar to the age-associated and IL-10-producing B-cells reported

recently,[23]preBoMs were CD1d^{+} and CD5^{+}. However, they also expressed F4/80, a mature macrophage marker. We were unable to evaluate CD11c expression within this population to confirm if these cells are one of the aforementioned novel B-cell subtypes, or a new subset residing within the peritoneal cavity. Because of the importance of innate-like B-cell subsets in peritoneal immunosurveillance, it needs to be determined whether this subset plays a role in metabolic disorders and peritoneal diseases.

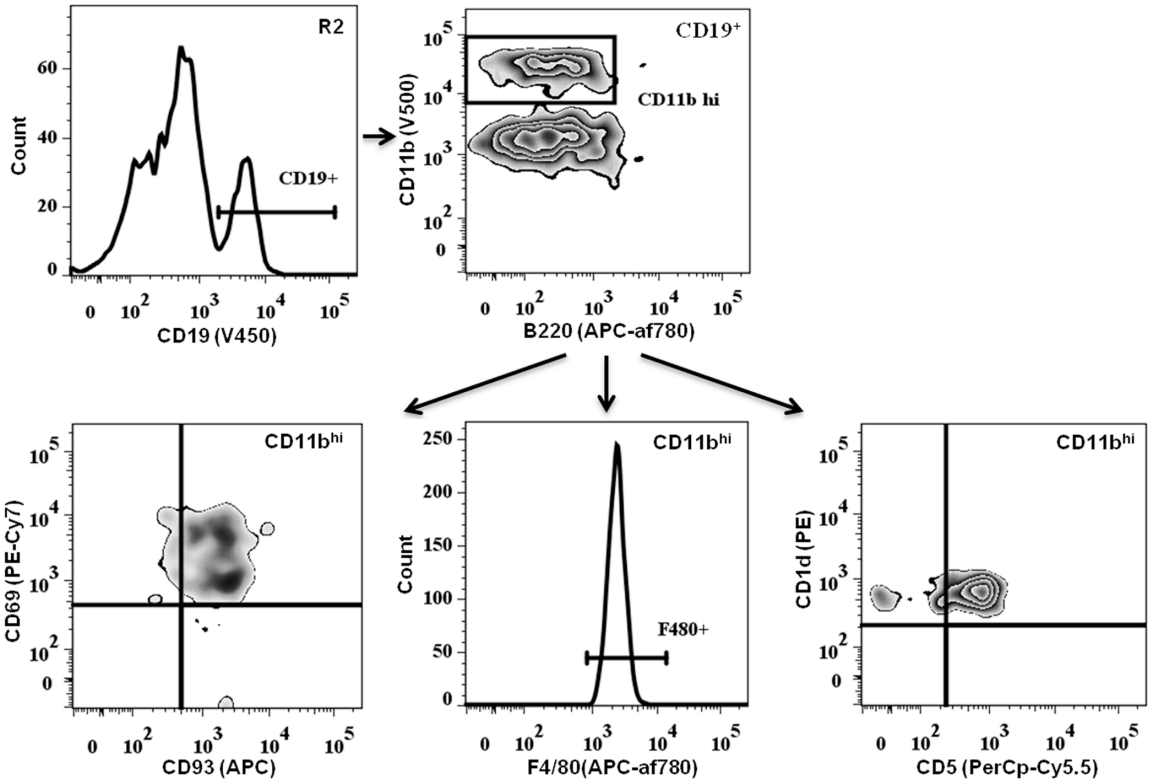

Figure 3.5. Identification of a unique CD45+ population in the PSF. Pre-B or –macrophage cells (PreBoMs) found within the R2 gate express CD19^{+}CD11b^{hi}F480^{+}CD93^{+}CD69^{+}CD1d^{+}CD5^{+} phenotype. This subset was not found in WAT.

Progenitor/Stem Populations

We also examined the prevalence of stem and progenitor cells as they may contribute to microenvironmental signaling and tissue-specific responses to energy. Additionally, they may be recruited and educated to participate in tissue repair and re-organization and may contribute to various disease states. Figure 3.6 A provides an

overview of some notable progenitor markers present on CD45$^-$ cells within pmWAT and omWAT. RpWAT did not contain a sufficient SVF content for analysis of both immune and progenitor populations in this tissue.

CD34, CD73, CD105, Sca1, CD31, and Flk1 were all differentially expressed in pmWAT and omWAT ($p<0.05$) (Figure 3.6 A). Of note, CD45$^-$CD105$^+$CD73$^+$ mesenchymal stem cells (MSCs)[24] were more prominent in omWAT ($p<0.0001$), while CD45$^-$Sca1$^+$CD34$^+$ adipocyte precursor cells (APCs)[25] and CD45$^-$ CD105$^+$CD31$^+$Sca1$^+$CD117$^+$ endothelial progenitor cells (EPCs)[26] were higher in pmWAT (both $p<0.0001$). However, based on total cell numbers, pmWAT contained a higher number of all three subsets due to the higher proportion of CD45$^-$ cells within the SVF (61.9% versus 24.5% respectively, $p<0.001$) (Figure 3.6 B). Thus, stem and progenitor populations may also contribute to depot-specific differences between intra-abdominal adipose tissues.

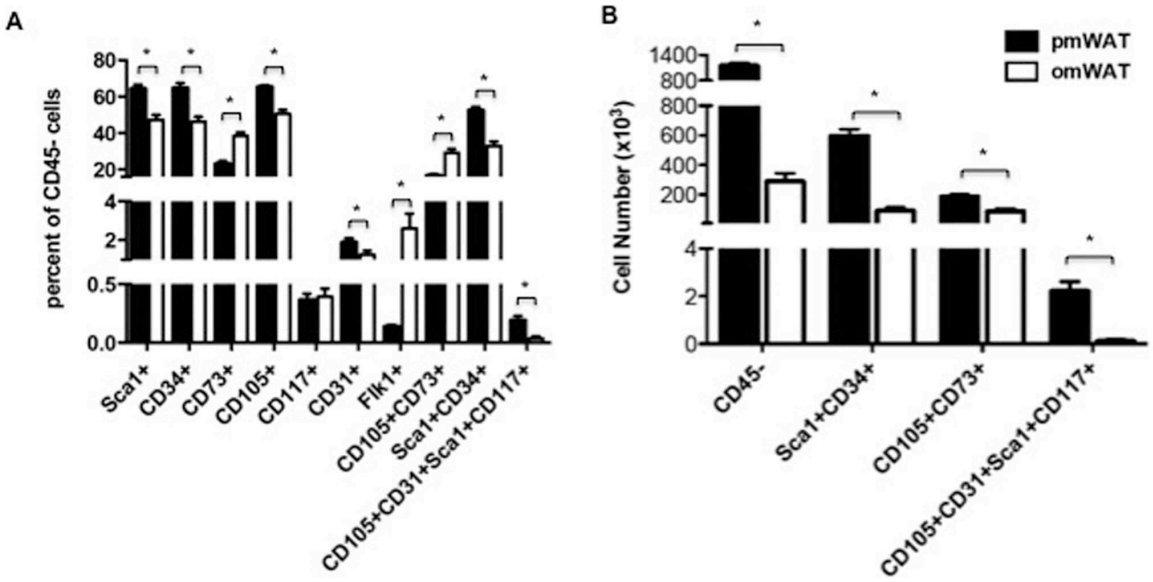

Figure 3.6. Flow cytometric analysis of stem and progenitor cell markers. (A) Percentage of CD452 cells that are positive for indicated markers. (B) Total number of SVF cells positive for selected markers in pmWAT and omWAT.

Fat depot specific mRNA expression profile

qRT-PCR was performed to more extensively characterize the overall adipose tissue signaling milieu in these unique microenvironments. It is important to note that expression patterns represent the tissue as a whole (except in PSF), and thus are reflective of both adipocytes and SVF. A panel of inflammatory mediators, angiogenesis-associated molecules, adipokines and lipolysis-associated enzymes were used to provide an overview of genes that may contribute to depot-specific differences.

RpWAT and pmWAT exhibited highly similar mRNA expression profiles (Figure 3.7, Table 3.2), potentially due to the prevalence of adipocytes and $CD45^-$ cells. In contrast, a significant ($p<0.05$) upregulation of cytokines (*Il-1b*, *Il-2*, *Il-10*) and chemokines (*Ccl2*, Ccl5, *Ccl7*, *Ccl19*, *Cxcl1*, *Cxcl2*, *Cxcl10*, *Cxcl13*) was observed in omWAT. While this may be due in part to the large resident leukocyte population, it may also be required for active recruitment and continual maintenance of high leukocyte numbers. OmWAT also expressed significantly higher levels of *Apoe*, and lower levels of *Adipoq*, *Agt,* and *Lpl* as compared to pmWAT and rpWAT, indicating differences in lipid homeostasis regulation. Additionally, omWAT displayed increased *Hif1a* expression, which may be the result of a chronic hypoxia[16]. However, this was not associated with a concomitant increase in *Vegfa*, perhaps because *Vegfa* was already highly expressed.

PSF, which was comprised almost exclusively of $CD45^+$-leukocytes, exhibited an mRNA expression profile similar to omWAT, denoted by decreased expression of *Tnfa* and *Il5*, and increased expression of *Ccl5, Cxcl1, Cxcl2, Cxcl13,* and *Tgfb* as compared to pmWAT. However, PSF expression of *Csf1, Ifng, Rorc, Il4, Ccl4, Ccl7, Ccl21, Cxcl12, Vegfa, C3*, and *Nos3* were significantly lower than all fat depots. Additionally, *Il2, Il10,*

Ccl19, and *Cxcl10* were significantly upregulated ($p<0.05$) in omWAT, but were significantly downregulated ($p<0.05$) in PSF. As anticipated, PSF was more similar to omWAT, which acts as its filtration system, than the other fat pads. However, as PSF is composed of primarily leukocytes, the cellular components and interactions among cell types in the two microenvironments are very different, resulting in unique expression profiles.

Table 3.2 Gene expression profiles of immune microenvironments

Gene	rpWAT	omWAT	PSF
Tnfa	0.50 (0.67)	−3.84 (0.39)*	−9.17 (1.70)*
Csf1	−1.04 (0.52)	−0.90 (0.47)	−11.84 (2.05)*
Nos2	1.14 (0.65)	−17.74 (4.02)*	−134.99 (30.80)*
Ifng	−1.55 (1.24)	0.26 (0.68)	−7.76 (1.712)*
Tgfb	−1.27 (.14)	−23.33 (1.26)*	−7.84 (0.99)*
Mif	0.01 (0.62)	−2.25 (0.22)*	−1.07 (0.77)
Ido	−0.71 (1.01)	−1.61 (0.25)	−1.02 (0.76)
Rorc	1.38 (1.94)	1.66 (0.90)	−17.99 (0.50)*
Gata3	−1.69 (0.81)	−8.80 (2.92)*	−13.99 (2.46)*
Tbx21	−1.10 (0.93)	1.39 (0.65)	−0.84 (1.02)
NFkB	−0.31 (0.74)	3.02 (0.24)*	4.62 (1.02)*
Il1b	0.20 (1.12)	114.42 (78.18)*	9.57 (7.71)
Il2	−1.80 (1.57)	6.36 (1.49)*	−6.19 (2.18)*
Il4	−6.31 (4.47)	−1.57 (0.72)	−6.10 (1.81)*
Il5	−0.84 (0.85)	−3.38 (0.59)*	−24.54 (7.77)*
Il6	−0.55 (0.69)	1.86 (0.70)	0.85 (0.85)
Il10	−1.00 (0.54)	9.62 (1.73)*	−2.58 (0.62)*
Il12a	0.50 (0.66)	−1.88 (0.25)	−0.31 (0.88)
Ccl2	2.29 (1.53)	67.59 (33.34)*	−2.80 (1.64)
Ccl3	−0.85 (0.81)	−1.82 (0.67)	14.30 (5.41)*
Ccl4	−2.44 (0.50)	2.39 (0.35)	−14.10 (4.18)*
Ccl5	−1.00 (0.50)	11.65 (2.08)*	2.73 (1.08)*
Ccl7	0.52 (0.97)	1.86 (2.0)*	−214.80 (112.99)*
Ccl19	−0.47 (0.80)	5.76 (0.90)*	−42.96 (10.35)*
Ccl21	−10.27 (5.81)*	−3.46 (1.60)	−4387.09 (1360.31)*
Cxcl1	2.95 (0.56)	54.61 (20.49)*	5.52 (2.07)*
Cxcl2	3.36 (0.90)	32.22 (15.48)*	96.50 (37.33)*
Cxcl10	−0.089 (0.87)	4.72 (0.86)*	−46.87 (12.43)*
Cxcl12	−2.32 (0.42)*	−0.98 (0.51)	−21.79 (3.19)*
Cxcl13	2.06 (1.08)	488.67 (56.84)*	67.45 (19.31)*
Crp	−2.18 (1.69)	22.73 (13.83)*	4.03 (1.77)
Prom1	0.51 (0.77)	−0.15 (1.10)	−17.06 (4.83)
IL1rn	1.27 (2.10)	50.39 (24.96)*	3.31 (0.99)
Vegfa	1.05 (0.53)	−1.64 (1.62)	−255.32 (31.63)*
Hif1a	−0.89 (0.51)	74.87 (10.38)*	33.99 (5.56)*
Nos3	1.25 (0.60)	−2.25 (0.52)	−112.30 (40.96)*
Lep	3.65 (1.19)	−4.62 (2.16)	−1233.93 (376.92)*
Adipoq	1.78 (0.24)	−31.56 (5.28)*	−287768.13 (57680.49)*
Retn	2.25 (0.20)*	−2.08 (0.45)	−28554.69 (8773.49)*
Agt	1.29 (0.13)	−3.14 (0.77)*	−31365.74 (0.00)*
Apoe	1.50 (0.26)	5.64 (0.46)*	5.55 (1.63)*
C3	−1.75 (0.85)	2.49 (0.38)	−17.65 (5.20)*
Msr1	−1.32 (0.14)	−0.99 (0.46)	−1.43 (0.67)
Lpl	2.21 (0.25)*	−3.76 (1.10)	−22.46 (0.74)

Data are presented as fold changes compared to pmWAT (± standard error of the mean), *$p<0.05$.

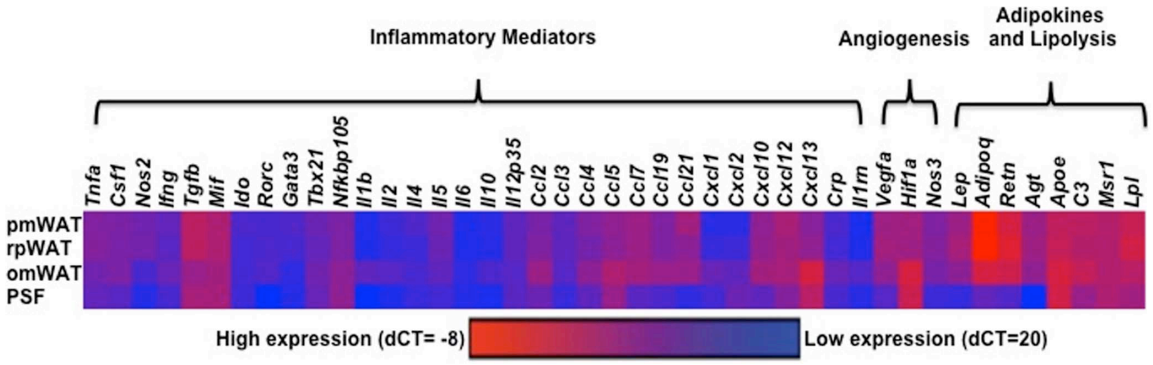

Figure 3.7. Heat map of mRNA expression profiles of adipose tissue depots (based on dCT values).

Discussion

Adipose tissue is a highly active and functionally diverse endocrine organ. V-WAT has been strongly associated with various metabolic disorders and certain cancers,[1,4] although the contribution of individual V-WAT depots to physiologic and pathologic functions is poorly understood. Here, we characterized SVF composition and homeostatic gene expression profiles of three intra-abdominal fat pads to determine depot-specific differences, as this may critically impact their functionality. This study highlights the unique immune profile of intra-abdominal fat depots and supports our hypothesis that they may each have distinct roles in biological functions and disease pathogenesis and thus should be evaluated independently.

In agreement with the previous designation of pmWAT and rpWAT as non-visceral intra-abdominal fat pads, the initial compositional profile of leukocytes based on lymphocyte (R1) versus monocyte/granulocyte (R2) fractions revealed an identical 1:2 ratio, while omWAT and PSF displayed a ratio of 3:2. This indicates that lymphocytes are the predominant leukocyte population in omWAT and PSF, while the monocytes/granulocyte fraction is dominant in pmWAT and rpWAT. However, upon further evaluation, high numbers of B1-cells were found within the R2 gate of rpWAT.

Although the R1:R2 ratios of pmWAT and rpWAT are very similar, when expressed as a proportion of total T- and B-cells, the immune cell composition of rpWAT more closely resembles that of omWAT and PSF. This was unexpected as the omWAT is considered "true" V-WAT while rpWAT has been described as a non-visceral intra-peritoneal fat pad.

B1-lymphocytes play an important role in immunosurveillance in the peritoneal cavity and are considered "innate-like" B-cells, possessing pattern recognition receptors to conserved bacterial and viral epitopes.[27] In naïve animals, there is a constant flux of B1-cells between omWAT and the PSF. However, their presence in other intra-abdominal fat pads has not been reported. Unexpectedly, we found a large proportion of B1-cells in rpWAT, comparable to PSF and higher than omWAT. Additionally, rpWAT expressed higher levels of IL-5, a stimulator of B-cell growth and immunoglobulin secretion,[28] than omWAT. In concordance with FACS data, qRT-PCR indicated constitutively high expression of CXCL13, a chemoattractant for B1-cells,[29] in all four microenvironments. Together, this suggests that the rpWAT may serve a yet undefined function in peritoneal B-cell immunomodulation.

An unexpected finding during the course of this study was the appearance of $CD19^{+}F4/80^{+}B220^{lo}CD11b^{hi}CD1d^{+}CD5^{+}D93^{+}CD69^{+}$ cells, which we have named PreBoMs based on their expression of B-cell-, macrophage- and progenitor-specific markers. It is unclear if this population represents the IL-10-producing regulatory (recently reported in spleen and PSF)[30,31]or age-associated B-cells (reported in spleen only),[32] since the expression of F4/80 has not been reported in either cell type. Further

analysis is needed to determine whether this PreBoM population is indeed a novel B-cell-like subset within the peritoneal cavity.

The $CD45^-$ component of the SVF includes fibroblasts, endothelial cells, and stem and progenitor populations. Adipose-associated stem and progenitor cells have been implicated in various biological processes and pathological conditions.[33,34] While not comprehensive, our analysis highlights significant depot-specific stem/progenitor populations present in pmWAT and omWAT. The higher numbers of MSCs, APCs, and EPCs in pmWAT suggest that it may be a more abundant source of recruitable stem/progenitor cells. Similar to fat depot-specific leukocyte trafficking, unique signaling milieus may account for differences in progenitor populations. More in-depth depot-specific analyses are warranted to determine the local and systemic implications of these populations in individual fat depots, particularly in the context of human disease states.

Conclusion

In summary, our results support the hypothesis that intra-abdominal fat pads represent distinct signaling microenvironments, each serving as its own "mini-organ".[35] In agreement with previous reports indicating important functional differences between true visceral and non-visceral intra-abdominal fat pads in various metabolic disorders, we have found distinct differences in the SVF even within these subgroups. Our comparison of SVF composition, as well as overall gene expression of pmWAT, rpWAT, and omWAT, indicate that intra-abdominal fat depots cannot be used interchangeably. Hence, a comprehensive characterization of these immunomodulatory microenvironments should provide insights into depot-specific impacts on peritoneal disease states.

References

1. Caspar-Bauguil S, Cousin B, Galinier A, et al. Adipose tissues as an ancestral immune organ: site-specific change in obesity. *FEBS Lett.* Jul 4 2005;579(17):3487-3492.

2. Park HT, Lee ES, Cheon YP, et al. The relationship between fat depot-specific preadipocyte differentiation and metabolic syndrome in obese women. *Clin Endocrinol (Oxf).* Jan 2012;76(1):59-66.

3. Baglioni S, Cantini G, Poli G, et al. Functional differences in visceral and subcutaneous fat pads originate from differences in the adipose stem cell. *PLoS One.* 2012;7(5):e36569.

4. Montague CT, Prins JB, Sanders L, et al. Depot-related gene expression in human subcutaneous and omental adipocytes. *Diabetes.* Sep 1998;47(9):1384-1391.

5. Lee MJ, Wu Y, Fried SK. Adipose tissue heterogeneity: implication of depot differences in adipose tissue for obesity complications. *Mol Aspects Med.* Feb 2013;34(1):1-11.

6. Foster MT, Shi H, Softic S, Kohli R, Seeley RJ, Woods SC. Transplantation of non-visceral fat to the visceral cavity improves glucose tolerance in mice: investigation of hepatic lipids and insulin sensitivity. *Diabetologia.* Nov 2011;54(11):2890-2899.

7. Wueest S, Yang X, Liu J, Schoenle EJ, Konrad D. Inverse regulation of basal lipolysis in perigonadal and mesenteric fat depots in mice. *Am J Physiol Endocrinol Metab.* Jan 1 2012;302(1):E153-160.

8. Foster MT, Shi H, Seeley RJ, Woods SC. Transplantation or removal of intra-abdominal adipose tissue prevents age-induced glucose insensitivity. *Physiol Behav.* Sep 1 2010;101(2):282-288.

9. Berberich S, Dahne S, Schippers A, et al. Differential molecular and anatomical basis for B cell migration into the peritoneal cavity and omental milky spots. *J Immunol.* Feb 15 2008;180(4):2196-2203.

10. Yu G, Wu X, Kilroy G, Halvorsen YD, Gimble JM, Floyd ZE. Isolation of murine adipose-derived stem cells. *Methods Mol Biol.* 2011;702:29-36.

11. Livak KJ, Schmittgen TD. Analysis of relative gene expression data using real-time quantitative PCR and the 2(-Delta Delta C(T)) Method. *Methods.* Dec 2001;25(4):402-408.

12. Wueest S, Schoenle EJ, Konrad D. Depot-specific differences in adipocyte insulin sensitivity in mice are diet- and function-dependent. *Adipocyte.* Jul 1 2012;1(3):153-156.

13. Kwon EY, Shin SK, Cho YY, et al. Time-course microarrays reveal early activation of the immune transcriptome and adipokine dysregulation leads to fibrosis in visceral adipose depots during diet-induced obesity. *BMC Genomics.* 2012;13:450.

14. Brake DK, Smith EO, Mersmann H, Smith CW, Robker RL. ICAM-1 expression in adipose tissue: effects of diet-induced obesity in mice. *Am J Physiol Cell Physiol.* Dec 2006;291(6):C1232-1239.

15. Kawanishi N, Yano H, Yokogawa Y, Suzuki K. Exercise training inhibits inflammation in adipose tissue via both suppression of macrophage infiltration and acceleration of phenotypic switching from M1 to M2 macrophages in high-fat-diet-induced obese mice. *Exerc Immunol Rev.* 2010;16:105-118.
16. Gerber SA, Rybalko VY, Bigelow CE, et al. Preferential attachment of peritoneal tumor metastases to omental immune aggregates and possible role of a unique vascular microenvironment in metastatic survival and growth. *Am J Pathol.* Nov 2006;169(5):1739-1752.
17. Ray A, Dittel BN. Isolation of mouse peritoneal cavity cells. *J Vis Exp.* 2010(35).
18. Sandoval P, Loureiro J, Gonzalez-Mateo G, et al. PPAR-gamma agonist rosiglitazone protects peritoneal membrane from dialysis fluid-induced damage. *Lab Invest.* Oct 2010;90(10):1517-1532.
19. Rangel-Moreno J, Moyron-Quiroz JE, Carragher DM, et al. Omental milky spots develop in the absence of lymphoid tissue-inducer cells and support B and T cell responses to peritoneal antigens. *Immunity.* May 2009;30(5):731-743.
20. Yu J, Wei M, Mao H, et al. CD94 defines phenotypically and functionally distinct mouse NK cell subsets. *J Immunol.* Oct 15 2009;183(8):4968-4974.
21. Smyth MJ, Cretney E, Kelly JM, et al. Activation of NK cell cytotoxicity. *Mol Immunol.* Feb 2005;42(4):501-510.
22. Ghosn EE, Cassado AA, Govoni GR, et al. Two physically, functionally, and developmentally distinct peritoneal macrophage subsets. *Proc Natl Acad Sci U S A.* Feb 9 2010;107(6):2568-2573.
23. Rubtsova K, Marrack P, Rubtsov AV. Age-associated B cells: are they the key to understanding why autoimmune diseases are more prevalent in women? *Expert Rev Clin Immunol.* Jan 2012;8(1):5-7.
24. Dromard C, Bourin P, Andre M, De Barros S, Casteilla L, Planat-Benard V. Human adipose derived stroma/stem cells grow in serum-free medium as floating spheres. *Exp Cell Res.* Apr 1 2011;317(6):770-780.
25. Macotela Y, Emanuelli B, Mori MA, et al. Intrinsic differences in adipocyte precursor cells from different white fat depots. *Diabetes.* Jul 2012;61(7):1691-1699.
26. Fang S, Wei J, Pentinmikko N, Leinonen H, Salven P. Generation of functional blood vessels from a single c-kit+ adult vascular endothelial stem cell. *PLoS Biol.* 2012;10(10):e1001407.
27. Montecino-Rodriguez E, Dorshkind K. New perspectives in B-1 B cell development and function. *Trends Immunol.* Sep 2006;27(9):428-433.
28. Horikawa K, Takatsu K. Interleukin-5 regulates genes involved in B-cell terminal maturation. *Immunology.* Aug 2006;118(4):497-508.
29. Ansel KM, Harris RB, Cyster JG. CXCL13 is required for B1 cell homing, natural antibody production, and body cavity immunity. *Immunity.* Jan 2002;16(1):67-76.
30. Poe JC, Smith SH, Haas KM, et al. Amplified B lymphocyte CD40 signaling drives regulatory B10 cell expansion in mice. *PLoS One.* 2011;6(7):e22464.
31. Matsushita T, Tedder TF. Identifying regulatory B cells (B10 cells) that produce IL-10 in mice. *Methods Mol Biol.* 2011;677:99-111.

32. Rubtsov AV, Rubtsova K, Fischer A, et al. Toll-like receptor 7 (TLR7)-driven accumulation of a novel CD11c(+) B-cell population is important for the development of autoimmunity. *Blood.* Aug 4 2011;118(5):1305-1315.
33. Zhang Y, Daquinag, A, Traktuev, D, Amaya-Manzanares, F, Simmons, P, March, K, Pasqualini, R, Arap, W, Kolonin, M. White adipose tissue cells are recruited by experimental tumors and promote cancer progression in mouse models. *Cancer Res.* 2009;69(12):5259-5266.
34. Kidd S, Spaeth E, Watson K, et al. Origins of the tumor microenvironment: quantitative assessment of adipose-derived and bone marrow-derived stroma. *PLoS One.* 2012;7(2):e30563.
35. Tchkonia T, Lenburg M, Thomou T, et al. Identification of depot-specific human fat cell progenitors through distinct expression profiles and developmental gene patterns. *Am J Physiol Endocrinol Metab.* Jan 2007;292(1):E298-307.

SUPPLEMENTARY MATERIAL

Table S3.1 FACS analysis of intra-abdominal fat depots. PmWAT, rpWAT, omWAT and PSF.

Leukocyte Characterization (% of CD45+, +/- SE)					
	Markers	pmWAT	rpWAT	omWAT	PSF
% $CD45^+$ (of viable)		38.1 (3.6)	38.1 (2.5)	75.4 (1.2)	99.1 (0.3)
% lymphocytes		29.0 (3.1)	29.1 (3.0)	53.0 (8.3)	62.0 (1.1)
% mono/granulocytes (R2)		62.2 (3.0)	61.1 (3.5)	39.3 (8.3)	34.7 (3.1)
R1					
B cells	$CD19^+$	12.9 (1.8)	43.4 (2.2)	35.5 (1.5)	46.5 (1.2)
B1	$CD19^+CD11b^+B220^{lo/+}$	11.5 (1.7)	40.0 (2.1)	25.0 (1.1)	38.1 (1.2)
B2	$CD19^+CD11b^-B220^{lo/+}$	0.9 (0.2)	2.2 (0.4)	7.1 (0.9)	4.9 (0.8)
T cells	$CD3^+$	8.2 (0.8)	7.3 (0.8)	21.5 (1.7)	4.3 (0.4)
T_H	$CD3^+CD4^+$	4.6 (0.8)	3.7 (0.6)	12.8 (1.8)	3.1 (0.2)
T_C	$CD3^+CD8^+$	1.2 (0.1)	1.2 (0.2)	3.9 (0.5)	0.7 (0.1)
NKT	$CD3^+NK1.1^+$	0.9 (0.1)	0.7 (0.1)	0.6 (0.1)	0.3 (0.1)
T_{REG}	$CD3^+CD4^+CD25^+$	0.8 (0.3)	1.5 (0.4)	2.5 (0.2)	1.6 (0.2)
$CD3^+CD4^-CD8^-NK1.1^-$		2.4 (0.2)	2.3 (0.4)	4.5 (0.4)	0.4 (0.1)
Myeloid precursors	$CD3^-B220^-NK1.1^-CD11b^{hi}$	5.1 (0.6)	5.2 (0.4)	4.8 (0.3)	2.0 (0.1)
mNK	$NK1.1^+CD11b^+CD3^-$	3.4 (0.3)	3.0 (0.3)	1.4 (0.2)	1.3 (0.1)
preNK	$NK1.1^+CD11b^-CD3^-$	0.9 (0.1)	0.5 (0.1)	0.6 (0.1)	0.1 (0.04)
DCs(I)	$CD11c^+CD11b^{lo/+}$	6.7 (0.4)	8.3 (0.5)	7.6 (0.7)	4.6 (0.4)
R2					
DCs (II)	$CD11b^{+/lo}CD11c^+F4/80^-$	3.7 (1.5)	11.3 (6.4)	11.5 (4.0)	3.8 (1.5)
LPMs	$CD11b^+F4/80^+$	3.6 (0.6)	3.1 (0.5)	1.1 (0.2)	21.0 (1.4)
SPMs	$CD11b^+F4/80^{lo}$	41.6 (2.1)	22.9 (1.2)	11.1 (1.2)	2.9 (1.1)
Monocytes (I)	$CD11b^+F4/80^-$	1.4 (0.6)	10.2 (3.8)	4.0 (1.7)	0.2 (0.1)
Monocytes (II)	$CD11b^{lo}F4/80^-$	1.4 (1.1)	4.4 (1.4)	6.1 (2.4)	5.0 (2.2)
PMNs	$CD11b^+Ly6G^+Ly6C^+$	0.4 (0.1)	0.8 (0.1)	0.04 (0.03)	0
PreBoMs	$CD19^+CD11b^{hi}B220^{lo}F480^+CD93^+CD69^+$	0	0	0	0.7 (0.1)

Table S3.2 Gene expression analysis of intra-abdominal fat depots. Data are presented as fold changes compared to pmWAT (± standard error of the mean), *p<0.05

Gene	rpWAT	omWAT	PSF
Tnfa	0.50 (0.67)	-3.84 (0.39)*	-9.17 (1.70)*
Csf1	-1.04 (0.52)	-0.90 (0.47)	-11.84 (2.05)*
Nos2	1.14 (0.65)	-17.74 (4.02)*	-134.99 (30.80)*
Ifng	-1.55 (1.24)	0.26 (0.68)	-7.76 (1.712)*
Tgfb	-1.27 (.14)	-23.33 (1.26)*	-7.84 (0.99)*
Mif	0.01 (0.62)	-2.25 (0.22)*	-1.07 (0.77)
Ido	-0.71 (1.01)	-1.61 (0.25)	-1.02 (0.76)
Rorc	1.38 (1.94)	1.66 (0.90)	-17.99 (0.50)*
Gata3	-1.69 (0.81)	-8.80 (2.92)*	-13.99 (2.46)*
Tbx21	-1.10 (0.93)	1.39 (0.65)	-0.84 (1.02)
NFkB	-0.31 (0.74)	3.02 (0.24)*	4.62 (1.02)*
Il1b	0.20 (1.12)	114.42 (78.18)*	9.57 (7.71)
Il2	-1.80 (1.57)	6.36 (1.49)*	-6.19 (2.18)*
Il4	-6.31 (4.47)	-1.57 (0.72)	-6.10 (1.81)*
Il5	-0.84 (0.85)	-3.38 (0.59)*	-24.54 (7.77)*
Il6	-0.55 (0.69)	1.86 (0.70)	0.85 (0.85)
Il10	-1.00 (0.54)	9.62 (1.73)*	-2.58 (0.62)*
Il12a	0.50 (0.66)	-1.88 (0.25)	-0.31 (0.88)
Ccl2	2.29 (1.53)	67.59 (33.34)*	-2.80 (1.64)
Ccl3	-0.85 (0.81)	-1.82 (0.67)	14.30 (5.41)*
Ccl4	-2.44 (0.50)	2.39 (0.35)	-14.10 (4.18)*
Ccl5	-1.00 (0.50)	11.65 (2.08)*	2.73 (1.08)*
Ccl7	0.52 (0.97)	1.86 (2.0)*	-214.80 (112.99)*
Ccl19	-0.47 (0.80)	5.76 (0.90)*	-42.96 (10.35)*
Ccl21	-10.27 (5.81)*	-3.46 (1.60)	-4387.09 (1360.31)*
Cxcl1	2.95 (0.56)	54.61 (20.49)*	5.52 (2.07)*
Cxcl2	3.36 (0.90)	32.22 (15.48)*	96.50 (37.33)*
Cxcl10	-0.089 (0.87)	4.72 (0.86)*	-46.87 (12.43)*
Cxcl12	-2.32 (0.42)*	-0.98 (0.51)	-21.79 (3.19)*
Cxcl13	2.06 (1.08)	488.67 (56.84)*	67.45 (19.31)*
Crp	-2.18 (1.69)	22.73 (13.83)*	4.03 (1.77)
Prom1	0.51 (0.77)	-0.15 (1.10)	-17.06 (4.83)
IL1rn	1.27 (2.10)	50.39 (24.96)*	3.31 (0.99)
Vegfa	1.05 (0.53)	-1.64 (1.62)	-255.32 (31.63)*
Hif1a	-0.89 (0.51)	74.87 (10.38)*	33.99 (5.56)*
Nos3	1.25 (0.60)	-2.25 (0.52)	-112.30 (40.96)*
Lep	3.65 (1.19)	-4.62 (2.16)	-1233.93 (376.92)*
Adipoq	1.78 (0.24)	-31.56 (5.28)*	-287768.13 (57680.49)*
Retn	2.25 (0.20)*	-2.08 (0.45)	-28554.69 (8773.49)*
Agt	1.29 (0.13)	-3.14 (0.77)*	-31365.74 (0.00)*
Apoe	1.50 (0.26)	5.64 (0.46)*	5.55 (1.63)*
C3	-1.75 (0.85)	2.49 (0.38)	-17.65 (5.20)*
Msr1	-1.32 (0.14)	-0.99 (0.46)	-1.43 (0.67)
Lpl	2.21 (0.25)*	-3.76 (1.10)	-22.46 (0.74)

Chapter 4: HIGH FAT FEEDING INTIATES CHANGES IN INTRA-ABDOMINAL FAT DEPOT PROGENITOR POPULATIONS

Abstract

Once thought to be a passive reservoir for the storage of excess energy, white adipose tissue (WAT) is increasingly being recognized for its diverse roles in metabolism, thermoregulation, immune function and disease pathogenesis. Visceral fat (V-WAT) especially, has been associated with numerous diseases and metabolic disorders, indicating specific functions related to anatomical location. Although visceral depots are often used interchangeably in V-WAT-associated disease studies, there is evidence that each depot may represent a unique microenvironment with distinct physiological roles, illustrating a need for more depot-specific information. As WAT hosts a substantial population of stem and progenitor cells, it is likely that these cells are critical to the biological role of each depot. Here, we use FACS analysis to comparatively characterize the progenitor populations in the stromal vascular fraction (SVF) of parametrial (pmWAT), retroperitoneal (rpWAT), and omental (omWAT) adipose tissue from mice on either a low fat or high fat diet. We found significant differences in SVF composition between all three microenvironments. OmWAT contained the smallest proportion of $CD45^-$ stromal cells (6.8%), almost six-fold less than pmWAT and rpWAT (40.6% and 45.5% respectively). Of the $CD45^-$ population, omWAT had the highest proportion of adipocyte progenitor cells, mesenchymal stem cells, and $Sca1^+CD31^{hi}CD44^+$ cells, although with the much smaller number of CD45- cells, there were significantly fewer total adipocyte progenitor and mesenchymal stem cells. PmWAT and rpWAT were more similar in regards to CD45+/- ratios, as well as in the proportions of progenitor

populations. With high fat feeding, there was a decrease in proportion of CD45- cells in pmWAT, no change in rpWAT, and an increase in omWAT. Additionally, in adipocyte progenitor cells, which made up the largest proportion of $CD45^-$ cells in all three depots, with high fat diet, there was a significant decrease in omWAT, an increase in rpWAT, and no change in pmWAT, indicating different responses to high fat feeding. Variations in gene expression profiles with high fat diet were also evident between the tissues, including more significant enhancement in inflammatory and stromal factors in omWAT. These results support the hypothesis that intra-abdominal fat pads represent independent microenvironments with potentially unique contributions to physiological and pathological processes.

Introduction

White adipose tissue (WAT) is the largest endocrine organ in the body, comprising up to 45% of total body composition in obese individuals (BMI>30). Once thought to be a passive reservoir for excess energy storage, WAT is increasingly recognized for its role in metabolism, immune and endocrine function, thermoregulation, and tissue repair.[1] Recent studies indicate functional differences in adipose tissue depots related to anatomical location, suggesting that different fat depots may differentially contribute to physiological and pathological conditions. Exemplary of this, excess visceral fat especially, has been strongly correlated with increased morbidity and mortality.[2,3]

Visceral fat is comprised of numerous fat pads within the peritoneal cavity. Each of these depots is reportedly unique in regards to tissue dynamics (hypertrophic versus hyperplastic response to excess calories), adipokine release, hormonal responses, vascularization, innervation, and abundance of non-adipocyte components.[4,5] Adipose

tissue is composed of tissue resident adipocytes and a stromal vascular fraction (SVF), which includes leukocytes, mesenchymal stem cells, adipocyte progenitors, fibroblasts, and endothelial cells.[6] The SVF of WAT can vary widely between depots and is critical to function. In support of this, research has demonstrated that differences in fat pad composition and functionality endure after transplantation to different anatomical sites, indicating that other factors, such as SVF content, may be more important to functional heterogeneity.[7]

Stem and progenitor populations account for a large percentage of most adipose depots, as stem cells are responsible in part for the ability of WAT to rapidly expand in response to sustained positive energy balance.[8] As a reference for their large population, even more stem cells can be retrieved from 100g of fat than from 100ml of bone marrow.[9-11] Importantly, these populations are also able to contribute to other biological and pathological conditions, such as in wound repair and tumor development.[12,13] Differences in progenitor populations between adipose depots may play a role in their abilities to differentially impact these conditions. Thus, it is critical that the inherent differences between intra-abdominal fat depots are more extensively characterized.

In addition to basal cellular frequencies, changes in these populations with high fat diet and obesity may also be critical. In 2010, 69.2% of adult Americans were overweight or obese,[14] and this number is projected to increase. With the strong correlation between obesity and other diseases such as diabetes, metabolic syndrome, heart disease, and many cancers,[15,16] any mechanistic link should be further investigated. While many studies focus on WAT transcriptomes, proteomes or secretomes, limited information exists on the cellular composition of individual depots. Given the relevance

of V-WAT to various disease states, there is clearly a need for elucidation of depot-specific SVF composition and gene expression profiles in order to provide a more comprehensive understanding of these distinct microenvironments within the peritoneal cavity. Thus, this study investigated not only the basal progenitor populations within intra-abdominal adipose depots of mice, but also how these populations change with high fat feeding. The three depots examined include parametrial (pmWAT), retroperitoneal (rpWAT), and omental (omWAT) WAT: pmWAT due to its widespread application in murine studies, omWAT due to its classification as a ‘‘true’’ visceral fat and importance in immunological surveillance, and rpWAT due to its characterization as a non-visceral intra-abdominal fat depot with a human counterpart. Blood and peritoneal serous fluid (PSF) were also included in the analysis as systemic points of reference. Our results indicate that pmWAT, rpWAT, and omWAT represent distinct microenvironments with unique progenitor compositions in both the homeostatic and obese states. We also found significant changes in their stroma, supporting our hypothesis that distinct fat depots possess inherent properties that may differentially impact disease states.

Methods and Materials

Animals

Female C57BL/6 mice (Harlan Laboratories) were housed one mouse per cage in a controlled environment (12 hour light/dark cycle at 21°) with free access to food and water. Mice were placed on diets and were weighed twice a week for 15 weeks. At 12 weeks, mice underwent body composition analysis using the Bruker nuclear magnetic resonance machine as well as a glucose tolerance test to examine metabolic changes. At 15 weeks, mice were sacrificed by CO_2 asphyxiation. Mouse studies were conducted in

accordance with the guidelines approved by the Virginia Tech Institutional Animal Care and Usage.

Diets

Animals were placed into one of two diet groups: a 17% low fat (AIN-93G purified rodent diet with 7% corn oil replacing soybean oil) or a 45% high fat (AIN-93G purified rodent diet with 7% corn oil replacing soybean oil and 16.5% lard; total fat- 45% of kilocalories) diet (Dyets, Inc.), with free access to food for 15 weeks. Diet composition can be found in appendix b.

Glucose tolerance test

Animals were fasted overnight (12 hours) prior to an intraperitoneal injection of 2mg pharmaceutical grade glucose per gram of body weight in a 10% solution of PBS. Blood was sampled six times per mouse over a two-hour period (at time point 0, 15, 30, 60, 90, and 120 minutes). To collect blood, the tail vein was nicked with a sterile lancet and approximately 5 μl was used to measure glucose via a hand held glucometer.

Tissue fat depot and peritoneal serous fluid harvest

OmWAT, pmWAT and rpWAT were harvested from each mouse, weighed, and rinsed with calcium- and magnesium deficient phosphate buffered saline (PBS-/-). OmWAT is attached posteriorly to the stomach, connected to the pancreas and the anterior of the spleen.[17] To ensure that there was no pancreatic contamination, omWAT samples were also tested for buoyancy.[18] PmWAT, the largest fat depot, is comprised of two fat pads, which are located directly under the muscle wall on the dorsal side of the abdomen and attached to the uterine horns. RpWAT also contains two fat pads, which are attached dorsally to the peritoneum, directly behind each kidney. Each tissue was processed for

FACS or placed into RNAlater (Qiagen) and stored at -80°C. Resident peritoneal cavity cells were collected via peritoneal lavage with 5 ml of PBS-/-. The effluent was centrifuged, subjected to erythrocyte lysis (lysis buffer: 155 mM NH_4Cl, 10 mM $KHCO_3$, 0.1 mM EDTA),[6] and further processed as described below.

Tissue digest

SVFs from individual fat depots (n= 10) were isolated from digested tissue according to standard protocol[19,20] with minor modifications to improve yields. OmWAT was digested in GKN-buffer containing 1.8 mg/ml type IV collagenase, 10% FBS, and 0.1 mg/ml DNase. PmWAT and rpWAT digest buffer included a 1:1 ratio of Krebs-Ringer bicarbonate buffer and collagenase solution (1 mg type I collagenase, 10 mg BSA, and 2 mM $CaCl_2$ in 1 ml PBS). Following digest at 37°C for 45 min, cells were passed through a 40 μm cell strainer, and erythrocytes were lysed.

FACS analysis

Tissues from five mice per group were used. Cell suspensions were washed in flow buffer (2% BSA in PBS-/-), blocked with Fc block (BD Biosciences) for 10 minutes at 4°C, rinsed, and subsequently incubated with fluorochrome-labeled antibody combinations (available upon request) for 20 min at 4°C. Fluorochrome-labeled antibodies specific for mouse CD45, CD34, CD31, CD44, CD73, CD133 and Flk-1 were obtained from eBioscience (San Diego, CA). CD105 antibody was obtained from BioLegend (San Diego, CA) and Sca1, CD44, and CD117 antibodies were obtained from BD Biosciences (San Jose, CA). Prior to analysis, cells were washed twice and resuspended in PBS-/- with propidium iodide for dead cell exclusion. FACS was performed on a FACSAria (BD Biosciences) and data was analyzed using Flowjo

(TreeStar) software.

RNA Extraction and cDNA synthesis

WAT was homogenized in Qiazol (Qiagen), and RNA was purified using an RNeasy Lipid Tissue Kit (Qiagen), according to manufacturer's instructions. RNA concentration was determined using a NanoDrop1000 spectrophotometer. RNA (n= 5 per tissue) was then subjected to the iScript cDNA synthesis system (Biorad) according to manufacturer's protocol.

PCR Array

Pooled cDNA samples for each group (5 mice each) were used with 1 μg total RNA for the whole plate (384 well). The SABiosciences RT^2 Profiler PCR Array (PAMM-3803E-12) was used according to standard protocol and was run on the ABI 7900HT (Applied Biosystems). Data was analyzed using the SABiosciences web-based RT^2 Profiler PCR Array data analysis program.

Quantitative real-time PCR (qRT-PCR)

Tissues from five mice per group were analyzed. qRT-PCR was performed with 12.5 ng cDNA per sample using gene-specific SYBR Green primers (primer sequences are available upon request) designed with Beacon Design software. SensiMix SYBR and Fluorescein mastermix (Bioline) was used in a 15 μl reaction volume. qRT-PCR was performed for 42 cycles at 95°C for 15 sec, 60°C for 15 sec, and 72°C for 15 sec, preceded by a 10 min incubation at 95°C on the ABI 7900HT (Applied Biosystems). Melt curves were performed to ensure fidelity of the PCR product. L19 was utilized as the housekeeping gene and the ddCt method[21] was used to determine fold differences.

Statistical analysis

Student t-tests were used to compare low fat and high fat groups. Comparisons across tissues utilized a one-way ANOVA coupled with a Tukey post-hoc test in Graphpad Prism. Differences were considered statistically significant at $p<0.05$.

Results

Effect of diet on body weight and composition

Eight-week old female C57BL/6 mice were placed on either a low fat (17% fat) or high fat (45% fat) diet for 15 weeks. As shown in figure 4.1 A and B, mice on the high fat diet had a significantly greater final body weight, with an average weight of 43.0 g as compared to 34.9 g in the low fat group ($p=0.0036$). Mice on the high fat diet also had significantly greater percentages of body fat (figure 4.1 C), with an average of 27.3% in the high fat group and 20.1% in the low fat group ($p<0.05$). Additionally, glucose tolerance tests (figure 4.1 D) confirmed that mice on a high fat diet had a reduced ability to uptake glucose as evidenced by a significantly higher blood glucose level at all time points after time 0 (all time points, $p<0.05$). There was not a significant difference in fasting blood glucose levels. Thus, the high fat diet mice are a good representation of early stages of weight gain and metabolic dysregulation due to high fat feeding, but are pre-metabolic syndrome.

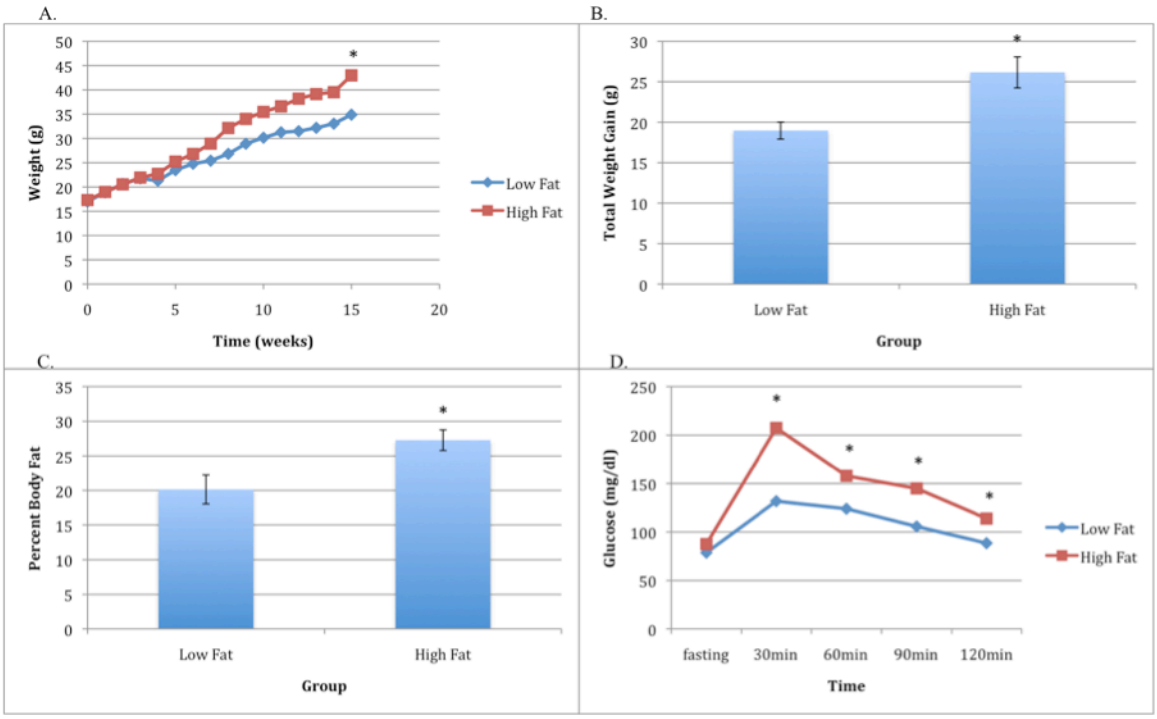

Figure 4.1. Effect of diet on body weight, body composition, and glucose tolerance. A) Total body weight at each week on diet. B) Total weight gain. C) Final percent body fat. D) Glucose tolerance test. *indicates significance of $p<0.05$

Adipose depot weight and cellularity

Each adipose depot was weighed following harvest and the number of SVF cells were counted post-tissue digest. As expected, pmWAT was the largest depot at approximately 1756 mg in low fat mice, followed by rpWAT at 408 mg, and omWAT at 38 mg (Figure 4.2 A). As shown in figure 4.2 B, in low fat diet mice, pmWAT had the largest total SVF cell content (pmWAT: 1.9 x 10^6 cells, rpWAT: 0.9 x 10^6 cells, omWAT: 1.4x 10^6 cells), although when viewed in terms of cells per mg tissue (figure 3.2 C), omWAT had the greatest cell number (pmWAT: 1142 cells/mg, rpWAT: 2294 cells/mg, omWAT: 35,270 cells/mg). All three depots were significantly larger following high fat feeding (pmwat: 3218 mg, p=0.0014; rpWAT: 656 mg, p=0.0018; omWAT: 60 mg, p=0.0420). However, pmWAT was the only depot with a significant increase in SVF cell number (low fat: 1.9

x 10^6 cells, high fat: 3.5 x 10^6 cells, $p<0.05$) with high fat diet. RpWAT also had a trend towards an increased cell number, but this was not significant.

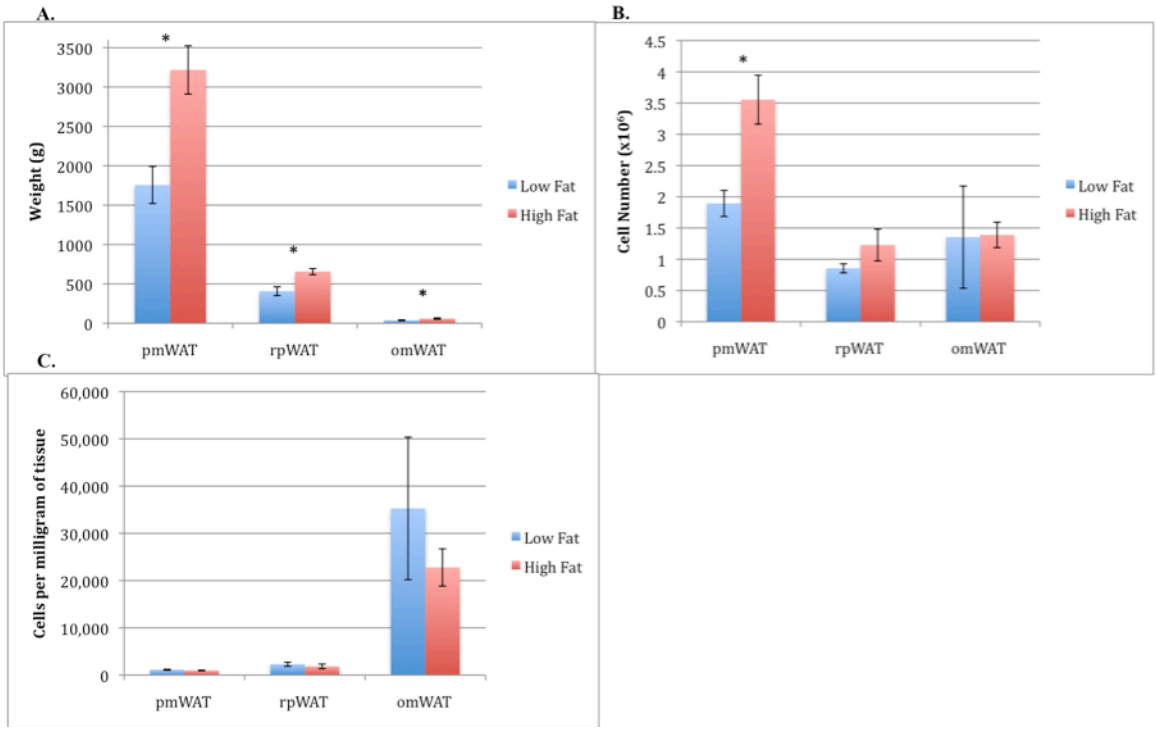

Figure 4.2. Effect of diet on adipose depot weights and cellularity. A) Adipose depot weight from mice on a low fat or high fat diet. B) Total number of cells in the SVF of each adipose depot. C) Number of cells per milligram of tissue in each adipose depot. *indicates significance of $p<0.05$

Fat depot SVF characterization

FACS analysis was used to identify changes in progenitor populations present in each adipose depot, as well as blood and PSF, of mice on a low fat versus a high fat diet. PSF was included as an established immunologically active microenvironment present within the peritoneal cavity[22,23] and blood was included since previous reports show systemic changes in circulating progenitor populations with obesity and cancer.[24,25]

For analysis, viable cells identified via propidium iodide exclusion (figure 4.3 A), were gated based on forward/side scatter to exclude doublets (figure 4.3 B and C) and were then separated into $CD45^+$ leukocytes and $CD45^-$ stromal constituents (figure 4.3 D).

The CD45$^-$ gate contains the majority of our progenitor populations of interest, although hematopoietic stem cells (HSCs) are found within the CD45$^+$ gate.

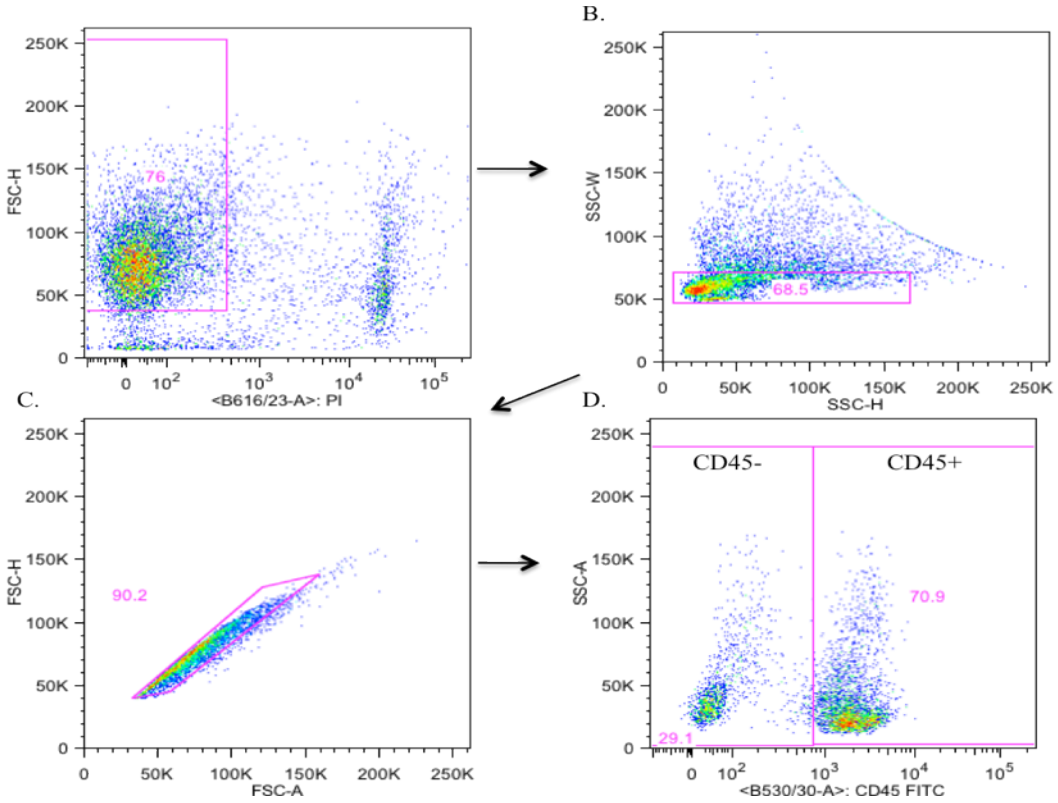

Figure 4.3. FACS gating strategy. A) Propidium iodide exclusion gating of viable cells. B) Doublet exclusion gating. C) Second doublet gating. D) CD45+/- gating.

Various populations were chosen based on those examined in current literature. It is important to note that adipocyte progenitor cells (APCs) are generally used interchangeably with adipose tissue-derived mesenchymal stem cells (MSCs).[26-28] However, there are vast arrays of surface marker combinations used to describe these cells. We chose two different combinations of markers: CD45$^-$Sca1$^+$CD34$^+$, which is a more common combination of markers for adipose tissue progenitors[26] and CD45$^-$CD44$^+$CD105$^+$CD73$^+$, which is a more standard combination for MSCs from any tissue.[29] We also investigated changes in CD45$^-$CD133$^+$Flk1$^+$CD31$^-$ endothelial progenitor cells (EPCs),[30] CD45$^-$CD34$^{lo/-}$CD133$^-$CD31$^+$ endothelial cells (ECs),[30] and

$CD45^-Flk1^+CD31^+CD133^+$ circulating endothelial cells (CECs).[31] $CD45^-Sca1^+CD31^{hi}CD44^+$ cells, which are likely additional endothelial progenitor cells, were included as well because there were distinct populations present in each tissue and they have not been previously reported on. As mentioned above, $CD45^+Sca1^+ckit^+$ hematopoietic stem cells[32,33] were also examined.

There were major differences between tissues on a basal level, which are depicted in table 4.1. In a homeostatic state, $CD45^-$ cells made up 40.6% of the SVF cells in pmWAT, 45.5% in rpWAT, and only 6.8% in omWAT, demonstrating a much larger stromal component in pmWAT and rpWAT and a larger leukocyte population in omWAT. Within the $CD45^-$ gate, as expected, the largest populations in all three tissues were APCs and MSCs. It should be noted that there was significant overlap between the APC and MSC populations, although the amount varied across tissues and animals. Thus the two should not be considered independently and more work is needed to better define the stem cells populations in WAT.

OmWAT had the highest proportion of APCs, MSCs, and $Sca1^+CD31^{hi}CD44^+$ cells, although with the much smaller number of CD45- cells, there were significantly fewer total APCs and MSCs ($p<0.05$). PmWAT and rpWAT were more similar in the proportions of progenitors populations, with little variation between tissues.

Blood and PSF included almost exclusively $CD45^+$ cells (97.8% and 99.2%, respectively). The majority of cells in the $CD45^-$ gate in the PSF were APCs (6.7%), MSCs (35%), ECs (15%), and HSCs (3.4%). The CD45- gate in the blood contained primarily ECs (41.1%) and MSCs (13.4%). However, in both cases, there were few $CD45^-$ cells total, so the actual cell numbers for these populations was low.

Table 4.1. Progenitor populations in tissues from mice on a low fat diet.

Progenitor Characterization- Low Fat Diet						
	Markers	pmWAT	rpWAT	omWAT	PSF	Blood
CD45+		59.4 (3.1)	54.2 (3.0)	93 (1.5)	99.2(0.1)	97.8 (0.2)
Percent of CD45+ cells						
HSC	Sca1+Ckit+	0.6 (0.1)	0.3 (0.1)	2.1 (0.2)	3.4 (0.3)	0.01 (0.01)
CD45-		40.6 (3.1)	45.4 (3.0)	6.8 (1.5)	0.8 (0.1)	2.0 (0.1)
Percent of CD45- Cells						
APC	Sca1+CD34+	42.1 (3.8)	36.5 (2.2)	52.3 (2.4)	6.7 (1.5)	1.1 (0.4)
MSC	CD44+CD105+CD73+	10.0 (1.9)	13.2 (2.0)	43.8 (1.1)	35.0 (2.4)	13.4 (2.0)
EPC	CD133+Flk1+CD31-	0.1 (0.0)	0.3 (0.1)	1.1 (0.4)	0 (0)	0.1 (0.1)
EC	$CD34^{-/lo}$, $CD133^{-}CD31^{+}$	5.9 (1.1)	3.7 (0.4)	3.6 (0.4)	15.2 (1.8)	41.1 (7.1)
CEC	Flk1+CD31+CD133+	0.04 (0.02)	0.1 (0.1)	0.6 (0.2)	0 (0)	0 (0)
	$Sca1^{+}CD31^{hi}CD44^{+}$	0.6 (0.2)	0.7 (0.3)	1.7 (0.5)	0 (0)	0 (0)

Table 4.2 presents the percentages of each population in mice on a low fat versus high fat diet. Interestingly, each fat depot responded differently to high fat feeding. PmWAT and rpWAT both had an increase in proportion of $CD45^{+}$ cells with high fat feeding (pmWAT p=0.04, rpWAT- not significant), while omWAT had a significantly decreased $CD45^{+}$ percentage of the total SVF cells (p=0.0039). Within the $CD45^{-}$ gate, pmWAT had a significant increase in $Sca1^{+}CD31^{hi}CD44^{+}$ cells ($p < 0.05$), rpWAT had a significant increase in APCs (p=0.0024) and $Sca1^{+}CD31^{hi}CD44^{+}$ cells (p=0.0003), and omWAT had a significant decrease in APCs and MSCs (both $p<0.0001$) with high fat feeding.

Blood and PSF contained greater than 97% $CD45^{+}$ cells with low fat and high fat diet. With high fat diet, blood had a significant decrease in APCs (from 1.1% to 0.1% of CD45- cells, p=0.03) and MSCs (from 13.4% to 2.1% of CD45- cells, p=0.0006) and an increase in CECs (0% to 0.5%, p=0.009). PSF had a significant increase only in HSCs (p=0.003).

Table 4.2. Progenitor population percentages in tissues from mice on a low fat versus high fat diet, organized by tissue. *p<0.05 (High fat as compared to low fat)

pmWAT		
Markers	Low Fat	High Fat
CD45+	59.4 (3.1)	67.4 (0.1)*

Percent of CD45+ cells			
HSC	Sca1+Ckit+	0.6 (0.1)	1.31 (0.2)
CD45-		40.6 (3.1)	32.6 (1.1)*
Percent of CD45- Cells			
APC	Sca1+CD34+	42.1 (3.8)	39.3 (4.6)
MSC	CD44+CD105+CD73+	10.0 (1.9)	12.4 (1.7)
EPC	CD133+Flk1+CD31-	0.1 (0.0)	5.1 (2.9)
EC	$CD34^{-/lo}$, $CD133^{-}CD31^{+}$	5.9 (1.1)	5.0 (1.3)
CEC	$Flk1^{+}CD31^{+}CD133^{+}$	0.04 (0.02)	0.9 (0.4)
	$Sca1^{+}CD31^{hi}CD44^{+}$	0.6 (0.2)	5.2 (2.1)*
rpWAT			
	Markers	Low Fat	High Fat
CD45+		54.2 (3.0)	61.9 (3.9)
Percent of CD45+ cells			
HSC	Sca1+Ckit+	0.3 (0.1)	1.2 (0.5)
CD45-		45.4 (3.0)	38.2 (3.9)
Percent of CD45- Cells			
APC	$Sca1^{+}CD34^{+}$	36.5 (2.2)	56.2(2.4)*
MSC	$CD44^{+}CD105^{+}CD73^{+}$	13.2 (2.0)	16.8 (5.8)
EPC	CD133+Flk1+CD31-	0.3 (0.1)	0.1 (0.04)
EC	$CD34^{-/lo}$, $CD133^{-}CD31^{+}$	3.7 (0.4)	4.1 (0.1)
CEC	Flk1+CD31+CD133+	0.1 (0.1)	0.1 (0.1)
	$Sca1+CD31^{hi}CD44+$	0.7 (0.3)	2.9 (0.2)*
omWAT			
	Markers	Low Fat	High Fat
CD45+		93.0 (1.5)	79.9 (2.9)*
Percent of CD45+ cells			
HSC	Sca1+Ckit+	2.1 (0.2)	0.8 (0.1)
CD45-		6.8 (1.5)	20.1 (2.9)*
Percent of CD45- Cells			
APC	Sca1+CD34+	52.3 (2.4)	17.6 (1.8)*
MSC	CD44+CD105+CD73+	43.8 (1.1)	12.8 (0.4)*
EPC	CD133+Flk1+CD31-	1.1 (0.4)	0 (0)
EC	$CD34^{-/lo}$, $CD133^{-}CD31^{+}$	3.6 (0.4)	2.3 (0.2)
CEC	Flk1+CD31+CD133+	0.6 (0.23)	0.1 (0.1)
	$Sca1^{+}CD31^{hi}CD44^{+}$	1.7 (0.5)	0.8 (0.1)
Peritoneal Serous Fluid			
	Markers	Low Fat	High Fat
CD45+		99.2(0.1)	98.4 (0.5)
Percent of CD45+ cells			
HSC	Sca1+Ckit+	3.4 (0.3)	6.8 (0.6)
CD45-		0.8 (0.1)	1.6 (0.5)
Percent of CD45- Cells			
APC	Sca1+CD34+	6.7 (1.5)	3.9 (0.9)*
MSC	CD44+CD105+CD73+	35.0 (2.4)	34.1 (1.8)
EPC	CD133+Flk1+CD31-	0 (0)	0.1 (0.1)

EC	$CD34^{-/lo}$, $CD133^{-}CD31^{+}$	15.2 (1.8)	15.5 (5.5)
CEC	Flk1+CD31+CD133+	0 (0)	0 (0)
	$Sca1^{+}CD31^{hi}CD44^{+}$	0 (0)	0.9 (0.6)
Blood			
	Markers	Low Fat	High Fat
CD45+		97.8 (0.2)	98.4 (0.3)
Percent of CD45+ cells			
HSC	Sca1+Ckit+	0.01 (0.01)	0 (0)
CD45-		2.0 (0.1)	1.6 (0.3)
Percent of CD45- Cells			
APC	Sca1+CD34+	1.1 (0.4)	0.1 (0.1)*
MSC	CD44+CD105+CD73+	13.4 (2.0)	2.1 (0.6)*
EPC	CD133+Flk1+CD31-	0.1 (0.1)	0.1 (0.1)
EC	$CD34^{-/lo}$, $CD133^{-}CD31^{+}$	41.1 (7.1)	42.1 (5.9)
CEC	Flk1+CD31+CD133+	0 (0)	0.5 (0.1)*
	$Sca1+CD31^{hi}CD44+$	0 (0)	0.1 (0.1)

Due to varying numbers of cells and proportions of $CD45^{+}$ versus $CD45^{-}$ cells in each tissue, total cell numbers provided a novel perspective on differences across depots. Table 4.3 contains estimated total cell numbers (x 10^5) extrapolated by multiplying the total cell numbers by percentage of $CD45^{+}$ or $CD45^{-}$ cells and then percentage of the population of interest. As expected since pmWAT had a much greater cell count, pmWAT had significantly more $CD45^{-}$ cells, APCs, MSCs and ECs than omWAT ($p<0.05$ for all). PmWAT also had significantly more CD45- cells and APCs than rpWAT. Additionally, with high fat diet, pmWAT responded with the greatest number of changes, displaying an increase in both $CD45^{+}$ and $CD45^{-}$ cells as well as an increase in HSCs, APCs, MSCs and $CD45^{-}CD31^{hi}CD44^{+}$ cells.

Table 4.3. Progenitor population total numbers (x10^5) in tissues from mice on a low fat versus high fat diet, organized by tissue. *p<0.05 (High fat as compared to low fat)

pmWAT			
	Markers	Low Fat	High Fat
CD45+		11.5 (3.7)	19.1 (2.1)*
HSC	Sca1+Ckit+	0.07 (0.03)	0.2 (0.03)*
CD45-		7.4 (3.2)	16.5 (2.0)*
APC	Sca1+CD34+	2.9 (1.9)	6.7 (1.4)*
MSC	CD44+CD105+CD73+	0.6 (0.4)	2.0 (0.3)*
EPC	CD133+Flk1+CD31-	0.01 (0.002)	1.0 (0.7)

EC	CD34-/lo, CD133-CD31+	0.65(0.1)	0.8 (0.1)
CEC	Flk1+CD31+CD133+	0.002 (0.002)	0.2 (0.1)
	Sca1+CD31^{hi}CD44+	0.05 (0.01)	0.8 (0.3)*
rpWAT			
	Markers	Low Fat	High Fat
CD45+		4.9 (1.3)	7.6 (1.4)
HSC	Sca1+Ckit+	0.01 (0.01)	0.1 (0.04)
CD45-		3.6 (2.1)	4.7 (1.2)
APC	Sca1+CD34+	1.4 (0.6)	2.6 (0.7)
MSC	CD44+CD105+CD73+	0.5 (0.2)	0.7 (0.2)
EPC	CD133+Flk1+CD31-	0.02 (0.01)	0.005 (0.0)
EC	CD34-/lo, CD133-CD31+	0.2 (0.1)	0.2 (0.06)
CEC	Flk1+CD31+CD133+	0.01 (0.004)	0.005 (0.003)
	Sca1+CD31^{hi}CD44+	0.02 (0.04)	0.1 (0.03)*
omWAT			
	Markers	Low Fat	High Fat
CD45+		12.1 (6.3)	10.0 (1.4)
HSC	Sca1+Ckit+	0.3 (0.2)	0.1 (0.03)
CD45-		1.4 (0.9)	2.7 (0.8)
APC	Sca1+CD34+	0.7 (0.5)	0.4 (0.1)
MSC	CD44+CD105+CD73+	0.5 (0.3)	0.4 (0.1)
EPC	CD133+Flk1+CD31-	0.03 (0.02)	0 (0)
EC	CD34-/lo, CD133-CD31+	0.06 (0.04)	0.1 (0.01)
CEC	Flk1+CD31+CD133+	0.01 (0.01)	0 (0)
	Sca1+CD31^{hi}CD44+	0.04 (0.03)	0.02 (0.004)

Fat depot mRNA expression profiles

PCR arrays using pooled samples of RNA from the adipose depots of mice on both diets (n=5 per diet) were performed to more extensively characterize the overall adipose tissue signaling milieu in each microenvironments. It is important to note that expression patterns represent the tissue as a whole, and thus are reflective of both adipocytes and SVF cells. Figure 4.4 depicts basal expression of selected chemokines/cytokines in each tissue and Ct values of each can be found in appendix A.

OmWAT appeared to be the most immunologically active with the highest expression of cytokines, cytokine receptors, and growth factors. Comparing across tissues, while omWAT appeared to have the highest expression of most cytokines/chemokines, pmWAT followed with the second highest expression, and rpWAT generally had the lowest expression of most genes investigated. The variations in

expression levels are likely due in large part to differences in cellular content of the SVF. For instance, omWAT had a much greater number of SVF cells per milligram of tissue and also a higher content of immune cells, corresponding to its greater expression of inflammatory mediators.

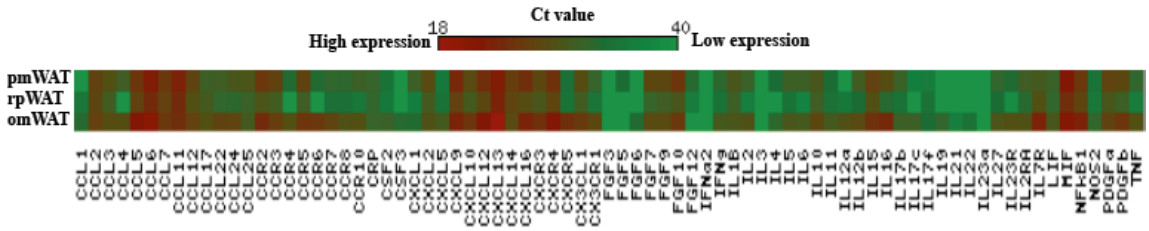

Figure 4.4. Heat map of gene expression in adipose depots from low fat mice.

Table 4.4 displays genes in each depot that were changed twofold or greater with high fat feeding. There was significant overlap between depots, specifically in an increase of cytokine/chemokine expression. All three depots had an increase in CCL2, CCL7, CCR2 and CCR5. Interestingly, although pmWAT and rpWAT were the most similar in progenitor population profiles, pmWAT and omWAT had the most similarities in the genes investigated. With high fat diet, they both had an increased expression of CCR3, CXCL5, IFNa2, IFNg, IL17f, IL21, NOS2, and a decrease in CXCR4, IL17b.

Table 4.4. PCR array changes in gene expression. Genes with greater than twofold difference higher (red) or lower (green) in high fat mice as compared to low fat were included. Fold changes are in parenthesis.

pmWAT	rpWAT	omWAT
CCL1 (3.4)	CCL2 (6.6)	CCL2 (2.4)
CCL2 (4.1)	CCL3 (2.1)	CCL7 (2.3)
CCL4 (5.3)	CCL4 (3.7)	CCL11 (2.7)
CCL7 (4.1)	CCL5 (3.0)	CCL12 (2.5)
CCL17 (4.4)	CCL7 (5.4)	CCR2 (2.6)
CCL22 (2.4)	CCL22 (3.1)	CCR3 (6.3)
CCR2 (2.5)	CCL24 (2.1)	CCR5 (2.6)
CCR3 (3.2)	CCR2 (2.4)	CSF2 (4.4)
CCR4 (2.4)	CCR4 (2.0)	CXCL1 (3.3)
CCR5 (2.9)	CCR5 (2.5)	CXCL2 (2.5)
CCR6 (6.0)	CSF2 (4.9)	CXCL5 (3.6)
CXCL5 (4.1)	CXCL1 (2.9)	CX3CR1 (2.2)

CXCL10 (2.3)
CXCR5 (10.2)
FGF3 (2.6)
IFNa2 (2.6)
IFNg (2.4)
IL10 (2.7)
IL17c (3.6)
IL17f (22.4)
IL12a (4.2)
IL21 (3.0)
NOS2 (100.0)
CCR10 (-2.8)
CXCL13 (-2.3)
CXCR4 (-2.0)
FGF5 (-2.2)
IL5 (-4.5)
IL12b (-2.2)
IL17b (-2.3)

CXCL9 (2.6)
CXCL10 (5.2)
CXCL12 (2.1)
CXCL14 (2.1)
CXCL16 (2.2)
CXCR3 (2.2)
CX3CL1 (2.4)
FGF10 (2.1)
FGF12 (7.3)
IL2 (10.4)
IL6 (5.9)
IL10 (2.5)
IL15 (2.1)
IL16 (3.3)
IL17b (3.3)
PDGFa (2.3)
PDGFb (2.2)
TNF (4.5)
CCL11 (-3.8)
CCL25 (-2.6)
CCR8 (-2.8))
CXCL13 (-2.8)
CRP (-3.3)
IL11 (-2.1)
IL12b (-3.7)
IL27 (-2.3)

FGF12 (8.9)
FGF5 (4.7)
FGF7 (2.8)
IFNa2 (2.8)
IFNg (2.0)
IL1b (4.0)
IL3 (2.2)
IL4 (2.5)
IL17f (4.7)
IL21 (18.8)
IL23a (3.8)
NOS2 (169.2)
TNF (2.5)
CCL6 (-2.1)
CCR7 (-2.3)
CCR8 (-3.0)
CXCR4 (-2.3)
CSF3 (-3.3)
FGF6 (-4.0)
FGF9 (-2.0)
IL2 (-2.0)
IL11 (-3.4)
IL12b (-2.0)
IL17b (-2.0)
IL19 (-8.3)
IL22 (-2.1)

Since the PCR array utilized pooled samples, qRT-PCR was used to confirm some cytokine expression levels and changes between groups. Additionally, genes associated with adipose tissue, angiogenesis, and stromal cells were added to gain a better overall picture of the adipose depot microenvironments. Average Ct values can be found in appendix a. Overall, the cytokine expression levels matched well with the PCR array data. Following with cytokine expression, omWAT had the highest expression of some adipose-related genes (LEP, NAMPT, VLDLR, PAI1), hypoxia/angiogenesis-related genes (NOS3, VEGFa, HIF1a, VEGFR2, AGT, CDH5, VCAM1) and other stromal markers (CD34, CD31, FN1). PmWAT had the highest expression of RETN, ADIPOQ,

IL1b, and IGF1, and generally had the second highest expression of most other genes. Again, rpWAT expression was usually the lowest of the three depots.

Changes in gene expression between mice on high fat versus low fat diets are presented in table 4.5. Most adipokines were not affected by the high fat diet, although there was a trend of increased leptin expression in pmWAT and rpWAT. There was however a significant increase in TNFa and IL1b in omWAT and pmWAT, as well as IL6 in pmWAT ($p<0.05$ for all), which are commonly associated with obesity.[34,35] In regards to angiogenesis-related genes, VEGFR2 was increased in omWAT. However, VEGFa was not increased, potentially due to high basal expression (average Ct of 24.5 in omWAT). TNC, which is increased during disease and injury,[36] had significantly increased expression in omWAT and rpWAT with high fat feeding.

Table 4.5. qRT-PCR gene expression fold changes in adipose tissue depots (n=5) in mice on a high fat diet as compared to a low fat diet. *p<0.05

	pmWAT	rpWAT	omWAT
VLDLR	1.4	1.6	1.37
NAMPT	0.2	-1.6	-1.44
RETN	-0.95	-0.4	0.28
ADIPOQ	0.8	0.97	1.2
LEP	3.7	3.7	0.65
CCL1	1.7	4	1
CCL2	4.8*	5.7	3.71*
CCL4	4*	6	2.1
CCL5	1.7	2	0.76
CCR5	4.8	4.7	2.9
CXCR2	3.9	0.42	1.8
CXCL13	-0.3	-0.6	-0.4
CX3CL1	1.1	1.9	2.2*
IL1b	2.8*	2.1*	3.5*
TNFa	7.6*	4.7*	3.7*
IL10	1.6	-1.2	2
IFNg	4.7	2.8	2.2*
IL6	4.1*	1.8	1.9
NOS3	1.4	-1.4	1.5
VEGFa	-0.6	-3.0	0.3
VEGFR2	1.2	-1.0	2.4*

HIF1a	0.8	-0.1	1.3
IGF1	0.3	-1.2	0.3
TGFb	1.8	0.9	1.6
Agt	-0.5	-4.1*	-0.4
Col1	1.3	-1.4	2.9*
TNC	0.2	5.9*	3.6*
IDO	-0.8	-0.9	-3.5*
CD34	0.8	0.5	-0.2
aSMA	0.2	2.7	1.6
MMP11	2.6	2.9	2.3*
CD31	2.7	0.8	1.5
PAI1	-1.1	-1.9	-7.1*
CDH5	1.0	0.7	1.7
FN1	0.8	-0.3	2.0
VCAM1	-1.5	-1.5	-1.5
UCP1	-1.8	32.6	0.5

Discussion

While V-WAT has been associated with various metabolic disorders and certain cancers,[1-3] the actual contributions of individual V-WAT depots to biological functions are poorly understood. An important component of functionality is the cellular composition of each depot. We have previously reported on significant differences in immune populations between depots[37] and here, we further characterize SVF stem and progenitor populations and their modulation by high fat diet.

Our three depots of interest are all traditionally considered visceral depots and were chosen due to the greater association of V-WAT with disease. We aimed to evaluate an early time point in progression to obesity, which was characterized by an increase in body weight, body fat percentage, and dysregulated glucose tolerance. As expected, along with whole body weight, all three depots became significantly larger with high fat diet. The adipose depots also began to exhibit signs of chronic low-grade inflammation as evidenced by increased expression of TNFa, IL1b, CCL2, IL6 and

iNOS, as well as the influx of leukocytes in pmWAT and rpWAT. It is important to note that our high fat diet mice were not models of severe obesity, as they did not have impaired fasting glucose levels and did not display significant changes in adipokines such as leptin, adiponectin, resistin, and visfatin. However, it should also be noted that a recent publication found that female mice are more resistant to the inflammatory and metabolic symptoms of obesity.[38] Thus while our mice may not have displayed all the symptoms of metabolic syndrome, they are a good indication of early events of obesity. It will also be important to characterize changes in later stages.

In our model, there was a concomitant increase in SVF cell numbers and number of APCs with the expansion of adipose tissue, although this was only evident in pmWAT. This fits with others such as Zhang et al.,[26] who have also reported an expansion of APCs with obesity. The lack of increase in the other visceral depots may be attributed to a tendency towards a hypertrophic response as compared to a hyperplastic response. Joe et al.[39] found that 60 days of high fat feeding resulted in an increase in adipocyte diameter of 17% in S-WAT, compared to a 65% increase in V-WAT, even with a comparable fold increase in mass in both depots. They additionally found that there was not a significant increase in $Sca1^{+}CD34^{+}$ cell proliferation in V-WAT (although there was in S-WAT) in mice on a high fat diet. However, it is also possible that V-WAT has a hypertrophic prior to a hyperplastic response, so 60 days may be too early to detect expansion of progenitors in these depots. Our study demonstrates that at 15 weeks of high fat diet, there is an increase in SVF cell numbers in pmWAT, but that within the V-WAT classification, there are differences in SVF proliferative responses, since this was not seen in rpWAT or omWAT.

Looking more specifically at cell populations, there were some important differences between tissues. omWAT is considered a secondary lymphoid organ and is critical to immunosurveillance in the peritoneal cavity.[40] It is composed of fatty tissue interspersed with immune cell aggregates, called "milky spots".[17] Complementary to this, omWAT contained a much greater proportion of $CD45^+$ leukocytes (>90%) than pmWAT and rpWAT (both closer to 50%). PmWAT and rpWAT were more similar in their CD45+/- and progenitor population ratios, although pmWAT contained a greater number of cells. However, rpWAT and pmWAT are not interchangeable as our previous studies have demonstrated that in regards to $CD45^+$ cell ratios, rpWAT more closely resembles omWAT.[37] Thus all three depots may serve as unique microenvironemts.

High fat diet induced some changes in SVF composition. In pmWAT and rpWAT, there was an influx of $CD45^+$ leukocytes, which was significant in pmWAT, and is indicative of an early inflammatory response to high fat feeding. Most of the other population proportions remained remarkably stable with high fat diet, suggesting that progenitor populations in these tissue may be tightly controlled. Influx or proliferation of progenitors could have resulted in differentiated adipocytes, endothelial cells, or fibroblasts instead of an accumulation of progenitors. In future studies, it will be important to characterize cellular flux in addition to population numbers at specific time points.

OmWAT had more significant changes in population rations. Interestingly, while omWAT is considered a secondary lymphoid organ, the $CD45^+$ fraction significantly decreased with high fat diet and the $CD45^-$ portion of omWAT was increased, suggesting that there was not an expansion of immune cells. However, omWAT did have the

greatest expression of inflammation-related genes, likely due to the more concentrated number of immune cells. It is possible that there were changes in leukocyte populations or activation states, which should be investigated in future studies.

Another interesting facet of the changes in populations within omWAT was that while there was an increase in CD45- cells, there was a decrease in APCs and MSCs. As our APCs are $CD45^{-}CD34^{+}Sca1^{+}$, this fits with a recent report that also found a decreased number of $CD45^{-}Sca1^{+}$ cells (which they called MSCs), in the omental fat of mice on a high fat diet.[41] It is possible that these cells differentiated into stromal cells not investigated in this study, such as fibroblasts or mesothelial cells, which are both prominent in omWAT.

A cell population that appeared in this study was $Sca1^{+}CD31^{hi}CD44^{+}$ cells, which to our knowledge, have never been reported on. Based on their surface marker expression, they are likely endothelial progenitor cells, but their CD31 expression was much higher than other cells. With high fat diet, there was an increase in this population in both pmWAT and rpWAT, but no significant change in omWAT.

There was also a trend towards an increase in proportions of other endothelial progenitors and endothelial cells with high fat diet in pmWAT and rpWAT and a trend towards decreased numbers in omWAT. This is counterintuitive considering the greater expression of most angiogenesis-related genes such as HIF1a, VEGFa, VEGFR2, CD31, VCAM1, CDH5, and PAI1 in omWAT. However, as pmWAT and rpWAT are much larger tissues, there is likely greater need for expansion of vasculature to maintain tissue growth with high fat feeding.

Blood and PSF were included in this analysis as a medium through which stem and progenitor cells could travel through between tissues. As expected, the cells in blood and PSF were primarily leukocytes, but there were $CD45^-$ cells present in both. High fat feeding initiated some changes in these locations, specifically a decrease in APCs and MSCs and increase in CECs in blood and a decrease in APCs in PSF. The increase in CECs in the blood with obesity correlates with previous reports that have found a positive relationship between obesity and circulating endothelial progenitor populations.[42,43] The decrease in APCs and MSCs may be due to recruitment from the blood and PSF into adipose tissues to accommodate tissue expansion.

There were also changes in stromal-related genes with high fat diet, which may enhance the ability of the adipose depots to serve as metastatic seeding sites. Tenascin C (TNC) was significantly increased in both rpWAT and omWAT. TNC is an extracellular matrix protein common in stem cell niches and is produced by cancer cells to promote survival and outgrowth of metastases.[44] The increased TNC with obesity may promote cancer cell adhesion and metastasis. OmWAT also had an increase in Col1 and MMP11. Collagen may be chemotactic for cancer cells[45] and studies have shown that some cancers respond to collagen 1 by increasing motility and up-regulating mesenchymal markers, such as N-cadherin, for invasion.[46] MMP11 is a negative regulator of adipocyte hypertrophy and is commonly expressed by cancer-associated fibroblasts.[47,48] Cells with enhanced MMP11 expression are beneficial as tumor-associated cells and may increase metastatic potential. OmWAT also had a trend, but not significant increase in FN1 and aSMA, suggesting that with obesity, there may be enhanced extracellular matrix deposition, potentially leading to firmer tissue in omWAT. IDO and PAI were

significantly decreased in omWAT with high fat diet, although it is unclear why as both are associated with an increased amount in obesity.[49,50]

PmWAT and rpWAT primarily responded to high fat diet with increases in inflammatory mediators, which may also be associated with cancer development. For instance, IL6 and TNFa were both increased in this study and have been shown to directly contribute to cancer initiation and development.[51] As to expression of other genes, pmWAT had no changes in stromal or angiogenesis-related genes. Besides TNC, rpWAT also had no significant increases in stromal or pro-angiogenic factors.

Conclusion

This study provides a comprehensive analysis of the stem and progenitor populations present in three intra-abdominal adipose depots and how they are modulated by early stages of obesity. There were also significant differences between the tissues in a homeostatic state. While omWAT was more immunologically active, with the SVF comprised primarily of leukocytes, pmWAT and rpWAT contained more stromal cells, with about a quarter of the SVF cells being adipocyte progenitors. Largely due to size, there were much greater total numbers of stem and progenitor cells in pmWAT. Thus, while pmWAT and rpWAT may not be as immunologically active as omWAT, the higher abundance of progenitor cells may allow them to be more efficient reservoirs of stem cells.

With expansion of each depot with high fat diet, there was a concomitant increase in total SVF cell numbers, although this was only significant in pmWAT. With the early stages of obesity, except for the decrease in adipose stem cells in omWAT, an increase in $Sca1^{+}CD31^{hi}CD44^{+}$ in pmWAT an increase in APCs and $Sca1^{+}CD31^{hi}CD44^{+}$ in rpWAT,

the progenitor population ratios remained relatively stable, suggesting a tight regulation of these cell types. In regards to gene expression, rpWAT was the least endocrinologically active, with the lowest expression of most genes investigated. Conversely, omWAT had the highest expression of most genes including inflammatory mediators and angiogenesis-related genes. It also had the most changes in expression of stroma-associated genes, including increases in COL1 and TNC, which may play a role in pathological conditions. These differences between adipose depots in cell populations, gene expression profiles, and response to high fat feeding may impact the ability of each depot to contribute to biological and pathological processes. Studies that investigate these adipose tissue-derived progenitor populations and their changes with cancer and other disease states, may provide insights on novel targets for the prevention of obesity-associated disorders.

References

1. Caspar-Bauguil S, Cousin B, Galinier A, et al. Adipose tissues as an ancestral immune organ: site-specific change in obesity. *FEBS Lett.* Jul 4 2005;579(17):3487-3492.

2. Montague CT, Prins JB, Sanders L, et al. Depot-related gene expression in human subcutaneous and omental adipocytes. *Diabetes.* Sep 1998;47(9):1384-1391.

3. Lee MJ, Wu Y, Fried SK. Adipose tissue heterogeneity: implication of depot differences in adipose tissue for obesity complications. *Mol Aspects Med.* Feb 2013;34(1):1-11.

4. Foster MT, Shi H, Softic S, Kohli R, Seeley RJ, Woods SC. Transplantation of non-visceral fat to the visceral cavity improves glucose tolerance in mice: investigation of hepatic lipids and insulin sensitivity. *Diabetologia.* Nov 2011;54(11):2890-2899.

5. Wueest S, Yang X, Liu J, Schoenle EJ, Konrad D. Inverse regulation of basal lipolysis in perigonadal and mesenteric fat depots in mice. *Am J Physiol Endocrinol Metab.* Jan 1 2012;302(1):E153-160.

6. Park HT, Lee ES, Cheon YP, et al. The relationship between fat depot-specific preadipocyte differentiation and metabolic syndrome in obese women. *Clin Endocrinol (Oxf).* Jan 2012;76(1):59-66.

7. Foster MT, Shi H, Seeley RJ, Woods SC. Transplantation or removal of intra-abdominal adipose tissue prevents age-induced glucose insensitivity. *Physiol Behav.* Sep 1 2010;101(2):282-288.
8. Carolyn Algire DM, and Stephan Herzig. Chapter 2 Adipose Stem Cells. In: Cao Y, ed. *Angiogenesis in Adipose Tissue*: Springer; 2013.
9. Strem BM, Hicok KC, Zhu M, et al. Multipotential differentiation of adipose tissue-derived stem cells. *Keio J Med.* Sep 2005;54(3):132-141.
10. Pittenger MF, Mackay AM, Beck SC, et al. Multilineage potential of adult human mesenchymal stem cells. *Science.* Apr 2 1999;284(5411):143-147.
11. Varma MJ, Breuls RG, Schouten TE, et al. Phenotypical and functional characterization of freshly isolated adipose tissue-derived stem cells. *Stem Cells Dev.* Feb 2007;16(1):91-104.
12. Zhang Y, Daquinag, A, Traktuev, D, Amaya-Manzanares, F, Simmons, P, March, K, Pasqualini, R, Arap, W, Kolonin, M. White adipose tissue cells are recruited by experimental tumors and promote cancer progression in mouse models. *Cancer Res.* 2009;69(12):5259-5266.
13. Patricia Semedo MB-S, Cassiano Donizetti-Oliveira and Niels Olsen Saraiva Camara. *Stem Cells in Clinic and Research*2011.
14. Statistics NCfH. *Health, United States, 2012: With Special Feature on Emergency Care.* Hyattsville: Department of Health and Human Services;2013.
15. van Kruijsdijk RC, van der Wall E, Visseren FL. Obesity and cancer: the role of dysfunctional adipose tissue. *Cancer Epidemiol Biomarkers Prev.* Oct 2009;18(10):2569-2578.
16. Bianchini F, Kaaks R, Vainio H. Overweight, obesity, and cancer risk. *Lancet Oncol.* Sep 2002;3(9):565-574.
17. Gerber SA, Rybalko VY, Bigelow CE, et al. Preferential attachment of peritoneal tumor metastases to omental immune aggregates and possible role of a unique vascular microenvironment in metastatic survival and growth. *Am J Pathol.* Nov 2006;169(5):1739-1752.
18. Khan SM, Funk HM, Thiolloy S, et al. In vitro metastatic colonization of human ovarian cancer cells to the omentum. *Clin Exp Metastasis.* Mar 2010;27(3):185-196.
19. Berberich S, Dahne S, Schippers A, et al. Differential molecular and anatomical basis for B cell migration into the peritoneal cavity and omental milky spots. *J Immunol.* Feb 15 2008;180(4):2196-2203.
20. Yu G, Wu X, Kilroy G, Halvorsen YD, Gimble JM, Floyd ZE. Isolation of murine adipose-derived stem cells. *Methods Mol Biol.* 2011;702:29-36.
21. Livak KJ, Schmittgen TD. Analysis of relative gene expression data using real-time quantitative PCR and the 2(-Delta Delta C(T)) Method. *Methods.* Dec 2001;25(4):402-408.
22. Ray A, Dittel BN. Isolation of mouse peritoneal cavity cells. *J Vis Exp.* 2010(35).
23. Sandoval P, Loureiro J, Gonzalez-Mateo G, et al. PPAR-gamma agonist rosiglitazone protects peritoneal membrane from dialysis fluid-induced damage. *Lab Invest.* Oct 2010;90(10):1517-1532.
24. Bellows CF, Zhang Y, Simmons PJ, Khalsa AS, Kolonin MG. Influence of BMI on Level of Circulating Progenitor Cells. *Obesity (Silver Spring).* Feb 3 2011.

25. Zhang Y, Bellows CF, Kolonin MG. Adipose tissue-derived progenitor cells and cancer. *World J Stem Cells.* Oct 26 2010;2(5):103-113.
26. Zhang Y, Daquinag AC, Amaya-Manzanares F, Sirin O, Tseng C, Kolonin MG. Stromal progenitor cells from endogenous adipose tissue contribute to pericytes and adipocytes that populate the tumor microenvironment. *Cancer Res.* Oct 15 2012;72(20):5198-5208.
27. Kern S, Eichler H, Stoeve J, Kluter H, Bieback K. Comparative analysis of mesenchymal stem cells from bone marrow, umbilical cord blood, or adipose tissue. *Stem Cells.* May 2006;24(5):1294-1301.
28. Timper K, Seboek D, Eberhardt M, et al. Human adipose tissue-derived mesenchymal stem cells differentiate into insulin, somatostatin, and glucagon expressing cells. *Biochem Biophys Res Commun.* Mar 24 2006;341(4):1135-1140.
29. Leyva-Leyva M, Barrera L, Lopez-Camarillo C, et al. Characterization of mesenchymal stem cell subpopulations from human amniotic membrane with dissimilar osteoblastic potential. *Stem Cells Dev.* Apr 15 2013;22(8):1275-1287.
30. Urbich C, Dimmeler S. Endothelial progenitor cells: characterization and role in vascular biology. *Circ Res.* Aug 20 2004;95(4):343-353.
31. Rae PC, Kelly RD, Egginton S, St John JC. Angiogenic potential of endothelial progenitor cells and embryonic stem cells. *Vasc Cell.* 2011;3:11.
32. Bryder D, Ramsfjell V, Dybedal I, et al. Self-renewal of multipotent long-term repopulating hematopoietic stem cells is negatively regulated by Fas and tumor necrosis factor receptor activation. *J Exp Med.* Oct 1 2001;194(7):941-952.
33. Health NIo. *Chapter 5. Hematopoietic Stem Cells.* Bethesda: US Department of Health and Human Services;2011.
34. Tzanavari T, Giannogonas P, Karalis KP. TNF-alpha and obesity. *Curr Dir Autoimmun.* 2010;11:145-156.
35. Rodriguez-Hernandez H, Simental-Mendia LE, Rodriguez-Ramirez G, Reyes-Romero MA. Obesity and inflammation: epidemiology, risk factors, and markers of inflammation. *Int J Endocrinol.* 2013;2013:678159.
36. Midwood KS, Orend G. The role of tenascin-C in tissue injury and tumorigenesis. *J Cell Commun Signal.* Dec 2009;3(3-4):287-310.
37. Cohen CA, Shea AA, Heffron CL, Schmelz EM, Roberts PC. Intra-abdominal fat depots represent distinct immunomodulatory microenvironments: a murine model. *PLoS One.* 2013;8(6):e66477.
38. Pettersson US, Walden TB, Carlsson PO, Jansson L, Phillipson M. Female mice are protected against high-fat diet induced metabolic syndrome and increase the regulatory T cell population in adipose tissue. *PLoS One.* 2012;7(9):e46057.
39. Joe AW, Yi L, Even Y, Vogl AW, Rossi FM. Depot-specific differences in adipogenic progenitor abundance and proliferative response to high-fat diet. *Stem Cells.* Oct 2009;27(10):2563-2570.
40. Van Vugt E, Van Rijthoven EA, Kamperdijk EW, Beelen RH. Omental milky spots in the local immune response in the peritoneal cavity of rats. *Anat Rec.* Feb 1996;244(2):235-245.
41. Crossno JT, Jr., Majka SM, Grazia T, Gill RG, Klemm DJ. Rosiglitazone promotes development of a novel adipocyte population from bone marrow-derived circulating progenitor cells. *J Clin Invest.* Dec 2006;116(12):3220-3228.

42. Bellows CF, Zhang Y, Simmons PJ, Khalsa AS, Kolonin MG. Influence of BMI on level of circulating progenitor cells. *Obesity (Silver Spring).* Aug 2011;19(8):1722-1726.
43. Bellows CF, Zhang Y, Chen J, Frazier ML, Kolonin MG. Circulation of progenitor cells in obese and lean colorectal cancer patients. *Cancer Epidemiol Biomarkers Prev.* Nov 2011;20(11):2461-2468.
44. Oskarsson T, Acharyya S, Zhang XH, et al. Breast cancer cells produce tenascin C as a metastatic niche component to colonize the lungs. *Nat Med.* Jul 2011;17(7):867-874.
45. Mundy GR, DeMartino S, Rowe DW. Collagen and collagen-derived fragments are chemotactic for tumor cells. *J Clin Invest.* Oct 1981;68(4):1102-1105.
46. Shintani Y, Hollingsworth MA, Wheelock MJ, Johnson KR. Collagen I promotes metastasis in pancreatic cancer by activating c-Jun NH(2)-terminal kinase 1 and up-regulating N-cadherin expression. *Cancer Res.* Dec 15 2006;66(24):11745-11753.
47. Peruzzi D, Mori F, Conforti A, et al. MMP11: a novel target antigen for cancer immunotherapy. *Clin Cancer Res.* Jun 15 2009;15(12):4104-4113.
48. Lijnen HR, Van HB, Frederix L, Rio MC, Collen D. Adipocyte hypertrophy in stromelysin-3 deficient mice with nutritionally induced obesity. *Thromb Haemost.* Mar 2002;87(3):530-535.
49. De Taeye B, Smith LH, Vaughan DE. Plasminogen activator inhibitor-1: a common denominator in obesity, diabetes and cardiovascular disease. *Curr Opin Pharmacol.* Apr 2005;5(2):149-154.
50. Brandacher G, Hoeller E, Fuchs D, Weiss HG. Chronic immune activation underlies morbid obesity: is IDO a key player? *Curr Drug Metab.* Apr 2007;8(3):289-295.
51. Park EJ, Lee JH, Yu GY, et al. Dietary and genetic obesity promote liver inflammation and tumorigenesis by enhancing IL-6 and TNF expression. *Cell.* Jan 22 2010;140(2):197-208.

Chapter 5: CHANGES IN ADIPOSE PROGENITOR POPULATIONS ARE ASSOCIATED WITH ENHANCED OVARIAN CANCER PROGRESSION IN MICE ON A HIGH FAT DIET

Abstract

Ovarian cancer is the fifth leading cause of cancer deaths in women in the United States and is typically undiscovered prior to peritoneal metastasis due to its asymptomatic nature and a lack of early detection methods. Epidemiological studies suggest that obesity is associated with increased ovarian cancer risk, although the mechanisms responsible for this have not been delineated. Waist-to-hip ratio has been especially correlated with risk,[1,2] suggesting that visceral fat may be the greatest contributor. There are multiple depots within the abdominal cavity, all with varying characteristics related to tissue dynamics, adipokine release, hormonal responses, vascularization, innervation, and abundance of non-adipocyte cells, which all impact the specific function of each individual fat depot. We have also previously demonstrated differences in the immune composition of each fat depot,[3] which may further increase functional differences. In the present study, we assessed how high fat diet impacts the peritoneal implantation of ovarian cancer and how intra-abdominal adipose progenitor populations are affected by both diet and cancer dispersion. Of note, animals on a high fat diet exhibited significantly enhanced tumor burden following intraperitoneal implantation, as compared to animals on a low fat diet. This was also associated with changes in progenitor populations within intra-abdominal adipose depots, most notably, a significant decrease in adipose progenitor cells in the omentum. There was also an increase in stromal components COL1, TNC, and FN1 in all depots, suggesting that these factors are both important for cancer progression and may also be markers of peritoneal cancer.

Introduction

Obesity is a major global health concern due to its steadily increasing rates and significant contribution to numerous diseases. In the United States alone, obesity has been associated with an estimated $147 billion per year in healthcare costs[4] related to conditions such as coronary heart disease, hypertension, diabetes, and increased risk of many cancers, including prostate,[5] breast,[6] colon,[7] kidney,[8] pancreas,[9] and more recently suggested, ovarian cancer.[10] Ovarian cancer is responsible for 140,000 deaths per year in women worldwide[11] and has one of the highest incidence-to-death ratios due to late detection, tumor heterogeneity and a high rate of metastasis.[12] Currently, the molecular mechanisms for the increased risk of ovarian cancer with obesity have not been delineated. Waist-to-hip ratio has especially been associated with risk,[1,2] suggesting that visceral fat may be the greatest contributor. There are multiple depots within the abdominal cavity, all with different characteristics from tissue dynamics (tendency to respond to excess calories with a hypertrophic versus a hyperplastic response), adipokine release, hormonal responses, vascularization, innervation, and abundance of non-adipocyte cells, which all impact the specific function of each individual fat depot. Nonetheless, little is known about the persistent molecular and cellular changes that modulate ovarian cancer development as a result of high fat feeding and weight gain.

As a largely asymptomatic disease in the early stages, ovarian cancer is rarely detected prior to metastasis. During metastasis, ovarian cancer cells exfoliate from the primary tumor, disseminate throughout the peritoneal cavity in the serous fluid and preferentially seed in the omental fat band.[13] As the primary metastatic site, the omentum is typically removed during surgical tumor debulking to slow disease progression. Importantly, there are other adipose depots within the peritoneal cavity, such as

perigonadal (parametrial in females and epididymal in males) and retroperitoneal fat that may also contribute to disease progression. As the omentum is a preferential seeding site, it appears that all adipose depots do not play the same role and thus differences between the tissues could offer critical insight into factors essential to disease progression.

We have shown previously that the homeostatic immune microenvironment of the omentum differs significantly from that of other intraperitoneal fat depots, with a distinct leukocyte profile and a robust cytokine signaling network.[3] However, other stromal cells are also integral to the tumor microenvironment and have critical implications for the generation of a permissive metastatic niche. In addition to neoplastic cells, stromal cells such as fibroblasts, endothelial cells, adipocytes or adipose tissue-derived stromal cells, stem and progenitor cells, and immune cells, can promote tumor growth, invasion, and metastasis through cellular cross-talk.[14] Stroma, consisting of vasculature, extracellular matrix, and supporting cells, provides mechanical support, a source of growth factors and cytokines, as well as the vascular supply for nutrients, gas exchange, and waste disposal. Indeed, in some common carcinomas, stroma can account for over 90% of the total tumor mass.[15]

Adipose tissue may be able to impact tumor progression by contributing to tumor stroma formation. Importantly, cells recruited from the stromal vascular fraction (SVF) of adipose tissue, especially stem and progenitor populations, have been shown to enhance cancer progression and stromal development.[16-18] An obese state may additionally alter adipose depots and associated cells, further enhancing the contribution of adipose tissue to cancer development and promotion. Here, we used a mouse model to confirm the correlation between increased body weight and ovarian cancer as well as

extensively characterized the progenitor populations present in three adipose depots: parametrial (pmWAT), retroperitoneal (rpWAT), and omental (omWAT) white adipose tissue in mice on either a low fat or high fat diet. We found that there were significant differences between tissues in both progenitor populations and expression of stromal markers with the presence of cancer. Thus, these stromal cells could potentially be key players in the correlation between obesity and ovarian cancer development and may also contribute to depot-specific differences in impact on disease.

Methods and Materials

Animals

Female C57BL/6 mice (Harlan Laboratories) were housed one mouse per cage in a controlled environment (12 hour light/dark cycle at 21°C) with free access to food and water. Mice were placed on diets and weighed twice a week for 15 weeks. At 12 weeks, animals were subjected to a glucose tolerance test and underwent body composition analysis using a Bruker nuclear magnetic resonance machine. They were then intraperitoneally injected with either PBS or MOSE-L FFL cells and maintained on their diets for three more weeks. At 15 weeks, mice were sacrificed by CO_2 asphyxiation. This study was conducted in accordance with the guidelines approved by the Virginia Tech Institutional Animal Care and Usage Committee.

Diets

Mice were placed on either a 17% low fat (AIN-93G purified rodent diet with 7% corn oil replacing soybean oil) or a 45% high fat (AIN-93G purified rodent diet with 7% corn oil replacing soybean oil and 16.5% lard; total fat- 45% of kilocalories) diet, with free access to food for a total of 15 weeks (12 before cancer initiation and three after). Diet

composition can be found in appendix b.

Glucose tolerance test

After 12 weeks of dietary treatment, mice were fasted overnight and given an intraperitoneal dose of 2mg pharmaceutical grade glucose/g body weight in a 10% solution of PBS. Blood was sampled six times per mouse over a two-hour period (at time point 0, 15, 30, 60, 90, and 120 minutes). To collect the blood, the tail vein was knicked with a sterile lancet and approximately 5 microliters of blood was used to measure glucose via a hand held glucometer.

Cell lines

The mouse ovarian surface epithelial (MOSE) cell model utilized in this study was developed from C57BL/6 mice and characterized previously.[19] Tumorigenic MOSE cells were passaged once *in vivo* by intraperitoneal (i.p.) injection into C57BL/6 mice and re-collected via peritoneal lavage following a 4-6 week incubation period to select for a more aggressive phenotype. These MOSE cell variants (MOSE-L FFL) were subsequently transduced with firefly luciferase (FFL) lentiviral particles (GeneCopoeia) as described[20] to facilitate live *in vivo* imaging of cancer cell outgrowth. The characteristics of MOSE-LFFL will be reported elsewhere. MOSE-L FFL cells were routinely maintained in high glucose Dulbecco's Modified Eagle Medium (Invitrogen), supplemented with 4% fetal bovine serum (Hyclone), 100mg/ml penicillin and streptomycin and 4μg/ml puromycin (lentiviral particles utilize a puromycin resistance marker for selection of transduced cells).

MOSE-L FFL injection

After 12 weeks of dietary treatment, mice (n=10 per group) were injected i.p. with either

$1x10^4$ MOSE-L FFL cells in 300µL sterile calcium- and magnesium-deficient phosphate buffered saline (PBS-/-), or mock-injected with 300µl of PBS-/- alone. Mice were maintained on their diets for 21 days post-injection.

Peritoneal cancer index (PCI)

In order to quantify relative tumor burden at the time of sacrifice, the PCI was determined as described previously,[21] with minor modifications. The original PCI was adapted to apply to tumor size and region in mice. "Quadrant areas" were modified to represent distinct organs and their mesentery in order to evaluate preferential seeding sites. Specific regions included peritoneal cavity lining, ovaries, lesser omentum, greater omentum, diaphragm, liver, stomach, pancreas, spleen, kidney, small intestine, small intestine mesentery, large intestine, large intestine mesentery, retroperitoneal WAT (2 pads), parametrial WAT (2 pads), and injection site. Tumor size was scored as **(0)**: no visible tumor, **(1):** < 1mm; **(2):** 1-5mm; **(3):** 5-10mm; **(4):** 10-20mm; or **(5):** >20mm. The maximum PCI score was 95, reflecting maximal lesion size in each of the 19 designated areas. Relative PCI scores were further validated by qRT-PCR analysis of FFL gene expression employed as a tumor cell reporter gene.

Fat depot and peritoneal serous fluid harvest

OmWAT, pmWAT and rpWAT were harvested from each mouse, weighed, and rinsed with PBS-/-. OmWAT is attached posteriorly to the stomach, connected to the pancreas and the anterior of the spleen.[13] To ensure that there was no pancreatic contamination, omWAT samples were also tested for buoyancy.[22] PmWAT, the largest fat depot, is comprised of two fat pads, which are located directly under the muscle wall on the dorsal side of the abdomen and attached to the uterine horns. RpWAT also contains two fat

pads, which are attached dorsally to the peritoneum, directly behind each kidney. Each tissue was processed for FACS or placed into RNAlater (Qiagen) and stored at -80°C. Resident peritoneal cavity cells were collected via peritoneal lavage with 5 ml of PBS-/-. The effluent was centrifuged, subjected to erythrocyte lysis (155 mM NH_4Cl, 10 mM $KHCO_3$, 0.1 mM EDTA),[23] and further processed as described below.

Tissue digest

SVF from individual fat depots (n= 10) were isolated from digested tissue according to standard protocols[24,25] with minor modifications to improve yields. OmWAT was digested in GKN-buffer containing 1.8 mg/ml type IV collagenase, 10% FBS, and 0.1 mg/ml DNase. The pmWAT and rpWAT digest buffer included a 1:1 ratio of Krebs-Ringer bicarbonate buffer and collagenase solution (1 mg type I collagenase, 10 mg BSA, and 2 mM $CaCl_2$ in 1 ml PBS). Following digest at 37°C for 45 min, cells were passed through a 40 μm cell strainer, and erythrocytes were lysed.

FACS analysis

SVF from the tissues of five mice per group were used. Cell suspensions were washed in flow buffer (2% BSA in PBS-/-), blocked with Fc block (BD Biosciences) for 10 minutes at 4°C, rinsed and subsequently incubated with fluorochrome-labeled antibody combinations (available upon request) for 20 min at 4°C. Fluorochrome-labeled antibodies specific for mouse CD45, CD34, CD31, CD44, CD73, CD133 and Flk-1 were obtained from eBioscience (San Diego, CA). CD105 antibody was obtained from BioLegend (San Diego, CA) and Sca1, CD44, and CD117 antibodies were obtained from BD Biosciences (San Jose, CA). Prior to analysis, cells were washed twice and resuspended in PBS-/- with propidium iodide for dead cell exclusion. FACS was

performed on a FACSAria (BD Biosciences) and data was analyzed using Flowjo (TreeStar) software.

RNA Extraction and cDNA synthesis

WAT was homogenized in Qiazol (Qiagen), and RNA was purified using an RNeasy Lipid Tissue Kit (Qiagen), according to manufacturer's instructions. RNA concentration was determined using a NanoDrop1000 spectrophotometer. RNA (n= 5 per tissue) was subjected to the iScript cDNA synthesis system (Biorad) according to manufacturer's protocol.

PCR Array

Pooled cDNA samples for each group (5 mice each) were used with 1μg total RNA for the whole plate (96 well). The SABiosciences RT^2 Profiler PCR Array (PAMM-3803E-12) was used according to standard protocol and was run on the ABI 7900HT (Applied Biosystems). The data was analyzed using the SABiosciences web-based RT^2 Profiler PCR Array data analysis program.

Quantitative real-time PCR (qRT-PCR)

qRT-PCR was performed with 12.5ng cDNA per sample using gene-specific SYBR Green primers (primer sequences are available upon request) designed with Beacon Design software. SensiMix SYBR and Fluorescein mastermix (Bioline) was used in a 15 μL reaction volume. qRT-PCR was performed for 42 cycles at 95°C for 15 sec, 60°C for 15 sec, and 72°C for 15 sec, preceded by a 10 min incubation at 95°C on the ABI 7900HT (Applied Biosystems). Melt curves were performed to ensure fidelity of the PCR product. L19 was utilized as the housekeeping gene and the ddCt method[26] was used to determine fold differences.

Statistical analysis

Data was expressed as mean ± standard error of mean (SEM). Student's t-tests were used to compare two groups. Comparisons between tissues or more than two groups utilized a one-way ANOVA coupled with a Tukey post-hoc test in Graphpad Prism. Differences were considered statistically significant at $p<0.05$.

Results

To determine if high fat feeding enhances ovarian cancer tumor burden, female C57BL/6 mice were placed on either a low fat (17% fat) or high fat (45%) diet for 12 weeks. After confirmation of significant differences in total body weight (figure 5.1 A), body fat percentages, and glucose tolerance (see chapter 4), mice were i.p. injected with 1 x 10^4 MOSE-L FFL cells in 300µl PBS -/- or mock injected with 300µl PBS-/- alone. This cell number was chosen based on time course experiments using varying dosages of MOSE-L FFL administration. With injection of 1 x 10^4 cells, mice rapidly develop severe tumor burdens and must be euthanized around 21 days (data not shown). Thus mice were injected and maintained on their respective diets for three weeks. Body weights, total weight gain, and final percent body fat are displayed in figure 5.1.

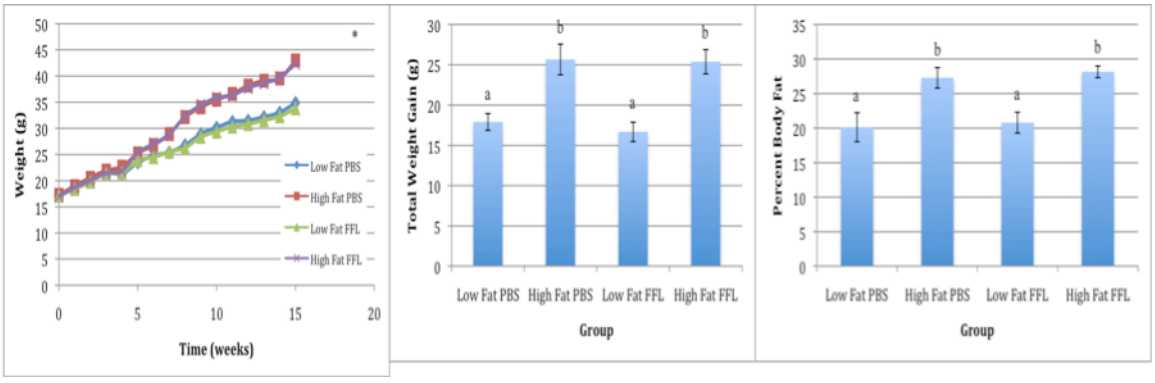

Figure 5.1. Effect of diet on body weight and composition. A) Total body weight at each week on diet. B) Total weight gain. C) Final percent body fat. * and [a,b] different letters indicate significance of $p<0.05$

Following euthanasia, tumor burden was determined via a modified Peritoneal Cancer Index (PCI)[21] protocol. Scoring of peritoneal cancers is difficult due to dissemination throughout the entire cavity. Thus, many tumors of varying sizes form. To measure this, we assigned a score, based on size, to the largest tumor in each tissue within the peritoneal cavity. The scores from each tissue were then summed to give a total score for each animal.

As shown in figure 5.3, there was a significant increase in tumor burden with mice on a high fat as compared to low fat diet ($p=0.049$). This was confirmed by qRT-PCR analysis of whole tissue firefly luciferase (FFL), which was only expressed by the MOSE-L FFL cells. There was significantly greater expression of FFL in the high fat group as compared the low fat group in omWAT (figure 5.3 B). There was also a trend towards increased FFL expression in pmWAT and rpWAT, but this was not significant due to variability. It is important to note that ovarian cancer frequently metastasizes to the omental fat band.[27,28] Additionally, after i.p. injection, a majority of ovarian cancer cells can be found localized to the omentum within 20 minutes.[29] Thus more consistent implantation of tumor cells in omWAT is expected. PmWAT and rpWAT are less frequent sites of metastasis and thus there was much more variation in FFL expression. However, the overall trend in increased FFL expression in all adipose depots is consistent with the increased PCI scores with high fat feeding. Additionally, as shown in figure 5.3 C, there was not a significant change in tissue weight in pmWAT or rpWAT with ovarian cancer dissemination. However, in omWAT, both MOSE-L FFL injected groups (low fat and high fat) had significantly heavier tissues. Indeed, omWAT was completely

overgrown by tumor tissue and was extremely fibrous, again supporting preferential seeding of cancer cells in the omentum. OmWAT also weighed significantly more in the high fat group, which correlates with higher FFL expression and a greater tumor burden with high fat diet.

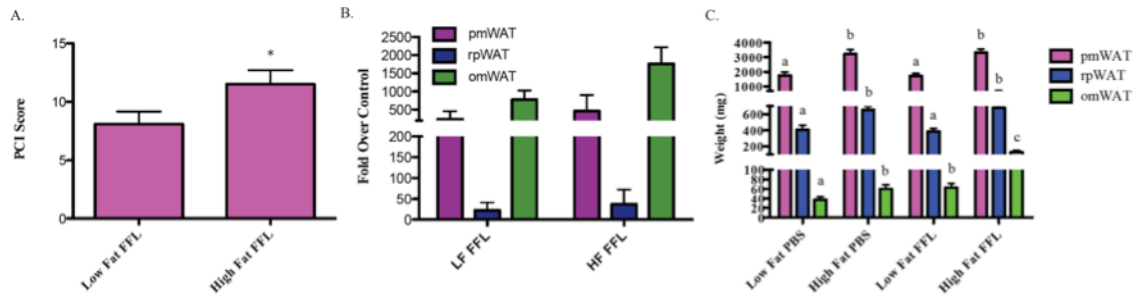

Figure 5.2. Tumor burden of mice 21 days post injection of 1 x 10^4 MOSE-L FFL cells. A)Peritoneal Cancer Index score of high fat and low fat groups with MOSE-L FFL injection. B) Firefly luciferase gene expression in each adipose depot from all groups. C) Tissue weights of adipose depots. [a, b, c]different letters indicate a p-value of <0.05

Progenitor Populations

PmWAT, rpWAT, and omWAT were examined to determine if there were depot-specific differences in response to ovarian cancer dissemination with low fat versus high fat feeding. Viable cells identified via propidium iodide exclusion (figure 5.4 A) were gated based on forward/side scatter to exclude doublets (figure 5.4 B and C) and were then separated into $CD45^+$ leukocytes and $CD45^-$ stromal constituents (figure 5.4 D). We were able to gate out the cancer cells based on forward/side scatter in the first doublet gate (figure 5.4 B). The lower box was included in the analysis, while the upper box is placed over the cancer cells, which have been excluded.

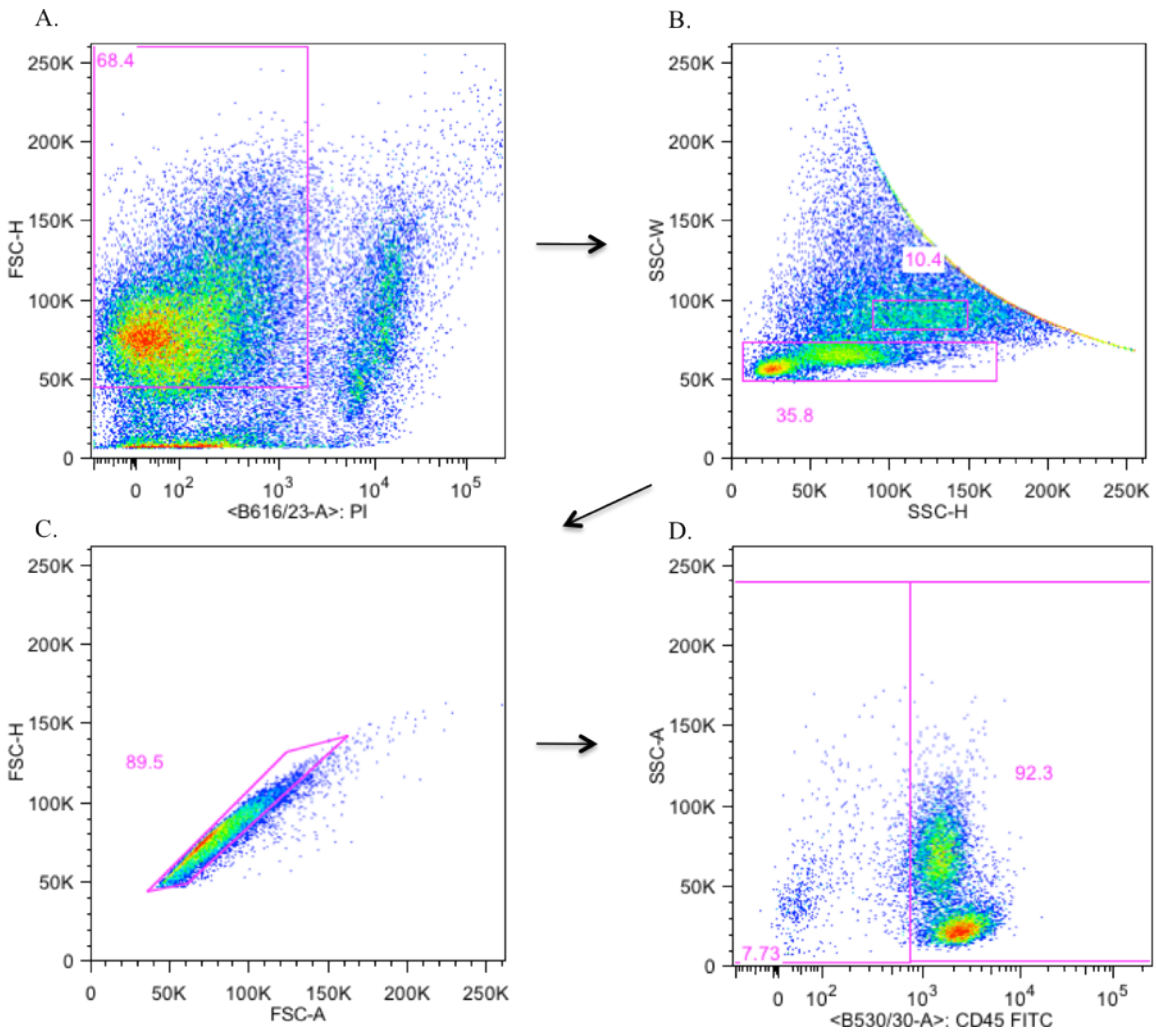

Figure 5.3. FACS gating strategy. A) Propidium iodide exclusion gating of viable cells. B) Doublet exclusion gating. C) Second doublet exclusion gating. D) CD45+/- gating.

Each adipose depot responded differently to dissemination of MOSE-L FFL cells. In pmWAT with the presence of cancer, there was a trend of decreased $CD45^-$ cells and an increase in APCs and MSCs in both cancer groups. In rpWAT, there were no notable changes in any populations with cancer. Conversely, the most significant changes were evident in omWAT. With the injection of cancer cells, there was a trend towards decreased $CD45^-$ cells in both groups, a major decrease in APCs with both high fat diet

and cancer dissemination alone ($p<0.05$), which was further decreased in the high fat cancer group (LF PBS-52.3%, LF FFL-13.7%, HF PBS-17.6%, HF FFL-3.6%), and a significant increase in ECs in both MOSE-L FFL groups over their dietary control groups ($p<0.05$) (LF PBS-3.6%, LF FFL-5.8%, HF PBS-2.3%, HF FFL-4.2%).

PSF and blood were included in the analysis as medium which may contain transitory progenitor populations. In addition, the dissemination of ovarian cancer is largely mediated by PSF, as metastatic ovarian cancer cells slough off of the ovaries into the peritoneal cavity where they are carried by PSF to novel seeding sites. While ovarian cancer less readily engages in hematogenous dissemination, the blood could be an important vehicle for the recruitment of progenitor cells from sites outside of the peritoneal cavity.

There were some significant changes in both blood and PSF with the presence of ovarian cancer cells in the peritoneal cavity. In blood, there was a trend towards an increase in $CD45^-$ cells in the high fat cancer group only (LF PBS-2.0%, LF FFL-1.6%, HF PBS-1.6%, HF FFL-4.5%), and for MSCs, a decrease in the low fat group with cancer and an increase in the high fat group with cancer (LF PBS-13.4%, LF FFL-9.6%, HF PBS-2.1%, HF FFL-4.1%). In PSF, there was a decrease in APCs in all groups compared to low fat PBS (LF PBS-6.7%, LF FFL-3.2%, HF PBS-1.6%, HF FFL-2.2%) and a significant increase in MSCs in the high fat cancer group compared to all others ($p<0.05$) (LF PBS-35.0%, LF FFL-36.1%, HF PBS-34.1%, HF FFL-47.3%).

Table 5.1. Progenitor populations in adipose depots, blood and PSF of mice on a high fat versus low fat diet with the addition of peritoneal dissemination of ovarian cancer cells. Data presented as a mean with standard error of the mean in parenthesis. [a,b]different letters indicate significant difference of $p<0.05$

	Parametrial WAT			
Markers	Low Fat PBS	Low Fat FFL	High Fat PBS	High Fat FFL
CD45+	59.4 (3.1)	70.1 (2.9)	67.4 (0.1)	71.6 (3.1)

Percent of CD45+ cells					
HSC	Sca1+Ckit+	0.6 (0.1)[a, c]	0.2 (0.1)[a]	1.3 (0.2)[b, c]	0.8 (0.2)[c]
CD45-		40.6 (3.1)	29.9 (2.9)	32.6 (1.1)	28.4 (3.1)
Percent of CD45- Cells					
APC	Sca1+CD34+	42.1 (3.8)	45.5 (2.1)	39.3 (4.6)	41.5 (3.1)
MSC	CD44+CD105+CD73+	10.0 (1.9)	13.8 (1.2)	12.4 (1.7)	13.8 (2.0)
EPC	CD133+Flk1+CD31-	0.1 (0.0)	0.2 (0.1)	5.1 (2.9)	1.3 (1.1)
EC	CD34-/lo, CD133-CD31+	5.9 (1.1)	6.0 (0.4)	5.0 (1.3)	3.8 (0.6)
CEC	Flk1+CD31+CD133+	0.04 (0.02)	0.1 (0.1)	0.9 (0.4)	0.4 (0.3)
	Sca1+CD31+CD44+	0.6 (0.2)[a,c,d]	0.5 (0.1)[a,b,c]	5.2 (2.1)[b,c,d]	2.7 (0.4)[a,b,d]
		Retroperitoneal WAT			
	Markers	Low Fat PBS	Low Fat FFL	High Fat PBS	High Fat FFL
CD45+		54.2 (3.0)	55.3 (4.2)	61.9 (3.9)	61.0 (1.7)
Percent of CD45+ cells					
HSC	Sca1+Ckit+	0.3 (0.1)	0.3 (0.1)	1.2 (0.5)	0.8 (0.1)
CD45-		45.4 (3.0)	44.4 (4.3)	38.2 (3.9)	40.4 (1.7)
Percent of CD45- Cells					
APC	Sca1+CD34+	36.5 (2.2)	39.0 (3.3)	56.2(2.4)	47.6 (2.6)
MSC	CD44+CD105+CD73+	13.2 (2.0)	13.5 (2.3)	16.8 (5.8)	8.1 (1.3)
EPC	CD133+Flk1+CD31-	0.3 (0.1)	0.1 (0.1)	0.1 (0.04)	0.1 (0.1)
EC	CD34-/lo, CD133-CD31+	3.7 (0.4)	3.9 (1.0)	4.1 (0.1)	4.1 (0.8)
CEC	Flk1+CD31+CD133+	0.1 (0.1)	0.1 (0.1)	0.1 (0.1)	0 (0)
	Sca1+CD31+CD44+	0.7 (0.3)	1.3 (0.5)	2.9 (0.2)	2.9 (1.0)
		Omental WAT			
	Markers	Low Fat PBS	Low Fat FFL	High Fat PBS	High Fat FFL
CD45+		93.0 (1.5)	93.6 (1.4)	79.9 (2.9)	87.9 (3.6)
Percent of CD45+ cells					
HSC	Sca1+Ckit+	2.1 (0.2)	2.0 (0.3)	0.8 (0.1)	0.5 (0.2)
CD45-		6.8 (1.5)	6.1 (1.3)	20.1 (2.9)	12.1 (3.6)
Percent of CD45- Cells					
APC	Sca1+CD34+	52.3 (2.4)[a]	13.7 (6.3)[b]	17.6 (1.8)[b]	3.6 (1.0)[b]
MSC	CD44+CD105+CD73+	43.8 (1.1)[a]	39.1 (1.3)[a]	12.8 (0.4)[b]	23.8 (4.0)[c]
EPC	CD133+Flk1+CD31-	1.1 (0.4)	0.3 (0.2)	0 (0)	0.2 (0.1)
EC	CD34-/lo, CD133-CD31+	3.6 (0.4)[a]	5.8 (0.6)[b]	2.3 (0.2)[a]	4.2 (0.6)[a,b]
CEC	Flk1+CD31+CD133+	0.6 (0.23)	0.2 (0.2)	0.1 (0.1)	0 (0)
	Sca1+CD31+CD44+	1.7 (0.5)	2.2 (0.8)	0.8 (0.1)	0.2 (0.1)
		Peritoneal Serous Fluid			
	Markers	Low Fat PBS	Low Fat FFL	High Fat PBS	High Fat FFL
CD45+		99.2(0.1)	98.4 (0.2)	98.4 (0.5)	97.8 (0.6)
Percent of CD45+ cells					
HSC	Sca1+Ckit+	3.4 (0.3)	2.9 (0.5)	6.8 (0.6)	1.2 (0.5)
CD45-		0.8 (0.1)	1.5 (0.2)	1.6 (0.5)	2.2 (0.6)
Percent of CD45- Cells					
APC	Sca1+CD34+	6.7 (1.5)	3.2 (1.1)	3.9 (0.9)	3.7 (2.6)
MSC	CD44+CD105+CD73+	35.0 (2.4)[a]	36.1 (3.9)[a]	34.1 (1.8)[a]	47.3 (2.9)[b]
EPC	CD133+Flk1+CD31-	0 (0)[a]	0 (0)[a]	0.1 (0.1)[a,b]	0.5 (0.2)[b]
EC	CD34-/lo, CD133-CD31+	15.2 (1.8)	13.3 (2.2)	15.5 (5.5)	13.2 (4.6)
CEC	Flk1+CD31+CD133+	0 (0)	0 (0)	0 (0)	0.2 (0.1)
	Sca1+CD31+CD44+	0 (0)	0.3 (0.1)	0.9 (0.6)	1.4 (0.5)
		Blood			
	Markers	Low Fat PBS	Low Fat FFL	High Fat PBS	High Fat FFL
CD45+		97.8 (0.2)	98.2 (0.4)	98.4 (0.3)	95.6 (1.5)
Percent of CD45+ cells					
HSC	Sca1+Ckit+	0.01 (0.01)	0.02 (0.01)	0 (0)	0 (0)
CD45-		2.0 (0.1)	1.6 (0.4)	1.6 (0.3)	4.5 (1.5)
Percent of CD45- Cells					

APC	Sca1+CD34+	1.1 (0.4)	1.1 (0.5)	0.1 (0.1)	0.1 (0.1)
MSC	CD44+CD105+CD73+	13.4 (2.0)[a]	9.6 (1.5)[a]	2.1 (0.6)[b,c]	4.1 (0.8)[c]
EPC	CD133+Flk1+CD31-	0.1 (0.1)	0 (0)	0.1 (0.1)	0.1 (0.1)
EC	CD34-/lo, CD133-CD31+	41.1 (7.1)	42.5 (3.8)	42.1 (5.9)	38.4 (5.7)
CEC	Flk1+CD31+CD133+	0 (0)	0 (0)	0.5 (0.1)	1.0 (0.5)
	Sca1+CD31+CD44+	0 (0)	0 (0)	0.1 (0.1)	0 (0)

However, the PSF analysis may not give a completely accurate picture of all cells present, as some may have been lost due to association with tumor spheroids. The PSF was filtered to remove debris during processing, resulting in the removal of multicellular aggregates, which may have contained MOSE-L FFLs as well as any associated cells. As a preliminary investigation, we collected all of the aggregates that were filtered from the PSF of the low fat diet mice with MOSE-L FFL injections, digested them, pooled the resulting cells, and analyzed them via FACS. These cells were labeled "PSF backwash" because they were washed from the inside of the filter. We also collected a tumor from the pmWAT of a mouse on the high fat diet, digested it and analyzed the resulting single cells. The progenitor populations from both are displayed in table 5.2.

The PSF backwash had a greater proportion of CD45- cells than the PSF single cells (12.1% versus 1.5%, respectively), suggesting a tendency for $CD45^-$ cells in the PSF to associate with the tumor cells instead of floating freely. There was a much greater proportion of APCs (27.8% in backwash as compared to 3.2% in PSF) and a decreased percentage of MSCs (5.6% in backwash as compared to 36.1% in PSF) and ECs (1.6% in backwash as compared to 13.3% in PSF). Surprisingly, there were no EPCs or CECs in the PSF backwash. Within the pmWAT tumor, excluding tumor cells, there were 65.2% $CD45^+$ cells and 33.5% $CD45^-$ cells. There was an almost identical number of CD45- cells associated with the tumor as compared to the tissue it came from (33.5% in pmWAT tumor as compared to 32.6% in high fat diet pmWAT). However, within the tumor, there

were few of the progenitor populations of interest. There were more MSCs (9.2%) than APCs (2.2%) and a few ECs (1.8%). As there were few of our populations of interest within the $CD45^-$ fraction, it is unclear what other cell types were present. Fibroblasts are reported to be CD44+,[30] and about 68.5% of the CD45- cells in the pmWAT tumor were CD44+(data not shown), which may account for some of the cells. However, we did not incorporate other markers that could further characterize these cells.

Table 5.2. Progenitor population percentages of PSF backwash and pmWAT tumor.

	Markers	PSF Backwash	pmWAT tumor
CD45+		87.9	65.2
Percent of CD45+ cells			
HSC	Sca1+Ckit+	2.5	0.06
CD45-		12.1	33.5
Percent of CD45- Cells			
APC	Sca1+CD34+	27.8	2.2
MSC	CD44+CD105+CD73+	5.6	9.2
EPC	CD133+Flk1+CD31-	0	0
EC	CD34-/lo, CD133-CD31+	1.6	1.8
CEC	Flk1+CD31+CD133+	0	0
	Sca1+CD31+CD44+	0	0.8

PCR Array and qRT-PCR

PCR arrays using pooled samples of RNA from the adipose depots of mice on both diets, with and without the presence of MOSE-L FFL cells (n=5 per group), were performed to more extensively characterize the overall adipose tissue signaling milieu in these unique microenvironments. qRT-PCR was used to confirm a subset of genes from the array as well as add a panel of genes related to adipose tissue, hypoxia/angiogenesis, and stromal factors. It is important to note that expression patterns represent the tissue as a whole, and thus are reflective of both adipocytes, SVF cells, and MOSE-L FFL cells in cancer groups. Thus, for the omWAT especially, which had a significant influx of cancer cells, the gene expression may be more indicative of MOSE-L FFL cells than adipose tissue. However, pmWAT and rpWAT had few tumors and are likely more indicative of changes

in adipocytes and SVF cells due to the presence of cancer in the peritoneal cavity than of the cancer cells themselves. Figure 5.5 depicts changes in the gene expression profiles (from both the PCR array and qRT-PCR) of each tissue with high fat diet, MOSE-L FFL implantation or both. As the PCR array utilized pooled samples, there are no statistics. Thus figure 5.5 includes only trends of an increase or decrease by twofold.

PmWAT had the fewest changes with ovarian cancer dissemination. With cancer, there was an increase in some cytokines (CCL1, CCL2, CCL4, CXCR1 CXCR2, and TNF), an increase in stromal factors (COL1, FN1, TNC), and a decrease in anti-inflammatory markers IL4 and IL10. Additionally, CXCL10, IFNg, IL1a, IL1b, and NOS2 increased with both cancer and high fat diet and were further increased in the high fat cancer group as compared to the low fat cancer group, indicating a combinatory effect on inflammation.

In rpWAT, there was a major inflammatory response with an increase in cytokines/chemokines as well as an increase in some stromal factors (COL1, FN1) with MOSE-L FFL dissemination. Many genes, especially inflammatory markers, were increased with both high fat diet and cancer individually and were further increased in the high fat cancer group as compared to the low fat cancer group.

OmWAT had a significant number of changes, although again, this incorporates gene expression of the cancer cells. With MOSE-L FFL seeding, there was an increased

expression of most cytokines and a decrease in many stromal and adipose-related genes.

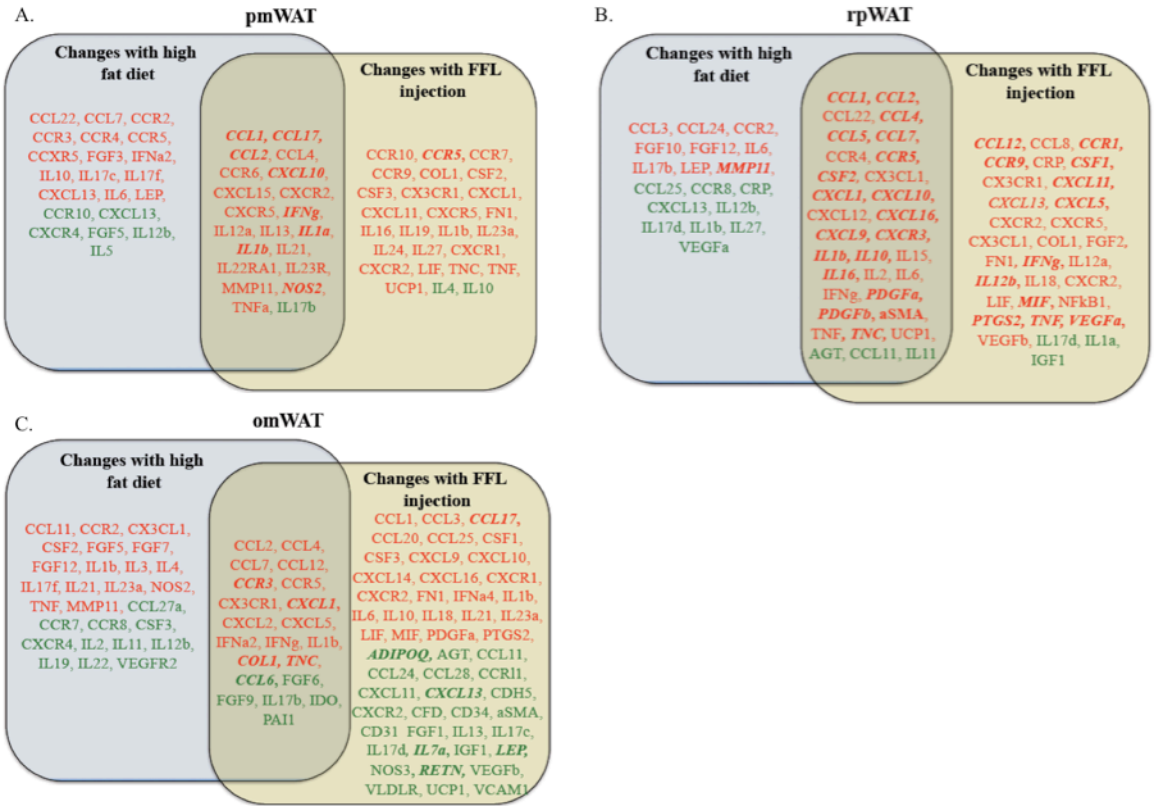

Figure 5.4. Venn diagram of gene expression changes. A) pmWAT, B) rpWAT, and C) omWAT, with high fat diet (left square), MOSE-L FFL injection (right square), or both (center). Red font indicates an increase in expression (twofold or greater) and green font indicates a decreased expression (twofold or greater). Bolded italics indicate that the gene increased with FFL injection and further increased in the MOSE-L FFL injected group on the high fat diet (over the injected group on the low fat diet). Includes PCR array and qRT-PCR analysis, so significance not included- changes indicative of trends less than or greater than twofold.

Table 5.3 displays qRT-PCR fold changes greater or less than twofold in the low fat MOSE-L FFL group as compared to the low fat PBS group. OmWAT had the greatest number of significant changes, again, largely reflective of a difference in gene expression of cancer cells as compared to adipose tissue. Notably, there was a decrease in adipokines (RETN, ADIPOQ, LEP, PAI1, and AGT), an increase in cytokines (CCL2, CCL4, CXCR2, IL10 and TNFa), a decrease in stromal markers (IDO, CD34, aSMA, CD31, CDH5, and VCAM1), and an increase in FN1 and TNC.

PmWAT and rpWAT had few significant changes, due in part to a small sample size and variation between mice. The variation may also be attributed to differences in tumor burden between animals. However, there were many trends. Both tissues displayed increases in CXCR2, IL1b, IFNg, Col1, TNC, MMP11, and FN1.

Table 5.3. Fold changes of low fat diet group plus MOSE-L FFL injection versus low fat diet group with PBS injection from qRT-PCR. *p<0.05

	pmWAT	rpWAT	omWAT
VLDLR	-0.1	1.1	-11.2*
NAMPT	1.0	1.8	-1.6
RETN	-1.2	1.0	-33.5*
ADIPOQ	0.4	1.4	-24.2*
LEP	1.5	1.8	-27.9*
CCL1	1.9	11.7	1.0
CCL2	1.7	2.2	10.4*
CCL4	0.4	4.1	3.9*
CCL5	0.7	2.6	-0.9
CCR5	1.9	3.2	1.7
CXCR2	36.9	27.0	8.3*
CXCL13	0	-0.5	-7.4*
CX3CL1	1.9	2.4	0.6
IL1b	10.3	3.8	6.7
TNFa	5.5	1.5	0.6
IL10	-2.3	-0.7	4.5*
IFNg	3.3	3.9	-0.4
IL6	1.3	0	2.2
NOS3	0	0	-2.8
VEGFa	0.5	-1.0	-0.1
VEGFR2	0.6	-0.5	-1.1
HIF1a	0.8	-0.4	1.6
IGF1	-1.1	-2.4	-2.6*
TGFb	1.2	0.4	1.3
AGT	0	-2.2	-18*
Col1	4.1	2.1	2.6
TNC	10.1	10.6	30.9*
IDO	0	-1.1	-17.6*
CD34	0.6	0.5	-2.8*
aSMA	0	2.6	-3.0*
MMP11	2.4	2.0	0.2
CD31	0	1.1	-3.0*
PAI1	0	0.2	-10.6*
CDH5	0.3	0.6	-2.6*
FN1	10.0	9.0	40.2*
VCAM1	0.4	1.8	-2.1*

Table 5.4 shows fold changes in gene expression of high fat diet mice with MOSE-L FFL injections as compared to high fat diet PBS mice. A majority of the trends appeared to be the same with cancer dissemination regardless of low fat or high fat diet. However, some trends were enhanced with high fat feeding. For instance, the increase in CXCR2 was significant across tissues, whereas IL1b was only significantly increased in pmWAT and omWAT, albeit IL1bdid trend upwards as well. IL6 expression increased in both pmWAT and rpWAT. The changes in stromal markers were also maintained across low fat and high fat groups with the presence of cancer. Both cancer groups displayed an increase in COL1, TNC (not increased in the cancer group with high fat diet in pmWAT, but became significantly increased in rpWAT with high fat diet), and FN1, which became significant in pmWAT with high fat diet.

Table 5.4. Fold changes of high fat diet group plus MOSE-L FFL injection versus high fat diet group with PBS injection from qRT-PCR. *p<0.05

	pmWAT	rpWAT	omWAT
VLDLR	-1.4	0.7	-30.9*
NAMPT	0.1	2.3*	-0.9
RETN	-0.8	-0.3	-112.4*
ADIPOQ	-0.8	-0.2	-77.2*
LEP	0.2	0.8	-83.5*
CCL1	9.7	2.3	-2.3
CCL2	1.7	0.4	4.0*
CCL4	1.5	-47.0	1.2
CCL5	1.2	2.6	-1.7
CCR5	0.4	1.3	-1.9
CXCR2	22.3*	29.2*	4.8*
CXCL13	-1.6	-0.9	-13.5*
CX3CL1	30.2	1.3	-2.2*
IL1b	6.0*	5.2	2.6*
TNFa	0.8	-0.6	-4.5*
IL10	-1.5	1.5	0.8
IFNg	0.9	2.6	-1.8
IL6	8.2	2.2	0.3
NOS3	-0.4	1.3	-4.9*
VEGFa	0.8	2.1	1.0
VEGFR2	0.5	0.7	-4.2*
HIF1a	1.9	1.3	0.2

IGF1	-0.1	-0.9	-3.3
TGFb	0.8	0.8	-0.5
AGT	-0.6	-0.7	-32.8*
Col1	2.1	3.3	2.3*
TNC	1.6	6.7*	19.6*
IDO	-1.2	1.5	-5.1
CD34	-0.3	1.0	-3.6*
aSMA	0.9	2.2	-5.3*
MMP11	-0.8	1.6	-1.1
CD31	0.0	2.1	-6.7*
PAI1	1.5	3.9	-0.7
CDH5	0.5	2.1	-4.8*
FN1	11.6*	10.2	32.9*
VCAM1	1.2	2.9*	-4.9*

Discussion

Recent studies have suggested that obesity is associated with an increased risk of ovarian cancer,[10,31] although the mechanism for this is currently unknown. This study demonstrates that in a mouse model, ovarian cancer implantation and tumor development is indeed augmented by high fat diet. As in chapter 4, it should be noted that our high fat diet mice displayed significant increases in total body weight, percent body fat, and dysregulation of glucose tolerance, but are indicative of early stages of obesity. However, even the pre-obese state resulted in a significant increase in tumor burden following i.p. injection of MOSE-L FFL cells. To investigate potential mechanisms for this correlation, we focused on adipose tissue-derived stromal cells.

Studies have shown that stem and progenitor cells from WAT are in fact able to contribute to tumor development,[16-18,32] yet few have examined these cells as potential players in a relationship between obesity and cancer risk. Here, we characterized changes that occur in these populations with dissemination of ovarian cancer cells in mice on either a low fat or high fat diet. We focused on omWAT, a frequent site of ovarian cancer metastasis,[33] as well as rpWAT and pmWAT, which are not common sites

of metastasis, but are proximal tissues that may be able to contribute cells or secreted factors.

As anticipated, the most changes were evident in omWAT, likely due to the high influx of cancer cells. Additionally, there appeared to be a combinatorial effect with high fat diet and cancer. While there was no change in $CD45^+$ cells with MOSE-L FFL dissemination in low fat diet mice, there was a significant increase in MOSE-L FFL mice on a high fat diet. This is indicative of an enhanced inflammatory response with high fat diet, a phenomenon that is commonly associated with obesity.[34] There was also a major loss of APCs with both high fat diet and cancer individually, and this was further enhanced by high fat diet and cancer concurrently. This could be due to a downregulation of markers used, efflux of these cells out of the tissue, or more probably, differentiation of the APCs. There was also an increase in ECs in both FFL groups and a significantly higher percentage in the high fat cancer group as compared to low fat cancer group. The increased presence of endothelial cells correlates with the necessity of blood vessels for access to oxygen and nutrients. Indeed, avascular tumors are severely restricted in their growth and metastatic potential,[35] making endothelial cell recruitment or proliferation critical to cancer progression.

There were fewer significant changes in progenitor populations in the less tumor-infiltrated sites. In pmWAT, there were a few trends such as an increase in $CD45^+$ cells, a decrease in HSCs with FFLs, and a slight increase in APCs and EPCs in both cancer groups as compared to PBS. RpWAT likewise had a few trends, but no significant differences. However, the few changes in these tissues may not give an accurate depiction of overall occurrences. It is possible that the populations in the tissues are

tightly regulated and that the tissue may compensate for cells that flux in or out. An analysis of proliferation and turnover of cells may be important for future studies. It is also possible that three weeks was too early to see significant changes in more distal tissues. A time course experiment may be able to shed light on the sequence of events for changes in progenitor populations.

PSF and blood were also included in the analysis as they may provide a depiction of cells in transit. Normally, peritoneal fluid serves as lubrication between the organs and lining of the peritoneal cavity and contains primarily water, leukocytes, electrolytes, and other signaling molecules. However, with some disease states, such as metastatic cancer in the peritoneal cavity, this fluid, termed ascites, accumulates and can contribute to the proliferation and spread of cancer calls. Various small molecules including inflammatory mediators, bioactive lipids, proteolytic enzymes, shed plasma membrane particles, growth factors and extracellular matrix components, as well as many different cell types such as leukocytes, stem and progenitor cells, and other stromal cells can be found at varying levels in cancerous ascites.[36] The recruitment of these additional cells into the ascites may help establish a permissive microenvironment for tumor metastasis.[37] In this study, we found that in the PSF, there was a significant increase in MSCs in the high fat cancer group compared to all others, a significant increase in EPCs in high fat diet PBS mice and further in high fat MOSE-L FFL mice, and a trend towards a decrease in APCs in all groups compared to low fat PBS animals. Both MSCs and EPCs appear to increase more drastically in response to MOSE-L FFL cells with high fat feeding, suggesting that high fat diet with cancer may encourage the mobilization of progenitors into the PSF even greater than MOSE-L FFL cells alone. It is also interesting that there was an

increase in MSCs, but a decrease in APCs. However, this may not give a complete picture of the events in the PSF. For the processing of PSF samples for FACS analysis, aggregates were filtered out. Thus, the PSF analysis only takes into account free-floating cells, and not those that may be associated with tumor spheroids. It is possible that while many populations may be recruited to the peritoneal cavity due to the increased production of signaling molecules by cancer cells, some populations may associate with cancer cells more rapidly. Indeed, in the PSF backwash, which included digested aggregates of cells from the PSF, there was a greater number of $CD45^-$ cells associated with tumor cells than those free-floating in the PSF. Additionally, there was a much greater proportion of APCs and a decreased percentage of MSCs and ECs, suggesting that at an early timepoint, of these cell types, APCs are the most frequently associated with tumor cells. However, it should be kept in mind that the percentages are of the CD45- population, so while it appears that the proportions of MSCs and ECs associated with tumor cells are less than those free-floating, the actual numbers are not significantly different because the CD45- fraction is much larger in tumor spheroids. Regardless, the number of APCs was substantially higher, suggesting that APCs especially associate with cancer cells at an early time point in the metastatic process.

Blood was also included because there are often systemic effects of cancer, including recruitment of immune and other cells via the blood.[38,39] In this study, there was a trend towards an increase in $CD45^-$ cells in the high fat cancer group only, but not in the high fat or cancer groups alone, again suggesting an enhanced combinatorial effect. There was also a trend towards a decrease in MSCs in the low fat cancer group, a decrease with high fat diet and an increase with high fat cancer over high fat PBS. There

was no change in ECs, which is contrary to previous studies that found an increase in circulating endothelial cells and progenitors.[38] This could potentially be due to the early time point of obesity and ovarian cancer dissemination.

We additionally characterized the progenitor populations within a pmWAT tumor to see if stromal cells had been recruited within three weeks. There was a large population of immune cells (65.2% $CD45^+$ cells of total SVF cells), but still a substantial number of $CD45^-$ cells (33.5%). Interestingly, within the tumor, there were few of the progenitor populations of interest. There were more MSCs than APCs, and a few ECs. It is unclear what other cell types may be comprising the $CD45^-$ cell fraction. It is possible that there are fibroblasts/myofibroblasts, mesothelial cells, or hospicells, which were not included in this study. As previously stated, fibroblasts are reportedly positive for CD44, which was present on 68.5% of the CD45- cells in the tumor, and could account for some of the unknown cells. Fibroblasts generally constitute the majority of stromal cells within the primary tumor in various types of human carcinomas[40] and secrete a plethora of modulatory proteins that can influence cancer cells, including matrix metalloproteinases that remodel extracellular matrix in support of invasion and metastasis, growth factors to promote cancer cell proliferation, cytokines and chemokines for cell recruitment, as well as extracellular matrix proteins for adhesion and motility support.[41] Fibroblasts are the most likely candidates. Another potential cell type present are hospicells, a novel peritoneal cell of unknown lineage, that stains for multidrug resistance proteins and has similar features to MSCs. Hospicells express surface markers not included in our study, such as CD9, CD10, CD29, CD146, CD166, and HLA-1. They have been found to be closely associated with tumoral cells from ascites of stage III ovarian adenocarcinoma-

bearing patients and were initially isolated for their specific adhesion to mammary or ovarian adenocarcinoma cells.[33] Mesothelial cells are specialized epithelial cells that line the internal organs and wall of the peritoneal, pleural, and pericardial cavities and may also be present. They contribute to peritoneal homeostasis, control of fluid and solute transport, immune surveillance, antigen presentation, inflammation and wound healing.[42] Importantly, cancer cells can cause mesothelial cells to dissociate from the lining and they may also incorporate into tumors.[42-45] Lastly, the stem and progenitor cells of the adipose SVF are currently very poorly characterized and different authors use various different surface marker combinations, some only using one marker (which could indicate a multitude of different cells). [46-53] It is possible that these unknown $CD45^-$ cells could be previously uncharacterized cells or the same cell types with different surface marker expression profiles. However, as we know that APCs and other stem cells associate with tumor spheroids early on (as in the PSF), it is likely that these CD45- cells are differentiated stem and progenitor cells. The association of progenitor cells and cancer cells may lead to significant changes in differentiation or activation status. Indeed, various studies have demonstrated that MSCs can be induced to differentiate into myofibroblasts or endothelial cells upon association with cancer cells, contributing to the stroma and vasculature of tumors.[54-56]

An additional finding of interest was the difference in the stromal component of tumors originating from different adipose depots. For instance, while the $CD45^-$ fraction in a pmWAT tumor was about 33%, and very similar to the tissue itself, the omentum that had been infiltrated with tumor cells had a $CD45^-$ component of about 12%, which was closer to the control omentum with 20%, than it was to the pmWAT tumor. Thus,

the microenvironment may be critical to the stromal development of tumors.

Fitting with the importance of stromal contributions, the most significant changes in the genes we investigated were in stromal markers such as COL1, TNC, and FN1. COL1, or collagen 1, may play an important role in cancer progression, and in fact, patients with collagen dense breast tissue possess a greater than fourfold increased risk of breast carcinoma.[57] Additionally in breast cancer, it has been shown that metastatic epithelial cells are actually able to migrate in direct contact along stromal collagen fibers[58] and that cancer cells can increase expression of collagens, fibronectin, and tenascin in myofibroblasts.[59] In both low fat and high fat diet mice, COL1 was increased between two and four-fold in all tissues with MOSE-L FFL dissemination. However, this was not significant except in omWAT in high fat diet mice, likely due to variation which could potentially be attributed to differences in tumor burden.

Tenascin C, encoded by the gene TNC, is an extracellular matrix protein common in stem cell niches and is produced by cancer cells to promote survival and outgrowth of metastases.[60] TNC is overexpressed in the stroma of malignant ovarian tumours particularly at the interface between epithelia and stroma and can facilitate the process of invasion.[61,62] Additionally, ovarian carcinomas can induce enhanced expression of TNC in fibroblasts.[62] Here, TNC was increased approximately tenfold in both pmWAT and rpWAT in low fat cancer mice (although not significant due to variation), and significantly, thirtyfold in omWAT, as compared to low fat PBS mice. TNC was also increased in all three tissues in high fat diet mice with cancer (approximately twofold, sevenfold, and twentyfold in pmWAT, rpWAT, and omWAT, respectively). The fold increases were not as drastic in high fat cancer mice as compared to low fat cancer mice

due to an already enhanced expression with high fat diet. However, the dCT values were either the same or lower in the high fat cancer group as compared to the low fat cancer group in all tissues. Thus TNC could be another indicator of cancer presence and higher expression levels could help create a conducive environment for tumor seeding and outgrowth.

Finally, fibronectin, encoded for by FN1, is an extracellular adhesion molecule that can promote the migration and invasion of ovarian cancer cells.[63] Additionally, fibronectin has been shown to promote ovarian cancer spheroid formation, anchorage and disaggregation and has been found in the ascites of ovarian cancer patients.[64] It is also produced by fibroblasts, vascular cells and cancer cells and may increase invasive capacity.[65] FN1 was significantly increased in both cancer groups in omWAT as well as in pmWAT in the high fat cancer group. While not statistically significantly, on average there was a tenfold increase in FN1 in rpWAT in both cancer groups and in pmWAT in the low fat cancer groups.

Importantly, COL1, TNC, and FN1 were all increased in omWAT in both MOSE-L FFL groups, when the tissue is primarily composed on tumor cells, which means that they are likely important for tumor development, and tumor cells either secrete them or encourage surrounding cells to secrete them. Since there was an increase in some of these (TNC in rpWAT and omWAT, COL1 in omWAT, trend of Fn1 in omWAT) with high fat diet, it suggests that these matrix proteins may predispose the tissues to being a more conducive environment for tumor growth, especially since the greatest increases occurred in omWAT, which also had the greatest tumor burden. COL1, TNC, and FN1

may also be indicators of tumor burden in distant tissues or of modulation of the microenvironment to support metastases.

Conclusion

Increased tumor burden was associated with mice on a high fat versus low fat diet. Accompanying the enhanced tumor burden were changes in progenitor populations within intra-abdominal adipose depots. While fewer changes were evident in pmWAT and rpWAT, there were significant changes in omWAT, which also had the greatest tumor infiltration. Importantly there was a significant decrease in APCs, which could be indicative of differentiation into cells such as myofibroblasts or endothelial cells. Indeed, the proportion of endothelial cells was increased in omWAT with cancer. This theory of differentiation is also supported by the high number of progenitors associated with tumor spheroids in the PSF, an early part of the metastatic process, and the lack of progenitors, but high number of $CD45^-$ cells present in a tumor isolated from the pmWAT. Additionally, the significant increase in stromal components COL1, TNC, and FN1, especially in omWAT, suggests an enhanced presence of stromal cells. The expression of these factors was also augmented in pmWAT and rpWAT, which were associated with a lower tumor burden. This indicates that ovarian cancer dissemination can impact the various adipose depots in the peritoneal cavity, and may be able to modify the microenvironment in the peritoneal cavity by influencing the number and activity of stromal cell, including stem and progenitors, in order to create a permissive niche for adhesion and outgrowth.

References

1. Mink PJ, Folsom AR, Sellers TA, Kushi LH. Physical activity, waist-to-hip ratio, and other risk factors for ovarian cancer: a follow-up study of older women. *Epidemiology.* Jan 1996;7(1):38-45.

2. Delort L, Kwiatkowski F, Chalabi N, Satih S, Bignon YJ, Bernard-Gallon DJ. Central adiposity as a major risk factor of ovarian cancer. *Anticancer Res.* Dec 2009;29(12):5229-5234.

3. Cohen CA, Shea AA, Heffron CL, Schmelz EM, Roberts PC. Intra-abdominal fat depots represent distinct immunomodulatory microenvironments: a murine model. *PLoS One.* 2013;8(6):e66477.

4. Finkelstein EA, Khavjou OA, Thompson H, et al. Obesity and severe obesity forecasts through 2030. *Am J Prev Med.* Jun 2012;42(6):563-570.

5. MacInnis RJ, English DR. Body size and composition and prostate cancer risk: systematic review and meta-regression analysis. *Cancer Causes Control.* Oct 2006;17(8):989-1003.

6. Key TJ, Appleby PN, Reeves GK, et al. Body mass index, serum sex hormones, and breast cancer risk in postmenopausal women. *J Natl Cancer Inst.* Aug 20 2003;95(16):1218-1226.

7. Moore LL, Bradlee ML, Singer MR, et al. BMI and waist circumference as predictors of lifetime colon cancer risk in Framingham Study adults. *Int J Obes Relat Metab Disord.* Apr 2004;28(4):559-567.

8. Bergstrom A, Hsieh CC, Lindblad P, Lu CM, Cook NR, Wolk A. Obesity and renal cell cancer--a quantitative review. *Br J Cancer.* Sep 28 2001;85(7):984-990.

9. Li D, Morris JS, Liu J, et al. Body mass index and risk, age of onset, and survival in patients with pancreatic cancer. *JAMA.* Jun 24 2009;301(24):2553-2562.

10. Olsen C, Green, A, Whiteman, D, Sadeghi, S, Kolahdooz, F, Webb, P. Obesity and the risk of epithelial ovarian cancer: a systemic review and meta-analysis. *Eur J Cancer.* 2007;43:690-709.

11. Siegel R, Naishadham D, Jemal A. Cancer statistics, 2012. *CA Cancer J Clin.* Jan-Feb 2012;62(1):10-29.

12. Saad AF, Hu W, Sood AK. Microenvironment and pathogenesis of epithelial ovarian cancer. *Horm Cancer.* Dec 2010;1(6):277-290.

13. Gerber SA, Rybalko VY, Bigelow CE, et al. Preferential attachment of peritoneal tumor metastases to omental immune aggregates and possible role of a unique vascular microenvironment in metastatic survival and growth. *Am J Pathol.* Nov 2006;169(5):1739-1752.

14. Wels J, Kaplan RN, Rafii S, Lyden D. Migratory neighbors and distant invaders: tumor-associated niche cells. *Genes Dev.* Mar 1 2008;22(5):559-574.

15. Dvorak HF. Tumors: wounds that do not heal. Similarities between tumor stroma generation and wound healing. *N Engl J Med.* Dec 25 1986;315(26):1650-1659.

16. Zhang Y, Daquinag, A, Traktuev, D, Amaya-Manzanares, F, Simmons, P, March, K, Pasqualini, R, Arap, W, Kolonin, M. White adipose tissue cells are recruited by experimental tumors and promote cancer progression in mouse models. *Cancer Res.* 2009;69(12):5259-5266.

17. Kidd S, Spaeth E, Watson K, et al. Origins of the tumor microenvironment: quantitative assessment of adipose-derived and bone marrow-derived stroma. *PLoS One.* 2012;7(2):e30563.

18. Klopp AH, Zhang Y, Solley T, et al. Omental adipose tissue-derived stromal cells promote vascularization and growth of endometrial tumors. *Clin Cancer Res.* Feb 1 2012;18(3):771-782.
19. Roberts PC, Mottillo EP, Baxa AC, et al. Sequential molecular and cellular events during neoplastic progression: a mouse syngeneic ovarian cancer model. *Neoplasia.* Oct 2005;7(10):944-956.
20. Swainson L, Mongellaz C, Adjali O, Vicente R, Taylor N. Lentiviral transduction of immune cells. *Methods Mol Biol.* 2008;415:301-320.
21. Carmignani CP, Sugarbaker PH. Synchronous extraperitoneal and intraperitoneal dissemination of appendix cancer. *Eur J Surg Oncol.* Oct 2004;30(8):864-868.
22. Khan SM, Funk HM, Thiolloy S, et al. In vitro metastatic colonization of human ovarian cancer cells to the omentum. *Clin Exp Metastasis.* Mar 2010;27(3):185-196.
23. Park HT, Lee ES, Cheon YP, et al. The relationship between fat depot-specific preadipocyte differentiation and metabolic syndrome in obese women. *Clin Endocrinol (Oxf).* Jan 2012;76(1):59-66.
24. Berberich S, Dahne S, Schippers A, et al. Differential molecular and anatomical basis for B cell migration into the peritoneal cavity and omental milky spots. *J Immunol.* Feb 15 2008;180(4):2196-2203.
25. Yu G, Wu X, Kilroy G, Halvorsen YD, Gimble JM, Floyd ZE. Isolation of murine adipose-derived stem cells. *Methods Mol Biol.* 2011;702:29-36.
26. Livak KJ, Schmittgen TD. Analysis of relative gene expression data using real-time quantitative PCR and the 2(-Delta Delta C(T)) Method. *Methods.* Dec 2001;25(4):402-408.
27. Lengyel E. Ovarian cancer development and metastasis. *Am J Pathol.* Sep 2010;177(3):1053-1064.
28. Steinberg JJ, Demopoulos RI, Bigelow B. The evaluation of the omentum in ovarian cancer. *Gynecol Oncol.* Jul 1986;24(3):327-330.
29. Nieman KM, Kenny HA, Penicka CV, et al. Adipocytes promote ovarian cancer metastasis and provide energy for rapid tumor growth. *Nat Med.* 2011;17(11):1498-1503.
30. Pilling D, Fan T, Huang D, Kaul B, Gomer RH. Identification of markers that distinguish monocyte-derived fibrocytes from monocytes, macrophages, and fibroblasts. *PLoS One.* 2009;4(10):e7475.
31. Fairfield KM, Willett WC, Rosner BA, Manson JE, Speizer FE, Hankinson SE. Obesity, weight gain, and ovarian cancer. *Obstet Gynecol.* Aug 2002;100(2):288-296.
32. Martin-Padura I, Gregato G, Marighetti P, et al. The white adipose tissue used in lipotransfer procedures is a rich reservoir of CD34+ progenitors able to promote cancer progression. *Cancer Res.* Nov 3 2011.
33. Rafii A, Mirshahi P, Poupot M, et al. Oncologic trogocytosis of an original stromal cells induces chemoresistance of ovarian tumours. *PLoS One.* 2008;3(12):e3894.
34. Gregor MF, Hotamisligil GS. Inflammatory mechanisms in obesity. *Annu Rev Immunol.* 2011;29:415-445.

35. Folkman J. Role of angiogenesis in tumor growth and metastasis. *Semin Oncol.* Dec 2002;29(6 Suppl 16):15-18.
36. Barbolina MV, Moss NM, Westfall SD, et al. Microenvironmental regulation of ovarian cancer metastasis. *Cancer Treat Res.* 2009;149:319-334.
37. Burleson KM, Casey RC, Skubitz KM, Pambuccian SE, Oegema TR, Jr., Skubitz AP. Ovarian carcinoma ascites spheroids adhere to extracellular matrix components and mesothelial cell monolayers. *Gynecol Oncol.* Apr 2004;93(1):170-181.
38. Bellows CF, Zhang Y, Chen J, Frazier ML, Kolonin MG. Circulation of progenitor cells in obese and lean colorectal cancer patients. *Cancer Epidemiol Biomarkers Prev.* Nov 2011;20(11):2461-2468.
39. Wolf AM, Wolf D, Steurer M, Gastl G, Gunsilius E, Grubeck-Loebenstein B. Increase of regulatory T cells in the peripheral blood of cancer patients. *Clin Cancer Res.* Feb 2003;9(2):606-612.
40. Sappino AP, Skalli O, Jackson B, Schurch W, Gabbiani G. Smooth-muscle differentiation in stromal cells of malignant and non-malignant breast tissues. *Int J Cancer.* May 15 1988;41(5):707-712.
41. De Wever O, Demetter P, Mareel M, Bracke M. Stromal myofibroblasts are drivers of invasive cancer growth. *Int J Cancer.* Nov 15 2008;123(10):2229-2238.
42. Yung S, Chan TM. Mesothelial cells. *Perit Dial Int.* Jun 2007;27 Suppl 2:S110-115.
43. Foley-Comer AJ, Herrick SE, Al-Mishlab T, Prele CM, Laurent GJ, Mutsaers SE. Evidence for incorporation of free-floating mesothelial cells as a mechanism of serosal healing. *J Cell Sci.* Apr 1 2002;115(Pt 7):1383-1389.
44. Yashiro M, Chung YS, Inoue T, et al. Hepatocyte growth factor (HGF) produced by peritoneal fibroblasts may affect mesothelial cell morphology and promote peritoneal dissemination. *Int J Cancer.* Jul 17 1996;67(2):289-293.
45. Lansley SM, Searles RG, Hoi A, et al. Mesothelial cell differentiation into osteoblast- and adipocyte-like cells. *J Cell Mol Med.* Oct 2011;15(10):2095-2105.
46. Baglioni S, Cantini G, Poli G, et al. Functional differences in visceral and subcutaneous fat pads originate from differences in the adipose stem cell. *PLoS One.* 2012;7(5):e36569.
47. Brzoska M, Geiger H, Gauer S, Baer P. Epithelial differentiation of human adipose tissue-derived adult stem cells. *Biochem Biophys Res Commun.* Apr 29 2005;330(1):142-150.
48. Dromard C, Bourin P, Andre M, De Barros S, Casteilla L, Planat-Benard V. Human adipose derived stroma/stem cells grow in serum-free medium as floating spheres. *Exp Cell Res.* Apr 1 2011;317(6):770-780.
49. Efimenko A, Starostina E, Kalinina N, Stolzing A. Angiogenic properties of aged adipose derived mesenchymal stem cells after hypoxic conditioning. *J Transl Med.* 2011;9:10.
50. Fang B, Song Y, Zhao RC, Han Q, Lin Q. Using human adipose tissue-derived mesenchymal stem cells as salvage therapy for hepatic graft-versus-host disease resembling acute hepatitis. *Transplant Proc.* Jun 2007;39(5):1710-1713.

51. Kern S, Eichler H, Stoeve J, Kluter H, Bieback K. Comparative analysis of mesenchymal stem cells from bone marrow, umbilical cord blood, or adipose tissue. *Stem Cells.* May 2006;24(5):1294-1301.
52. Lin G, Yang R, Banie L, et al. Effects of transplantation of adipose tissue-derived stem cells on prostate tumor. *Prostate.* Jul 1 2010;70(10):1066-1073.
53. Mitchell JB, McIntosh K, Zvonic S, et al. Immunophenotype of human adipose-derived cells: temporal changes in stromal-associated and stem cell-associated markers. *Stem Cells.* Feb 2006;24(2):376-385.
54. Spaeth EL, Dembinski JL, Sasser AK, et al. Mesenchymal stem cell transition to tumor-associated fibroblasts contributes to fibrovascular network expansion and tumor progression. *PLoS One.* 2009;4(4):e4992.
55. Bexell D, Gunnarsson S, Tormin A, et al. Bone marrow multipotent mesenchymal stroma cells act as pericyte-like migratory vehicles in experimental gliomas. *Mol Ther.* Jan 2009;17(1):183-190.
56. Suzuki K, Sun R, Origuchi M, et al. Mesenchymal stromal cells promote tumor growth through the enhancement of neovascularization. *Mol Med.* 2011;17(7-8):579-587.
57. Boyd NF, Martin LJ, Stone J, Greenberg C, Minkin S, Yaffe MJ. Mammographic densities as a marker of human breast cancer risk and their use in chemoprevention. *Curr Oncol Rep.* Jul 2001;3(4):314-321.
58. Wang W, Wyckoff JB, Frohlich VC, et al. Single cell behavior in metastatic primary mammary tumors correlated with gene expression patterns revealed by molecular profiling. *Cancer Res.* Nov 1 2002;62(21):6278-6288.
59. Faouzi S, Le Bail B, Neaud V, et al. Myofibroblasts are responsible for collagen synthesis in the stroma of human hepatocellular carcinoma: an in vivo and in vitro study. *J Hepatol.* Feb 1999;30(2):275-284.
60. Oskarsson T, Acharyya S, Zhang XH, et al. Breast cancer cells produce tenascin C as a metastatic niche component to colonize the lungs. *Nat Med.* Jul 2011;17(7):867-874.
61. Wilson KE, Langdon SP, Lessells AM, Miller WR. Expression of the extracellular matrix protein tenascin in malignant and benign ovarian tumours. *Br J Cancer.* Oct 1996;74(7):999-1004.
62. Wilson KE, Bartlett JM, Miller EP, et al. Regulation and function of the extracellular matrix protein tenascin-C in ovarian cancer cell lines. *Br J Cancer.* May 1999;80(5-6):685-692.
63. Yousif NG. Fibronectin promotes migration and invasion of ovarian cancer cells through up-regulation of FAK-PI3K/Akt pathway. *Cell Biol Int.* Sep 21 2013.
64. Carduner L, Agniel R, Kellouche S, et al. Ovarian cancer ascites-derived vitronectin and fibronectin: combined purification, molecular features and effects on cell response. *Biochim Biophys Acta.* Oct 2013;1830(10):4885-4897.
65. Hanamura N, Yoshida T, Matsumoto E, Kawarada Y, Sakakura T. Expression of fibronectin and tenascin-C mRNA by myofibroblasts, vascular cells and epithelial cells in human colon adenomas and carcinomas. *Int J Cancer.* Sep 26 1997;73(1):10-15.

Chapter 6: WHITE ADIPOSE TISSUE STROMAL VASCULAR CELLS ENHANCE OVARIAN CANCER AGGRESSIVENESS IN VITRO

Abstract

Obesity is a major global health concern due to its steadily increasing rates and significant contribution to numerous diseases, including cancer. Ovarian cancer specifically, is associated with a 30% increased risk with obesity, although the mechanisms for this are unknown. We have previously shown that progenitor populations in visceral adipose tissue change with obesity and cancer presence. Additionally, many studies have demonstrated that stem and progenitor populations from white adipose tissue (WAT) are recruited by cancer cells and can enhance tumor development. Here, we show that stem cells from the stromal vascular fraction of visceral adipose tissue in mice can directly associate with mouse ovarian cancer cells. Additionally, co-culturing of these cells induces changes in structural formation and enhances proliferation, mobility, and invasive potential of ovarian cancer cells. These may all be contributing factors for the mechanism behind enhanced progression of ovarian cancer in obese individuals.

Introduction

Obesity is a major global health concern due to its steadily increasing rates and significant contribution to numerous diseases. In the United States alone, obesity has been associated with an estimated $147 billion per year in healthcare costs[1] related to conditions such as coronary heart disease, hypertension, diabetes, and increased risk of many cancers, including prostate,[2] breast,[3] colon,[4] kidney,[5] pancreas,[6] and more recently suggested, ovarian cancer.[7] Ovarian cancer is responsible for 140,000 deaths per year in

women worldwide[8] and has one of the highest incidence-to-death ratios due to late detection, tumor heterogeneity and a high rate of metastasis.[9] Currently, the molecular mechanisms for the increased risk of ovarian cancer with obesity have not been delineated.

Stromal cells such as fibroblasts, endothelial cells, progenitor cells, and immune cells are critical for tumor development due to their promotion of tumor growth, invasion, and metastasis.[10] This is achieved via provision of mechanical support, production of growth factors and cytokines, protection from immune destruction, and formation of a vascular supply for nutrients, gas exchange, and waste disposal. Adipose tissue may be able to impact tumor progression by contributing to tumor stroma formation. Importantly, the stromal vascular fraction (SVF) of adipose tissue is a rich source of stem and progenitor cells,[11] potentially even more so than bone marrow. Indeed, between 0.5 x 10^6 and 20 x 10^6 stem cells can be retrieved from 100g of fat, while approximately 0.006-0.06 x 10^6 stem cells can be isolated from 100ml of BM.[12-14] Additionally, visceral adipose tissue may be a more advantageous source of stem and progenitor cells for ovarian tumors as it is more proximal to the ovaries and other sites within the peritoneal cavity.

Studies have shown that stem and progenitor populations are able to be recruited by tumors, incorporate into the stroma, and enhance cancer progression.[15-17] An obese state may additionally alter adipose depots and associated cells, further enhancing the contribution of adipose tissue to cancer development and promotion. However, little is known about the actual role of adipose tissue-derived stem cells in tumor development. Here, we found that stem cells from visceral WAT were able to directly associate with

ovarian cancer cells and enhance cancer cell proliferation, migration, and invasive capacity. Additionally, co-culture of SVF stem cells with ovarian cancer cell initiated changes in structure formation of tumor outgrowths, which could impact metastatic success. By further characterizing these mechanisms, we could develop novel targets for decreasing ovarian cancer development and metastasis in at-risk obese populations.

Methods and Materials

Isolation of SVF progenitor cells

SVF cells were isolated from the parametrial WAT of female C57BL/6 mice on a high fat (45%kcal from fat) diet for 15 weeks, according to standard protocol.[18] Briefly, approximately 1 gram of pmWAT was rinsed in PBS, minced, and placed into digest buffer (1:1 ratio of Krebs-Ringer bicarbonate buffer and collagenase solution (1 mg type I collagenase, 10 mg BSA, and 2 mM CaCl2 in 1 ml PBS)). The tissue was digested in a shaker at 37°C for 45 min, then centrifuged to separate the SVF from adipocytes. The SVF was rinsed, passed through a 40 μm cell strainer, and erythrocytes were lysed (3 minutes in erythrocyte lysis buffer: 155mM NH4Cl, 10mM KHCO3, 0.1mM EDTA). The remaining cells were then plated in tissue-culture treated flasks in high glucose Dulbecco's Modified Eagle Medium (DMEM) (Invitrogen) supplemented with 4% fetal bovine serum (FBS) (Hyclone), 100mg/ml penicillin/streptomycin and 1x ciprofloxacin. After 24 hours, the medium was pulled off to remove dead cells. Attached cells were washed and fresh medium was added back. Once cells proliferated to ~80% confluence, they were trypsinized and used for experiments. For co-culture studies, the SVF cells were stained with CellTracker™ CM-DiI Cell-Labeling Solution (Molecular Probes) according to standard protocol.

FACS Analysis

Cultured SVF cells (grown to 80% confluence, but not passaged) were analyzed via flow cytometry. Cell suspensions were washed in flow buffer (2% BSA in PBS-/-), blocked with Fc block (BD Biosciences) for 10 minutes at 4°C, rinsed and subsequently incubated with fluorochrome-labeled antibodies (available upon request) for 20 min at 4°C. Fluorochrome-labeled antibodies specific for mouse CD29, CD31, CD44, CD45, and CD73 were obtained from eBioscience (San Diego, CA). CD105 and CD271 antibodies were obtained from BioLegend (San Diego, CA) and Sca1 and CD34 antibodies were obtained from BD Biosciences (San Jose, CA). FACS was performed on a FACSAria (BD Biosciences) and data was analyzed using Flowjo (TreeStar) software.

Cell lines

The mouse ovarian surface epithelial (MOSE) cell model utilized in this study was developed from C57BL/6 mice and characterized previously.[19] Tumorigenic MOSE cells were passaged once *in vivo* by intraperitoneal (i.p.) injection into C57BL/6 mice and re-collected via peritoneal lavage following a 4-6 week incubation period to select for a more aggressive phenotype. These MOSE cell variants (MOSE-L FFL) were subsequently transduced with firefly luciferase (FFL) lentiviral particles (GeneCopoeia) as described[20] to facilitate live *in vivo* imaging of cancer cell outgrowth. The characteristics of MOSE-LFFL will be reported elsewhere. MOSE-L FFL cells were routinely maintained in high glucose DMEM, supplemented with 4% FBS, 100mg/ml penicillin and streptomycin and 4μg/ml puromycin (lentiviral particles utilize a puromycin resistance marker for selection of transduced cells). MOSE-L FFL cells were

also stably transfected with pIRES-EGFP (Clontech), which expresses the enhanced green fluorescent protein (EGFP) as a bicistronic messenger RNA together with the puromycin resistance gene under control of an IRES segment for *in vitro* monitoring. Cells were selected for EGFP expression by flow cytometry and maintained under puromycin selection during routine culturing of the cells.

Early passages of MOSE cells (MOSE-E) were utilized in the invasion assays. MOSE-E cells have also been characterized previously[19] and represent non-aggressive, ovarian epithelial cells. They were routinely maintained in high glucose DMEM, supplemented with 4% FBS and 100mg/ml penicillin and streptomycin. They were labeled with CellTracker™ CM-DiI Cell-Labeling Solution for monitoring

MILE SVEN 1 (MS1), mouse pancreatic endothelial cells, were obtained from ATCC and were used as controls in the MTT and invasion assays. MS1 cells were routinely maintained in high glucose DMEM, supplemented with 4% FBS and 100mg/ml penicillin and streptomycin. MS1 cells were transfected with mCherry for monitoring.

Co-culture

CM-Dil-labeled SVF cells and MOSE-L FFL EGFP cells were co-cultured in non-tissue culture treated dishes in high glucose DMEM, supplemented with 4% FBS and 100 mg/ml penicillin/streptomycin. Images were taken via live-cell imaging using NIS Elements (Nikon Instruments).

MTT Assay

Cells (3000 MOSE-L FFL cells or 4000 SVF or MS1 cells per well) were seeded in a 96-well tissue culture treated plate in high glucose DMEM supplemented with 2% charcoal stripped FBS and 100mg/ml penicillin and streptomycin. After cells adhered to the plate

(approximately 5 hours), the medium was changed to 100μl of treatment medium: 1) high glucose DMEM plus 2% charcoal stripped FBS, 2) high glucose DMEM plus 4% FBS, 3) 50% high glucose DMEM plus 2% charcoal stripped FBS and 50% serum free high glucose DMEM, 4) 50% high glucose DMEM plus 2% charcoal stripped FBS and 50% SVF cell conditioned medium (for MOSE-L FFLs) or 5) 50% high glucose DMEM plus 2% charcoal stripped FBS and 50% MOSE-L FFL conditioned medium (for SVF cells) or 6) 50% high glucose DMEM plus 2% charcoal stripped FBS and 50% MS1 conditioned medium (for MOSE-L FFL cells). Conditioned medium was made by growing cells to approximately 90% confluence in tissue cultured-treated dishes with normal medium, rinsing, and then incubating in serum free high glucose DMEM for 48 hours. Conditioned medium was centrifuged and supernatant was filtered with a 2 μm filter. It was then aliquoted and frozen until use. Cells were incubated with their treatment media for 48 hours, then 50 μl MTT (3-(4,5-dimethylthiazol-2-yl)-2,5-diphenyltetrazolium bromide) solution was added and cells were incubated for 4 additional hours. Medium was removed and 100μl of dimethyl sulfoxide was added to each well. Absorbance was read on a BioTek Synergy 2 platereader (BioTek Instruments) at a wavelength of 570nm.

Transwell Migration Assay

Cells (65,000 MOSE-L FFL or SVF cells per well) were seeded in a 24-well tissue culture-treated plate in high glucose DMEM supplemented with 4% FBS and 100 mg/ml penicillin and streptomycin. After cells became approximately 95% confluent, wells were washed and 1ml of serum free high glucose DMEM was added. After 48 hours, inserts with 8 μm pores were added to wells with either serum-free high glucose DMEM, high

glucose DMEM with 4% FBS, or the wells containing cells. Fifty thousand cells of the opposing cell type in 600μl serum free high glucose DMEM were added to each insert. The plates were incubated at 37°C for 4 hours. The top of the inserts were then scraped, the inserts were rinsed with PBS -/-, and the cells on the bottom of the inserts were fixed in 3% paraformaldehyde in PBS-/- plus 250mM HEPES. The cells were then stained with crystal violet and images of 4 fields of view (north, south, east, and west) were taken at 10X magnification using NIS Elements. The number of cells in each image was then counted.

Invasion Assay

Spheroids of an exact cell number (1000 cells per spheroid) were formed by seeding cells in low-attachment round bottom plates in high glucose DMEM with 4% FBS and 100mg/ml penicillin and streptomycin. Spheroids contained the following: 1) 1000 MOSE-L FFLS, 2) 1000 SVF cells, 3) 750 MOSE-L FFLs and 250 SVF cells, 4) 500 MOSE-L FFLs and 500 SVF cells, or 5) 250 MOSE-L FFL cells and 750 SVF cells. As a control, SVF cells were replaced with either MOSE-E or MS1 cells. EGFP labeled MOSE-L FFL and CM-Dil labeled SVF, MOSE-E or mCherry-labeled MS1 cells were used so that each cell type could be monitored. After 48 hours, the preformed spheroids were embedded in collagen (For 10 wells: 20 μl 10X DMEM, 2.5 μl 1N NaOH, 68.5 μl water, 109 μl type I collagen (BD Biosciences)). The bottom layer of collagen was formed the day before spheroid seeding. To embed, the spheroids were seeded in their growth medium and incubated for 5 hours to allow for attachment to the collagen. Then the medium was pulled off, the top layer of collagen was added and 50 μl DMEM with

4% FBS was added over the collagen. Images were taken at time 0 and then every 48 hours for 6 days. Area of outgrowth was measured using NIS Elements.

Statistics

Each experiment was repeated in at least three times with at least three biological replicates. When comparing only two groups, a standard t-test was used. For comparing more than two groups, one-way ANOVAs with a Tukey post-test was utilized.

Results

Stem cells were isolated from the parametrial WAT of mice that had been placed on a high fat diet for 15 weeks. To ensure collection of the correct cells, the surface marker expression profile was determined using FACS analysis. The results are shown in table 6.1. The SVF cells were almost all $CD29^+$, a majority (60.7%) were $Sca1^+$, about half (42.6%) were positive for CD105, and about a quarter (24.7) were $CD73^+$. Less than 10% were positive for CD271, CD31, CD34, CD44, or CD45. CD45 and CD31 are lineage markers for leukocytes and endothelial cells, respectively, so their low levels of expression were expected. CD34 is generally present on adipose progenitor cells, but is lost in tissue culture.[21] Overall, our results matched well with previous studies. Yamamoto el al.[22] characterized the surface marker expression of cultured adipose stem cells from mice, and had similar results to ours (CD29-93.3%, CD31-1.9%, CD34-4.6%, CD45- 0.7%, CD105-49.7, Sca1- 89.4%), excepting a higher percentage of Sca1+ cells.

Table 6.1 SVF characterization. SVF cells were isolated from adipose tissue, plated, grown to 80% confluency, and then analyzed via FACS analysis.

Marker	Percentage of positive SVF cells
CD105	42.60
CD271	1.75
CD29	96.00
CD31	4.53
CD34	9.53

CD44	5.43
CD45	5.65
CD73	24.70
Sca1	60.70

After confirming isolation of the correct cells, the SVF stem cells were labeled with CM-Dil for monitoring *in vitro*. MS1, mouse endothelial progenitor cells, were used as a control for stromal cells and were transfected with mCherry. SVF and MS1 cells were each co-cultured with EGFP-transfected MOSE-L FFL cells. To mimic the *in vivo* environment of the peritoneal cavity where cells float unattached as spheroids, cells were grown in 3D culture in low attachment dishes. Grown alone (data not shown), both SVF and MOSE-L FFL cells were capable of anchorage-independent growth, demonstrated by survival and formation of spheroids. However, MS1 cells died within a few days when cultured alone. When cultured together starting as single cells, both SVF and MS1 cells associated with MOSE-L FFL cells within an hour. By 24 hours, the SVF and MS1 cells were found in the center of the spheroids with the MOSE cells surrounding them (figure 6.1). Even when SVF or MS1 cells were added to preformed MOSE-L FFL spheroids, they were able to attach to the spheroids and migrate to the center. As shown in figure 6.1E, within three days, MS1 cells were even able to form vasculature-like networks within the center of the tumor spheroids. While these structures were not evident with SVF cells, it is possible that they may form more complex structures at a later timepoint.

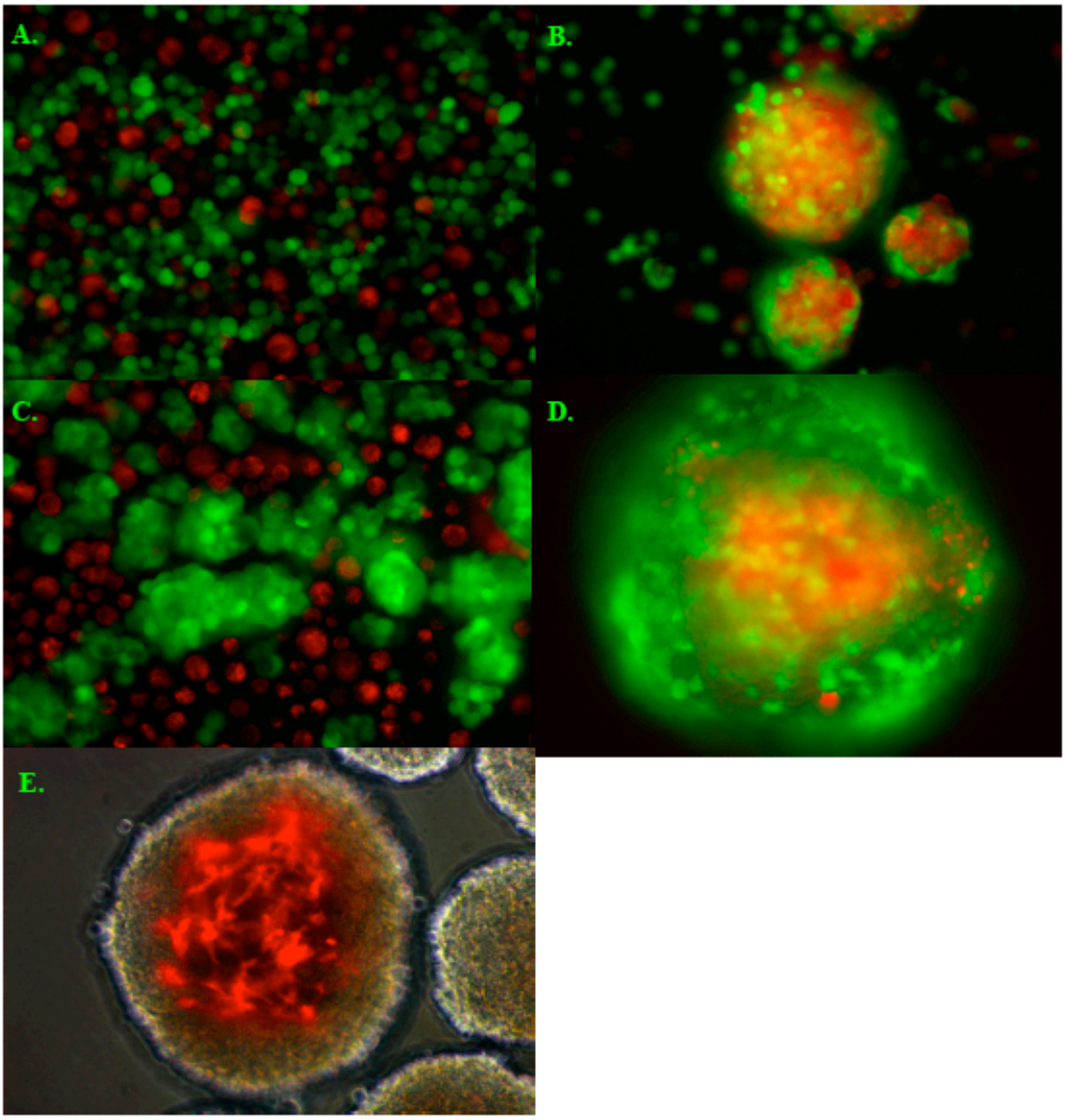

Figure 6.1. Fluorescent images of interactions between SVF (red) and MOSE-L FFL (green) cells. A) MOSE-L FFL and SVF cells added together, time 0. B) MOSE-L FFL and SVF cells added together, 20 hours after seeding. C) SVF cells added 24 hours after MOSE-L FFL, time 0. D) SVF cells added 24 hours after MOSE-L FFL, 20 hours after seeding of SVF cells. E) MOSE-L FFL and MS1 cells after 3 days.

After confirming that the cells could directly associate, we performed MTT assays with conditioned medium, to determine if SVF or MS1 cells secreted factors that could enhance proliferation of MOSE-L FFL cells or vice versa (figure 6.2). Within 48 hours, conditioned medium from all three cell types were able to increase the proliferation of the

other cells. The greatest increase in proliferation was in MOSE-L FFL cells incubated with SVF conditioned medium, although MS1 conditioned medium also significantly enhanced the number of MOSE-L FFL cells. Conversely, MOSE-L FFL conditioned medium was also able to significantly enhance the proliferation of both SVF cells and MS1 cells.

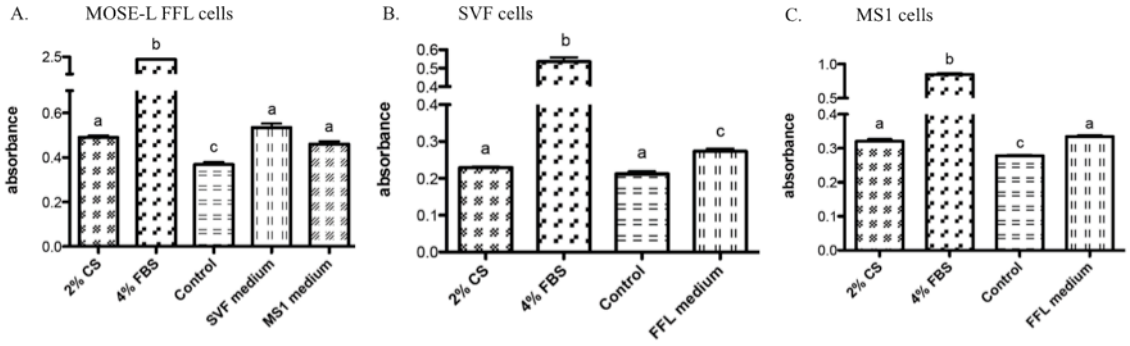

Figure 6.2. Absorbances from MTT assays for A) MOSE-L FFLs, B) SVF cells, and C) MS1 cells. 2% CS (charcoal stripped FBS) was a base medium for treatments and used as a control. 4% FBS medium was used as a positive control. Control medium consisted of 50% serum free medium and 50% 2% CS medium and treatment groups included 50% serum free medium and 50% conditioned medium from the labeled cell type (made in serum free medium). [a,b,c]different letters indicate $p<0.05$

We next determined that MOSE-L FFL cells and SVF cells secreted factors that could enhance the mobility of the other cell type. Serum-free medium was used as a negative control, 4% FBS medium was used as a positive control and the experimental wells included the opposing cell type incubated in serum free medium for 48 hours. MOSE-L FFLs were mobile even in serum-free medium, while SVF cells were not. Both cells were able to significantly enhance the migration of the opposing cell type (figure 6.3).

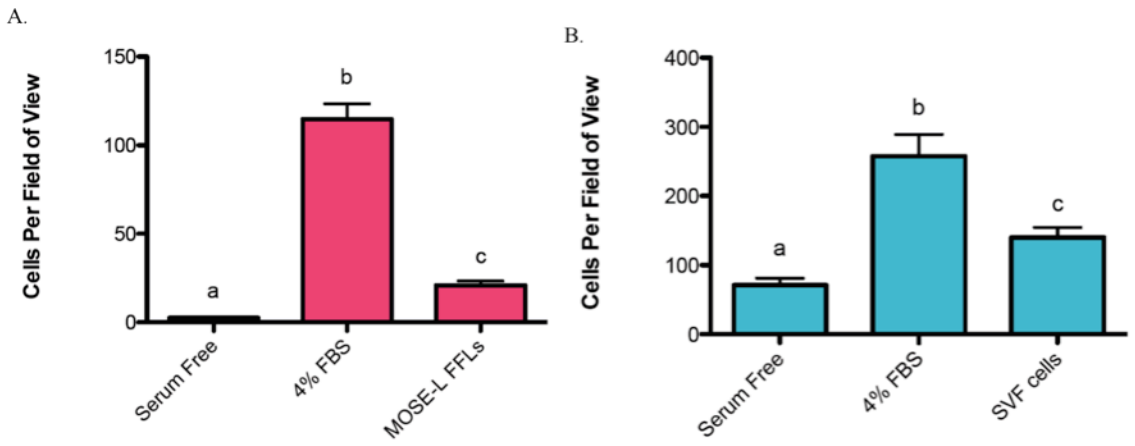

Figure 6.3. Migration of A) SVF cells and B) MOSE-L FFL cells. Serum free medium was used as a positive control and 4% FBS medium served as a positive control. The experimental wells contained the opposing cell type incubated in serum free medium for 48 hours. [a,b,c]different letters indicate $p<0.05$

We additionally wanted to determine if co-culturing MOSE-L FFL and SVF cells could enhance the invasive outgrowth of the cancer cells. Spheroids of 1000 cells were made with varying ratios of SVF and MOSE-L FFL cells. MOSE-E or MS1 cells replaced SVF cells in control spheroids. MOSE-E cells are early passages of MOSE cells that represent a more normal epithelial phenotype and do not form tumors when injected into mice. The spheroids were formed with an exact cell number and ratio and were then embedded in collagen. Outgrowth was measured every 48 hours for 6 days.

At 48 hours, there were significant differences in outgrowth areas (figure 6.4). When embedded alone, MOSE-L FFLs were able to invade the collagen, but not as effectively as spheroids which contained SVF cells. The spheroids that were most effective at collagen invasion were those that contained 50% MOSE-L FFL cells and 50% SVF cells. Other ratios of MOSE-L FFL and SVF cells also increased invasion over controls, but not significantly at 48 hours. There was also collagen invasion with co-culture of MOSE-L FFL with MOSE-E cells, although less substantial than that with SVF cells. MOSE-L FFLs cultured with MS1 cells had the least outgrowth, forming compact

spheroids. When grown alone, MS1 cells and SVF cells did not grow out and often the spheroids became smaller in size, likely due to cell death.

After 48 hours, the differences in outgrowth areas across spheroids were attenuated (data not shown). At 6 days, there were no significant differences across groups, except for less outgrowth of spheroids containing MS1 cells or spheroids that began with 250 MOSE-L FFL cells and 750 SVF or MOSE-E cells.

Another interesting facet of the invasion assay was that co-culturing with other cell types modulated the structure of the tumor outgrowths. While spheroids with MOSE-L FFL cells alone had very even outgrowth around the spheroids, the SVF co-cultured spheroids appeared to have more branch-like outgrowths (figure 6.5 B). Additionally, co-culture with MS1 cells resulted in invasive structure formation (figure 6.5 C). Surprisingly, co-culture with MOSE-E cells also resulted in the formation of branch-like structures (data not shown).

Viewing the outgrowths under higher magnification demonstrated that both SVF (figure 6.6) and MSI cells were able to migrate out of the spheroids with the cancer cells. However, the MOSE-E cells did not (data not shown).

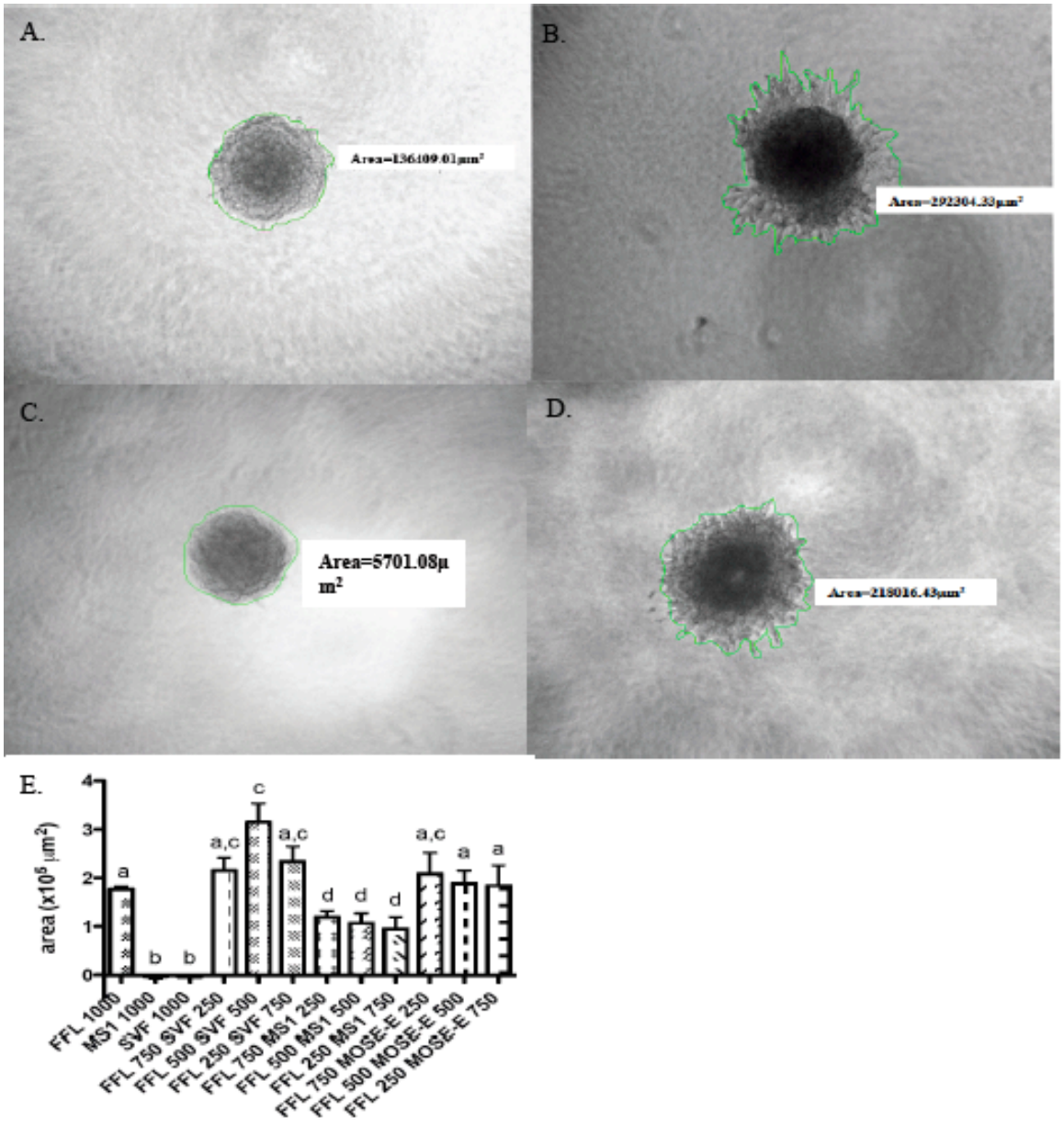

Figure 6.4. Invasion Assay at 48 hours after collagen embedding. A) 1000 MOSE-L FFL cells alone. B) 500 MOSE-L FFL cells and 500 SVF cells. C) 500 MOSE-L FFL cells and 500 MS1 cells. D) 500 MOSE-L FFL cells and 500 MOSE-E cells. E) Mean outgrowth area of embedded spheroids. [a,b,c,d]different letters indicate significant difference of $p<0.05$

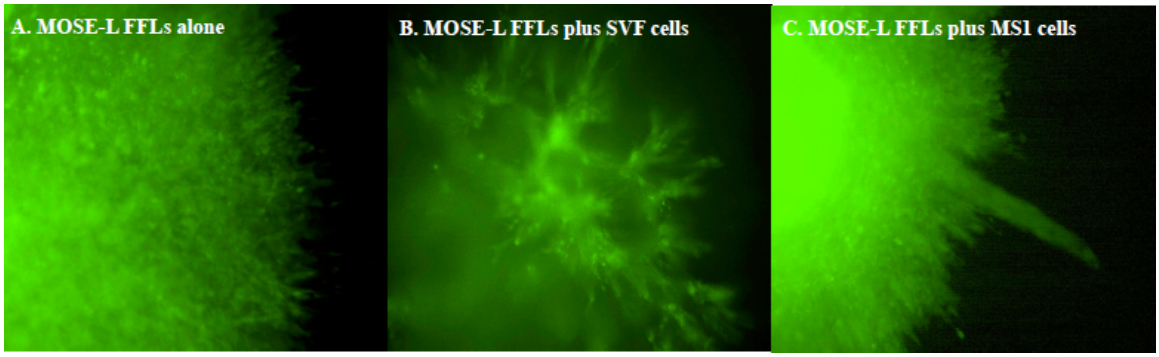

Figure 6.5. Fluorescent images of MOSE-L FFL outgrowth when cultured A) alone, B) with SVF cells, or C) with MS1 cells.

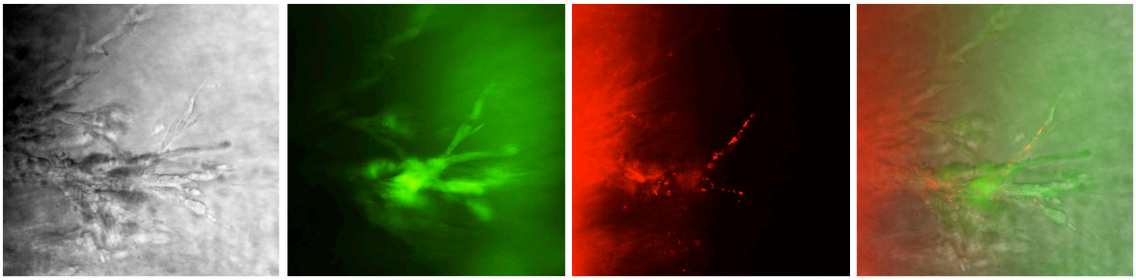

Figure 6.6. Images of outgrowths from MOSE-L FFL and SVF co-cultured spheroids. A) Brightfield. B) EGFP- MOSE-L FFL cells. C) CM-Dil SVF cells. D) Overlay.

Discussion

Recent studies suggest that adipose tissue-derived stem and progenitor cells may be recruited by cancer cells and function in cancer progression, potentially contributing to the association between obesity and cancer risk. However, the exact role of stem cells in tumor growth is not well established. Here, we confirmed that mouse ovarian cancer cells are able to directly interact with endothelial cells as well as stem cells isolated from intra-abdominal adipose tissue. Indeed, these stromal cells associated with cancer cells within 24 hours *in vitro*. SVF and MS1 cells were even able to rapidly migrate to the center of pre-formed tumor spheroids, suggesting a chemotactic gradient from the spheroid centers, potentially due to hypoxia or other factors. How this allows for the survival of MS1 and SVF cells needs to be evaluated in greater detail since it may represent targets for intervention strategies to prevent metastasis.

SVF and MS1 cells were also able to enhance other behaviors of MOSE-L FFL cells. There was an increase in proliferation of both MOSE-L FFL cells and SVF or MS1 cells when grown in conditioned medium of the opposing cell type, indicating that all cell types likely produce growth factors capable of stimulating the proliferation of the others. This correlates with other studies that found that conditioned medium from visceral adipocytes from obese individuals was able to significantly increase proliferation of esophageal and colorectal cancer cells.[23] Our SVF cells were isolated from mice in early stages of obesity and were able to significantly enhance proliferation of cancer cells. This effect may also be enhanced with more severe obesity. Additionally, since both of the stromal cell types were able to directly interact with ovarian cancer cells, it is also likely that there is cellular crosstalk which may be augmented when the cells are grown together.

Co-culturing was also able to enhance migration of both SVF and MOSE-L FFL cells. This substantiates work by Shinagawa et al.[24] who found that mesenchymal stem cells stimulated migration and invasion of colon cancer cells *in vitro*. The stem cells were also able to migrate to colon tumors and significantly increase the cancer cell proliferation *in vivo*. As both SVF and MOSE-L FFL cells are both able to increase the mobility of the other, it is unclear which happens more frequently *in vivo*. Tumor cells could potentially migrate towards areas that contain high numbers of stem cells, or after seeding, cancer cells could recruit stem cells from proximal tissues. It has been suggested that CXCL12, CCL2, and PDGF are involved in the modulation of mesenchymal stem cell homing to tumors.[24] As discussed in chapter 5 (data in appendix a), while CXCL12 and PDGF are not increased in cancer groups, CCL2 is increased,

especially in the omentum, in mice with cancer on either a high fat or low fat diet (omentum dCTs from qRT-PC:- LF PBS- 26.31, LF FFL- 22.19, HF PBS- 25.19, HF FFL- 21.86). CCL2 expression was also slightly increased by high fat diet, but not as drastically as with cancer. Additionally, CCL2 expression was increased in the other adipose tissues but less so than the omentum (which was primarily tumor tissue in the cancer groups), suggesting that CCL2 may be predominantly being produced by the cancer cells and may be a chemoattractant for stem cells. However, there was not an increase in MSCs in the omentum (Chapter 4, table 4.2), although this may be due to differentiation of the MSCs upon association with cancer cells. The large percentage of APCs and MSCs associated with early spheroids in the peritoneal serous fluid, but small percentage of stem cells and larger proportion of stromal cells present in the pmWAT tumor (Chapter 4) indicate that differentiation of stem cells towards stromal cells is a possibility.

Lastly, we found that co-culturing of MOSE-L FFL cells with other cell types increased early invasive events. At 48 hours, spheroids composed of cancer cells and SVF cells as opposed to cancer cells alone or cancer cells cultured with benign epithelial cells, demonstrated greater collagen invasion. However, this effect was mitigated after this time point. Surprisingly, co-culturing MOSE-L FFL cells with MS1 cells did not enhance outgrowth, which is counterintuitive since other studies have indicated that stromal cells enhanced cancer invasiveness and that endothelial cells were frequently present within the stroma.[16,25]

In regards to the culture of MOSE-L FFL cells with SVF or MOSE- E cell, since the differences between groups were attenuated after 48 hours, this could indicate that our

cancer cells are growing so aggressively that the impact of other cells is minimal. Alternatively, it is possible that the outgrowth of single cells may not reveal the larger picture or that the immediate invasive advantage within the first 48 hours could be essential to attachment and metastasis of ovarian cancer. The changes in the formation of outgrowth structures may be more indicative of metastatic or invasive success *in vivo*.

When the cancer cells were cultured alone, areas of outgrowth were equally distributed around the spheroid. However, when cultured with SVF cells, the outgrowths formed branchlike structures that also contained SVF cells. These structures may be invasive formations that help penetrate tissues at metastatic seeding sites or early vessel-like formations that may be early precursors contributing to neoangiogenesis. Other studies have shown that stem cells can indeed contribute to vessel formation in tumors.[11,25,26] Suzuki et al.[26] co-injected mesenchymal stem cells with melanoma cells, resulting in a significant increase in tumor volume with more blood vessels and larger vessel area as compared to melanoma cells injected alone.[26] Interestingly, MOSE-E cells also promoted the formation of these branchlike structures. This may be because the MOSE-E cells are significantly firmer and less malleable than MOSE-L cells.[27] Stiffer microenvironments have been shown to contribute to the aggressiveness and invasive capacity of cancer cells.[28] Thus by incorporation of stiffer cells into the tumor, it is possible that this enhanced mechanical support could enhance cancer progression. However, further examination of the impact of structural formation of outgrowths is warranted.

It also still needs to be delineated how these stem cells are recruited and what determines preferential location of recruitment. This could lead to important targets for

decreasing the risk of ovarian cancer progression and metastasis in at-risk obese populations.

Conclusion

Adipose-derived stem cells comprise a large portion of the SVF in white adipose tissue and may be key players in contribution of WAT to diseases, including cancer. Here, we confirmed that WAT SVF stem cells are able to directly associate with MOSE-L FFL cells, an aggressive ovarian cancer cell line. Additionally, SVF cells increased the proliferation, mobility, and invasiveness of MOSE-L FFL cells *in vitro*. Co-culture with SVF cells also changed the morphology of spheroid outgrowth, forming more branch-like structures that may contribute to enhanced metastatic success. Conversely, co-culturing also enhanced the proliferation and mobility of SVF cells, providing further evidence that SVF cells may be recruited by cancer cells and that their relationship may be bilateral. This study supports the hypothesis that SVF cells may play a role in the association between obesity and cancer risk. Additional studies should investigate these mechanisms further, including how these cells are recruited and if more are indeed recruited in obese individuals. This could lead to targets for decreasing cancer risk with obesity.

References

1. Finkelstein EA, Khavjou OA, Thompson H, et al. Obesity and severe obesity forecasts through 2030. *Am J Prev Med.* Jun 2012;42(6):563-570.

2. MacInnis RJ, English DR. Body size and composition and prostate cancer risk: systematic review and meta-regression analysis. *Cancer Causes Control.* Oct 2006;17(8):989-1003.

3. Key TJ, Appleby PN, Reeves GK, et al. Body mass index, serum sex hormones, and breast cancer risk in postmenopausal women. *J Natl Cancer Inst.* Aug 20 2003;95(16):1218-1226.

4. Moore LL, Bradlee ML, Singer MR, et al. BMI and waist circumference as predictors of lifetime colon cancer risk in Framingham Study adults. *Int J Obes Relat Metab Disord.* Apr 2004;28(4):559-567.
5. Bergstrom A, Hsieh CC, Lindblad P, Lu CM, Cook NR, Wolk A. Obesity and renal cell cancer--a quantitative review. *Br J Cancer.* Sep 28 2001;85(7):984-990.
6. Li D, Morris JS, Liu J, et al. Body mass index and risk, age of onset, and survival in patients with pancreatic cancer. *JAMA.* Jun 24 2009;301(24):2553-2562.
7. Olsen C, Green, A, Whiteman, D, Sadeghi, S, Kolahdooz, F, Webb, P. Obesity and the risk of epithelial ovarian cancer: a systemic review and meta-analysis. *Eur J Cancer.* 2007;43:690-709.
8. Siegel R, Naishadham D, Jemal A. Cancer statistics, 2012. *CA Cancer J Clin.* Jan-Feb 2012;62(1):10-29.
9. Saad AF, Hu W, Sood AK. Microenvironment and pathogenesis of epithelial ovarian cancer. *Horm Cancer.* Dec 2010;1(6):277-290.
10. Wels J, Kaplan RN, Rafii S, Lyden D. Migratory neighbors and distant invaders: tumor-associated niche cells. *Genes Dev.* Mar 1 2008;22(5):559-574.
11. Martin-Padura I, Gregato G, Marighetti P, et al. The white adipose tissue used in lipotransfer procedures is a rich reservoir of CD34+ progenitors able to promote cancer progression. *Cancer Res.* Nov 3 2011.
12. Strem BM, Hicok KC, Zhu M, et al. Multipotential differentiation of adipose tissue-derived stem cells. *Keio J Med.* Sep 2005;54(3):132-141.
13. Pittenger MF, Mackay AM, Beck SC, et al. Multilineage potential of adult human mesenchymal stem cells. *Science.* Apr 2 1999;284(5411):143-147.
14. Varma MJ, Breuls RG, Schouten TE, et al. Phenotypical and functional characterization of freshly isolated adipose tissue-derived stem cells. *Stem Cells Dev.* Feb 2007;16(1):91-104.
15. Zhang Y, Daquinag, A, Traktuev, D, Amaya-Manzanares, F, Simmons, P, March, K, Pasqualini, R, Arap, W, Kolonin, M. White adipose tissue cells are recruited by experimental tumors and promote cancer progression in mouse models. *Cancer Res.* 2009;69(12):5259-5266.
16. Kidd S, Spaeth E, Watson K, et al. Origins of the tumor microenvironment: quantitative assessment of adipose-derived and bone marrow-derived stroma. *PLoS One.* 2012;7(2):e30563.
17. Klopp AH, Zhang Y, Solley T, et al. Omental adipose tissue-derived stromal cells promote vascularization and growth of endometrial tumors. *Clin Cancer Res.* Feb 1 2012;18(3):771-782.
18. Yu G, Wu X, Kilroy G, Halvorsen YD, Gimble JM, Floyd ZE. Isolation of murine adipose-derived stem cells. *Methods Mol Biol.* 2011;702:29-36.
19. Roberts PC, Mottillo EP, Baxa AC, et al. Sequential molecular and cellular events during neoplastic progression: a mouse syngeneic ovarian cancer model. *Neoplasia.* Oct 2005;7(10):944-956.
20. Swainson L, Mongellaz C, Adjali O, Vicente R, Taylor N. Lentiviral transduction of immune cells. *Methods Mol Biol.* 2008;415:301-320.
21. Suga H, Matsumoto D, Eto H, et al. Functional implications of CD34 expression in human adipose-derived stem/progenitor cells. *Stem Cells Dev.* Oct 2009;18(8):1201-1210.

22. Yamamoto N, Akamatsu H, Hasegawa S, et al. Isolation of multipotent stem cells from mouse adipose tissue. *J Dermatol Sci.* Oct 2007;48(1):43-52.
23. Lysaght J, van der Stok EP, Allott EH, et al. Pro-inflammatory and tumour proliferative properties of excess visceral adipose tissue. *Cancer Lett.* Dec 15 2011;312(1):62-72.
24. Shinagawa K, Kitadai Y, Tanaka M, et al. Mesenchymal stem cells enhance growth and metastasis of colon cancer. *Int J Cancer.* Nov 15 2010;127(10):2323-2333.
25. Zhang Y, Daquinag A, Traktuev DO, et al. White adipose tissue cells are recruited by experimental tumors and promote cancer progression in mouse models. *Cancer Res.* Jun 15 2009;69(12):5259-5266.
26. Suzuki K, Sun R, Origuchi M, et al. Mesenchymal stromal cells promote tumor growth through the enhancement of neovascularization. *Mol Med.* 2011;17(7-8):579-587.
27. Ketene AN, Schmelz EM, Roberts PC, Agah M. The effects of cancer progression on the viscoelasticity of ovarian cell cytoskeleton structures. *Nanomedicine.* Jan 2012;8(1):93-102.
28. Wirtz D, Konstantopoulos K, Searson PC. The physics of cancer: the role of physical interactions and mechanical forces in metastasis. *Nat Rev Cancer.* Jul 2011;11(7):512-522.

Conclusion

The obesity epidemic is a major health concern in the United States that despite much attention, is not subsiding. In 2010, 69.2% of adult Americans were overweight or obese,[1] and if the trend continues, this number is projected to be at 86.3% by 2030.[2,3] Importantly, obesity has been linked to numerous health conditions including cancer. In 2003, it was estimated that overweight and obesity were responsible for 14% of all cancer deaths in men and 20% of those in women in the United States.[4] Of particular interest is ovarian cancer. Ovarian cancer has limited early symptoms, resulting in greater than 70% of patients presenting with late-stage disease, and ultimately, 140,000 deaths per year in women worldwide.[5] A meta-analysis of 28 studies on the association between obesity and ovarian cancer found that there is an estimated 30% increased risk of ovarian cancer with overweight and obesity.[6] Currently, the mechanism for how obesity contributes to ovarian cancer is unknown.

A potential clue is the greater correlation of ovarian cancer risk with waist-to-hip ratio as compared to body mass index,[7,8] suggesting that visceral fat may be the greatest contributor. Visceral fat is a broad grouping of multiple adipose depots within the peritoneal cavity, all with different characteristics from tissue dynamics (tendency to respond to excess calories with a hypertrophic versus a hyperplastic response), adipokine release, hormonal responses, vascularization, innervation, and abundance of non-adipocyte cells, which all impact the specific function of each individual depot. Thus it seems that each depot may have the potential to differentially contribute to both biological and pathological conditions.

In this series of studies, we aimed to delineate differences in visceral fat depots that may contribute to ovarian cancer progression. We focused on one of the lesser studied facets of adipose tissue- the stromal vascular constituents. In preliminary studies, we found that the intra-abdominal parametrial (pmWAT), retroperitoneal (rpWAT), and omental (omWAT) white adipose tissue (WAT) depots were all unique in regards to leukocyte and basic progenitor populations. Confirming previous reports, omWAT was more immunologically active, with a much greater proportion of leukocytes present (75.4% versus 38.1% in both pmWAT and rpWAT). The depots additionally differed in their immune composition with the largest proportion in pmWAT being macrophages and much larger populations of dendritic cells and B cells in omWAT and rpWAT. Interestingly, while omWAT is the only depot considered a secondary lymphoid organ, the immune cell ratios in rpWAT more closely resembled omWAT than pmWAT.

We next wanted to further examine the stem and progenitor populations present within these depots as these populations constitute a large proportion of the SVF and can be recruited by cancer cells to participate in tumor development. We investigated the stem and progenitor cells present in all three depots in mice on either a low fat or high fat diet. To more closely mimic dietary patterns of modern Americans, we chose 17% fat as our low fat diet and 45% fat as our high fat diet. The mice were maintained on their diets for 15 weeks. At 15 weeks, the high fat group had significantly greater whole body weight, percent body fat, and dysregulation of glucose tolerance. However, the high fat mice were not significantly different in regards to expression of adipokines such as leptin, adiponectin, and resistin and did not have significantly different fasting glucose levels. Thus these mice were indicative of early stages of obesity.

For the progenitor populations, rpWAT was more similar to pmWAT than omWAT. As omWAT contains a much greater proportion of leukocytes, it had a much smaller proportion of $CD45^-$ stromal cells. However, within the $CD45^-$ gate, omWAT had a greater percentage of adipose progenitor cells (APCs), mesenchymal stem cells (MSCs), hematopoietic stem cells (HSCs), and endothelial cells (ECs). It is thus likely that pmWAT and rpWAT contained greater proportions of stromal cells such as fibroblasts, that were not examined in this study. It is important to remember that when multiplying by total cell numbers, pmWAT had by far the largest number of APCs and MSCs as compared to other tissues, in part due to its larger size.

While there was a significant increase in the size of all fat depots in mice fed a high fat diet, there was surprisingly only a significant increase in SVF cell numbers in pmWAT, although there was also an increased trend in rpWAT. This suggests that pmWAT may have a greater hyperplastic response than the other tissues. There was also surprising stability in the proportions of most progenitors in all tissues. There was only an increase in $CD45^+$ cells and $Sca1^+CD31^{hi}CD44^+$ cells in pmWAT, an increase in APCs and $Sca1^+CD31^{hi}CD44^+$ cells in rpWAT and a decrease in APCs and MSCs in omWAT. The gene expression profiles were also remarkably stable, but importantly, there was an increase in inflammatory markers such as IL1b, TNFa, IL6, and CCL2 in most tissues. Interestingly, there was also an increase in stromal factors, such as COL1 and TNC in omWAT and TNC in rpWAT with high fat diet.

We next wanted to see if any of these changes were also associated with cancer dissemination and if high fat diet and weight gain were indeed associated with enhanced ovarian cancer progression. We found that with the injection of ovarian cancer cells after

12 weeks on a high fat diet, there was a significantly increased tumor burden as compared to mice on a low fat diet. This was confirmed by a significantly increased expression of firefly luciferase (which was only expressed by cancer cells) in the adipose depots of high fat diet mice, indicating a greater cancer cell number. Consistent with the reported preferential seeding of ovarian cancer metastases in the omentum, the omentum had the greatest tumor burden and was almost entirely overcome by tumor cells.

Interestingly, there were few changes in progenitor populations with cancer dissemination. The greatest difference was a significant decrease in APCs and MSCs in omWAT, which was enhanced in the high fat cancer group. However, there was also an increase (although not significant) in $CD45^-$ cells in omWAT, suggesting that some of these stem cells may have differentiated into stromal cells not identified in this study.

Another interesting finding, although examined in only one pooled sample, was that the cellular aggregates, which were filtered from the PSF, had an even greater proportion of $CD45^-$ cells than the single cells in the PSF. This suggests that there may have been an influx of progenitors into the PSF, but they associated with other cells, including cancer cells and may have been filtered out during FACS processing. The aggregates also had a greater proportion of APCs and a smaller proportion of MSCs. One tumor from pmWAT was also analyzed. Within the tumor, a large percentage of the non-cancer cell component were $CD45^-$ cells, but surprisingly few were APCs and MSCs. As it is likely that APCs and MSCs associate with the tumor cells early on (as evidenced by the number of both in the PSF aggregates), and because 33.5% of the non-tumor cells were $CD45^-$, it is probable that at least a proportion of the cells differentiated into cells such as fibroblasts, which were not examined in this study. These cells could also be

hospicells or mesothelial cells.

Also implicating the importance of high fat diet and adipose tissue to a stromal contribution in tumor development was the increase in expression of stromal factors with cancer. COL1, TNC, and FN1 were all increased in the omentum with cancer in both diet groups. All three were also increased in pmWAT and rpWAT in both groups, although this was only significant with FN1 in pmWAT and TNC in rpWAT, both in the high fat group. Since these factors are increased the most in omWAT, which was primarily tumor tissue, it indicates that these stromal markers may be important for cancer development. Since they were also increased in omWAT with high fat diet alone, it is possible that these are also markers of a permissive metastatic niche. The less substantial increases in pmWAT and rpWAT may be indicators of environmental modulation by cancer cells to create additional pre-metastatic niches.

In the final portion of this study, we wanted to further characterize the relationship between MOSE-L FFL cancer cells and SVF stem cells. We did this through various *in vitro* assays aimed at further delineating potential mechanisms that SVF cells could enhance cancer development. MOSE-L FFL and SVF cells were able to directly interact and when added to culture as single cells, they associated within 24 hours. When SVF cells were added to cultures of pre-formed MOSE-L FFL spheroids, the SVF cells were able to migrate to the center of the spheroids within 24 hours, indicating cellular cross-talk. SVF cells were also able to increase the proliferation, mobility, and invasiveness of MOSE-L FFL cells. Conversely, co-culturing also enhanced the proliferation and mobility of SVF cells, providing further evidence that SVF cells may be recruited by cancer cells and that their relationship may be bilateral.

Another interesting finding in the invasion assay was that co-culture of SVF cells with MOSE-L FFL cells changed the structural formation of spheroid outgrowths in collagen. Outgrowths appeared to be evenly distributed around the spheroids of only MOSE-L FFL cells or when co-cultured with early passage, non-malignant MOSE cells. However, when MOSE-L FFL cells were cultured with SVF cells, the outgrowths appeared to form branch-like structures. It is unclear how this may affect success of metastases, but it is possible that this structural formation may play a role in vasculogenesis.

Thus, this study found that visceral omWAT, pmWAT, and rpWAT depots represent distinct microenvironments with different SVF composition profiles (in regards to both leukocytes and stem cell populations) and unique gene expression profiles. Additionally, these SVF populations are differentially impacted by high fat diet and ovarian cancer cell dissemination. As changes in stem and progenitor populations are associated with cancer dissemination, it is possible that these cells may play a role in cancer development. Also, many changes in both cell populations and gene expression were enhanced by concomitant high fat feeding and the presence of cancer, supporting a potential cellular mechanism for the correlation between obesity and ovarian cancer risk. Thus, this study provides a good foundation for examining the cellular contributions of adipose tissue to cancer. However, much work is left to be done. It is still unclear how these stem and progenitor cells are actually recruited, what determines where cells are recruited from (adipose tissue versus bone marrow), and what the timeline of events is. It is well known that stromal cells are required for cancer progression, but less is known about the actual process of stromal development. Are cells recruited in a specific order?

In the case of ovarian cancer, are cells recruited before or after metastasis? Is the migration of stem and progenitor cells an important part of pre-metastatic niche development? Is modulation of stromal components such as TNC, FN1, and COL1 also an important part of niche formation? Additionally, studies in humans to determine if more stem cells and other stromal cells are actually present in ovarian tumors with obesity are necessary. In regards to our *in vitro* assays, further studies to determine which factors are responsible for enhancement of proliferation, migration, and invasion are required. It would also be beneficial to determine what regulates the structural changes that occur upon co-culturing and if these structures are important to metastatic success. Thus there are still many questions left to answer, but by further characterizing the mechanism for the association between obesity and cancer development, we could find novel targets to decrease the progress of cancer development in at-risk obese individuals. As the worldwide population is becoming increasingly obese, this could be a critical development that could decrease healthcare costs and more importantly, save lives.

References

1. Statistics NCfH. *Health, United States, 2012: With Special Feature on Emergency Care.* Hyattsville: Department of Health and Human Services;2013.

2. Flegal K, Carroll, M, Ogden, C, Curtin, L. Prevalence and trends in obesity among US adults, 1999-2008. *JAMA.* 2010;303(3):235-241.

3. Wang Y, Beydoun, M, Liang, L, Caballero, B, Kumanyika, S. Will all Americans become overweight or obese? Estimating the progression and cost of the US obesity epidemic. *Obesity.* 2008;16(10):2323-2330.

4. Calle EE, Rodriguez C, Walker-Thurmond K, Thun MJ. Overweight, obesity, and mortality from cancer in a prospectively studied cohort of U.S. adults. *N Engl J Med.* Apr 24 2003;348(17):1625-1638.

5. Siegel R, Naishadham D, Jemal A. Cancer statistics, 2012. *CA Cancer J Clin.* Jan-Feb 2012;62(1):10-29.

6. Olsen C, Green, A, Whiteman, D, Sadeghi, S, Kolahdooz, F, Webb, P. Obesity and the risk of epithelial ovarian cancer: a systemic review and meta-analysis. *Eur J Cancer.* 2007;43:690-709.
7. Mink PJ, Folsom AR, Sellers TA, Kushi LH. Physical activity, waist-to-hip ratio, and other risk factors for ovarian cancer: a follow-up study of older women. *Epidemiology.* Jan 1996;7(1):38-45.
8. Delort L, Kwiatkowski F, Chalabi N, Satih S, Bignon YJ, Bernard-Gallon DJ. Central adiposity as a major risk factor of ovarian cancer. *Anticancer Res.* Dec 2009;29(12):5229-5234.

Appendix A- dCT tables

Table A.1. CT and dCT values from omental WAT (from PCR array)

	LF PBS CT	LF PBS dCT	HF PBS CT	HF PBS dCT	LF FFL CT	LF FFL dCT	HF FFL CT	HF FFL dCT
Adora1	26.73	2.54	26.45	2.14	29.77	5.59	31.67	7.42
Ahsg	29.24	5.05	29.69	5.38	27.71	3.53	31.35	7.09
Aif1	22.88	-1.30	22.91	-1.41	21.59	-2.59	21.86	-2.40
Apcs	35.00	10.81	32.06	7.75	34.46	10.28	35.00	10.74
Apoa2	28.50	4.32	28.89	4.58	25.72	1.54	27.99	3.73
Apol7a	28.39	4.20	27.82	3.50	25.14	0.96	25.37	1.12
Apol8	32.10	7.91	31.88	7.57	31.96	7.78	31.26	7.00
Areg	35.00	10.81	33.44	9.12	28.59	4.42	27.93	3.67
Bcl6	23.66	-0.53	24.19	-0.13	23.93	-0.25	24.25	-0.01
Blnk	25.30	1.11	24.86	0.54	24.73	0.56	24.34	0.08
Bmp1	23.26	-0.92	22.77	-1.54	22.80	-1.38	22.34	-1.92
Bmp2	27.61	3.43	27.33	3.01	29.09	4.92	29.72	5.46
Bmp3	24.44	0.25	24.50	0.18	27.76	3.58	28.08	3.82
Bmp7	27.25	3.06	25.95	1.63	28.12	3.94	28.24	3.99
C3	18.20	-5.99	18.26	-6.06	19.20	-4.98	19.90	-4.36
C3ar1	23.44	-0.75	22.85	-1.46	22.66	-1.51	22.76	-1.50
Cast	21.75	-2.44	22.29	-2.03	22.26	-1.92	22.54	-1.72
Ccl1	32.37	8.18	32.40	8.08	29.57	5.39	29.47	5.21
Ccl11	24.20	0.01	22.90	-1.41	27.39	3.21	26.83	2.57
Ccl12	26.35	2.16	25.18	0.87	23.34	-0.84	22.45	-1.80
Ccl17	28.45	4.26	29.38	5.07	27.27	3.09	26.11	1.85
Ccl19	23.22	-0.97	23.58	-0.74	23.51	-0.67	24.14	-0.11
Ccl2	26.31	2.12	25.18	0.87	22.19	-1.99	21.86	-2.39
Ccl20	35.00	10.81	35.00	10.69	31.92	7.74	31.99	7.73
Ccl22	26.67	2.48	27.12	2.81	26.40	2.22	26.99	2.73
Ccl24	26.87	2.68	26.66	2.34	28.77	4.59	30.17	5.91
Ccl25	29.79	5.60	29.33	5.01	26.89	2.71	26.32	2.06
Ccl27a	24.17	-0.01	25.33	1.02	24.30	0.12	24.13	-0.13
Ccl28	29.92	5.74	29.29	4.97	30.95	6.77	30.97	6.71
Ccl3	28.07	3.89	28.17	3.85	25.77	1.59	25.83	1.57
Ccl4	28.15	3.96	27.77	3.46	25.29	1.11	26.02	1.76
Ccl5	21.77	-2.42	22.31	-2.01	21.20	-2.98	21.49	-2.77
Ccl6	20.31	-3.87	21.52	-2.79	21.62	-2.56	22.98	-1.28
Ccl7	25.35	1.16	24.27	-0.05	22.67	-1.51	22.28	-1.98
Ccl8	21.52	-2.67	21.98	-2.34	20.92	-3.26	21.48	-2.78
Ccl9	22.43	-1.76	23.27	-1.05	23.36	-0.82	23.31	-0.95
Ccr1	23.83	-0.35	23.60	-0.72	23.48	-0.70	23.38	-0.88
Ccr10	28.35	4.16	28.01	3.70	27.91	3.73	28.09	3.83
Ccr2	23.76	-0.43	22.49	-1.82	22.97	-1.21	22.19	-2.07
Ccr3	25.80	1.62	23.28	-1.03	24.72	0.54	23.17	-1.09
Ccr4	28.51	4.32	28.13	3.82	28.43	4.25	29.22	4.96

Ccr5	24.90	0.71	23.65	-0.67	23.36	-0.82	22.90	-1.36
Ccr6	25.40	1.22	24.55	0.23	24.56	0.39	24.47	0.21
Ccr7	26.91	2.72	28.21	3.89	26.10	1.92	26.67	2.41
Ccr8	28.69	4.50	30.40	6.09	27.80	3.62	28.42	4.16
Ccr9	27.48	3.29	26.85	2.54	27.08	2.90	27.48	3.22
Ccrl1	28.49	4.30	29.13	4.81	30.19	6.01	30.61	6.35
Ccrl2	25.79	1.60	25.56	1.25	26.13	1.95	26.43	2.17
Cd14	21.78	-2.41	22.51	-1.81	22.33	-1.85	22.67	-1.59
Cd180	24.80	0.62	23.94	-0.38	24.44	0.26	24.46	0.20
Cd27	26.92	2.73	26.88	2.56	26.99	2.81	27.28	3.02
Cd28	25.63	1.44	26.00	1.69	25.67	1.49	26.12	1.86
Cd4	25.62	1.43	25.85	1.53	25.36	1.18	25.72	1.46
Cd40	24.75	0.57	25.57	1.26	24.89	0.71	25.52	1.26
Cd40lg	27.34	3.15	26.79	2.48	27.75	3.57	27.58	3.33
Cd70	32.27	8.09	33.51	9.20	29.93	5.75	31.52	7.26
Cd74	16.29	-7.90	16.46	-7.86	16.62	-7.55	16.47	-7.79
Cd86	23.57	-0.62	23.84	-0.47	23.85	-0.33	24.29	0.03
Cd97	20.91	-3.27	21.21	-3.10	21.54	-2.64	22.00	-2.26
Cebpb	20.23	-3.95	21.83	-2.49	19.66	-4.52	19.71	-4.55
Cer1	35.00	10.81	35.00	10.69	35.00	10.82	33.32	9.06
Cklf	24.51	0.33	24.82	0.50	23.99	-0.19	24.50	0.24
Clcf1	25.42	1.23	24.92	0.61	24.50	0.33	25.00	0.74
Cmtm1	35.00	10.81	34.64	10.33	35.00	10.82	34.19	9.93
Cmtm2a	35.00	10.81	35.00	10.69	35.00	10.82	35.00	10.74
Cntfr	27.55	3.37	28.59	4.28	29.23	5.05	30.58	6.32
Crp	31.39	7.20	31.10	6.78	30.70	6.53	33.25	8.99
Csf1	22.88	-1.30	23.14	-1.18	21.80	-2.38	21.82	-2.44
Csf2	31.16	6.97	29.13	4.82	30.78	6.60	29.94	5.68
Csf2ra	23.97	-0.22	24.70	0.39	24.50	0.32	25.58	1.32
Csf3	32.56	8.37	33.69	9.37	30.81	6.63	30.60	6.35
Csf3r	26.10	1.92	26.11	1.80	24.35	0.17	24.86	0.61
Ctf1	27.14	2.95	27.92	3.60	25.88	1.70	26.95	2.69
Ctf2	31.47	7.28	32.74	8.42	29.56	5.38	29.83	5.57
Cx3cl1	25.52	1.34	25.58	1.26	25.19	1.01	24.73	0.47
Cx3cr1	27.35	3.17	26.33	2.02	24.84	0.66	24.47	0.21
Cxcl1	32.74	8.55	31.15	6.84	27.09	2.91	25.78	1.52
Cxcl10	24.94	0.75	24.70	0.39	22.62	-1.56	22.47	-1.79
Cxcl11	28.57	4.38	28.16	3.85	29.98	5.81	30.33	6.07
Cxcl12	21.72	-2.47	21.83	-2.48	22.49	-1.69	22.93	-1.33
Cxcl13	17.79	-6.39	17.99	-6.33	18.24	-5.94	19.74	-4.52
Cxcl14	27.63	3.44	27.84	3.53	25.25	1.07	25.22	0.96
Cxcl15	35.00	10.81	35.00	10.69	35.00	10.82	33.38	9.12
Cxcl16	23.01	-1.17	23.28	-1.04	21.92	-2.26	21.69	-2.57
Cxcl2	28.63	4.44	27.44	3.13	25.87	1.69	24.89	0.63
Cxcl5	29.63	5.44	27.90	3.58	21.81	-2.37	20.80	-3.46
Cxcl9	23.31	-0.88	23.80	-0.51	21.96	-2.21	21.79	-2.47
Cxcr3	24.61	0.43	24.52	0.21	24.40	0.22	23.96	-0.30

Cxcr4	21.93	-2.25	23.28	-1.03	21.73	-2.45	22.10	-2.15
Cxcr5	24.25	0.06	24.54	0.23	24.77	0.59	25.76	1.50
Cxcr6	24.70	0.51	24.62	0.30	25.13	0.95	25.42	1.16
Cybb	22.64	-1.55	23.00	-1.32	22.59	-1.59	22.99	-1.27
Cyp26b1	29.93	5.74	29.10	4.79	30.59	6.41	30.57	6.31
D17Wsu104e	22.46	-1.73	22.70	-1.62	21.54	-2.64	21.68	-2.57
Dock2	23.37	-0.82	23.64	-0.68	23.73	-0.45	24.46	0.20
Ebi3	24.90	0.71	25.27	0.96	24.79	0.61	25.44	1.18
Eda	26.44	2.26	27.46	3.15	28.85	4.68	29.88	5.62
Ephx2	23.33	-0.86	23.11	-1.20	26.58	2.40	26.22	1.96
Epo	35.00	10.81	35.00	10.69	35.00	10.82	35.00	10.74
Epor	28.57	4.38	28.18	3.87	27.97	3.79	28.42	4.16
Erbb2	27.17	2.99	27.12	2.80	26.96	2.78	27.15	2.89
Erbb2ip	22.87	-1.32	23.39	-0.93	22.11	-2.07	22.51	-1.75
F11r	23.50	-0.69	23.91	-0.41	21.61	-2.56	21.97	-2.28
F2	31.10	6.91	31.26	6.95	29.75	5.57	32.42	8.16
F3	24.40	0.21	24.34	0.03	25.65	1.48	25.57	1.31
F8	27.12	2.93	27.60	3.29	27.26	3.09	27.57	3.31
Fasl	29.12	4.93	29.16	4.85	29.11	4.93	28.68	4.42
Fgf1	21.22	-2.97	21.87	-2.45	22.95	-1.22	23.90	-0.36
Fgf10	25.14	0.95	24.51	0.20	24.89	0.71	24.10	-0.16
Fgf12	35.00	10.81	31.96	7.65	35.00	10.82	32.49	8.24
Fgf2	23.92	-0.27	24.71	0.40	24.45	0.28	24.43	0.18
Fgf3	35.00	10.81	35.00	10.69	35.00	10.82	35.00	10.74
Fgf4	35.00	10.81	35.00	10.69	35.00	10.82	35.00	10.74
Fgf5	35.00	10.81	32.90	8.59	35.00	10.82	35.00	10.74
Fgf6	32.90	8.71	35.00	10.69	35.00	10.82	35.00	10.74
Fgf7	27.69	3.50	26.33	2.02	28.63	4.45	28.22	3.96
Fgf8	35.00	10.81	35.00	10.69	35.00	10.82	35.00	10.74
Fgf9	27.54	3.35	28.70	4.39	29.64	5.46	30.63	6.37
Figf	22.54	-1.65	23.10	-1.22	23.71	-0.47	23.79	-0.47
Flt3l	23.90	-0.29	23.76	-0.56	25.00	0.82	25.40	1.14
Fn1	20.31	-3.88	20.38	-3.93	17.51	-6.67	17.72	-6.54
Fos	24.29	0.11	25.29	0.97	24.36	0.18	23.52	-0.74
Fpr1	25.25	1.07	25.47	1.16	24.32	0.14	26.72	2.46
Gdf1	29.47	5.29	28.98	4.66	29.60	5.42	31.51	7.25
Gdf2	35.00	10.81	35.00	10.69	35.00	10.82	33.84	9.58
Gdf3	29.36	5.17	29.79	5.47	27.67	3.49	27.86	3.60
Gdf5	31.86	7.67	31.02	6.71	30.57	6.39	32.00	7.74
Gdf6	30.81	6.62	30.91	6.59	27.43	3.25	28.25	3.99
Gdf7	30.41	6.22	30.18	5.86	30.72	6.54	31.82	7.56
Gdf9	27.99	3.81	28.15	3.84	29.32	5.14	28.90	4.64
Gfra1	28.57	4.39	29.59	5.28	29.61	5.43	31.26	7.01
Gfra2	25.27	1.09	25.17	0.86	26.54	2.36	27.34	3.08
Ghr	19.62	-4.57	19.95	-4.36	21.57	-2.61	21.90	-2.35
Glmn	25.39	1.20	25.25	0.94	24.54	0.36	24.63	0.37
Gpi1	20.73	-3.46	21.02	-3.30	19.58	-4.60	19.49	-4.77

Gpr68	27.40	3.21	28.85	4.53	26.84	2.66	27.54	3.29
Grem1	28.73	4.54	28.19	3.87	28.43	4.25	27.90	3.64
Grem2	25.85	1.66	25.88	1.56	28.10	3.92	29.44	5.19
Grn	20.65	-3.54	20.96	-3.35	20.64	-3.54	21.10	-3.16
Hdac4	24.01	-0.18	25.51	1.20	23.99	-0.19	24.61	0.36
Hdac5	24.61	0.42	24.96	0.65	25.37	1.19	26.16	1.90
Hdac7	22.84	-1.35	22.80	-1.51	21.66	-2.52	21.24	-3.02
Hdac9	25.54	1.35	24.84	0.53	26.22	2.04	25.26	1.00
Hrh1	28.76	4.58	27.92	3.60	29.32	5.14	29.73	5.47
Ifna11	35.00	10.81	35.00	10.69	34.42	10.24	33.72	9.46
Ifna14	35.00	10.81	35.00	10.69	35.00	10.82	31.68	7.42
Ifna2	35.00	10.81	33.63	9.32	33.36	9.18	32.48	8.22
Ifna4	35.00	10.81	34.14	9.83	32.77	8.59	33.43	9.17
Ifna9	35.00	10.81	35.00	10.69	35.00	10.82	33.09	8.83
Ifnab	35.00	10.81	35.00	10.69	35.00	10.82	31.54	7.28
Ifnar1	22.95	-1.24	23.28	-1.03	22.46	-1.72	22.58	-1.68
Ifnar2	21.66	-2.53	22.58	-1.73	21.78	-2.40	22.19	-2.07
Ifnb1	34.98	10.79	35.00	10.69	35.00	10.82	34.15	9.89
Ifne	35.00	10.81	35.00	10.69	32.42	8.24	31.17	6.91
Ifng	29.79	5.60	28.89	4.57	28.66	4.48	28.57	4.31
Ifngr1	20.62	-3.57	21.57	-2.75	21.68	-2.50	21.87	-2.39
Ifngr2	22.86	-1.32	23.01	-1.31	22.28	-1.90	22.29	-1.97
Ifnk	27.74	3.56	27.77	3.45	28.42	4.24	29.31	5.05
Ik	24.43	0.24	27.83	3.52	24.08	-0.10	26.33	2.07
Il10	27.23	3.04	26.57	2.25	25.35	1.17	25.82	1.56
Il10ra	24.34	0.16	24.55	0.24	23.91	-0.27	24.41	0.15
Il10rb	21.59	-2.60	22.00	-2.31	21.75	-2.43	21.84	-2.42
Il11	29.93	5.74	31.86	7.55	30.45	6.28	30.90	6.64
Il11ra1	22.80	-1.39	23.15	-1.16	23.13	-1.05	22.86	-1.40
Il12a	28.76	4.57	28.46	4.15	27.78	3.60	28.59	4.33
Il12b	27.84	3.66	28.99	4.68	26.98	2.80	27.01	2.75
Il12rb1	32.13	7.95	32.31	7.99	31.87	7.69	31.23	6.97
Il12rb2	30.89	6.70	32.88	8.57	31.61	7.43	33.48	9.22
Il13	31.40	7.21	32.26	7.94	33.76	9.58	32.15	7.89
Il13ra1	24.67	0.48	25.18	0.87	23.50	-0.68	23.35	-0.91
Il13ra2	31.21	7.02	32.92	8.61	33.45	9.27	31.94	7.68
Il15	24.65	0.47	24.91	0.60	25.23	1.05	25.33	1.08
Il15ra	24.60	0.42	25.72	1.41	26.41	2.23	27.28	3.02
Il16	23.47	-0.71	23.72	-0.60	23.36	-0.82	23.67	-0.59
Il17a	35.00	10.81	35.00	10.69	35.00	10.82	35.00	10.74
Il17b	30.77	6.59	31.90	7.59	32.76	8.58	30.64	6.39
Il17c	30.97	6.78	30.97	6.65	32.43	8.25	32.31	8.06
Il17d	29.39	5.20	30.44	6.13	31.86	7.68	32.36	8.10
Il17f	33.26	9.08	31.15	6.84	33.41	9.23	31.70	7.44
Il17ra	24.86	0.67	25.12	0.80	24.75	0.57	25.35	1.09
Il17rb	27.92	3.74	28.69	4.37	28.89	4.71	30.18	5.92
Il18	23.88	-0.31	23.99	-0.33	22.18	-2.00	21.95	-2.30

Il18r1	26.38	2.19	25.70	1.39	23.69	-0.49	23.32	-0.94
Il18rap	27.09	2.90	27.14	2.83	26.30	2.12	25.80	1.54
Il19	31.86	7.67	35.00	10.69	32.68	8.50	31.65	7.39
Il1a	28.92	4.74	28.33	4.02	28.28	4.10	27.62	3.37
Il1b	29.25	5.06	27.36	3.05	25.35	1.17	24.24	-0.02
Il1f10	35.00	10.81	35.00	10.69	35.00	10.82	35.00	10.74
Il1f5	35.00	10.81	35.00	10.69	35.00	10.82	35.00	10.74
Il1f6	34.23	10.04	35.00	10.69	35.00	10.82	35.00	10.74
Il1f8	35.00	10.81	34.85	10.54	35.00	10.82	35.00	10.74
Il1f9	31.10	6.91	31.90	7.58	28.44	4.26	28.19	3.93
Il1r1	22.92	-1.27	23.46	-0.86	21.97	-2.21	21.86	-2.39
Il1r2	28.25	4.06	28.56	4.24	24.47	0.29	24.61	0.36
Il1rap	26.16	1.97	26.48	2.16	24.98	0.80	25.27	1.02
Il1rapl2	35.00	10.81	35.00	10.69	35.00	10.82	35.00	10.74
Il1rl1	25.80	1.61	25.78	1.47	26.66	2.48	27.46	3.20
Il1rl2	28.90	4.71	29.24	4.93	27.10	2.93	27.24	2.98
Il1rn	30.57	6.38	30.94	6.63	26.99	2.82	26.19	1.94
Il2	28.63	4.44	29.76	5.45	29.51	5.34	30.30	6.04
Il20	35.00	10.81	35.00	10.69	35.00	10.82	34.27	10.01
Il20ra	31.65	7.46	33.77	9.46	32.73	8.55	35.00	10.74
Il21	35.00	10.81	30.90	6.58	31.19	7.01	30.78	6.52
Il21r	26.18	1.99	25.50	1.19	25.60	1.42	25.77	1.51
Il22	33.80	9.62	35.00	10.69	33.82	9.64	33.69	9.43
Il22ra1	26.11	1.93	26.23	1.92	26.81	2.63	27.36	3.10
Il22ra2	27.47	3.28	29.48	5.16	31.35	7.17	32.42	8.16
Il23a	35.00	10.81	33.20	8.89	30.61	6.43	31.81	7.55
Il23r	28.51	4.32	27.68	3.37	29.09	4.91	29.31	5.05
Il24	28.50	4.32	28.67	4.36	27.90	3.72	28.57	4.31
Il27	28.99	4.80	29.18	4.87	28.48	4.31	29.34	5.08
Il28ra	28.15	3.96	28.49	4.17	26.95	2.77	27.53	3.28
Il2ra	28.65	4.46	28.76	4.44	29.39	5.21	29.43	5.18
Il2rb	25.30	1.11	25.65	1.34	25.40	1.22	25.94	1.68
Il2rg	22.50	-1.69	22.46	-1.86	22.34	-1.84	22.58	-1.68
Il3	35.00	10.81	33.97	9.66	35.00	10.82	35.00	10.74
Il31	35.00	10.81	35.00	10.69	35.00	10.82	33.38	9.12
Il31ra	25.82	1.64	27.28	2.97	28.51	4.33	29.42	5.16
Il3ra	28.44	4.25	28.84	4.53	29.12	4.94	31.09	6.84
Il4	32.11	7.92	30.93	6.62	32.90	8.72	31.73	7.48
Il4ra	26.24	2.05	26.98	2.67	25.84	1.66	25.87	1.61
Il5	29.44	5.26	29.40	5.09	30.23	6.05	30.10	5.84
Il5ra	25.50	1.31	25.99	1.68	26.15	1.97	27.19	2.93
Il6	29.91	5.72	29.39	5.08	28.58	4.40	28.55	4.29
Il6ra	22.94	-1.25	24.25	-0.07	24.19	0.01	24.88	0.62
Il6st	20.70	-3.48	20.77	-3.54	20.92	-3.26	20.86	-3.39
Il7	26.90	2.71	27.89	3.58	28.64	4.47	29.67	5.41
Il7r	22.91	-1.28	24.10	-0.21	23.59	-0.59	24.43	0.17
Cxcr1	33.14	8.95	33.59	9.27	31.96	7.78	31.32	7.06

Cxcr2	29.20	5.01	28.67	4.35	26.01	1.83	25.54	1.28
Il9	35.00	10.81	35.00	10.69	35.00	10.82	35.00	10.74
Il9r	28.97	4.78	28.25	3.93	29.29	5.11	28.70	4.44
Inha	27.84	3.65	28.49	4.18	28.76	4.58	29.02	4.76
Inhba	26.34	2.15	27.35	3.03	25.26	1.08	25.52	1.27
Inhbb	25.75	1.57	25.75	1.43	26.58	2.40	27.61	3.35
Ins1	35.00	10.81	35.00	10.69	35.00	10.82	32.39	8.13
Ins2	26.51	2.33	28.40	4.08	30.02	5.84	31.24	6.98
Irf4	24.31	0.12	24.73	0.41	25.16	0.98	25.78	1.52
Irf7	23.53	-0.66	24.30	-0.01	22.44	-1.74	22.92	-1.33
Itgb2	21.46	-2.73	21.78	-2.54	21.16	-3.02	21.30	-2.96
Itih4	29.38	5.20	27.38	3.07	29.45	5.27	29.89	5.63
Kitl	22.91	-1.28	22.84	-1.48	22.85	-1.33	22.71	-1.55
Kng1	35.00	10.81	33.82	9.51	30.87	6.69	35.00	10.74
Lbp	23.80	-0.39	24.53	0.21	25.56	1.38	26.30	2.04
Lefty1	25.88	1.69	26.00	1.69	23.98	-0.20	23.77	-0.49
Lefty2	31.91	7.72	33.39	9.07	35.00	10.82	33.50	9.24
Lepr	23.60	-0.59	24.27	-0.05	25.30	1.12	26.24	1.98
Lif	29.44	5.25	29.85	5.54	26.58	2.40	26.29	2.03
Lifr	22.31	-1.88	22.69	-1.62	21.77	-2.41	21.98	-2.28
Lta	27.77	3.58	27.21	2.90	27.95	3.77	27.88	3.62
Ltb	23.24	-0.95	22.60	-1.71	22.61	-1.57	22.88	-1.38
Ltb4r1	30.40	6.21	30.78	6.47	31.39	7.21	32.65	8.40
Ly75	26.71	2.52	26.52	2.21	25.52	1.34	25.72	1.46
Ly86	22.76	-1.43	22.36	-1.95	22.01	-2.17	21.51	-2.75
Ly96	23.91	-0.28	24.37	0.06	24.38	0.21	24.62	0.36
Mdk	23.49	-0.69	23.92	-0.40	24.89	0.71	25.24	0.99
Mefv	28.74	4.55	28.55	4.24	27.44	3.26	28.01	3.75
Mgll	21.73	-2.46	22.52	-1.79	24.40	0.22	25.30	1.04
Mif	21.52	-2.66	21.90	-2.42	19.50	-4.68	18.95	-5.30
Mmp25	29.82	5.63	30.36	6.04	30.27	6.09	29.91	5.65
Mpl	35.00	10.81	31.70	7.38	33.47	9.29	33.77	9.51
Mstn	34.10	9.91	33.73	9.42	35.00	10.82	35.00	10.74
Muc4	35.00	10.81	35.00	10.69	34.45	10.27	34.26	10.00
Myd88	26.55	2.37	26.98	2.66	26.24	2.06	27.25	3.00
Nfam1	26.86	2.67	27.34	3.03	26.93	2.76	28.81	4.55
Nfatc3	23.35	-0.84	23.54	-0.77	22.82	-1.36	22.85	-1.41
Nfatc4	31.89	7.70	30.68	6.36	32.91	8.73	33.17	8.91
Nfe2l1	22.44	-1.75	22.55	-1.76	23.14	-1.04	23.81	-0.45
Nfkb1	22.82	-1.37	23.33	-0.98	22.46	-1.72	22.91	-1.35
Nfrkb	25.62	1.43	25.90	1.58	25.60	1.42	25.81	1.55
Nfx1	25.67	1.48	25.75	1.44	25.64	1.47	25.46	1.20
Nlrp12	32.92	8.74	35.00	10.69	30.30	6.12	30.64	6.38
Nmi	22.95	-1.24	23.63	-0.69	22.64	-1.53	22.93	-1.33
Nodal	35.00	10.81	31.91	7.59	32.39	8.21	35.00	10.74
Nos2	31.99	7.80	24.72	0.40	31.00	6.82	25.83	1.57
Nr3c1	22.57	-1.62	22.46	-1.85	22.23	-1.95	22.15	-2.11

Nrg1	31.93	7.74	31.34	7.02	28.17	3.99	27.68	3.42
Ntf3	27.46	3.27	27.10	2.79	28.91	4.73	29.49	5.23
Olr1	28.71	4.52	29.20	4.89	24.85	0.67	25.22	0.96
Osm	27.19	3.01	27.70	3.39	26.83	2.65	26.56	2.31
Osmr	22.54	-1.65	23.22	-1.09	22.35	-1.83	22.56	-1.70
Parp4	23.65	-0.53	23.92	-0.40	24.00	-0.18	24.00	-0.25
Nampt	21.77	-2.42	23.00	-1.31	22.37	-1.81	22.14	-2.12
Pdgfa	26.71	2.53	26.95	2.63	25.48	1.31	25.32	1.06
Pdgfb	24.93	0.75	24.61	0.30	24.81	0.63	24.53	0.27
Pdgfc	24.30	0.11	24.98	0.67	25.35	1.17	25.66	1.40
Pf4	21.23	-2.96	21.59	-2.72	22.71	-1.47	22.82	-1.44
Pglyrp1	24.11	-0.08	24.20	-0.12	24.21	0.03	24.38	0.13
Pla2g2d	23.90	-0.29	23.67	-0.65	25.30	1.12	24.93	0.67
Pla2g7	21.89	-2.30	22.78	-1.54	21.63	-2.54	21.93	-2.33
Ppbp	29.21	5.03	29.43	5.11	28.46	4.28	28.31	4.05
Prdx5	20.56	-3.63	21.32	-3.00	20.36	-3.82	20.72	-3.54
Prg2	25.18	0.99	25.52	1.21	26.11	1.93	26.37	2.11
Prg3	29.61	5.42	28.85	4.54	28.91	4.73	29.65	5.39
Prl	35.00	10.81	35.00	10.69	30.16	5.98	29.82	5.56
Prlr	25.41	1.22	25.95	1.64	27.25	3.07	28.48	4.22
Procr	24.24	0.05	24.39	0.07	23.75	-0.43	23.90	-0.36
Prok2	31.36	7.18	31.37	7.06	31.41	7.23	31.80	7.55
Ptafr	24.67	0.48	24.24	-0.08	25.21	1.03	25.60	1.35
Ptgs2	29.14	4.95	29.68	5.36	27.72	3.54	26.92	2.66
Ptn	29.69	5.50	31.13	6.82	31.61	7.43	34.13	9.87
Ptpra	21.57	-2.62	22.34	-1.98	21.85	-2.32	21.89	-2.37
Ptx3	26.48	2.30	26.44	2.13	24.66	0.48	23.84	-0.42
Pxmp2	24.34	0.15	25.38	1.07	26.25	2.07	26.67	2.41
Reg3a	26.37	2.19	25.30	0.98	31.30	7.12	29.83	5.57
Reg3g	27.26	3.07	26.77	2.46	30.68	6.50	30.98	6.72
Ripk2	25.12	0.93	24.88	0.56	25.08	0.90	24.12	-0.14
S100a11	18.88	-5.31	19.21	-5.10	18.77	-5.41	18.58	-5.68
S100a8	22.61	-1.58	22.38	-1.93	21.19	-2.99	20.76	-3.50
S100b	27.00	2.82	27.19	2.88	28.93	4.75	29.14	4.88
Saa4	35.00	10.81	35.00	10.69	35.00	10.82	33.60	9.35
Scg2	34.13	9.94	33.80	9.49	35.00	10.82	35.00	10.74
Scube1	32.58	8.39	32.58	8.27	32.43	8.25	32.73	8.47
Aimp1	21.69	-2.49	22.32	-1.99	20.81	-3.37	20.64	-3.62
Sdcbp	20.33	-3.86	20.58	-3.73	20.27	-3.91	20.35	-3.90
Sectm1b	35.00	10.81	35.00	10.69	34.12	9.94	34.73	10.47
Sele	29.22	5.03	29.23	4.91	30.32	6.14	29.82	5.56
Serpina1a	26.34	2.15	26.52	2.21	26.92	2.74	28.67	4.41
Serpina3n	21.67	-2.51	22.52	-1.79	22.88	-1.30	24.26	0.00
Serpinf2	31.81	7.62	31.84	7.52	29.82	5.64	30.55	6.29
Sftpd	34.67	10.48	32.81	8.49	35.00	10.82	35.00	10.74
Sigirr	27.27	3.09	27.35	3.04	26.29	2.12	26.89	2.63
Siglec1	22.76	-1.43	24.25	-0.07	22.47	-1.71	22.52	-1.74

Siva1	22.97	-1.22	23.59	-0.73	21.63	-2.55	21.58	-2.68
Slco1a4	29.86	5.67	31.34	7.02	32.58	8.40	34.22	9.96
Slurp1	31.40	7.21	32.20	7.89	30.41	6.23	31.25	6.99
Socs2	23.52	-0.67	25.47	1.16	25.46	1.28	25.99	1.73
Spaca3	35.00	10.81	35.00	10.69	34.84	10.66	35.00	10.74
Spp1	27.37	3.18	25.21	0.89	22.61	-1.57	20.43	-3.83
Spred1	22.89	-1.30	23.24	-1.08	22.71	-1.47	22.64	-1.62
Srgap1	26.61	2.42	26.94	2.62	27.92	3.74	29.18	4.92
Stab1	22.99	-1.20	23.52	-0.79	22.89	-1.29	23.21	-1.04
Stat3	25.17	0.98	24.96	0.65	24.75	0.57	25.48	1.22
Sykb	25.16	0.98	25.61	1.29	25.52	1.34	26.45	2.19
Tacr1	27.24	3.05	28.68	4.37	28.22	4.04	29.79	5.53
Thpo	31.41	7.23	31.91	7.60	33.33	9.15	32.39	8.13
Tirap	24.95	0.76	24.96	0.65	24.60	0.42	24.41	0.15
Tlr1	25.49	1.30	23.95	-0.36	25.28	1.10	23.48	-0.78
Tlr2	25.92	1.73	25.73	1.42	24.87	0.69	25.17	0.91
Tlr3	35.00	10.81	25.45	1.14	27.31	3.13	26.24	1.98
Tlr4	22.94	-1.25	23.65	-0.66	23.27	-0.91	23.57	-0.69
Tlr5	24.17	-0.01	25.18	0.87	25.30	1.12	25.32	1.06
Tlr6	27.67	3.48	26.34	2.03	26.94	2.76	26.50	2.25
Tlr7	25.85	1.67	24.50	0.19	25.72	1.54	24.68	0.42
Tlr8	24.15	-0.03	24.41	0.10	24.31	0.14	24.24	-0.02
Tlr9	25.71	1.52	25.39	1.07	25.61	1.43	25.94	1.68
Tnf	28.43	4.25	27.25	2.93	27.70	3.52	27.97	3.71
Tnfaip6	27.11	2.92	27.68	3.37	26.77	2.59	26.43	2.17
Tnfrsf11b	27.60	3.41	25.02	0.70	27.39	3.21	26.52	2.26
Tnfsf10	26.11	1.93	25.13	0.82	26.08	1.90	26.15	1.89
Tnfsf11	28.58	4.39	27.35	3.03	28.65	4.47	27.42	3.17
Tnfsf13	23.68	-0.51	24.50	0.19	23.41	-0.77	23.85	-0.40
Tnfsf13b	25.92	1.73	25.84	1.52	26.57	2.39	26.83	2.57
Tnfsf14	27.36	3.18	26.72	2.40	26.47	2.29	26.31	2.05
Tnfsf15	31.94	7.75	29.37	5.05	29.63	5.45	27.85	3.59
Tnfsf18	29.60	5.41	30.64	6.33	30.67	6.49	32.16	7.91
Tnfsf4	29.73	5.54	29.20	4.89	29.65	5.47	29.30	5.04
Tnfsf8	28.96	4.78	27.95	3.64	28.27	4.09	27.85	3.59
Tnfsf9	30.63	6.44	28.59	4.27	28.17	3.99	26.38	2.12
Tollip	23.57	-0.61	24.10	-0.21	23.40	-0.78	23.42	-0.84
Tpst1	22.86	-1.32	22.77	-1.55	22.41	-1.77	22.35	-1.90
Trap1	22.54	-1.65	23.11	-1.20	22.62	-1.56	22.65	-1.60
Ttn	28.69	4.50	29.28	4.97	28.20	4.02	28.41	4.16
Tymp	33.27	9.08	31.26	6.94	32.14	7.96	30.66	6.40
Vegfa	22.87	-1.32	22.77	-1.54	22.30	-1.88	21.78	-2.48
Vegfb	23.11	-1.08	23.97	-0.34	25.35	1.17	25.89	1.63
Vps45	25.32	1.14	25.79	1.48	25.15	0.98	25.57	1.31
Xcl1	27.57	3.38	27.18	2.87	25.83	1.65	25.33	1.07
Xcr1	27.50	3.31	26.17	1.86	27.50	3.32	26.92	2.66
Yars	25.26	1.07	25.63	1.32	24.26	0.08	24.98	0.72

Gusb	24.15	-0.03	23.56	-0.75	23.55	-0.63	23.64	-0.61
Hprt	21.60	-2.58	21.84	-2.48	21.53	-2.65	21.33	-2.93
Hsp90ab1	18.67	-5.52	19.68	-4.63	17.53	-6.65	17.63	-6.63
Gapdh	19.82	-4.37	20.13	-4.18	18.71	-5.47	18.92	-5.33
Actb	18.32	-5.87	18.10	-6.21	17.70	-6.48	18.27	-5.99

Table A.2. CT and dCT values from parametrial WAT (from PCR array)

	LF PBS CT	LF PBS dCT	HF PBS CT	HF PBS dCT	LF FFL CT	LF FFL dCT	HF FFL CT	HF FFL dCT
Adora1	27.64	4.09	27.16	3.62	26.93	3.40	26.98	3.49
Ahsg	29.38	5.83	29.95	6.42	29.68	6.15	30.42	6.93
Aif1	25.80	2.25	24.64	1.11	23.86	0.33	23.35	-0.15
Apcs	35.00	11.45	35.00	11.47	35.00	11.47	35.00	11.51
Apoa2	28.33	4.78	29.13	5.59	27.61	4.08	28.28	4.78
Apol7a	29.07	5.52	28.55	5.01	28.75	5.23	27.45	3.96
Apol8	35.00	11.45	35.00	11.47	33.55	10.02	35.00	11.51
Areg	34.25	10.71	32.47	8.93	32.49	8.96	30.35	6.86
Bcl6	25.16	1.61	25.27	1.73	25.22	1.69	25.59	2.10
Blnk	27.59	4.05	26.26	2.73	26.26	2.74	26.48	2.98
Bmp1	24.22	0.67	24.24	0.71	23.97	0.44	24.33	0.84
Bmp2	30.38	6.83	30.19	6.66	30.26	6.73	29.95	6.46
Bmp3	23.58	0.03	23.86	0.33	23.56	0.03	24.23	0.74
Bmp7	29.22	5.67	29.52	5.98	30.85	7.32	29.44	5.95
C3	21.73	-1.82	21.44	-2.10	20.90	-2.63	21.49	-2.01
C3ar1	25.59	2.04	23.34	-0.19	23.77	0.25	23.08	-0.42
Cast	23.25	-0.30	23.16	-0.37	23.13	-0.40	22.95	-0.55
Ccl1	35.00	11.45	33.20	9.67	31.42	7.89	29.85	6.35
Ccl11	22.99	-0.55	22.69	-0.84	23.12	-0.41	22.91	-0.58
Ccl12	26.79	3.24	26.00	2.46	25.96	2.44	24.01	0.52
Ccl17	30.96	7.41	28.83	5.29	28.62	5.09	27.24	3.75
Ccl19	26.78	3.23	26.37	2.83	26.48	2.95	26.44	2.95
Ccl2	26.52	2.97	24.46	0.93	24.71	1.19	23.13	-0.36
Ccl20	35.00	11.45	35.00	11.47	35.00	11.47	33.52	10.03
Ccl22	30.44	6.90	29.17	5.64	29.46	5.93	27.57	4.08
Ccl24	29.41	5.86	28.73	5.19	28.94	5.42	29.98	6.48
Ccl25	29.07	5.52	29.33	5.79	28.31	4.78	28.23	4.73
Ccl27a	25.32	1.77	26.08	2.55	25.02	1.49	25.66	2.16
Ccl28	29.92	6.38	30.70	7.16	30.54	7.02	30.09	6.60
Ccl3	28.42	4.87	28.40	4.86	28.01	4.48	27.16	3.67
Ccl4	30.62	7.07	28.19	4.66	28.91	5.38	27.00	3.51
Ccl5	24.94	1.40	24.35	0.82	24.31	0.79	23.21	-0.29
Ccl6	22.21	-1.34	22.53	-1.01	22.52	-1.00	22.46	-1.03
Ccl7	25.41	1.86	23.36	-0.17	24.44	0.92	22.16	-1.33
Ccl8	22.17	-1.38	21.80	-1.74	21.91	-1.62	20.67	-2.83
Ccl9	23.59	0.05	23.83	0.29	24.13	0.60	23.58	0.08
Ccr1	27.22	3.67	26.96	3.43	26.52	2.99	25.16	1.67
Ccr10	30.90	7.35	32.35	8.82	29.54	6.02	30.47	6.97

Ccr2	25.15	1.61	23.79	0.26	24.24	0.72	23.35	-0.14
Ccr3	26.63	3.08	24.94	1.41	25.64	2.12	24.35	0.86
Ccr4	32.76	9.21	31.47	7.94	32.20	8.68	30.68	7.19
Ccr5	26.50	2.95	24.93	1.40	25.40	1.87	24.13	0.64
Ccr6	32.99	9.44	30.39	6.85	29.57	6.04	29.12	5.63
Ccr7	31.70	8.16	31.89	8.36	30.59	7.06	30.16	6.67
Ccr8	32.10	8.56	32.36	8.83	31.41	7.89	29.68	6.19
Ccr9	31.31	7.76	30.80	7.26	29.48	5.95	30.12	6.63
Ccrl1	29.84	6.30	30.11	6.57	30.95	7.43	32.46	8.97
Ccrl2	27.62	4.07	26.31	2.77	27.19	3.66	26.43	2.94
Cd14	23.50	-0.04	23.63	0.10	23.55	0.02	23.54	0.05
Cd180	28.68	5.13	26.32	2.78	26.97	3.44	26.33	2.83
Cd27	30.88	7.34	30.69	7.15	30.48	6.95	29.66	6.16
Cd28	29.16	5.61	28.12	4.59	28.62	5.09	27.99	4.50
Cd4	29.76	6.21	28.69	5.16	28.16	4.63	27.87	4.38
Cd40	28.27	4.72	28.24	4.71	28.20	4.67	27.50	4.01
Cd40lg	31.13	7.59	30.36	6.83	29.96	6.43	29.56	6.07
Cd70	33.22	9.67	35.00	11.47	33.26	9.74	32.91	9.41
Cd74	18.81	-4.74	18.31	-5.23	18.58	-4.95	18.12	-5.38
Cd86	25.78	2.23	25.50	1.97	25.29	1.76	25.16	1.67
Cd97	23.29	-0.25	22.87	-0.66	23.57	0.04	23.29	-0.21
Cebpb	21.19	-2.35	22.26	-1.27	21.48	-2.05	21.32	-2.18
Cer1	35.00	11.45	35.00	11.47	35.00	11.47	35.00	11.51
Cklf	26.75	3.21	26.62	3.08	26.22	2.70	25.72	2.23
Clcf1	30.65	7.10	29.60	6.07	28.83	5.31	28.16	4.66
Cmtm1	34.01	10.46	34.59	11.06	34.66	11.14	34.14	10.65
Cmtm2a	35.00	11.45	35.00	11.47	32.52	8.99	32.84	9.35
Cntfr	31.30	7.75	32.61	9.07	30.43	6.91	30.73	7.24
Crp	31.44	7.90	31.65	8.11	32.00	8.47	32.79	9.29
Csf1	25.34	1.79	25.69	2.15	24.85	1.32	24.58	1.08
Csf2	34.28	10.73	30.76	7.23	32.93	9.40	31.64	8.14
Csf2ra	27.41	3.86	27.46	3.93	26.56	3.03	27.17	3.67
Csf3	35.00	11.45	33.30	9.77	32.25	8.72	33.68	10.19
Csf3r	29.86	6.32	28.34	4.81	27.14	3.62	27.39	3.89
Ctf1	28.15	4.60	29.22	5.68	27.61	4.09	28.38	4.89
Ctf2	33.18	9.63	35.00	11.47	33.51	9.98	33.41	9.91
Cx3cl1	27.91	4.36	27.87	4.34	27.59	4.06	27.33	3.84
Cx3cr1	31.48	7.93	30.61	7.08	27.55	4.03	27.35	3.86
Cxcl1	30.96	7.41	30.60	7.06	28.84	5.32	28.39	4.90
Cxcl10	27.61	4.06	26.38	2.85	25.31	1.78	23.81	0.32
Cxcl11	29.83	6.29	29.38	5.85	28.37	4.85	28.85	5.36
Cxcl12	24.13	0.58	23.91	0.38	23.44	-0.08	23.88	0.38
Cxcl13	21.98	-1.56	23.20	-0.33	21.97	-1.56	24.32	0.83
Cxcl14	25.80	2.26	26.53	3.00	26.35	2.82	25.46	1.97
Cxcl15	35.00	11.45	35.00	11.47	35.00	11.47	33.26	9.77
Cxcl16	24.38	0.83	23.93	0.40	23.92	0.40	23.30	-0.20
Cxcl2	27.81	4.26	27.91	4.37	27.79	4.26	27.50	4.00

Cxcl5	35.00	11.45	32.94	9.41	24.44	0.92	23.88	0.38
Cxcl9	23.51	-0.03	23.74	0.20	22.91	-0.62	21.90	-1.60
Cxcr3	27.38	3.83	26.69	3.16	27.13	3.61	26.42	2.92
Cxcr4	24.68	1.13	25.69	2.15	24.49	0.97	24.67	1.18
Cxcr5	33.67	10.12	30.31	6.77	30.36	6.84	31.42	7.93
Cxcr6	27.83	4.28	27.26	3.73	27.13	3.61	26.44	2.95
Cybb	26.30	2.75	25.01	1.47	25.21	1.69	24.72	1.22
Cyp26b1	33.84	10.29	33.28	9.74	34.80	11.28	33.52	10.03
D17Wsu104e	23.52	-0.03	22.92	-0.61	22.90	-0.62	22.73	-0.76
Dock2	27.35	3.80	26.57	3.04	26.29	2.77	26.31	2.82
Ebi3	27.26	3.71	26.57	3.03	26.55	3.03	26.75	3.26
Eda	27.50	3.95	27.60	4.07	27.80	4.28	28.35	4.86
Ephx2	21.87	-1.68	21.51	-2.03	21.36	-2.17	21.16	-2.33
Epo	35.00	11.45	35.00	11.47	35.00	11.47	35.00	11.51
Epor	29.42	5.88	28.85	5.32	28.72	5.20	28.65	5.16
Erbb2	29.58	6.04	31.43	7.90	29.87	6.35	29.55	6.06
Erbb2ip	25.18	1.63	24.82	1.28	24.48	0.95	24.31	0.82
F11r	25.62	2.07	25.52	1.99	24.69	1.16	24.59	1.10
F2	35.00	11.45	35.00	11.47	35.00	11.47	32.44	8.94
F3	24.56	1.01	24.01	0.48	24.55	1.02	24.35	0.86
F8	27.20	3.66	27.37	3.84	26.79	3.27	27.33	3.84
Fasl	32.61	9.07	30.08	6.55	31.52	7.99	29.95	6.46
Fgf1	22.77	-0.78	22.37	-1.16	22.75	-0.77	23.00	-0.49
Fgf10	24.92	1.37	24.34	0.80	24.78	1.25	24.53	1.04
Fgf12	32.43	8.88	33.10	9.56	33.37	9.84	31.72	8.23
Fgf2	25.92	2.37	25.90	2.37	25.59	2.07	25.36	1.86
Fgf3	35.00	11.45	33.59	10.06	35.00	11.47	33.84	10.35
Fgf4	35.00	11.45	35.00	11.47	35.00	11.47	35.00	11.51
Fgf5	33.27	9.73	34.38	10.85	33.57	10.04	34.80	11.31
Fgf6	35.00	11.45	35.00	11.47	35.00	11.47	35.00	11.51
Fgf7	27.50	3.96	27.09	3.55	27.70	4.18	27.33	3.83
Fgf8	35.00	11.45	35.00	11.47	34.52	10.99	35.00	11.51
Fgf9	27.43	3.88	27.49	3.95	27.91	4.39	28.56	5.06
Figf	22.78	-0.77	23.32	-0.22	23.51	-0.02	23.68	0.19
Flt3l	27.24	3.69	26.73	3.19	26.40	2.87	27.29	3.80
Fn1	23.25	-0.30	23.32	-0.22	21.50	-2.03	20.80	-2.70
Fos	23.43	-0.12	24.57	1.03	24.30	0.77	23.27	-0.22
Fpr1	28.60	5.06	28.65	5.12	26.60	3.08	28.66	5.17
Gdf1	32.96	9.41	32.94	9.41	30.44	6.91	31.37	7.87
Gdf2	35.00	11.45	33.28	9.75	35.00	11.47	33.17	9.68
Gdf3	33.69	10.15	29.74	6.20	30.20	6.68	29.28	5.79
Gdf5	29.19	5.64	29.83	6.30	29.34	5.82	30.42	6.93
Gdf6	35.00	11.45	35.00	11.47	34.14	10.61	31.10	7.61
Gdf7	30.74	7.19	30.38	6.85	30.26	6.73	31.13	7.64
Gdf9	28.70	5.15	28.98	5.44	28.51	4.99	28.83	5.34
Gfra1	30.50	6.95	30.18	6.65	29.72	6.19	30.30	6.80
Gfra2	26.83	3.28	26.44	2.91	26.47	2.94	26.63	3.13

Ghr	19.23	-4.32	18.95	-4.58	19.36	-4.17	19.75	-3.74
Glmn	26.30	2.75	26.53	2.99	25.94	2.42	25.84	2.35
Gpi1	21.50	-2.05	21.24	-2.29	21.47	-2.05	21.34	-2.15
Gpr68	30.55	7.00	31.10	7.57	30.61	7.08	30.27	6.78
Grem1	35.00	11.45	31.64	8.10	32.40	8.87	32.19	8.70
Grem2	28.13	4.59	27.86	4.33	28.00	4.48	29.28	5.78
Grn	22.21	-1.34	21.77	-1.76	21.78	-1.74	21.92	-1.58
Hdac4	25.75	2.20	26.83	3.29	25.96	2.44	26.17	2.68
Hdac5	26.96	3.42	27.01	3.48	26.89	3.37	27.53	4.04
Hdac7	24.18	0.63	24.17	0.63	23.90	0.38	24.19	0.70
Hdac9	29.17	5.62	27.64	4.10	28.21	4.69	27.39	3.90
Hrh1	31.48	7.94	30.83	7.30	31.61	8.08	30.42	6.92
Ifna11	34.71	11.17	35.00	11.47	35.00	11.47	35.00	11.51
Ifna14	35.00	11.45	35.00	11.47	35.00	11.47	34.62	11.13
Ifna2	35.00	11.45	33.60	10.07	35.00	11.47	32.99	9.50
Ifna4	33.79	10.24	34.73	11.19	33.94	10.41	34.54	11.05
Ifna9	35.00	11.45	35.00	11.47	35.00	11.47	35.00	11.51
Ifnab	35.00	11.45	35.00	11.47	35.00	11.47	35.00	11.51
Ifnar1	25.13	1.58	24.38	0.84	24.49	0.97	24.30	0.81
Ifnar2	22.52	-1.02	22.29	-1.25	22.17	-1.36	22.19	-1.31
Ifnb1	35.00	11.45	35.00	11.47	35.00	11.47	35.00	11.51
Ifne	32.43	8.89	35.00	11.47	32.49	8.96	35.00	11.51
Ifng	32.24	8.69	30.95	7.41	30.54	7.02	30.33	6.84
Ifngr1	22.11	-1.43	21.97	-1.57	22.81	-0.71	22.79	-0.71
Ifngr2	24.59	1.05	24.47	0.94	24.35	0.82	23.67	0.18
Ifnk	30.46	6.91	30.67	7.14	30.59	7.07	29.99	6.49
Ik	25.94	2.40	27.64	4.10	27.30	3.77	27.77	4.27
Il10	29.41	5.86	27.98	4.44	28.70	5.18	27.93	4.44
Il10ra	27.19	3.64	27.56	4.03	27.02	3.49	26.37	2.88
Il10rb	23.63	0.08	23.16	-0.38	23.26	-0.26	23.02	-0.47
Il11	33.15	9.60	32.74	9.20	33.31	9.78	33.22	9.72
Il11ra1	24.59	1.04	24.57	1.04	24.27	0.74	24.42	0.92
Il12a	35.00	11.45	32.92	9.39	31.85	8.33	30.99	7.50
Il12b	30.25	6.71	31.35	7.81	30.63	7.11	28.27	4.78
Il12rb1	35.00	11.45	35.00	11.47	35.00	11.47	35.00	11.51
Il12rb2	35.00	11.45	35.00	11.47	34.23	10.71	33.54	10.05
Il13	35.00	11.45	32.97	9.44	33.62	10.09	34.11	10.62
Il13ra1	26.62	3.07	26.72	3.18	25.53	2.01	25.47	1.98
Il13ra2	27.75	4.20	27.48	3.95	29.65	6.12	27.89	4.39
Il15	26.44	2.90	26.09	2.56	25.89	2.37	25.71	2.21
Il15ra	26.84	3.29	27.70	4.17	26.60	3.07	27.12	3.63
Il16	28.12	4.57	27.70	4.17	26.95	3.42	26.83	3.34
Il17a	35.00	11.45	35.00	11.47	35.00	11.47	35.00	11.51
Il17b	30.99	7.44	32.15	8.62	32.69	9.16	33.53	10.03
Il17c	35.00	11.45	33.15	9.61	35.00	11.47	33.30	9.81
Il17d	30.43	6.88	31.27	7.74	30.29	6.77	30.77	7.27
Il17f	35.00	11.45	30.50	6.96	34.71	11.18	31.58	8.09

Il17ra	28.36	4.81	28.61	5.07	27.71	4.19	27.54	4.04
Il17rb	29.23	5.69	29.26	5.73	28.87	5.34	29.18	5.68
Il18	25.20	1.65	25.22	1.68	24.53	1.01	24.02	0.53
Il18r1	29.63	6.08	29.31	5.77	28.18	4.65	27.28	3.78
Il18rap	30.92	7.37	29.79	6.26	28.81	5.29	27.16	3.66
Il19	35.00	11.45	35.00	11.47	33.78	10.25	35.00	11.51
Il1a	35.00	11.45	32.83	9.30	33.18	9.65	29.88	6.39
Il1b	29.44	5.89	30.11	6.57	27.24	3.72	27.13	3.64
Il1f10	35.00	11.45	35.00	11.47	35.00	11.47	35.00	11.51
Il1f5	35.00	11.45	35.00	11.47	35.00	11.47	35.00	11.51
Il1f6	33.69	10.14	34.95	11.42	35.00	11.47	35.00	11.51
Il1f8	33.49	9.95	35.00	11.47	35.00	11.47	35.00	11.51
Il1f9	35.00	11.45	35.00	11.47	29.58	6.06	31.20	7.71
Il1r1	24.64	1.09	25.01	1.47	24.45	0.92	23.93	0.44
Il1r2	27.62	4.07	28.32	4.79	27.36	3.84	26.68	3.19
Il1rap	28.96	5.41	28.50	4.96	27.30	3.78	27.22	3.72
Il1rapl2	35.00	11.45	35.00	11.47	35.00	11.47	35.00	11.51
Il1rl1	27.38	3.83	27.70	4.17	26.99	3.46	27.47	3.98
Il1rl2	30.97	7.42	30.91	7.38	30.38	6.85	30.60	7.10
Il1rn	31.92	8.37	27.69	4.16	29.87	6.34	27.35	3.86
Il2	31.01	7.46	30.66	7.12	30.64	7.11	30.12	6.63
Il20	35.00	11.45	35.00	11.47	35.00	11.47	35.00	11.51
Il20ra	35.00	11.45	35.00	11.47	33.80	10.28	34.97	11.48
Il21	35.00	11.45	33.38	9.85	33.79	10.27	34.28	10.79
Il21r	32.47	8.92	32.51	8.98	28.60	5.07	29.27	5.78
Il22	35.00	11.45	35.00	11.47	35.00	11.47	35.00	11.51
Il22ra1	30.95	7.40	29.87	6.34	29.90	6.38	29.54	6.05
Il22ra2	28.72	5.18	28.71	5.18	28.28	4.76	29.81	6.31
Il23a	35.00	11.45	34.21	10.67	32.93	9.41	32.73	9.24
Il23r	32.72	9.18	31.58	8.05	31.52	7.99	31.93	8.43
Il24	35.00	11.45	34.21	10.68	33.87	10.35	34.31	10.82
Il27	31.68	8.13	32.28	8.74	30.62	7.10	30.14	6.65
Il28ra	32.40	8.85	32.13	8.60	30.16	6.63	30.22	6.73
Il2ra	30.43	6.89	30.47	6.94	30.36	6.84	29.70	6.20
Il2rb	30.13	6.58	30.90	7.36	29.20	5.68	28.44	4.95
Il2rg	25.69	2.15	24.94	1.41	24.75	1.22	24.21	0.72
Il3	35.00	11.45	35.00	11.47	35.00	11.47	35.00	11.51
Il31	35.00	11.45	35.00	11.47	35.00	11.47	35.00	11.51
Il31ra	26.80	3.26	27.52	3.99	26.76	3.24	28.16	4.67
Il3ra	32.13	8.58	31.84	8.30	30.83	7.30	31.39	7.89
Il4	33.29	9.75	32.78	9.25	35.00	11.47	32.75	9.25
Il4ra	28.37	4.82	28.64	5.10	28.09	4.56	27.84	4.35
Il5	30.94	7.39	33.10	9.56	31.57	8.04	31.60	8.11
Il5ra	29.63	6.08	30.18	6.65	29.80	6.28	30.56	7.06
Il6	30.85	7.31	30.12	6.58	29.94	6.41	28.61	5.12
Il6ra	25.23	1.68	25.71	2.17	24.92	1.39	25.71	2.21
Il6st	22.43	-1.12	22.63	-0.90	21.98	-1.54	22.24	-1.25

Il7	29.76	6.21	29.60	6.06	30.54	7.01	30.14	6.64
Il7r	26.87	3.32	25.86	2.33	26.64	3.11	25.95	2.46
Cxcr1	35.00	11.45	34.19	10.66	32.57	9.04	33.54	10.05
Cxcr2	32.41	8.87	32.36	8.83	28.97	5.44	28.21	4.72
Il9	35.00	11.45	35.00	11.47	35.00	11.47	35.00	11.51
Il9r	35.00	11.45	35.00	11.47	33.53	10.00	32.66	9.17
Inha	31.10	7.55	31.31	7.77	30.20	6.68	32.31	8.82
Inhba	29.69	6.14	29.77	6.24	28.77	5.24	28.26	4.77
Inhbb	28.36	4.81	28.22	4.68	27.40	3.88	27.60	4.10
Ins1	35.00	11.45	35.00	11.47	35.00	11.47	35.00	11.51
Ins2	33.73	10.18	35.00	11.47	33.43	9.90	32.79	9.29
Irf4	26.35	2.80	27.84	4.31	26.43	2.91	28.60	5.11
Irf7	26.64	3.09	26.30	2.76	25.33	1.81	24.99	1.49
Itgb2	23.90	0.35	22.93	-0.60	23.90	0.37	23.16	-0.34
Itih4	29.69	6.15	30.43	6.90	30.88	7.35	30.61	7.12
Kitl	24.25	0.71	23.92	0.38	23.86	0.34	23.68	0.19
Kng1	33.49	9.94	32.01	8.48	31.62	8.09	33.12	9.62
Lbp	23.45	-0.10	23.37	-0.16	23.61	0.09	23.31	-0.18
Lefty1	27.63	4.08	27.89	4.36	27.15	3.62	26.47	2.98
Lefty2	35.00	11.45	31.85	8.31	35.00	11.47	33.25	9.76
Lepr	26.76	3.22	27.93	4.40	26.00	2.48	28.37	4.87
Lif	31.18	7.64	30.65	7.12	29.31	5.78	28.92	5.43
Lifr	24.99	1.44	25.27	1.74	24.56	1.04	24.35	0.86
Lta	35.00	11.45	32.86	9.32	32.45	8.92	31.21	7.72
Ltb	29.33	5.78	29.23	5.69	28.27	4.74	27.65	4.16
Ltb4r1	33.39	9.84	34.89	11.36	33.57	10.04	33.41	9.91
Ly75	31.33	7.78	30.35	6.82	29.24	5.71	28.38	4.89
Ly86	24.99	1.45	23.70	0.17	23.68	0.15	22.85	-0.65
Ly96	25.12	1.57	25.20	1.67	24.59	1.07	24.64	1.14
Mdk	24.65	1.10	24.40	0.87	24.38	0.86	24.63	1.14
Mefv	33.69	10.14	32.83	9.30	29.81	6.29	30.25	6.75
Mgll	22.10	-1.44	22.08	-1.45	22.12	-1.41	22.01	-1.48
Mif	21.68	-1.87	21.69	-1.85	21.55	-1.97	21.21	-2.28
Mmp25	33.74	10.20	32.52	8.99	33.71	10.19	31.40	7.91
Mpl	35.00	11.45	30.30	6.77	35.00	11.47	31.59	8.10
Mstn	31.40	7.85	32.74	9.21	32.27	8.75	27.79	4.30
Muc4	35.00	11.45	35.00	11.47	35.00	11.47	35.00	11.51
Myd88	29.66	6.11	29.39	5.86	28.54	5.01	28.53	5.03
Nfam1	31.22	7.67	31.12	7.58	31.08	7.55	30.39	6.90
Nfatc3	24.51	0.96	24.52	0.98	24.62	1.09	24.42	0.93
Nfatc4	35.00	11.45	33.34	9.80	34.64	11.12	33.69	10.20
Nfe2l1	24.57	1.02	24.64	1.11	24.29	0.76	24.42	0.93
Nfkb1	25.17	1.62	24.98	1.45	24.89	1.36	24.82	1.32
Nfrkb	28.42	4.87	28.08	4.55	27.83	4.31	28.18	4.69
Nfx1	27.21	3.66	26.60	3.07	26.73	3.20	27.25	3.76
Nlrp12	33.38	9.83	35.00	11.47	33.93	10.41	32.62	9.13
Nmi	24.29	0.74	24.57	1.03	24.30	0.77	23.99	0.50

Nodal	35.00	11.45	35.00	11.47	33.55	10.03	35.00	11.51
Nos2	34.26	10.72	27.61	4.07	32.30	8.77	27.35	3.85
Nr3c1	23.24	-0.31	23.09	-0.45	23.12	-0.41	23.13	-0.37
Nrg1	32.43	8.88	33.42	9.88	30.82	7.29	29.61	6.11
Ntf3	27.58	4.03	27.45	3.92	27.79	4.26	27.58	4.09
Olr1	28.17	4.62	27.89	4.35	27.75	4.23	26.74	3.25
Osm	29.86	6.31	30.88	7.34	30.50	6.97	29.17	5.68
Osmr	24.53	0.99	24.56	1.02	24.16	0.63	23.90	0.41
Parp4	25.13	1.58	25.01	1.47	25.16	1.64	25.42	1.93
Nampt	22.46	-1.09	23.20	-0.34	22.45	-1.08	22.98	-0.52
Pdgfa	26.97	3.42	26.99	3.46	26.95	3.42	26.63	3.14
Pdgfb	27.18	3.63	26.37	2.83	26.86	3.34	26.18	2.69
Pdgfc	25.58	2.03	25.45	1.92	25.06	1.53	25.63	2.14
Pf4	22.24	-1.31	22.11	-1.42	22.44	-1.09	21.67	-1.82
Pglyrp1	26.35	2.80	26.41	2.87	26.38	2.85	25.84	2.35
Pla2g2d	26.55	3.01	26.46	2.93	25.64	2.11	26.38	2.89
Pla2g7	22.66	-0.89	22.96	-0.58	22.49	-1.03	22.78	-0.71
Ppbp	28.81	5.26	28.57	5.04	28.72	5.19	27.44	3.95
Prdx5	20.18	-3.37	20.31	-3.23	20.43	-3.09	20.51	-2.98
Prg2	28.99	5.44	29.21	5.68	28.95	5.43	29.86	6.36
Prg3	35.00	11.45	32.51	8.97	35.00	11.47	32.82	9.33
Prl	35.00	11.45	35.00	11.47	35.00	11.47	31.81	8.32
Prlr	26.19	2.65	25.93	2.40	25.90	2.37	26.65	3.16
Procr	26.39	2.84	26.28	2.75	26.13	2.60	25.87	2.37
Prok2	35.00	11.45	34.74	11.21	33.94	10.41	35.00	11.51
Ptafr	26.45	2.90	25.47	1.93	25.75	2.22	25.47	1.98
Ptgs2	29.09	5.54	29.62	6.08	29.11	5.58	28.67	5.18
Ptn	27.29	3.74	29.80	6.26	26.72	3.20	28.67	5.18
Ptpra	22.49	-1.06	22.59	-0.95	22.61	-0.91	22.63	-0.87
Ptx3	26.58	3.03	26.40	2.87	26.25	2.73	24.17	0.67
Pxmp2	25.24	1.69	25.59	2.05	24.84	1.32	25.76	2.27
Reg3a	35.00	11.45	34.90	11.36	35.00	11.47	34.36	10.87
Reg3g	35.00	11.45	35.00	11.47	35.00	11.47	35.00	11.51
Ripk2	26.43	2.88	25.61	2.07	26.15	2.62	25.69	2.19
S100a11	18.59	-4.96	18.22	-5.32	18.60	-4.93	18.44	-5.05
S100a8	24.22	0.67	23.51	-0.02	23.49	-0.03	23.15	-0.35
S100b	26.69	3.14	26.94	3.40	26.72	3.20	27.45	3.96
Saa4	31.29	7.74	33.00	9.47	32.52	9.00	32.77	9.28
Scg2	35.00	11.45	35.00	11.47	35.00	11.47	35.00	11.51
Scube1	34.12	10.57	35.00	11.47	35.00	11.47	35.00	11.51
Aimp1	22.42	-1.13	22.59	-0.95	22.16	-1.37	22.17	-1.32
Sdcbp	21.25	-2.30	20.90	-2.63	20.97	-2.56	20.85	-2.64
Sectm1b	35.00	11.45	35.00	11.47	35.00	11.47	35.00	11.51
Sele	32.77	9.22	30.54	7.01	31.34	7.81	33.42	9.93
Serpina1a	27.48	3.93	27.53	3.99	27.51	3.98	27.50	4.00
Serpina3n	20.50	-3.05	20.48	-3.06	20.80	-2.73	20.62	-2.87
Serpinf2	35.00	11.45	32.84	9.31	35.00	11.47	31.93	8.43

Sftpd	35.00	11.45	35.00	11.47	35.00	11.47	35.00	11.51
Sigirr	30.76	7.21	30.14	6.61	30.78	7.26	28.99	5.50
Siglec1	25.34	1.80	24.97	1.43	24.95	1.42	24.32	0.83
Siva1	23.74	0.19	23.78	0.24	23.55	0.02	23.40	-0.10
Slco1a4	33.14	9.60	35.00	11.47	33.75	10.23	35.00	11.51
Slurp1	35.00	11.45	31.23	7.69	33.54	10.02	30.84	7.34
Socs2	25.30	1.75	26.77	3.24	26.28	2.76	26.41	2.91
Spaca3	35.00	11.45	35.00	11.47	35.00	11.47	35.00	11.51
Spp1	27.69	4.15	25.68	2.14	26.10	2.57	23.40	-0.10
Spred1	25.14	1.59	24.98	1.45	24.56	1.03	24.31	0.81
Srgap1	27.28	3.73	27.95	4.42	27.83	4.31	28.12	4.63
Stab1	25.45	1.91	25.23	1.70	24.48	0.95	24.80	1.30
Stat3	27.97	4.43	28.24	4.71	27.52	3.99	27.30	3.81
Sykb	29.33	5.78	29.32	5.78	28.57	5.05	28.76	5.27
Tacr1	35.00	11.45	32.57	9.04	33.22	9.70	33.13	9.63
Thpo	35.00	11.45	33.84	10.31	34.22	10.69	32.30	8.81
Tirap	26.40	2.85	26.16	2.62	25.89	2.36	25.95	2.45
Tlr1	28.73	5.18	25.93	2.39	26.49	2.97	25.50	2.00
Tlr2	28.49	4.95	27.73	4.20	27.17	3.64	26.90	3.41
Tlr3	28.51	4.96	26.31	2.78	27.17	3.64	26.67	3.17
Tlr4	24.43	0.89	24.59	1.06	23.82	0.29	24.33	0.83
Tlr5	25.83	2.28	26.83	3.30	25.61	2.09	26.30	2.81
Tlr6	29.27	5.72	28.42	4.89	28.33	4.81	27.67	4.18
Tlr7	27.64	4.09	25.95	2.42	25.88	2.35	25.82	2.32
Tlr8	26.08	2.53	25.24	1.70	25.12	1.59	24.99	1.50
Tlr9	29.89	6.34	29.03	5.49	29.29	5.77	29.29	5.80
Tnf	31.75	8.21	30.87	7.33	29.93	6.41	29.56	6.07
Tnfaip6	26.99	3.44	26.55	3.02	27.18	3.65	25.73	2.23
Tnfrsf11b	26.31	2.76	25.12	1.59	26.16	2.63	25.70	2.20
Tnfsf10	28.53	4.99	27.69	4.15	27.75	4.23	27.29	3.80
Tnfsf11	32.54	8.99	31.35	7.81	30.30	6.77	29.12	5.62
Tnfsf13	27.51	3.96	27.37	3.84	26.35	2.82	26.60	3.11
Tnfsf13b	27.86	4.32	27.85	4.32	27.65	4.13	27.79	4.29
Tnfsf14	28.89	5.34	28.45	4.92	28.02	4.49	28.22	4.73
Tnfsf15	34.76	11.22	32.64	9.10	31.82	8.29	30.83	7.34
Tnfsf18	31.11	7.56	32.32	8.78	30.72	7.19	32.97	9.48
Tnfsf4	31.38	7.84	31.70	8.16	30.38	6.85	30.86	7.37
Tnfsf8	35.00	11.45	32.59	9.05	31.76	8.23	30.51	7.02
Tnfsf9	32.28	8.74	29.77	6.23	30.36	6.84	29.53	6.04
Tollip	24.48	0.93	24.68	1.15	24.57	1.05	24.59	1.09
Tpst1	23.91	0.37	23.38	-0.15	23.63	0.11	23.55	0.06
Trap1	22.60	-0.95	22.80	-0.73	22.77	-0.76	22.75	-0.74
Ttn	31.28	7.73	31.72	8.18	30.49	6.96	25.49	1.99
Tymp	35.00	11.45	35.00	11.47	33.29	9.77	31.94	8.45
Vegfa	24.24	0.69	24.61	1.07	23.96	0.44	24.41	0.92
Vegfb	24.65	1.10	24.90	1.36	24.45	0.93	25.32	1.82
Vps45	26.44	2.90	26.60	3.07	26.58	3.06	26.50	3.00

Xcl1	29.12	5.58	28.61	5.08	28.43	4.90	26.01	2.51
Xcr1	32.82	9.27	29.53	6.00	29.76	6.24	28.16	4.66
Yars	26.97	3.42	27.50	3.96	27.18	3.65	26.46	2.96
Gusb	24.97	1.42	23.66	0.12	25.29	1.77	24.12	0.63
Hprt	21.16	-2.39	21.09	-2.44	21.27	-2.25	20.99	-2.50
Hsp90ab1	19.51	-4.04	19.90	-3.64	19.64	-3.89	19.59	-3.90
Gapdh	20.54	-3.01	20.83	-2.70	20.20	-3.32	19.99	-3.50
Actb	19.49	-4.06	18.98	-4.55	19.25	-4.27	18.64	-4.86

Table A.3. CT and dCT values from retroperitoneal WAT (from PCR array)

	LF PBS CT	LF PBS dCT	HF PBS CT	HF PBS dCT	LF FFL CT	LF FFL dCT	HF FFL CT	HF FFL dCT
Adora1	31.25	5.47	29.49	3.73	30.00	4.32	28.90	3.61
Ahsg	35.00	9.23	31.30	5.54	29.21	3.52	31.68	6.39
Aif1	26.98	1.20	25.63	-0.13	24.66	-1.02	23.50	-1.79
Apcs	32.37	6.59	35.00	9.24	34.26	8.57	35.00	9.72
Apoa2	27.74	1.96	27.78	2.02	25.24	-0.44	28.71	3.43
Apol7a	32.15	6.37	31.87	6.11	30.49	4.80	28.46	3.17
Apol8	35.00	9.23	35.00	9.24	35.00	9.32	35.00	9.72
Areg	34.68	8.91	33.22	7.46	32.20	6.51	29.25	3.96
Bcl6	27.52	1.75	26.91	1.15	26.63	0.94	25.64	0.35
Blnk	29.20	3.42	29.01	3.25	28.55	2.87	26.34	1.06
Bmp1	27.36	1.58	27.28	1.52	27.12	1.44	24.94	-0.34
Bmp2	34.22	8.45	34.99	9.23	33.85	8.16	31.64	6.35
Bmp3	28.43	2.66	27.60	1.84	27.33	1.65	26.33	1.04
Bmp7	31.11	5.33	29.79	4.03	30.66	4.97	30.42	5.14
C3	24.58	-1.19	24.32	-1.44	23.59	-2.10	23.19	-2.09
C3ar1	27.08	1.31	25.42	-0.34	25.66	-0.03	24.20	-1.09
Cast	25.72	-0.06	25.28	-0.48	24.93	-0.75	24.52	-0.77
Ccl1	34.86	9.08	35.00	9.24	31.29	5.61	31.64	6.36
Ccl11	23.79	-1.98	25.68	-0.08	25.85	0.17	23.65	-1.63
Ccl12	28.54	2.76	27.68	1.92	26.88	1.19	24.10	-1.19
Ccl17	29.69	3.92	29.94	4.18	28.89	3.21	28.20	2.92
Ccl19	27.57	1.79	27.69	1.93	27.36	1.68	26.61	1.32
Ccl2	27.36	1.59	24.62	-1.14	25.13	-0.55	23.52	-1.76
Ccl20	35.00	9.23	35.00	9.24	35.00	9.32	35.00	9.72
Ccl22	31.72	5.95	30.08	4.32	30.52	4.84	29.45	4.16
Ccl24	32.18	6.41	31.11	5.35	32.11	6.43	30.37	5.09
Ccl25	31.01	5.24	32.40	6.64	31.45	5.77	29.31	4.03
Ccl27a	27.15	1.38	27.07	1.31	26.26	0.58	26.28	1.00
Ccl28	32.75	6.97	32.50	6.74	32.87	7.19	31.32	6.03
Ccl3	29.94	4.17	28.84	3.08	28.95	3.26	27.22	1.93
Ccl4	31.55	5.78	29.64	3.88	29.37	3.69	27.26	1.98
Ccl5	26.78	1.01	25.21	-0.55	24.78	-0.91	23.42	-1.86
Ccl6	23.88	-1.89	23.90	-1.86	23.62	-2.06	22.98	-2.31
Ccl7	26.42	0.65	23.97	-1.79	25.24	-0.44	22.94	-2.34
Ccl8	24.86	-0.91	24.50	-1.26	23.16	-2.52	21.94	-3.35

Ccl9	24.96	-0.81	24.73	-1.03	24.82	-0.86	24.43	-0.85
Ccr1	28.92	3.14	28.35	2.59	27.71	2.03	25.81	0.52
Ccr10	34.80	9.03	35.00	9.24	35.00	9.32	31.66	6.38
Ccr2	28.99	3.22	27.73	1.97	28.16	2.47	25.11	-0.17
Ccr3	29.99	4.22	29.81	4.05	29.78	4.10	26.70	1.42
Ccr4	35.00	9.23	33.98	8.22	33.84	8.16	32.78	7.50
Ccr5	30.41	4.63	29.09	3.33	28.98	3.30	25.65	0.36
Ccr6	35.00	9.23	35.00	9.24	34.50	8.81	30.38	5.10
Ccr7	33.70	7.93	33.77	8.01	33.11	7.43	30.22	4.94
Ccr8	33.53	7.75	35.00	9.24	34.37	8.69	31.49	6.21
Ccr9	35.00	9.23	34.36	8.60	33.87	8.18	31.62	6.33
Ccrl1	35.00	9.23	33.80	8.04	34.41	8.72	31.88	6.60
Ccrl2	29.93	4.16	29.29	3.53	29.12	3.43	27.49	2.21
Cd14	25.25	-0.52	25.29	-0.47	24.43	-1.26	24.41	-0.88
Cd180	30.72	4.95	28.87	3.11	29.87	4.19	26.62	1.33
Cd27	35.00	9.23	33.84	8.08	33.08	7.40	30.73	5.45
Cd28	32.42	6.64	31.65	5.89	30.63	4.94	28.57	3.29
Cd4	32.97	7.20	33.08	7.32	30.55	4.87	29.27	3.99
Cd40	29.65	3.87	28.80	3.04	29.25	3.56	27.36	2.07
Cd40lg	34.18	8.41	34.20	8.44	34.74	9.06	30.92	5.64
Cd70	34.57	8.80	35.00	9.24	33.65	7.96	31.16	5.88
Cd74	21.69	-4.09	21.12	-4.64	20.76	-4.92	18.83	-6.46
Cd86	27.28	1.50	26.77	1.01	26.41	0.73	26.25	0.97
Cd97	25.97	0.19	25.42	-0.35	25.44	-0.24	23.98	-1.30
Cebpb	22.41	-3.36	22.70	-3.06	21.91	-3.77	21.72	-3.56
Cer1	35.00	9.23	35.00	9.24	35.00	9.32	35.00	9.72
Cklf	28.19	2.42	27.53	1.77	27.41	1.72	26.49	1.20
Clcf1	35.00	9.23	32.10	6.34	32.50	6.81	30.25	4.97
Cmtm1	35.00	9.23	35.00	9.24	35.00	9.32	34.92	9.64
Cmtm2a	33.97	8.19	35.00	9.24	35.00	9.32	33.47	8.19
Cntfr	32.25	6.47	31.96	6.20	31.51	5.82	30.78	5.50
Crp	31.72	5.95	33.46	7.69	30.33	4.65	33.12	7.83
Csf1	28.80	3.02	28.36	2.60	26.99	1.31	25.19	-0.10
Csf2	35.00	9.23	32.68	6.92	33.34	7.66	31.92	6.64
Csf2ra	30.56	4.79	29.16	3.40	29.12	3.43	28.60	3.32
Csf3	35.00	9.23	35.00	9.24	35.00	9.32	34.27	8.99
Csf3r	31.53	5.76	30.61	4.85	29.55	3.87	29.25	3.97
Ctf1	33.30	7.53	33.09	7.33	30.35	4.67	29.94	4.65
Ctf2	35.00	9.23	35.00	9.24	35.00	9.32	35.00	9.72
Cx3cl1	30.13	4.35	28.85	3.09	28.34	2.66	27.69	2.41
Cx3cr1	34.67	8.90	34.69	8.92	29.72	4.04	28.95	3.66
Cxcl1	35.00	9.23	33.47	7.71	31.76	6.08	28.84	3.56
Cxcl10	29.77	4.00	27.37	1.61	26.45	0.77	24.09	-1.19
Cxcl11	32.71	6.94	32.19	6.43	31.17	5.48	29.56	4.27
Cxcl12	27.50	1.72	26.39	0.63	26.39	0.71	25.58	0.29
Cxcl13	23.23	-2.54	24.69	-1.07	22.53	-3.15	24.68	-0.60
Cxcl14	26.96	1.18	25.87	0.11	26.31	0.63	25.63	0.35

Cxcl15	35.00	9.23	35.00	9.24	35.00	9.32	34.68	9.39
Cxcl16	28.08	2.30	26.90	1.14	26.26	0.58	24.50	-0.79
Cxcl2	29.69	3.92	30.24	4.47	29.73	4.04	27.58	2.30
Cxcl5	34.42	8.65	33.51	7.74	26.57	0.88	24.15	-1.14
Cxcl9	26.38	0.60	24.97	-0.79	24.91	-0.77	22.67	-2.61
Cxcr3	29.27	3.50	28.13	2.37	27.91	2.23	26.34	1.06
Cxcr4	26.98	1.21	27.87	2.11	26.30	0.62	24.97	-0.32
Cxcr5	34.38	8.60	34.95	9.19	33.22	7.53	31.98	6.70
Cxcr6	30.35	4.58	29.67	3.91	29.36	3.68	27.38	2.09
Cybb	28.30	2.52	27.15	1.39	26.51	0.83	25.50	0.21
Cyp26b1	35.00	9.23	35.00	9.24	34.15	8.47	34.78	9.49
D17Wsu104e	26.16	0.38	25.21	-0.55	24.90	-0.79	23.56	-1.73
Dock2	29.16	3.38	28.38	2.62	28.17	2.49	27.49	2.21
Ebi3	29.67	3.90	28.59	2.83	27.70	2.02	27.17	1.89
Eda	28.72	2.95	28.39	2.63	28.17	2.49	27.76	2.48
Ephx2	24.43	-1.35	24.44	-1.32	24.16	-1.53	22.39	-2.89
Epo	35.00	9.23	35.00	9.24	35.00	9.32	35.00	9.72
Epor	33.78	8.01	33.48	7.72	32.72	7.04	30.97	5.68
Erbb2	32.20	6.43	31.97	6.21	31.99	6.31	30.21	4.93
Erbb2ip	27.11	1.33	26.43	0.67	26.13	0.45	25.40	0.12
F11r	28.86	3.09	28.30	2.54	26.66	0.98	25.76	0.48
F2	33.26	7.49	34.14	8.38	31.23	5.55	33.01	7.73
F3	26.60	0.83	25.09	-0.67	25.56	-0.13	24.78	-0.51
F8	28.64	2.87	28.62	2.86	28.21	2.52	28.00	2.72
Fasl	33.71	7.93	33.33	7.57	33.99	8.31	30.40	5.11
Fgf1	24.23	-1.54	24.28	-1.48	24.39	-1.30	24.18	-1.11
Fgf10	29.29	3.51	28.20	2.44	28.51	2.83	26.44	1.15
Fgf12	35.00	9.23	32.13	6.37	35.00	9.32	31.27	5.98
Fgf2	28.99	3.21	28.56	2.80	27.85	2.16	27.32	2.03
Fgf3	35.00	9.23	35.00	9.24	35.00	9.32	35.00	9.72
Fgf4	35.00	9.23	35.00	9.24	35.00	9.32	35.00	9.72
Fgf5	35.00	9.23	35.00	9.24	35.00	9.32	35.00	9.72
Fgf6	35.00	9.23	35.00	9.24	35.00	9.32	35.00	9.72
Fgf7	31.41	5.63	30.43	4.67	31.90	6.22	29.36	4.08
Fgf8	35.00	9.23	35.00	9.24	35.00	9.32	35.00	9.72
Fgf9	30.53	4.76	30.09	4.33	30.85	5.17	28.96	3.67
Figf	25.33	-0.44	25.89	0.13	25.43	-0.25	24.62	-0.67
Flt3l	29.93	4.16	29.61	3.85	28.69	3.01	28.01	2.72
Fn1	25.67	-0.10	25.80	0.04	23.18	-2.50	21.94	-3.35
Fos	27.34	1.57	28.52	2.76	27.19	1.50	25.27	-0.01
Fpr1	31.25	5.47	31.77	6.01	28.00	2.31	29.01	3.73
Gdf1	35.00	9.23	35.00	9.24	35.00	9.32	35.00	9.72
Gdf2	35.00	9.23	35.00	9.24	35.00	9.32	35.00	9.72
Gdf3	33.67	7.89	32.26	6.50	32.90	7.22	29.69	4.41
Gdf5	34.28	8.51	32.57	6.81	32.41	6.73	30.38	5.09
Gdf6	34.23	8.46	35.00	9.24	32.87	7.18	32.56	7.28
Gdf7	35.00	9.23	35.00	9.24	33.93	8.25	32.64	7.36

Gdf9	31.15	5.38	29.91	4.15	30.40	4.72	29.21	3.93
Gfra1	32.18	6.41	35.00	9.24	32.26	6.58	31.10	5.82
Gfra2	28.33	2.56	27.98	2.22	28.15	2.46	27.56	2.27
Ghr	24.41	-1.37	20.23	-5.53	20.19	-5.49	19.81	-5.48
Glmn	28.45	2.68	27.85	2.09	27.38	1.70	26.75	1.47
Gpi1	24.17	-1.61	23.49	-2.27	22.93	-2.75	21.84	-3.45
Gpr68	35.00	9.23	33.56	7.80	33.29	7.61	32.28	6.99
Grem1	35.00	9.23	35.00	9.24	35.00	9.32	33.77	8.49
Grem2	32.56	6.78	34.12	8.36	31.98	6.30	31.81	6.52
Grn	24.27	-1.50	23.39	-2.37	23.23	-2.45	22.45	-2.83
Hdac4	29.10	3.32	28.42	2.66	28.08	2.40	26.81	1.53
Hdac5	30.53	4.76	30.38	4.62	29.59	3.91	28.54	3.26
Hdac7	27.11	1.34	26.55	0.79	25.67	-0.01	24.33	-0.95
Hdac9	33.78	8.01	31.66	5.90	31.89	6.20	29.34	4.06
Hrh1	35.00	9.23	34.75	8.99	33.53	7.84	32.25	6.97
Ifna11	35.00	9.23	35.00	9.24	35.00	9.32	35.00	9.72
Ifna14	35.00	9.23	35.00	9.24	35.00	9.32	35.00	9.72
Ifna2	35.00	9.23	35.00	9.24	35.00	9.32	35.00	9.72
Ifna4	35.00	9.23	35.00	9.24	34.43	8.75	33.62	8.34
Ifna9	35.00	9.23	35.00	9.24	35.00	9.32	35.00	9.72
Ifnab	35.00	9.23	35.00	9.24	35.00	9.32	35.00	9.72
Ifnar1	27.77	2.00	26.90	1.13	26.49	0.81	24.93	-0.35
Ifnar2	24.09	-1.69	23.35	-2.41	23.10	-2.58	22.50	-2.78
Ifnb1	35.00	9.23	35.00	9.24	35.00	9.32	35.00	9.72
Ifne	35.00	9.23	35.00	9.24	34.39	8.70	34.15	8.86
Ifng	34.41	8.63	34.39	8.63	32.42	6.74	30.65	5.37
Ifngr1	24.88	-0.90	24.98	-0.79	23.90	-1.78	22.75	-2.53
Ifngr2	28.24	2.47	26.94	1.18	26.68	0.99	24.78	-0.50
Ifnk	31.80	6.03	32.37	6.60	32.22	6.53	30.64	5.35
Ik	29.13	3.36	28.17	2.41	28.11	2.42	27.07	1.78
Il10	30.58	4.80	29.26	3.50	29.46	3.77	27.73	2.44
Il10ra	30.10	4.33	29.11	3.35	28.30	2.62	26.85	1.57
Il10rb	24.13	-1.64	24.85	-0.91	24.43	-1.25	23.62	-1.66
Il11	33.92	8.14	35.00	9.24	35.00	9.32	35.00	9.72
Il11ra1	27.32	1.54	26.97	1.20	26.28	0.60	25.97	0.68
Il12a	35.00	9.23	34.73	8.97	32.59	6.91	32.73	7.45
Il12b	33.14	7.37	35.00	9.24	31.40	5.71	29.45	4.17
Il12rb1	35.00	9.23	35.00	9.24	35.00	9.32	35.00	9.72
Il12rb2	35.00	9.23	35.00	9.24	35.00	9.32	35.00	9.72
Il13	34.39	8.61	34.21	8.45	33.83	8.15	35.00	9.72
Il13ra1	28.18	2.40	27.26	1.50	26.59	0.91	25.64	0.36
Il13ra2	29.48	3.71	28.99	3.23	30.95	5.27	28.65	3.36
Il15	28.55	2.77	27.47	1.71	27.28	1.60	26.55	1.27
Il15ra	28.94	3.16	29.43	3.67	28.47	2.78	27.63	2.35
Il16	32.52	6.75	30.78	5.02	30.60	4.91	28.53	3.24
Il17a	35.00	9.23	35.00	9.24	35.00	9.32	35.00	9.72
Il17b	34.31	8.54	32.69	6.93	35.00	9.32	32.58	7.30

Il17c	35.00	9.23	35.00	9.24	35.00	9.32	35.00	9.72
Il17d	31.36	5.59	34.46	8.70	34.63	8.95	32.46	7.17
Il17f	33.98	8.21	34.71	8.95	34.39	8.71	32.69	7.40
Il17ra	29.84	4.06	29.90	4.13	29.59	3.90	28.90	3.62
Il17rb	32.62	6.85	30.88	5.12	30.76	5.08	30.11	4.82
Il18	26.84	1.07	26.39	0.63	25.48	-0.20	25.14	-0.14
Il18r1	35.00	9.23	35.00	9.24	31.22	5.54	29.10	3.82
Il18rap	35.00	9.23	33.34	7.58	32.23	6.55	29.36	4.08
Il19	35.00	9.23	35.00	9.24	35.00	9.32	35.00	9.72
Il1a	33.89	8.12	34.82	9.06	35.00	9.32	31.74	6.45
Il1b	30.96	5.19	32.14	6.38	30.26	4.58	28.39	3.10
Il1f10	35.00	9.23	35.00	9.24	35.00	9.32	35.00	9.72
Il1f5	35.00	9.23	35.00	9.24	35.00	9.32	35.00	9.72
Il1f6	35.00	9.23	35.00	9.24	35.00	9.32	35.00	9.72
Il1f8	35.00	9.23	35.00	9.24	35.00	9.32	35.00	9.72
Il1f9	34.77	9.00	35.00	9.24	32.10	6.42	32.20	6.92
Il1r1	26.43	0.66	26.22	0.46	25.21	-0.47	24.54	-0.74
Il1r2	27.30	1.53	28.26	2.50	27.60	1.92	27.31	2.03
Il1rap	31.54	5.77	29.64	3.88	29.66	3.97	28.51	3.23
Il1rapl2	35.00	9.23	35.00	9.24	35.00	9.32	35.00	9.72
Il1rl1	30.16	4.38	29.95	4.19	29.32	3.63	28.29	3.01
Il1rl2	35.00	9.23	33.97	8.21	34.00	8.31	32.35	7.07
Il1rn	31.08	5.30	29.69	3.93	31.82	6.14	27.99	2.71
Il2	35.00	9.23	31.60	5.84	32.30	6.61	31.78	6.49
Il20	35.00	9.23	35.00	9.24	35.00	9.32	35.00	9.72
Il20ra	35.00	9.23	35.00	9.24	34.36	8.68	35.00	9.72
Il21	35.00	9.23	35.00	9.24	35.00	9.32	33.01	7.73
Il21r	35.00	9.23	35.00	9.24	31.93	6.25	30.35	5.07
Il22	35.00	9.23	35.00	9.24	35.00	9.32	35.00	9.72
Il22ra1	35.00	9.23	35.00	9.24	33.00	7.32	31.93	6.65
Il22ra2	30.77	4.99	31.44	5.68	30.92	5.24	29.53	4.24
Il23a	35.00	9.23	35.00	9.24	35.00	9.32	35.00	9.72
Il23r	35.00	9.23	34.39	8.63	35.00	9.32	33.76	8.47
Il24	35.00	9.23	35.00	9.24	35.00	9.32	34.22	8.94
Il27	33.20	7.42	34.41	8.65	32.90	7.22	31.99	6.70
Il28ra	35.00	9.23	34.19	8.42	34.09	8.41	32.90	7.62
Il2ra	32.52	6.75	31.18	5.42	31.48	5.80	30.58	5.30
Il2rb	33.13	7.36	33.76	8.00	31.91	6.23	29.82	4.54
Il2rg	27.94	2.17	27.36	1.60	26.23	0.55	25.00	-0.28
Il3	35.00	9.23	35.00	9.24	34.78	9.10	34.94	9.66
Il31	35.00	9.23	35.00	9.24	35.00	9.32	35.00	9.72
Il31ra	29.55	3.77	31.33	5.57	29.41	3.73	29.99	4.71
Il3ra	35.00	9.23	35.00	9.24	33.99	8.31	32.18	6.89
Il4	35.00	9.23	35.00	9.24	34.62	8.94	33.68	8.39
Il4ra	30.19	4.42	30.09	4.33	29.68	4.00	28.13	2.85
Il5	34.18	8.41	35.00	9.24	34.87	9.19	31.68	6.40
Il5ra	32.14	6.37	33.69	7.93	32.99	7.31	31.62	6.34

Il6	35.00	9.23	32.42	6.66	33.38	7.70	31.30	6.01
Il6ra	27.42	1.64	27.59	1.83	26.59	0.90	26.14	0.86
Il6st	25.11	-0.66	24.85	-0.91	23.93	-1.75	23.13	-2.16
Il7	29.64	3.86	29.75	3.99	30.42	4.73	29.56	4.27
Il7r	28.52	2.75	27.43	1.67	28.32	2.64	26.69	1.41
Cxcr1	35.00	9.23	35.00	9.24	35.00	9.32	35.00	9.72
Cxcr2	35.00	9.23	35.00	9.24	31.86	6.18	30.59	5.31
Il9	35.00	9.23	35.00	9.24	35.00	9.32	35.00	9.72
Il9r	35.00	9.23	35.00	9.24	35.00	9.32	35.00	9.72
Inha	35.00	9.23	34.76	9.00	32.09	6.41	33.30	8.01
Inhba	35.00	9.23	30.71	4.95	29.97	4.28	28.33	3.05
Inhbb	31.98	6.21	30.82	5.06	30.34	4.66	28.99	3.71
Ins1	35.00	9.23	35.00	9.24	35.00	9.32	35.00	9.72
Ins2	35.00	9.23	33.95	8.19	34.69	9.01	34.50	9.21
Irf4	29.57	3.80	31.10	5.34	28.56	2.88	29.25	3.97
Irf7	29.17	3.40	28.97	3.21	27.40	1.71	26.08	0.80
Itgb2	24.29	-1.48	23.44	-2.32	23.75	-1.93	22.57	-2.72
Itih4	34.14	8.36	32.62	6.86	30.08	4.40	31.75	6.47
Kitl	27.47	1.69	27.39	1.63	26.66	0.98	25.35	0.07
Kng1	35.00	9.23	34.70	8.94	31.58	5.90	35.00	9.72
Lbp	25.49	-0.28	24.36	-1.40	24.92	-0.77	23.60	-1.68
Lefty1	29.12	3.35	28.52	2.76	27.51	1.82	26.68	1.40
Lefty2	35.00	9.23	35.00	9.24	35.00	9.32	35.00	9.72
Lepr	30.58	4.81	29.68	3.92	29.44	3.76	29.20	3.92
Lif	32.01	6.24	31.50	5.74	30.78	5.09	28.54	3.25
Lifr	28.19	2.42	28.09	2.33	27.01	1.33	25.73	0.44
Lta	35.00	9.23	34.51	8.75	34.25	8.57	31.31	6.03
Ltb	32.80	7.03	32.43	6.67	31.70	6.02	27.94	2.66
Ltb4r1	35.00	9.23	35.00	9.24	35.00	9.32	35.00	9.72
Ly75	32.80	7.03	32.42	6.66	31.08	5.39	29.49	4.20
Ly86	26.41	0.64	26.08	0.32	25.61	-0.08	23.64	-1.65
Ly96	26.37	0.59	26.18	0.42	25.85	0.17	25.31	0.03
Mdk	27.52	1.75	25.94	0.18	26.17	0.48	25.26	-0.03
Mefv	35.00	9.23	34.59	8.83	31.90	6.21	31.80	6.51
Mgll	24.67	-1.10	23.55	-2.22	23.42	-2.26	22.49	-2.79
Mif	24.32	-1.46	23.91	-1.85	23.13	-2.55	21.50	-3.78
Mmp25	34.97	9.20	35.00	9.24	35.00	9.32	32.26	6.97
Mpl	35.00	9.23	35.00	9.24	35.00	9.32	35.00	9.72
Mstn	33.39	7.62	32.55	6.79	32.00	6.31	30.49	5.21
Muc4	35.00	9.23	35.00	9.24	35.00	9.32	35.00	9.72
Myd88	34.47	8.70	33.94	8.18	33.47	7.79	31.11	5.83
Nfam1	34.09	8.31	33.99	8.23	34.19	8.50	30.95	5.66
Nfatc3	26.56	0.78	25.75	-0.01	25.35	-0.33	24.57	-0.72
Nfatc4	35.00	9.23	35.00	9.24	35.00	9.32	33.11	7.83
Nfe2l1	28.22	2.45	27.80	2.04	27.33	1.65	26.21	0.93
Nfkb1	26.91	1.13	26.44	0.68	25.64	-0.04	24.68	-0.60
Nfrkb	30.76	4.99	30.96	5.20	30.16	4.48	28.90	3.61

Nfx1	29.24	3.47	29.42	3.66	28.49	2.81	27.16	1.87
Nlrp12	35.00	9.23	35.00	9.24	35.00	9.32	35.00	9.72
Nmi	25.90	0.13	25.43	-0.33	25.18	-0.51	24.38	-0.90
Nodal	35.00	9.23	35.00	9.24	35.00	9.32	35.00	9.72
Nos2	34.97	9.20	35.00	9.24	35.00	9.32	34.18	8.90
Nr3c1	24.97	-0.80	24.77	-0.99	24.47	-1.22	23.54	-1.75
Nrg1	35.00	9.23	35.00	9.24	31.64	5.96	30.29	5.01
Ntf3	29.95	4.18	29.08	3.32	29.23	3.54	28.28	3.00
Olr1	31.10	5.33	29.40	3.63	29.55	3.87	27.88	2.59
Osm	34.49	8.72	33.35	7.59	32.12	6.43	29.77	4.49
Osmr	26.84	1.07	26.84	1.08	25.98	0.29	24.81	-0.48
Parp4	26.93	1.16	26.45	0.69	26.16	0.48	25.37	0.09
Nampt	24.69	-1.08	25.09	-0.67	23.66	-2.02	23.49	-1.80
Pdgfa	29.48	3.70	28.29	2.53	28.01	2.33	26.47	1.19
Pdgfb	30.66	4.89	29.54	3.78	29.28	3.60	27.19	1.90
Pdgfc	28.23	2.45	27.51	1.75	27.25	1.57	26.54	1.26
Pf4	24.88	-0.89	23.87	-1.89	23.87	-1.81	22.96	-2.32
Pglyrp1	29.38	3.60	29.42	3.66	28.38	2.70	26.60	1.32
Pla2g2d	29.26	3.49	28.92	3.16	27.41	1.73	27.30	2.02
Pla2g7	24.46	-1.32	24.25	-1.51	23.35	-2.33	22.96	-2.32
Ppbp	29.95	4.18	29.41	3.65	29.61	3.93	28.71	3.42
Prdx5	22.67	-3.10	21.83	-3.94	21.57	-4.11	20.82	-4.47
Prg2	34.44	8.67	33.84	8.08	32.12	6.44	30.58	5.30
Prg3	35.00	9.23	35.00	9.24	35.00	9.32	34.12	8.83
Prl	35.00	9.23	35.00	9.24	34.40	8.72	35.00	9.72
Prlr	27.94	2.16	27.62	1.86	27.38	1.70	26.88	1.59
Procr	27.75	1.98	27.58	1.82	27.12	1.44	26.42	1.14
Prok2	35.00	9.23	35.00	9.24	35.00	9.32	32.84	7.56
Ptafr	28.83	3.05	27.61	1.85	28.21	2.53	26.72	1.44
Ptgs2	33.92	8.15	34.55	8.79	31.74	6.06	29.97	4.68
Ptn	34.59	8.82	31.69	5.93	34.61	8.93	32.32	7.03
Ptpra	24.28	-1.49	23.67	-2.09	23.65	-2.04	22.84	-2.45
Ptx3	25.39	-0.38	26.50	0.74	26.10	0.42	26.09	0.80
Pxmp2	27.50	1.72	27.67	1.91	26.41	0.72	26.58	1.29
Reg3a	35.00	9.23	35.00	9.24	35.00	9.32	35.00	9.72
Reg3g	35.00	9.23	35.00	9.24	35.00	9.32	33.49	8.21
Ripk2	28.35	2.58	27.88	2.12	27.11	1.43	25.82	0.54
S100a11	20.43	-5.34	19.87	-5.89	19.65	-6.03	18.79	-6.49
S100a8	25.00	-0.77	24.24	-1.52	24.63	-1.06	23.23	-2.05
S100b	28.47	2.70	28.07	2.31	27.26	1.58	27.66	2.37
Saa4	33.81	8.03	33.98	8.22	31.69	6.01	35.00	9.72
Scg2	35.00	9.23	35.00	9.24	35.00	9.32	35.00	9.72
Scube1	33.77	8.00	35.00	9.24	35.00	9.32	35.00	9.72
Aimp1	24.55	-1.23	23.98	-1.78	23.45	-2.24	22.81	-2.47
Sdcbp	23.29	-2.49	22.44	-3.32	22.35	-3.34	21.52	-3.77
Sectm1b	35.00	9.23	35.00	9.24	35.00	9.32	35.00	9.72
Sele	34.90	9.13	33.22	7.46	32.17	6.49	32.31	7.03

Serpina1a	28.38	2.61	28.20	2.44	26.39	0.71	27.84	2.55
Serpina3n	22.84	-2.93	22.16	-3.60	22.14	-3.55	21.62	-3.67
Serpinf2	29.67	3.90	30.35	4.59	30.92	5.23	29.22	3.93
Sftpd	35.00	9.23	35.00	9.24	35.00	9.32	35.00	9.72
Sigirr	32.28	6.50	31.99	6.23	30.99	5.31	28.74	3.45
Siglec1	28.25	2.48	27.66	1.90	26.55	0.86	24.86	-0.43
Siva1	26.81	1.04	26.41	0.65	25.31	-0.37	24.08	-1.20
Slco1a4	35.00	9.23	35.00	9.24	35.00	9.32	35.00	9.72
Slurp1	34.27	8.50	32.39	6.63	32.41	6.73	32.49	7.21
Socs2	28.73	2.96	30.19	4.43	28.64	2.96	27.86	2.57
Spaca3	35.00	9.23	35.00	9.24	35.00	9.32	35.00	9.72
Spp1	30.10	4.32	27.51	1.75	26.99	1.31	23.31	-1.97
Spred1	27.82	2.05	26.93	1.17	26.31	0.63	25.60	0.32
Srgap1	30.51	4.74	29.46	3.70	29.72	4.03	28.25	2.97
Stab1	28.35	2.57	27.47	1.71	26.24	0.56	25.28	-0.01
Stat3	31.21	5.44	30.58	4.82	29.62	3.94	27.69	2.40
Sykb	31.66	5.89	32.09	6.33	31.01	5.33	29.54	4.25
Tacr1	35.00	9.23	35.00	9.24	34.91	9.23	33.44	8.15
Thpo	35.00	9.23	35.00	9.24	35.00	9.32	35.00	9.72
Tirap	29.30	3.53	28.51	2.75	27.70	2.02	26.76	1.48
Tlr1	30.80	5.02	28.66	2.90	28.77	3.09	26.59	1.30
Tlr2	30.85	5.08	29.88	4.12	29.11	3.43	28.26	2.98
Tlr3	30.55	4.78	30.26	4.50	29.46	3.77	27.62	2.34
Tlr4	31.64	5.86	26.76	1.00	26.40	0.72	25.50	0.22
Tlr5	29.18	3.41	29.61	3.85	28.29	2.61	27.81	2.52
Tlr6	32.10	6.33	32.43	6.67	31.40	5.72	29.64	4.36
Tlr7	31.20	5.43	32.01	6.25	30.28	4.60	28.64	3.35
Tlr8	28.40	2.63	28.38	2.62	27.96	2.28	26.31	1.03
Tlr9	35.00	9.23	31.85	6.09	31.46	5.78	30.14	4.86
Tnf	35.00	9.23	32.81	7.05	31.31	5.63	29.97	4.68
Tnfaip6	26.84	1.06	27.30	1.53	26.95	1.27	26.71	1.43
Tnfrsf11b	30.18	4.40	28.89	3.13	29.34	3.65	27.40	2.12
Tnfsf10	31.85	6.07	31.11	5.35	30.39	4.70	28.34	3.06
Tnfsf11	34.44	8.66	34.86	9.10	35.00	9.32	30.91	5.63
Tnfsf13	29.99	4.21	29.17	3.41	27.60	1.92	27.40	2.12
Tnfsf13b	32.71	6.94	32.71	6.95	31.21	5.53	29.37	4.08
Tnfsf14	32.12	6.35	30.72	4.96	30.69	5.00	28.68	3.39
Tnfsf15	35.00	9.23	35.00	9.24	35.00	9.32	31.79	6.51
Tnfsf18	34.96	9.19	35.00	9.24	35.00	9.32	33.49	8.21
Tnfsf4	35.00	9.23	35.00	9.24	34.01	8.33	29.61	4.33
Tnfsf8	35.00	9.23	35.00	9.24	35.00	9.32	32.90	7.62
Tnfsf9	35.00	9.23	34.33	8.57	33.50	7.82	30.18	4.90
Tollip	26.42	0.64	26.00	0.24	25.33	-0.35	24.85	-0.43
Tpst1	26.79	1.01	26.00	0.23	25.46	-0.23	24.22	-1.07
Trap1	25.32	-0.45	24.18	-1.58	23.80	-1.89	23.54	-1.74
Ttn	32.80	7.03	32.81	7.05	30.51	4.82	28.48	3.19
Tymp	35.00	9.23	35.00	9.24	34.41	8.72	35.00	9.72

Vegfa	27.15	1.37	27.91	2.15	25.78	0.10	24.42	-0.86
Vegfb	28.30	2.53	27.63	1.87	26.88	1.20	26.18	0.89
Vps45	28.87	3.10	28.64	2.88	27.99	2.30	27.23	1.95
Xcl1	31.19	5.42	29.01	3.25	27.90	2.22	27.12	1.84
Xcr1	33.98	8.21	32.19	6.43	32.78	7.10	29.21	3.93
Yars	30.67	4.89	30.65	4.89	29.39	3.71	28.63	3.35
Gusb	25.36	-0.41	26.14	0.37	25.99	0.30	23.89	-1.39
Hprt	22.25	-3.52	22.26	-3.50	22.16	-3.52	21.45	-3.83
Hsp90ab1	21.34	-4.43	21.24	-4.52	20.48	-5.20	19.86	-5.43
Gapdh	23.49	-2.28	23.45	-2.31	22.58	-3.11	21.47	-3.82
Actb	22.41	-3.36	21.98	-3.79	21.81	-3.88	20.30	-4.98

Table A.4. Mean Ct values of genes in adipose depots from low fat PBS group (from qRT-PCR)

Gene	pmWAT	rpWAT	omWAT
VLDLR	26.1	27.8	24.7
NAMPT	24.3	25.5	22.9
RETN	18.1	19.7	20.7
ADIPOQ	17.3	18.6	17.9
LEP	24.3	26.1	22.4
CCL1	38.8	40.5	36.4
CCL2	27.3	27.7	27.1
CCL4	31.7	33.7	30.5
CCL5	26.0	27.3	24.0
CCR5	29.1	31.2	26.5
CXCR2	37.0	37.4	33.1
CXCL13	26.9	27.2	20.3
CX3CL1	31.0	33.3	28.5
IL1b	33.3	34.0	31.0
TNFa	33.1	33.9	28.2
IL10	37.8	40.0	36.6
IFNg	35.3	36.8	31.7
IL6	38.4	39.5	38.6
NOS3	29.9	31.7	28.3
VEGFa	25.4	27.0	24.5
VEGFR2	27.1	28.8	25.6
HIF1a	25.2	27.1	24.4
IGF1	23.0	23.7	24.1
TGFb	27.0	29.0	24.8
AGT	25.0	26.1	24.6
Col1	32.1	34.5	30.5
TNC	34.4	37.8	33.9
IDO	34.1	35.3	31.3
CD34	24.7	27.0	22.3
aSMA	21.0	23.8	23.0
MMP11	28.6	31.3	28.7
CD31	24.9	26.9	22.6

PAI1	24.1	25.4	22.9
CDH5	25.4	26.9	24.7
FN1	30.2	31.1	28.1
VCAM1	25.6	27.7	23.7

Table A.5. MOSE-L FFL CT values (PCR Array)

Adora1	31.145
Ahsg	31.870
Aif1	31.560
Apcs	32.756
Apoa2	26.907
Apol7a	23.630
Apol8	28.601
Areg	25.969
Bcl6	24.629
Blnk	29.328
Bmp1	22.343
Bmp2	30.705
Bmp3	32.455
Bmp7	33.833
C3	21.282
C3ar1	26.907
Cast	21.217
Ccl1	31.340
Ccl11	30.897
Ccl12	30.912
Ccl17	31.510
Ccl19	28.232
Ccl2	21.222
Ccl20	26.409
Ccl22	30.649
Ccl24	30.636
Ccl25	25.417
Ccl27a	25.219
Ccl28	31.512
Ccl3	29.750
Ccl4	29.794
Ccl5	23.966
Ccl6	30.501
Ccl7	22.165
Ccl8	28.269
Ccl9	25.824
Ccr1	29.997
Ccr10	27.491
Ccr2	30.465

Ccr3	30.274
Ccr4	29.932
Ccr5	32.763
Ccr6	30.642
Ccr7	30.258
Ccr8	33.496
Ccr9	29.969
Ccrl1	30.716
Ccrl2	28.150
Cd14	25.135
Cd180	32.401
Cd27	31.304
Cd28	30.137
Cd4	31.653
Cd40	33.952
Cd40lg	29.992
Cd70	31.298
Cd74	27.165
Cd86	30.400
Cd97	23.440
Cebpb	19.445
Cer1	31.594
Cklf	24.348
Clcf1	22.678
Cmtm1	32.732
Cmtm2a	31.149
Cntfr	32.299
Crp	33.373
Csf1	19.785
Csf2	31.095
Csf2ra	27.723
Csf3	28.831
Csf3r	31.685
Ctf1	24.797
Ctf2	29.187
Cx3cl1	24.459
Cx3cr1	30.013
Cxcl1	24.440
Cxcl10	23.436
Cxcl11	31.764
Cxcl12	22.541
Cxcl13	30.538
Cxcl14	31.505
Cxcl15	31.904
Cxcl16	22.511

Cxcl2	31.425
Cxcl5	20.406
Cxcl9	29.504
Cxcr3	31.716
Cxcr4	34.179
Cxcr5	29.554
Cxcr6	28.382
Cybb	32.764
Cyp26b1	30.883
D17Wsu104e	20.651
Dock2	31.249
Ebi3	29.710
Eda	32.014
Ephx2	32.698
Epo	30.384
Epor	27.234
Erbb2	24.706
Erbb2ip	22.507
F11r	19.646
F2	31.677
F3	25.398
F8	27.561
Fasl	31.585
Fgf1	27.876
Fgf10	21.992
Fgf12	31.620
Fgf2	23.329
Fgf3	30.765
Fgf4	32.625
Fgf5	31.638
Fgf6	30.615
Fgf7	30.969
Fgf8	32.265
Fgf9	33.548
Figf	25.129
Flt3l	26.133
Fn1	16.819
Fos	24.885
Fpr1	29.599
Gdf1	29.531
Gdf2	29.425
Gdf3	30.886
Gdf5	30.943
Gdf6	24.402
Gdf7	29.614

Gdf9	29.926
Gfra1	29.587
Gfra2	29.692
Ghr	22.305
Glmn	24.460
Gpi1	18.309
Gpr68	28.913
Grem1	26.478
Grem2	31.672
Grn	20.138
Hdac4	23.897
Hdac5	24.406
Hdac7	20.136
Hdac9	31.275
Hrh1	28.280
Ifna11	30.763
Ifna14	29.562
Ifna2	29.405
Ifna4	30.267
Ifna9	30.969
Ifnab	29.684
Ifnar1	22.249
Ifnar2	22.727
Ifnb1	31.537
Ifne	29.873
Ifng	32.162
Ifngr1	23.481
Ifngr2	21.603
Ifnk	31.776
Ik	25.640
Il10	29.179
Il10ra	32.233
Il10rb	23.142
Il11	28.532
Il11ra1	22.753
Il12a	29.255
Il12b	30.826
Il12rb1	28.654
Il12rb2	35.324
Il13	30.818
Il13ra1	23.731
Il13ra2	32.293
Il15	30.317
Il15ra	31.782
Il16	23.241

Il17a	33.180
Il17b	29.726
Il17c	29.511
Il17d	33.349
Il17f	28.636
Il17ra	24.514
Il17rb	29.319
Il18	22.925
Il18r1	26.237
Il18rap	25.250
Il19	31.599
Il1a	27.600
Il1b	33.339
Il1f10	32.808
Il1f5	30.156
Il1f6	32.831
Il1f8	32.529
Il1f9	32.479
Il1r1	23.695
Il1r2	29.464
Il1rap	23.709
Il1rapl2	31.389
Il1rl1	27.373
Il1rl2	26.580
Il1rn	27.789
Il2	31.489
Il20	30.876
Il20ra	31.975
Il21	32.879
Il21r	31.461
Il22	30.829
Il22ra1	24.786
Il22ra2	30.945
Il23a	29.567
Il23r	31.777
Il24	30.738
Il27	29.869
Il28ra	27.013
Il2ra	32.760
Il2rb	30.152
Il2rg	23.692
Il3	31.481
Il31	31.407
Il31ra	31.848
Il3ra	Undetermined

Il4	31.590
Il4ra	27.944
Il5	30.990
Il5ra	25.148
Il6	28.962
Il6ra	26.607
Il6st	20.499
Il7	30.814
Il7r	29.351
Cxcr1	32.591
Cxcr2	27.784
Il9	37.750
Il9r	31.346
Inha	28.690
Inhba	21.870
Inhbb	30.943
Ins1	31.518
Ins2	30.623
Irf4	30.753
Irf7	24.976
Itgb2	24.895
Itih4	29.571
Kitl	22.306
Kng1	32.499
Lbp	30.557
Lefty1	22.493
Lefty2	29.143
Lepr	30.497
Lif	23.949
Lifr	22.425
Lta	29.826
Ltb	30.754
Ltb4r1	32.742
Ly75	25.471
Ly86	30.887
Ly96	23.941
Mdk	28.114
Mefv	30.561
Mgll	27.683
Mif	17.444
Mmp25	30.303
Mpl	30.684
Mstn	31.957
Muc4	30.616
Myd88	25.524

Nfam1	35.264
Nfatc3	22.579
Nfatc4	32.773
Nfe2l1	21.353
Nfkb1	23.001
Nfrkb	24.609
Nfx1	24.830
Nlrp12	31.910
Nmi	26.723
Nodal	34.290
Nos2	23.570
Nr3c1	22.324
Nrg1	24.940
Ntf3	30.537
Olr1	21.671
Osm	31.392
Osmr	22.106
Parp4	24.564
Nampt	21.221
Pdgfa	24.441
Pdgfb	22.121
Pdgfc	23.753
Pf4	30.696
Pglyrp1	29.166
Pla2g2d	31.981
Pla2g7	23.775
Ppbp	25.182
Prdx5	20.507
Prg2	31.012
Prg3	31.596
Prl	29.910
Prlr	30.812
Procr	22.863
Prok2	31.882
Ptafr	30.980
Ptgs2	23.781
Ptn	30.849
Ptpra	21.528
Ptx3	21.584
Pxmp2	24.776
Reg3a	30.303
Reg3g	32.139
Ripk2	23.744
S100a11	16.677
S100a8	27.635

S100b	31.243
Saa4	31.871
Scg2	30.845
Scube1	30.969
Aimp1	20.163
Sdcbp	20.656
Sectm1b	30.727
Sele	32.469
Serpina1a	29.558
Serpina3n	27.895
Serpinf2	28.511
Sftpd	33.016
Sigirr	26.797
Siglec1	31.505
Siva1	20.515
Slco1a4	34.212
Slurp1	28.146
Socs2	26.202
Spaca3	31.766
Spp1	19.227
Spred1	21.769
Srgap1	29.574
Stab1	26.445
Stat3	23.443
Sykb	33.296
Tacr1	30.134
Thpo	29.718
Tirap	23.770
Tlr1	26.817
Tlr2	25.308
Tlr3	30.967
Tlr4	23.426
Tlr5	24.673
Tlr6	26.546
Tlr7	27.618
Tlr8	32.304
Tlr9	31.192
Tnf	31.728
Tnfaip6	26.410
Tnfrsf11b	30.526
Tnfsf10	33.182
Tnfsf11	31.394
Tnfsf13	23.583
Tnfsf13b	28.850
Tnfsf14	30.478

Tnfsf15	28.943
Tnfsf18	34.412
Tnfsf4	32.310
Tnfsf8	31.206
Tnfsf9	24.991
Tollip	22.355
Tpst1	22.144
Trap1	21.559
Ttn	29.520
Tymp	28.471
Vegfa	22.300
Vegfb	23.354
Vps45	24.469
Xcl1	30.748
Xcr1	31.688
Yars	21.656
Gusb	23.377
Hprt	20.851
Hsp90ab1	16.632
Gapdh	15.758
Actb	15.125
MGDC	34.164
MGDC	33.605
MGDC	33.207
RTC	33.135
RTC	34.570
RTC	38.103
PPC	18.199
PPC	18.170
PPC	17.955

Appendix B- Diet Composition

Low fat diet

Dyets Inc.

2508 Easton A Bethlehem, Pennsylvania 18017
Within 610 Area Code: 868-7701, FAX -868-5170
Outside 610 Area Code: 800-275-3938
FAX: 800-329-3938
E-Mail Address: dyets@enter.net

DYET# 110186

AIN-93G Purified Rodent Diet with 7% Corn Oil Replacing Soybean Oil (no added antioxidants)

Ingredient	kcal./gm	grams/kg	kcal./kg
Casein	3.58	200	716
L-Cystine	4	3	12
Sucrose	4	100	400
Cornstarch	3.6	397.5	1431.0
Dyetrose	3.8	132	501.6
Corn Oil	9	70	630
Cellulose	0	50	0
Mineral Mix #210025	0.88	35	30.8
Vitamin Mix # 310025	3.87	10	38.7
Choline Bitartrate	0	2.5	0
		1000.00	**3760.10**

Journal of Nutrition v123, 1941(1993)
Laura Kresty, Ohio State Univ., 2/5/96

High Fat Diet

Dyets Inc.
2508 Easton A Bethlehem, Pennsylvania 18017
Within 610 Area Code: 868-7701, FAX -868-5170
Outside 610 Area Code: 800-275-3938
FAX: 800-329-3938
E-Mail Address: dyets@enter.net

DYET# 182103

Custom AIN-93G Purified Rodent Diet with 7% Corn Oil Replacing Soybean Oil and 16.5% Lard (45% FDC)

Ingredient	kcal./gm	grams/kg	kcal./kg
Casein	3.58	200	716
L-Cystine	4	3	12
Sucrose	4	100	400
Cornstarch	3.6	232.5	837.0
Dyetrose	3.8	132	501.6
Corn Oil	9	70	630
Lard (wet rendered)	9	165	1485
Cellulose	0	50	0
Mineral Mix #210025	0.88	35	30.8
Vitamin Mix # 310025	3.87	10	38.7
Choline Bitartrate	0	2.5	0
		1000.00	**4651.10**

Journal of Nutrition v123, 1941(1993)
Eva Schmelz, Virginia Tech, 5/3/2011